SAR Theory and Applications to Forest Cover and Disturbance Mapping and Forest Biomass Assessment

PD Dr. Christian Thiel

Friedrich-Schiller-University Jena, Germany

Outline

1. Introduction: Why Forest Observation?
2. SAR Techniques of interest for forestry applications
3. SAR for Forestry Applications – Some Basics
4. Forest Cover and Biomass Mapping – Excurses
    1. BIOMASAR – Hypertemporal C-band Data Assimilation
    2. Forest Cover Mapping Using Backscatter and Coherence
    3. Forest Biomass Mapping Using Backscatter and Coherence
    4. Polarimetry for Forest Cover Mapping
    5. INSAR Phase and Tree Height
    6. Seasonality of C-band Backscatter in Siberia
    7. Seasonality of Coherence in Siberia
    8. X-band coherence over the Thuringian Forest
    9. Mapping of woody cover in KNP using L-band backscatter

Introduction - Why Forest Observation?

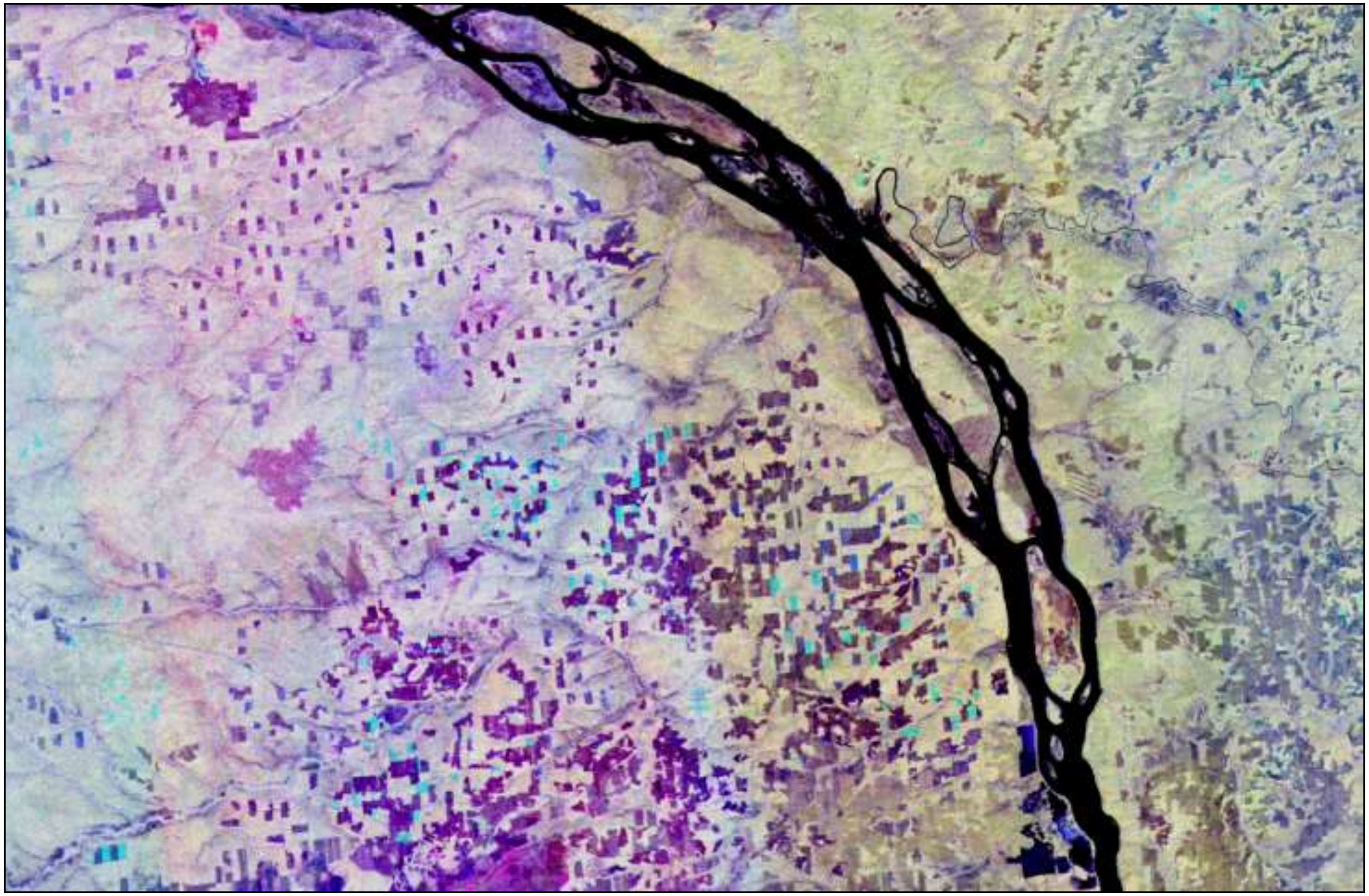

Observe clear-felling (ALOS PALSAR, Multitemporal Composite, Siberia)

Introduction - Why Forest Observation?

Observe damage by forest fires (mid-August 2010, fires close to Moscow)

Forest fire scar – mind the shadows from remaining stems

Forest fire scar (3 years old)

Forest fire scar (3 years old)

Wind damage area

The wood stack on the photo contains approx. 1.000.000 m3. It is 60 m wide, 16 m high, and more than 2 km long. The storm “Gudrun”, which hit southern Sweden in January 2005 fell approx. 75.000.000 m3, which is almost the annual cut in Sweden.
Photo: Ola Nilsson

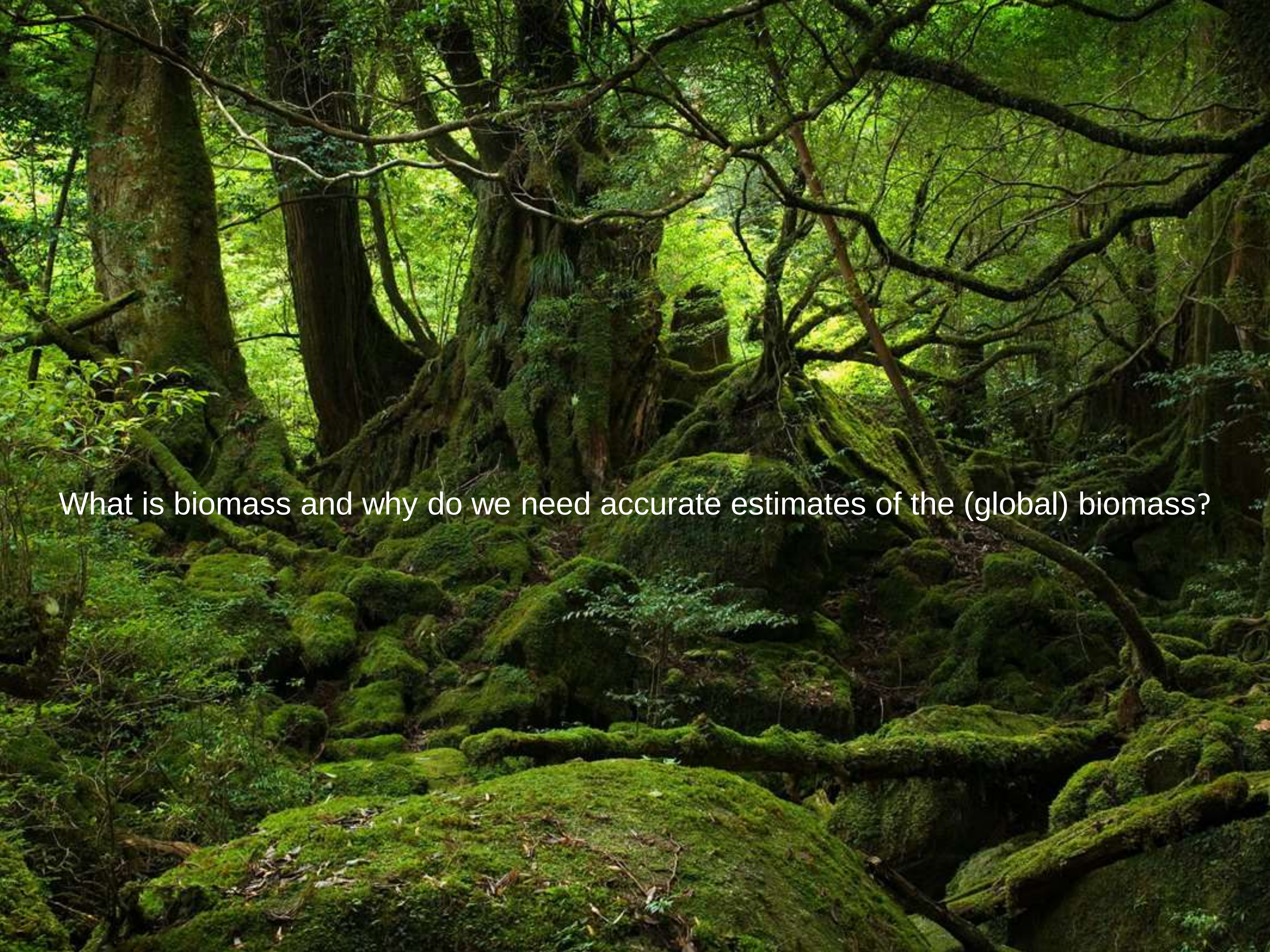
What is biomass and why do we need accurate estimates of the (global) biomass?

Introduction - Main components of biomass distribution

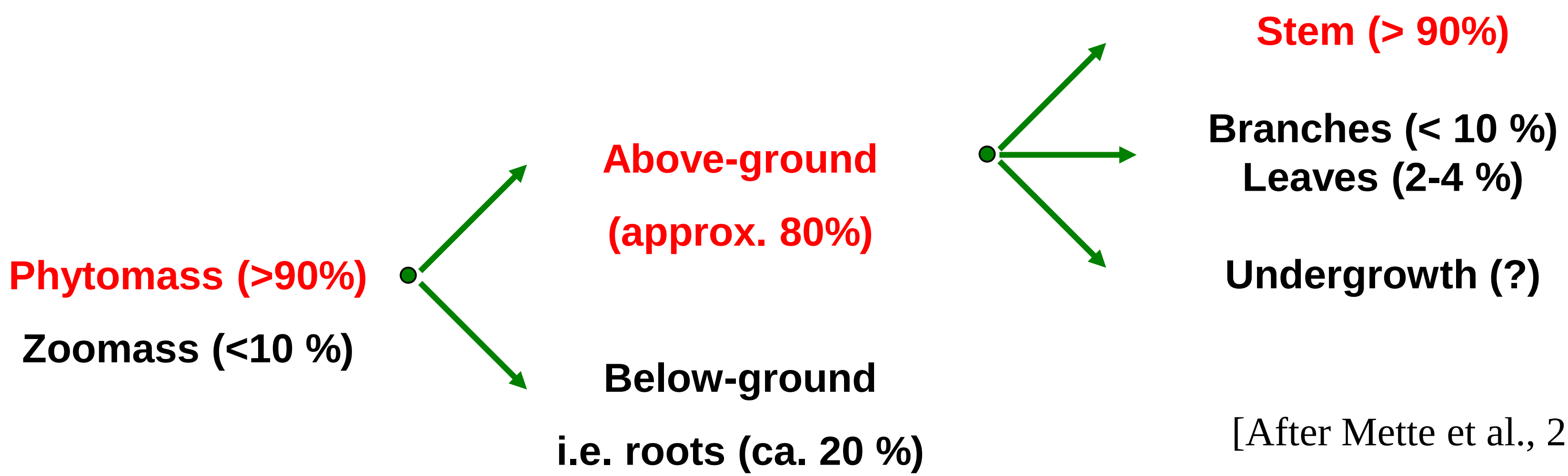

[After Mette et al., 2002]

- Stem Biomass is strongly related to the commercially interesting biomass.
- The major part of forest biomass is concentrated in the major trees. The contribution of minor trees (and hidden biomass) to total biomass is rather low
- Characterizing biomass using tree height will cover 75-95% of the vegetated earth and could directly characterize 80-90% of the aboveground biomass stock

DID YOU KNOW?

- ***Forests*** cover approximately ***33% of the Earth's land surface*** (JENSEN, 2000)

- Forests play an important role in the global carbon cycle, since ***each year forests absorb approximately 1/12 of the Earth's atmospheric CO_2 stock*** (MALHI et al., 2002)

- ***Forested*** ecosystems account for app. ***72% of the Earth's terrestrial carbon storage*** (MALHI et al., 2002)

- Therefore, Vegetation biomass is a ***larger global store of carbon than the atmosphere*** (FAO, 2009)

- Between 1850 and 2011, humans have released app. ***480 Gt (480 BILLION TONS!!!) of CO_2 into the atmosphere*** through fossil fuel burning and land use changes (e.g. deforestation and fires) (GHASEMI et al., 2011)

Forest Biomass

In Forestry, the biomass calculation is based on measurements of trunk diameter and height of sample populations of trees:

$$Biomass_{forest} = N \times \pi \times \left(\frac{1}{2}\,\mathrm{dbhmid}\right)^2 \times hmid \times \rho \times fz$$

$\boldsymbol{Biomass_{forest}}$ **[t/ha]**	is defined as aboveground woody of trunk and branches where exceeding 7 cm diameter
$\mathbf{dbh_{mid}}$ **[cm]**	is the (dbh^2 weighted) mean diameter at breast height 1.3 m
$\boldsymbol{h_{mid}}$ **[m]**	is the height of the tree
$\boldsymbol{\rho}$ **[g/cm³]**	is the species-specific wood density
$\boldsymbol{f_z}$ **[]**	is a form factor (= 0.4-0.5, constant in a first order approximation)
$\boldsymbol{N}$	is the tree density (tree number per area unit)

The product of $\boldsymbol{N} \times \boldsymbol{\pi} \times \left(\frac{1}{2}\,\mathbf{dbh}_{mid}\right)^2$ is also called **basal area g**.

WHY DO WE NEED TO OBSERVE (GLOBAL) FOREST BIOMASS?

- For a better understanding and quantification of:
  - the ***global carbon cycle***
  - ***global warming***
  - terrestrial ***carbon stocks and fluxes*** in forests
  - terrestrial ***carbon sources and sinks***
- Information of forest biomass is needed to ***support sustainable forest resource management***

Outline

SAR Techniques

1. Backscatter analysis (wavelength, polarisation, incidence angle, number of images)
2. Interferometry: Coherence analysis (wavelength, polarisation, incidence angle, temporal and spatial baseline, number of images, acquisition conditions)
3. Interferometry: Phase analysis (wavelength, incidence angle, high coherence required, acquisition conditions)
4. Polarimetry (wavelength, incidence angle, number of images)
5. Polarimetric Interferometry (wavelength, polarisation, incidence angle, temporal and spatial baseline)
6. SAR (Polarimetric) Tomography (wavelength, polarisation, incidence angle, spatial baseline, high coherence required, number of images)

SAR Techniques: Backscatter analysis

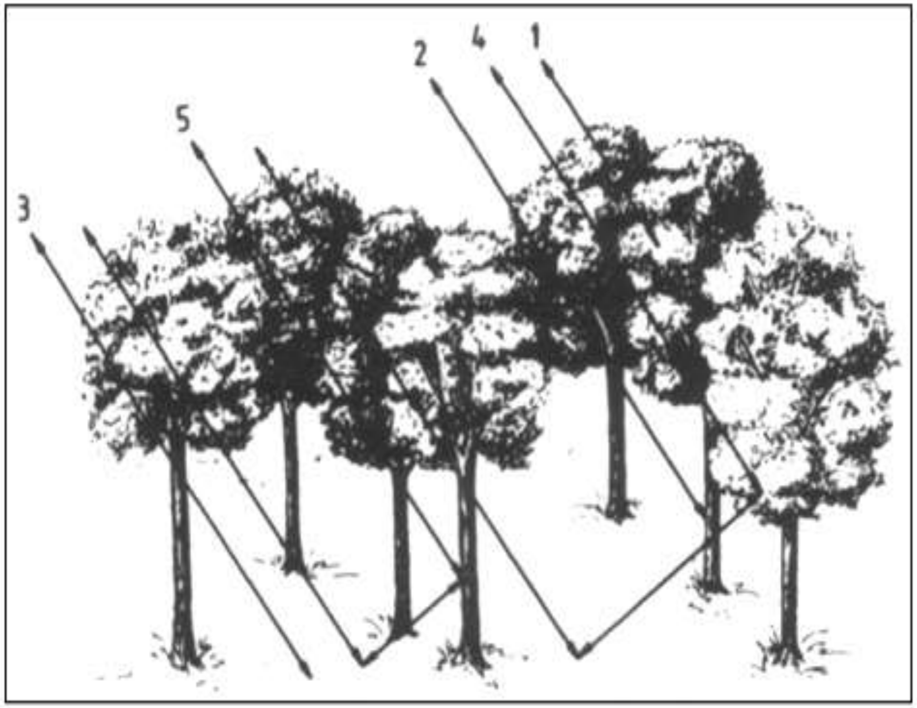

Stem volume vs. backscatter (HV)
(05aug2007) – 12.5 m data

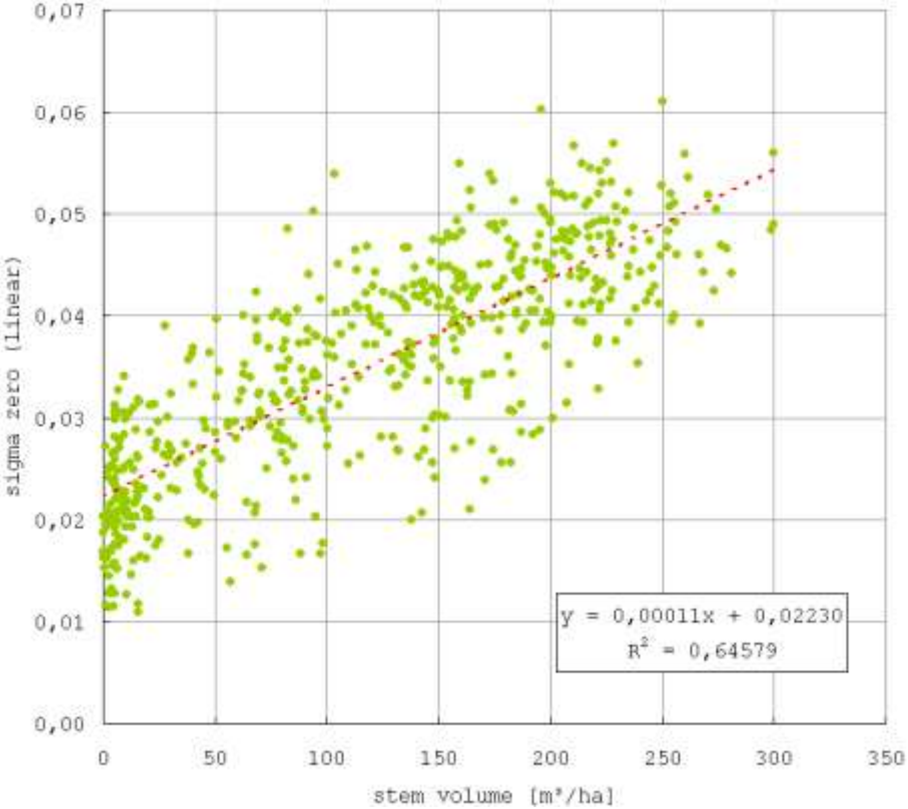

Correlation between SAR data and stem volume

SAR Techniques: Interferometry vs. Polarimetry

The Phase is essential for **Interferometry** and **Polarimetry**

- Both techniques require at least two complex SAR images

A) Same polarisation – different position

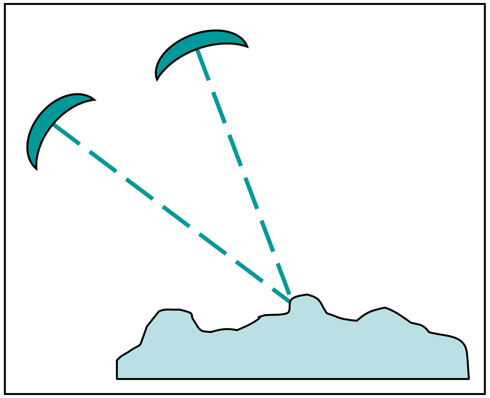

Interferometry

B) Same position – different polarisation

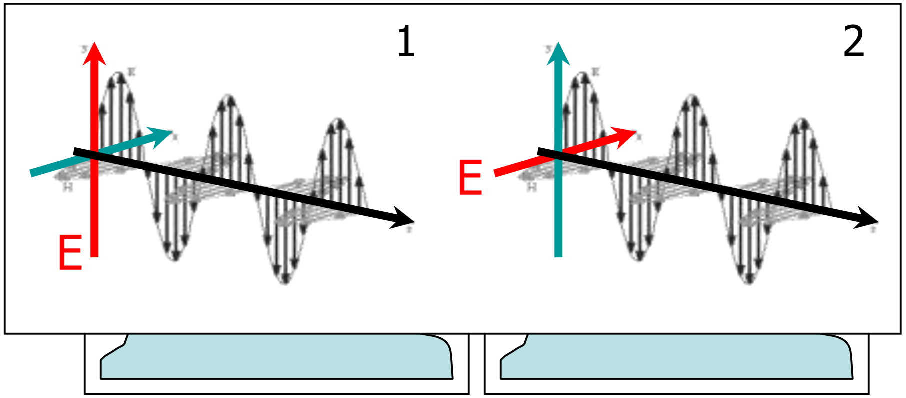

Polarimetry

SAR Techniques: Interferometry

Coherence and INSAR phase contain information on forest

- Interferometric Coherence – correlation of two complex SAR images

Stem volume vs. Coherence
(05feb2008-22mar2008) – 12.5 m data

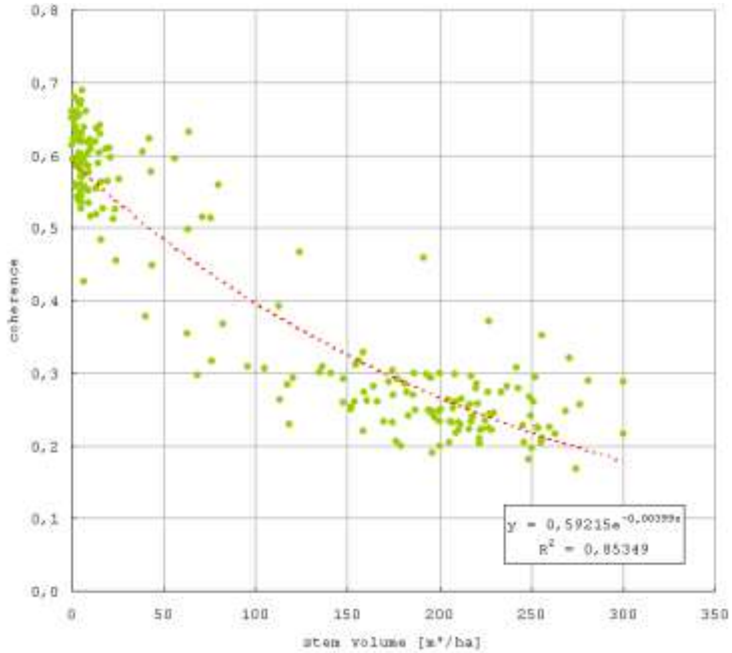

$$\gamma = \frac{\langle s_2 s_1^* \rangle}{\sqrt{\langle s_1 s_1^* \rangle \langle s_2 s_2^* \rangle}}$$

Is reduced by

- Temporal decorrelation
- Geometric decorrelation
- Atmosphere
- Noise

Interferometric Coherence for Image Interpretation

Backscatter image

coherence

Flevoland, NL

SAR Techniques: Interferometric Coherence

Fig. 33: Temporal Change of the surface (PALLAN o. J.:o. S.).

SAR Techniques: Interferometric Coherence

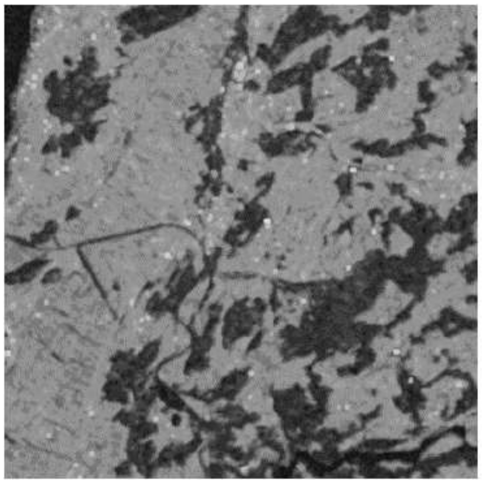

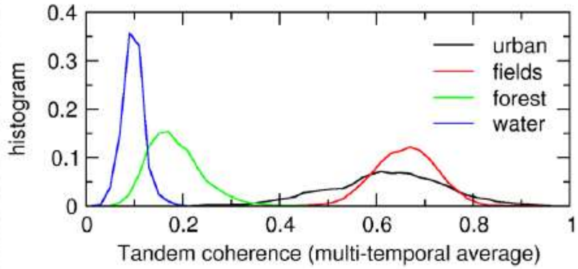

Histogram of averaged coherence
of main classes

ERS tandem

(1 day)

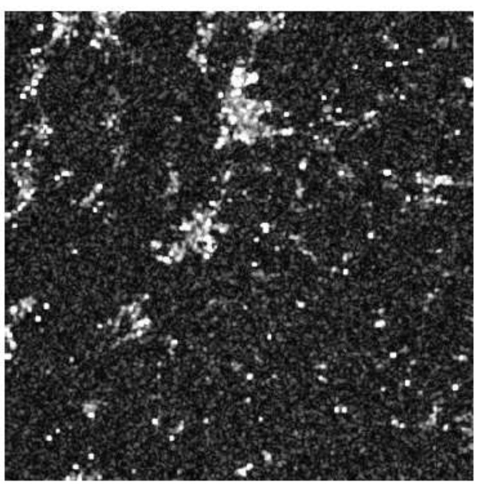

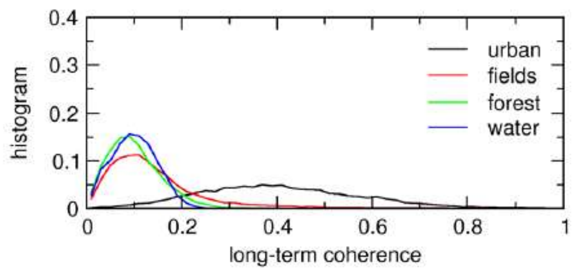

Histogram of long-time coherence
of main classes

ERS

long-term

(35 days)

Strozzi, T., InSAR Sommerschule 2002

SAR Techniques: Interferometry

Coherence and INSAR phase contain information on forest

- Interferometric Phase

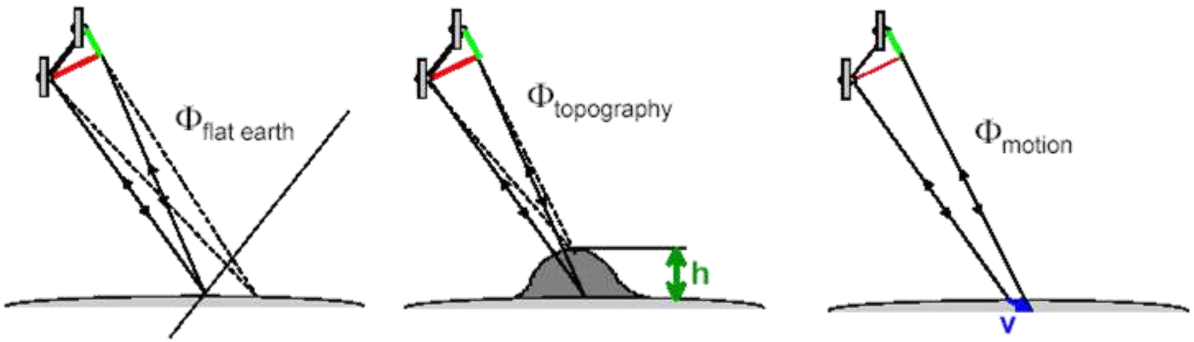

$$\Phi = \Phi_{flatearth} + \Phi_{topography} + \Phi_{motion} + \Phi_{atmosphere} + \Phi_{noise}$$

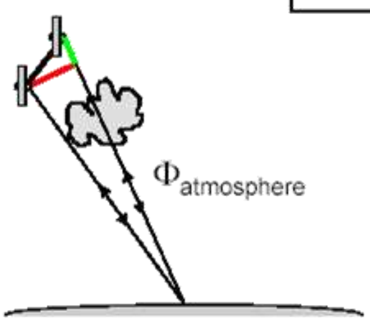

SAR Techniques: Interferometry

Coherence and INSAR phase contain information on forest

- Interferometric Phase

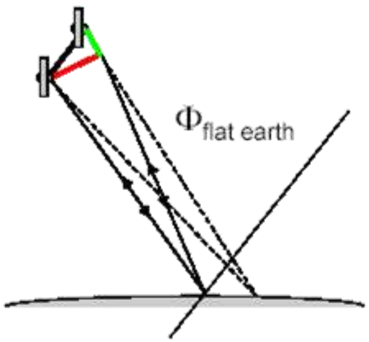

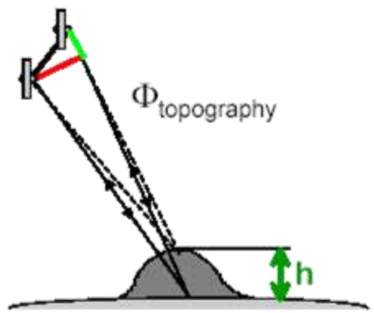

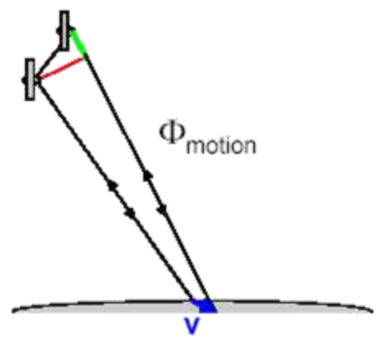

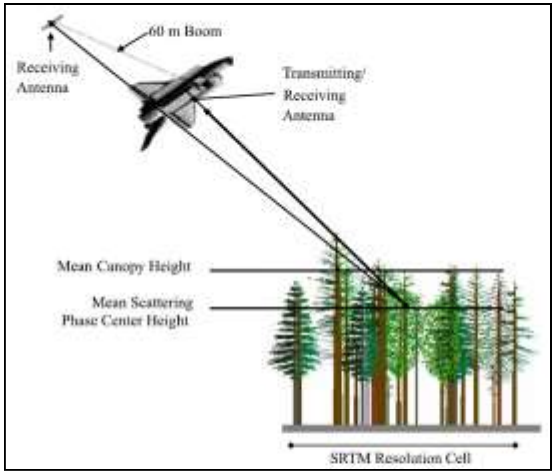

$$\Phi = \Phi_{\text{flatearth}} + \Phi_{\text{topography}} + \Phi_{\text{motion}} + \Phi_{\text{atmosphere}} + \Phi_{\text{noise}}$$

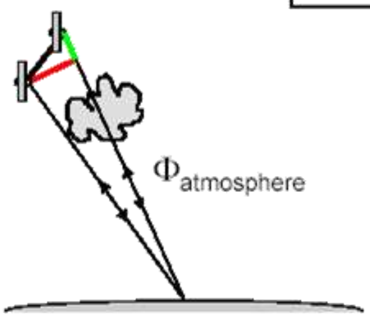

$$\Phi_{\text{flat earth}} = \frac{4\pi B_{\parallel}}{\lambda}$$

$$\Phi_{\text{topography}} \approx \frac{4\pi B_{\perp}}{\lambda} \frac{h}{r \sin\theta}$$

$$\Phi_{\text{motion}} = \frac{4\pi}{\lambda} \langle \mathbf{n}_{LOS} \cdot \mathbf{v} \Delta t \rangle$$

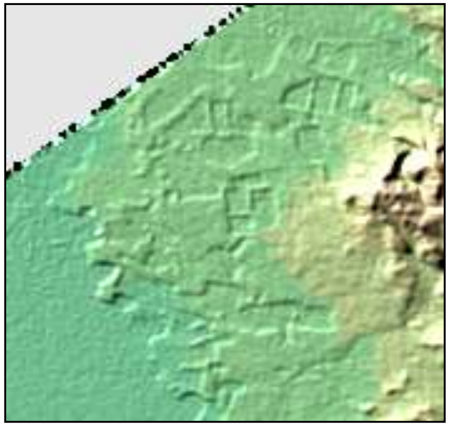

A complex SAR image can be decomposed into …

Amplitude and Phase

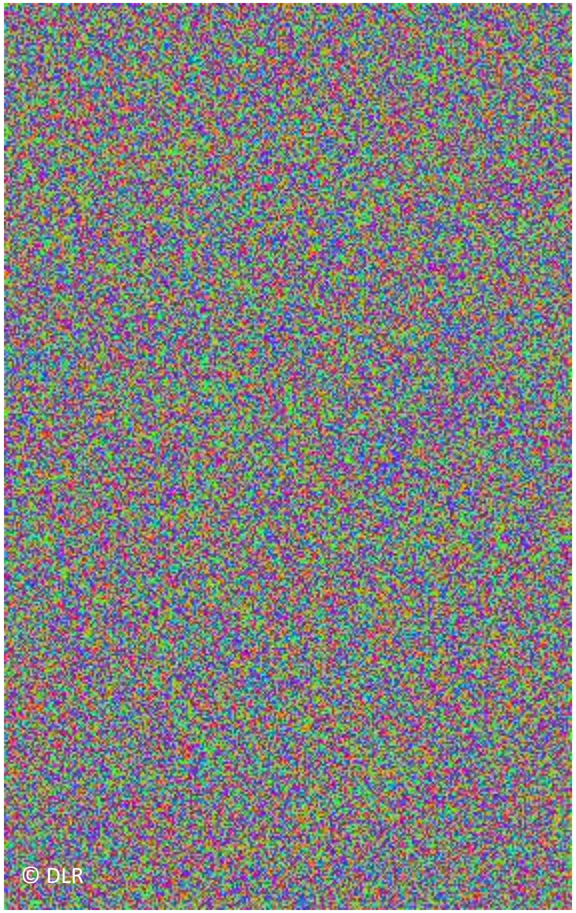

Phase Difference of Two SAR Images

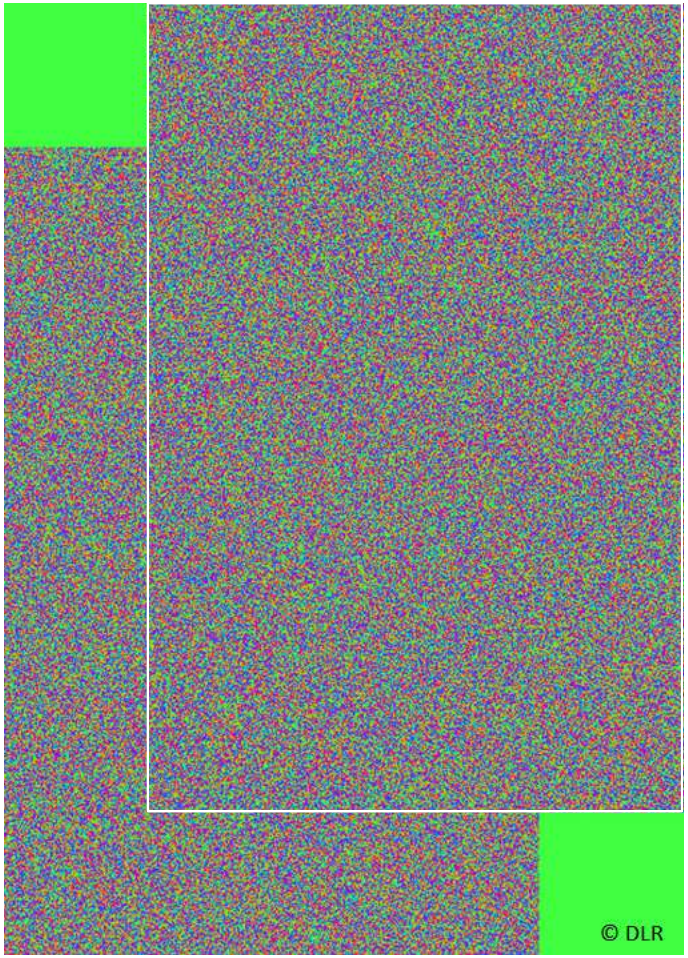

Phase in one SAR image looks random (→speckle effect!).
Only after accurate co-registraton the phase difference reveals the interferogram.

Phase Difference of Two SAR Images

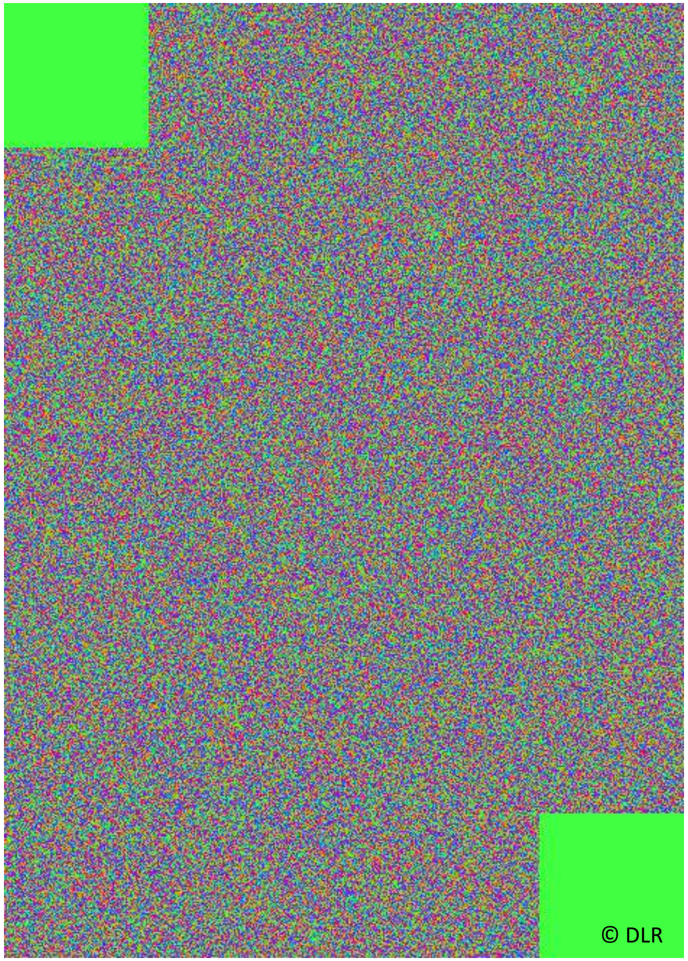

Phase in one SAR image looks random (→speckle effect!).
Only after accurate co-registraton the phase difference reveals the interferogram.

Phase Representation

- Phase is always ambiguous w.r.t. integer multiples of 2π
- → phase unwrapping required!

- pictorial representation of phase:
  - grey value
  - color wheel

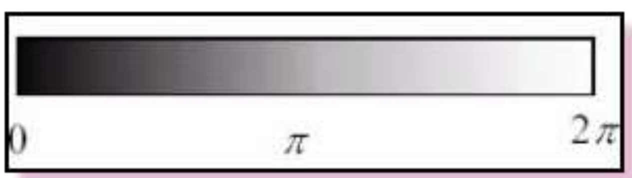

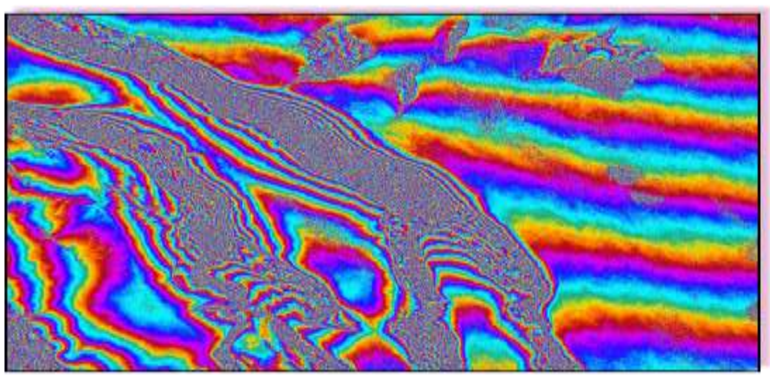

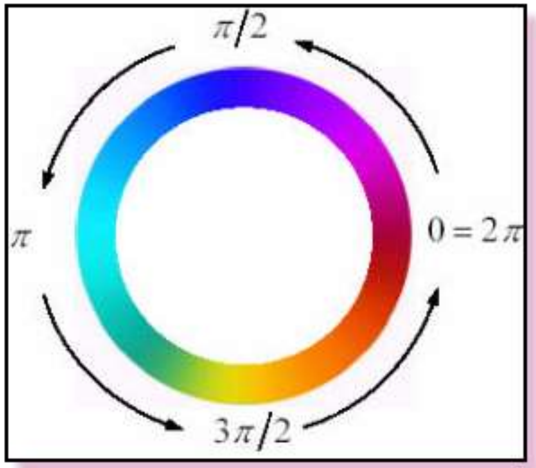

Interferometric phase

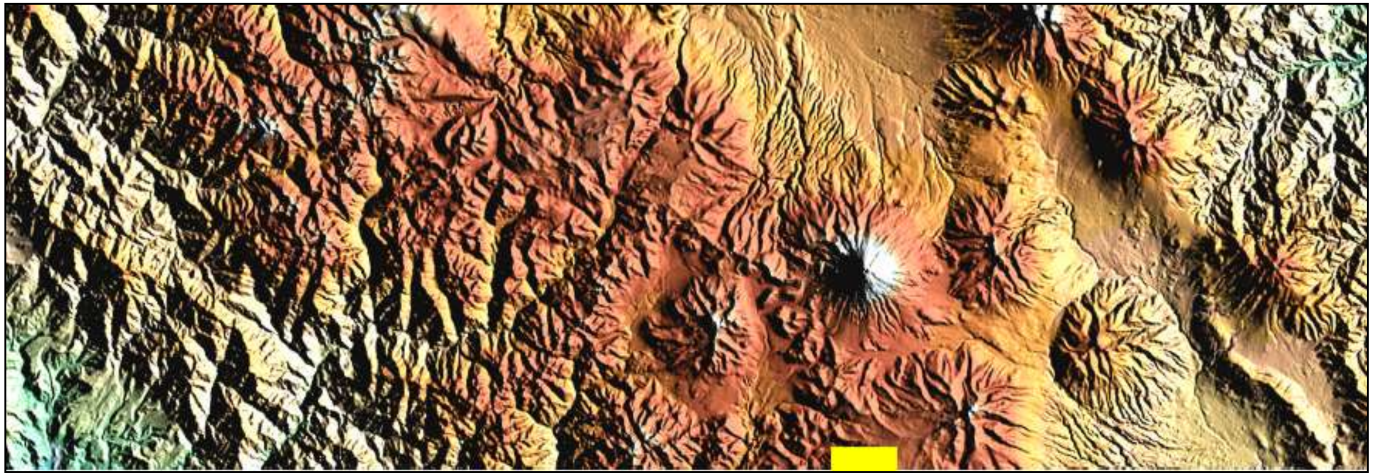

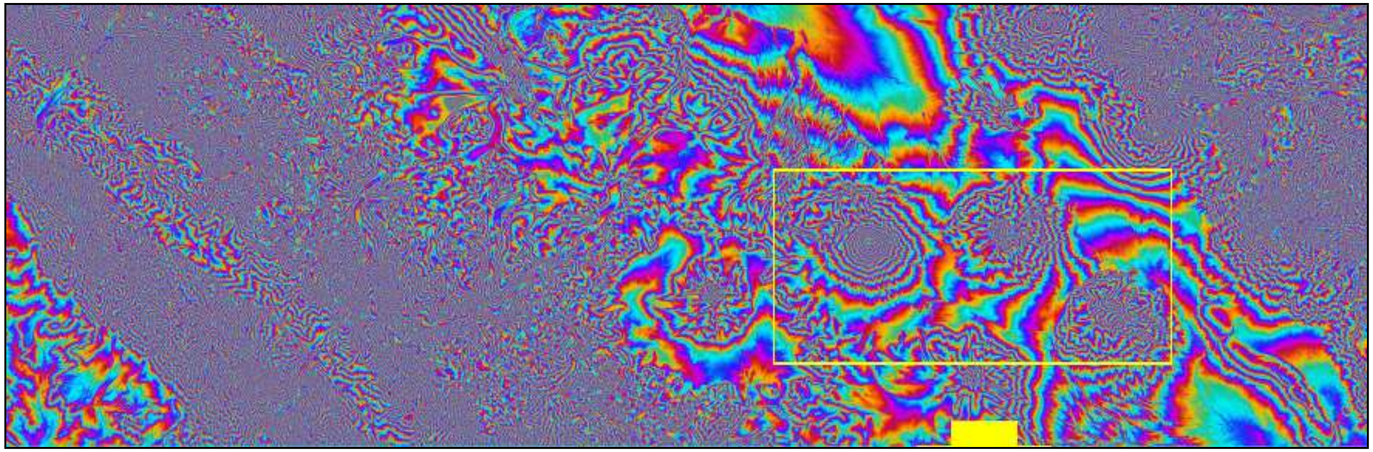

Cotopaxi volcano

Ecuador

(SRTM/X-SAR)

Interferometric Sensitivity as a Function of Wavelength

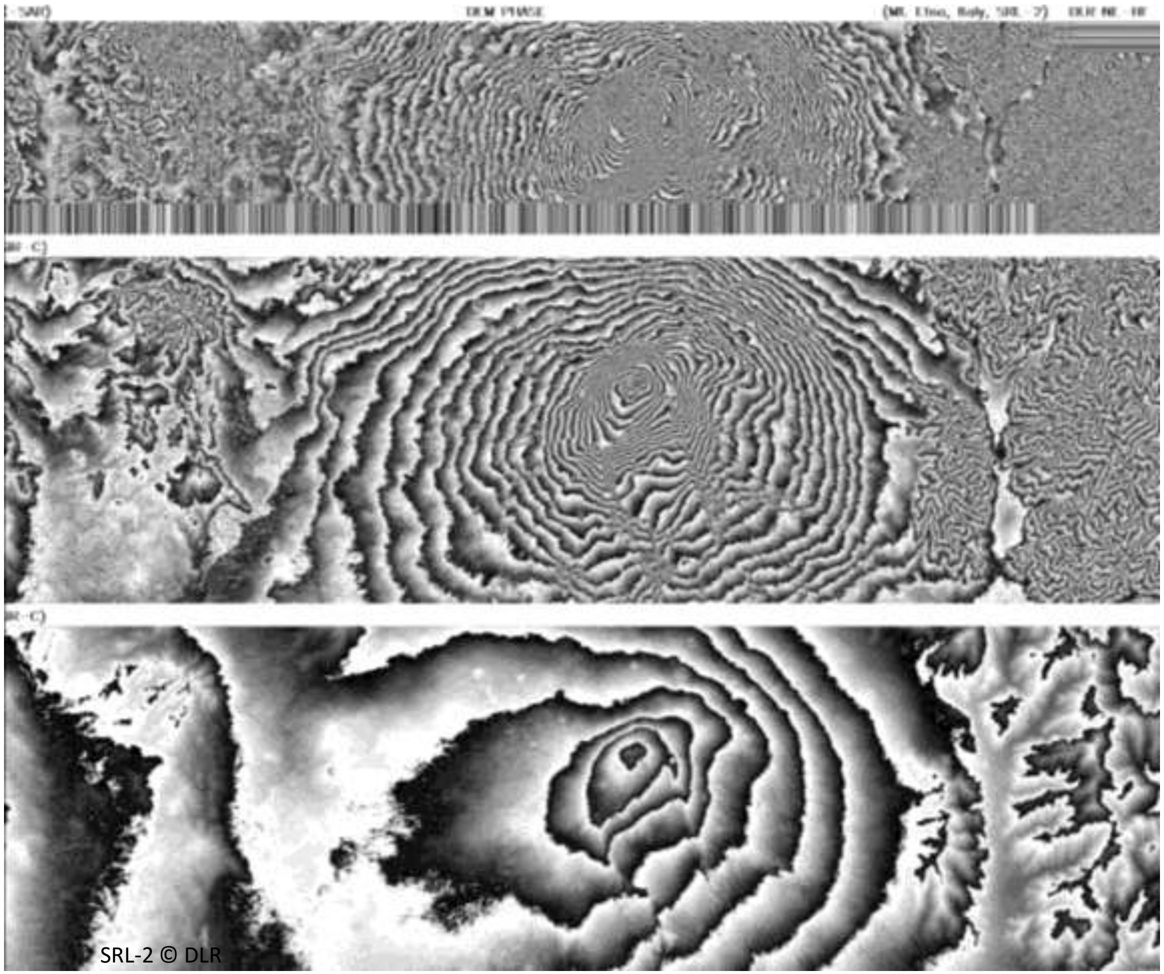

X-band

C-band

L-band

Mt. Etna
data: SRL-2

Dual-Pass vs. Single-Pass interferometry

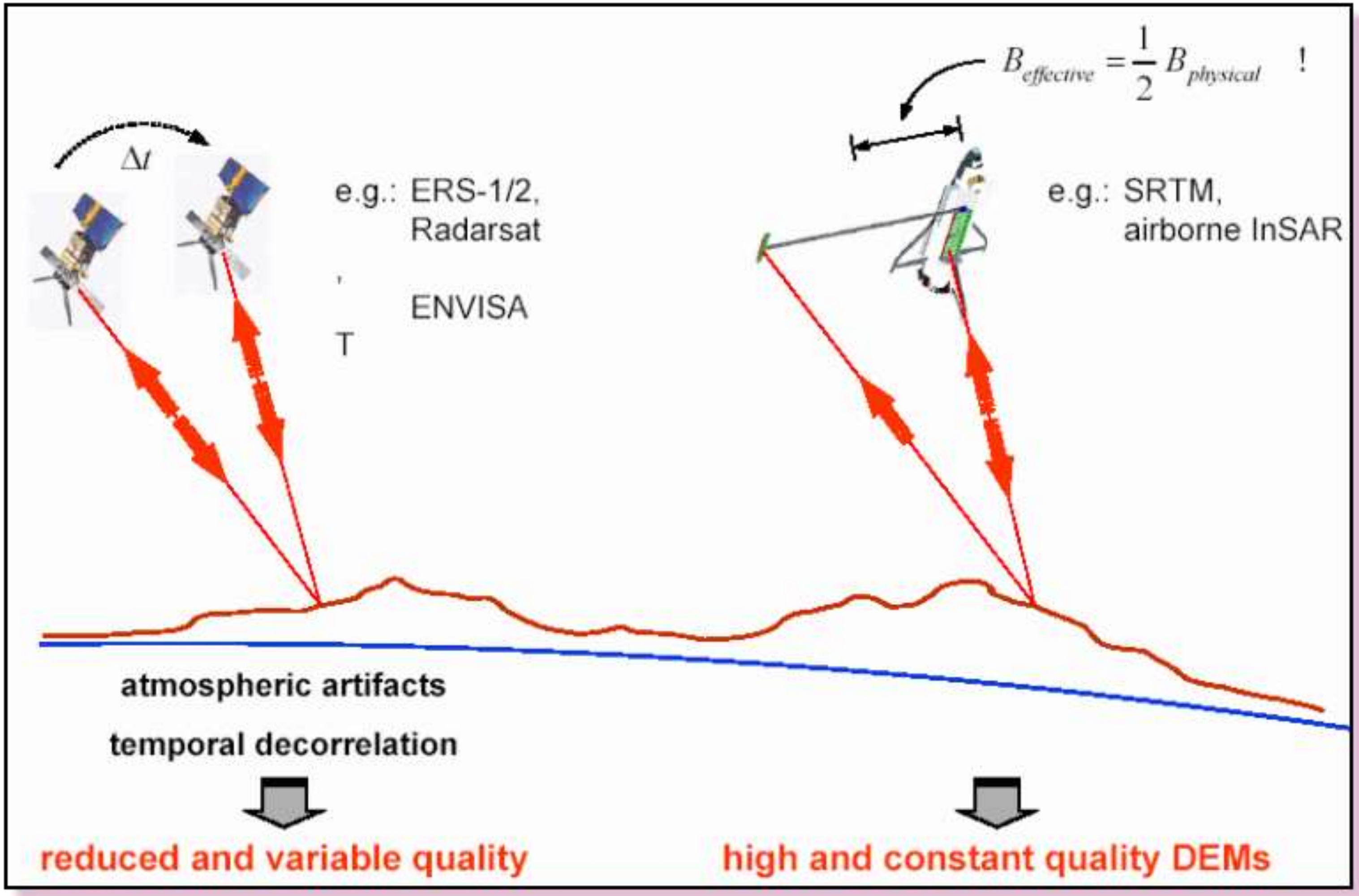

Interferometric Phase Error Sources

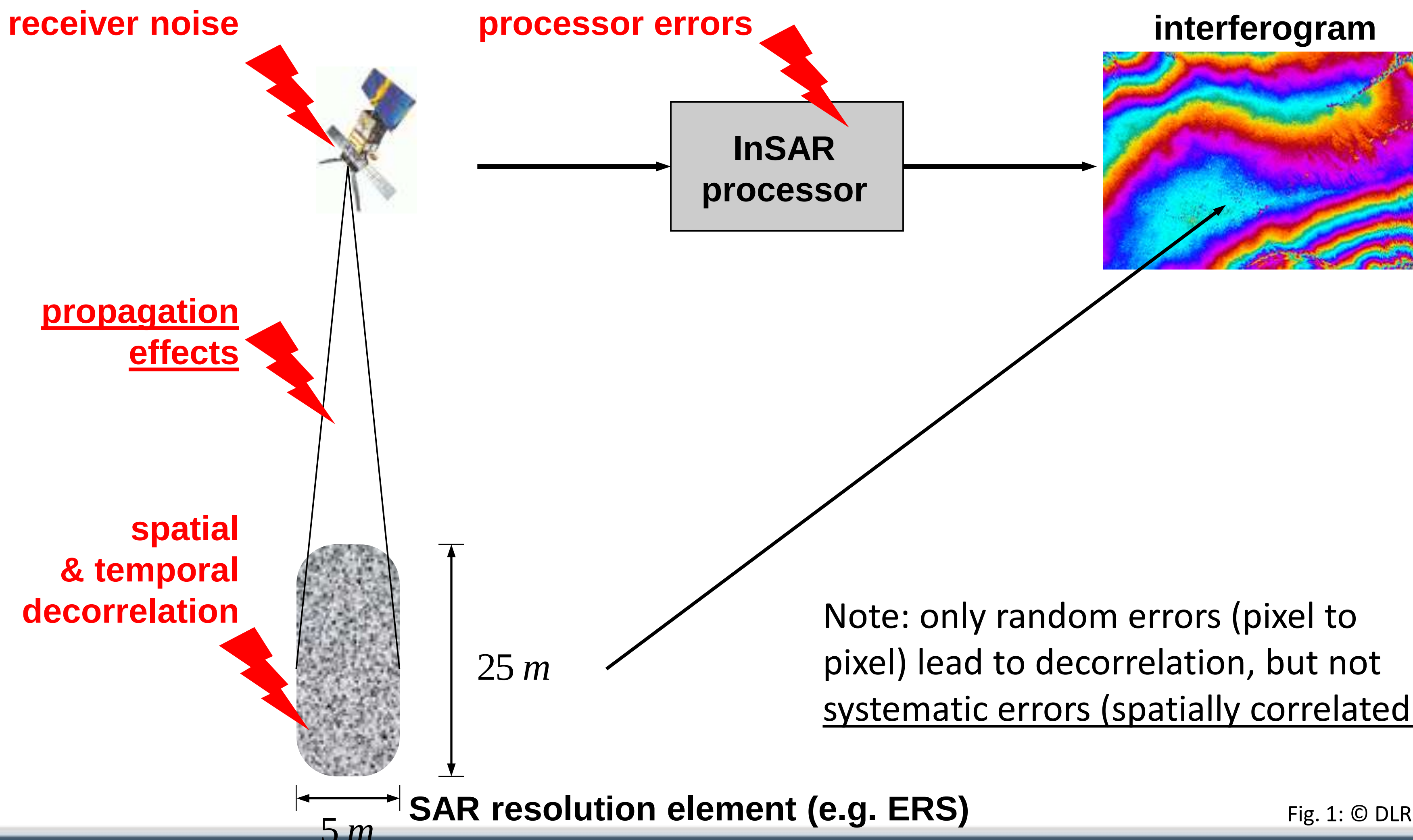

Note: only random errors (pixel to pixel) lead to decorrelation, but not systematic errors (spatially correlated)

Fig. 1: © DLR

Coherence and InSAR phase

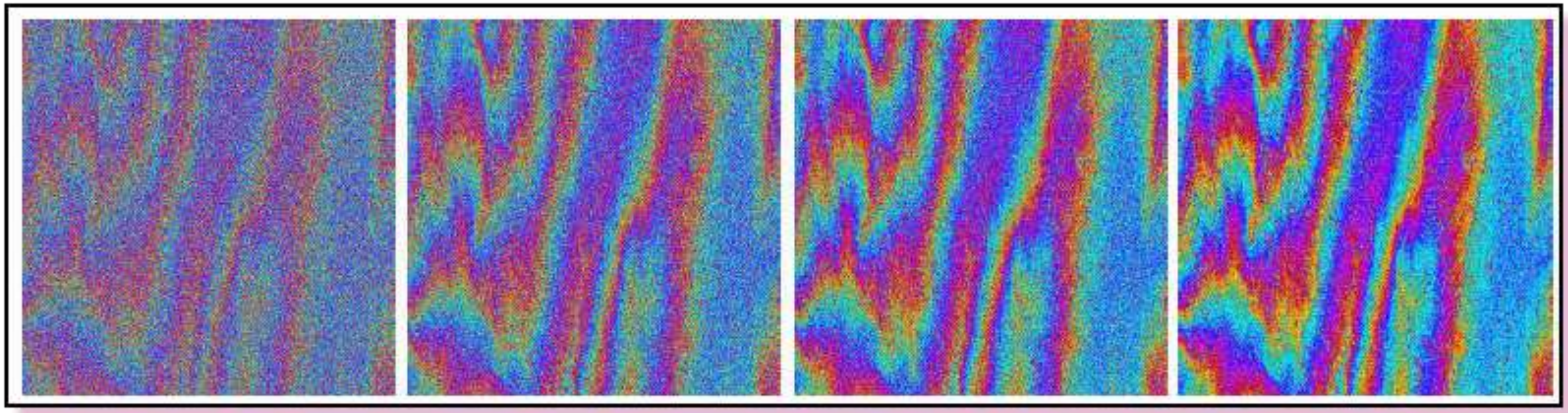

$|\gamma| = 0{,}28$ $|\gamma| = 0{,}5$ $|\gamma| = 0{,}65$ $|\gamma| = 0{,}82$

[MFFU Sommerschule 2000]

Forest Height based on EO Data

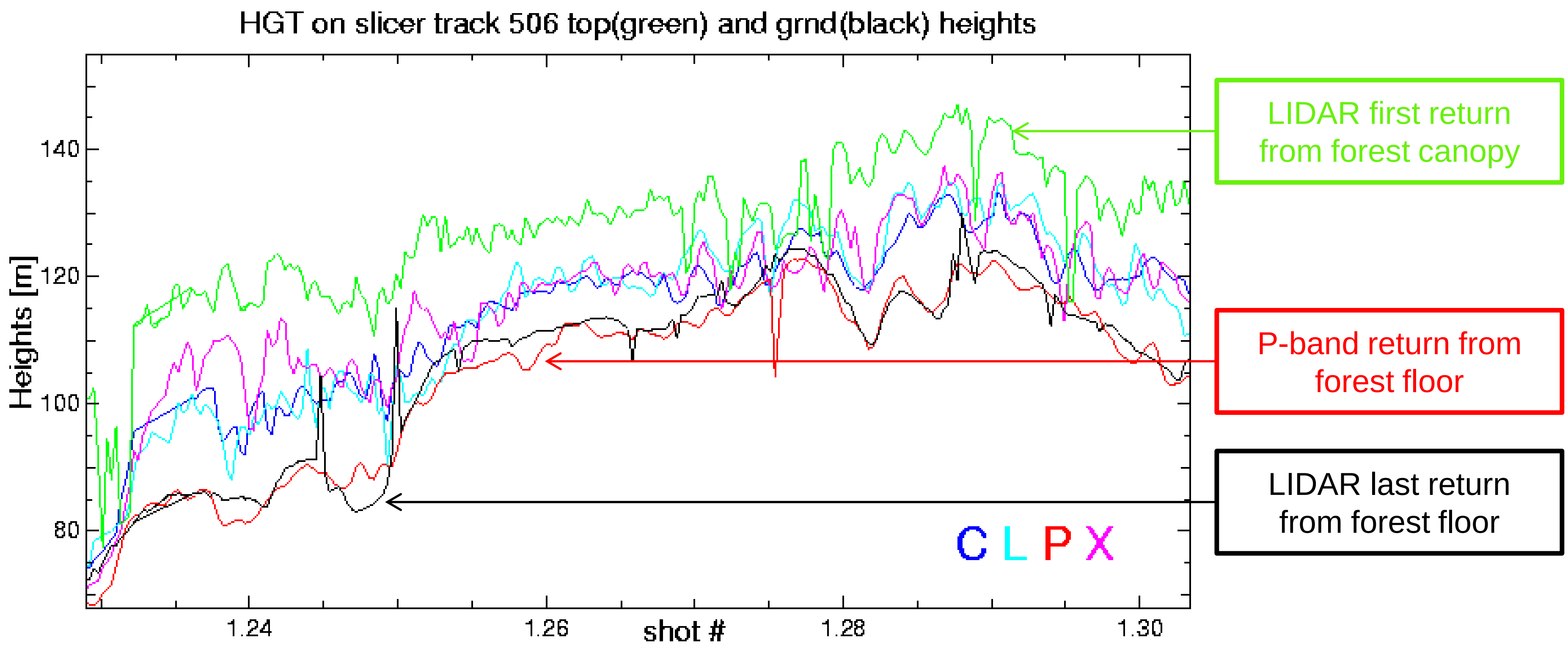

(Woodhouse; Data from Sassan Saatchi, JPL).

Forest Height based on EO Data

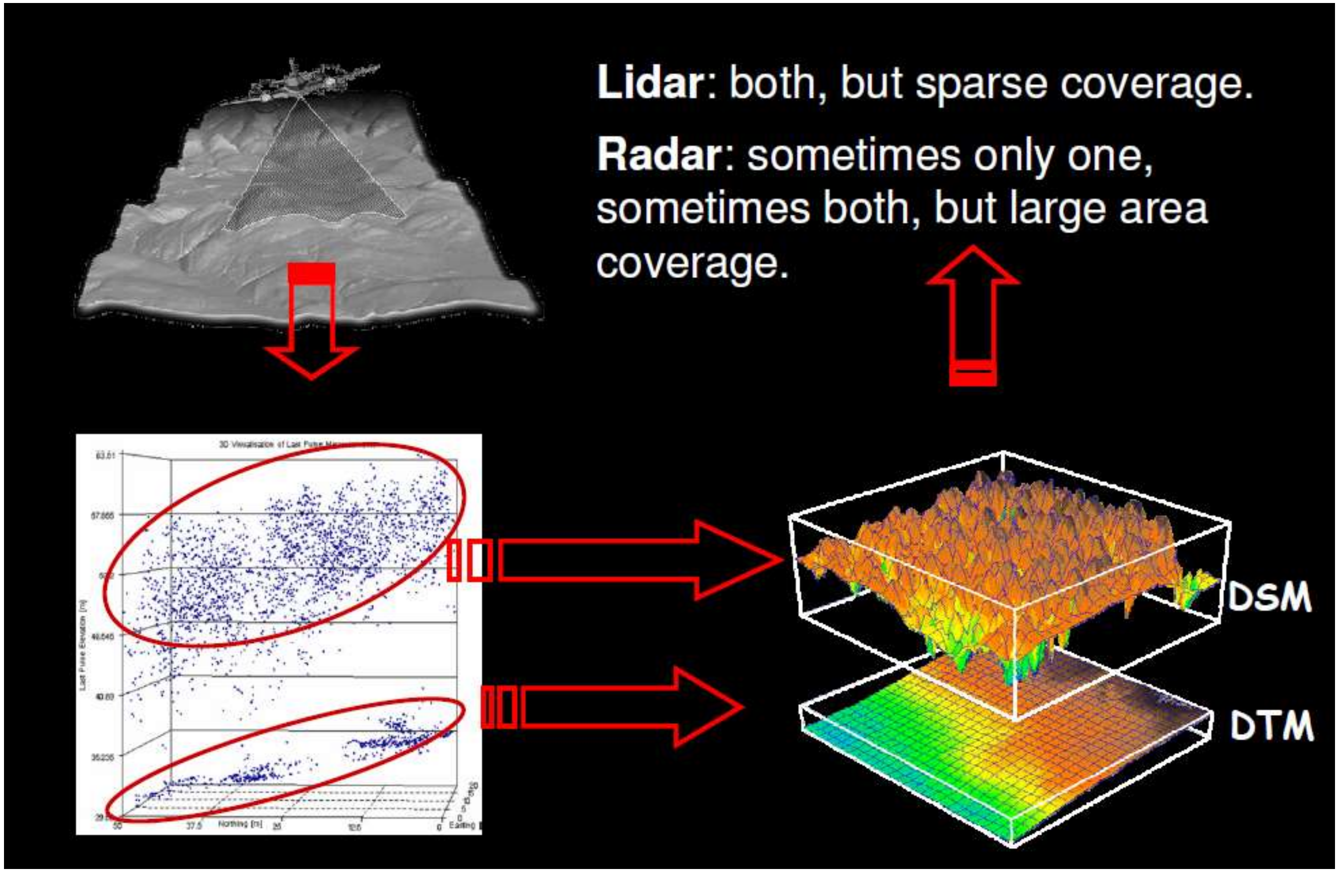

1 - Forest Height
↓
2 - Conversion
↓
3 - Forest Biomass

(Woodhouse)

SAR Techniques

1. Backscatter analysis (wavelength, polarisation, incidence angle, number of images)
2. Interferometry: Coherence analysis (wavelength, polarisation, incidence angle, temporal and spatial baseline, number of images, acquisition conditions)
3. Interferometry: Phase analysis (wavelength, incidence angle, high coherence required, acquisition conditions)
4. Polarimetry (wavelength, incidence angle, number of images)
5. Polarimetric Interferometry (wavelength, polarisation, incidence angle, temporal and spatial baseline)
6. SAR (Polarimetric) Tomography (wavelength, polarisation, incidence angle, spatial baseline, high coherence required, number of images)

SAR Techniques: Interferometry vs. Polarimetry

The Phase is essential for **Interferometry** and **Polarimetry**

- Both techniques require at least two complex SAR images

A) Same polarisation – different position

B) Same position – different polarisation

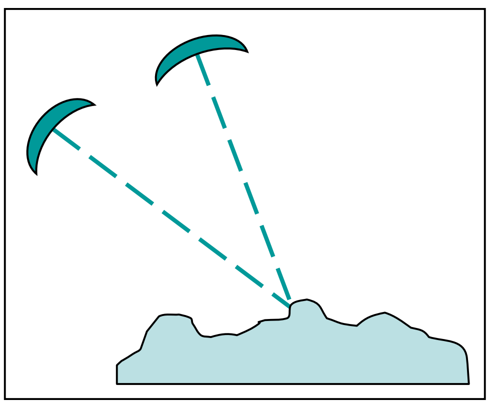

Interferometry

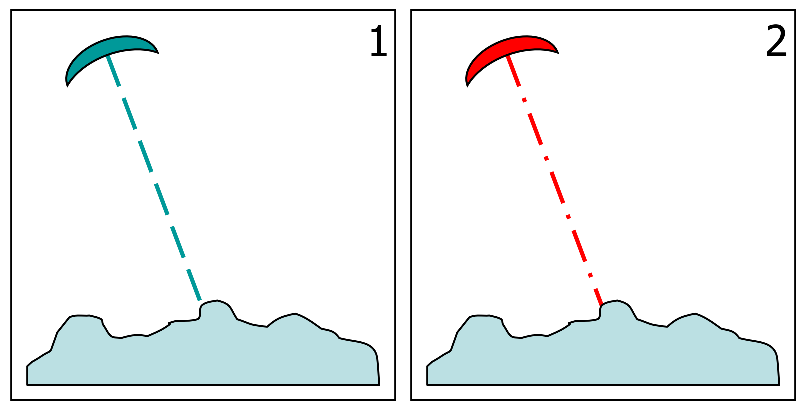

Polarimetry

Motivation for Radar Polarimetry in Remote Sensing

Polarimetric Radar Parameters ⟷ Modeling ⟷ **Geo-/Biophysical Parameters**

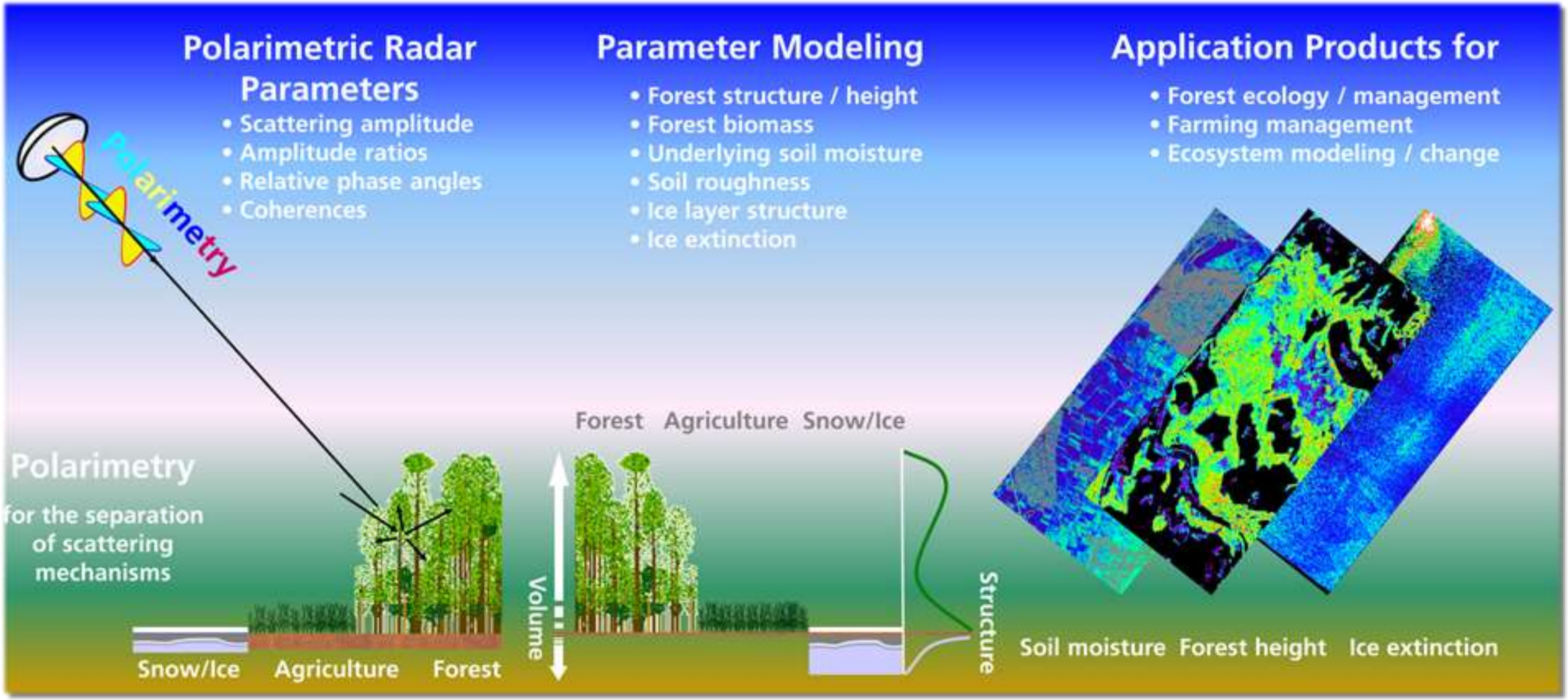

From Linear to Circular polarized EM Waves…

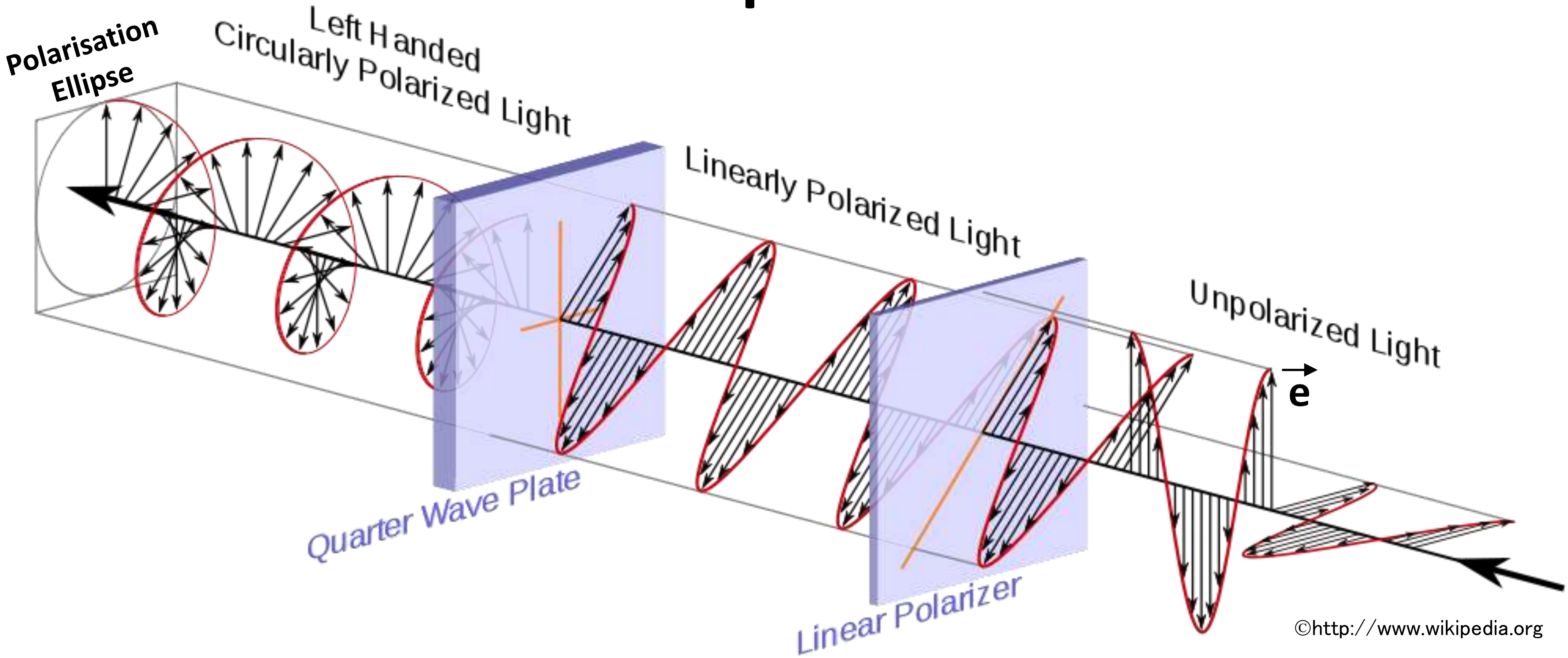

For all vector waves polarisation refers to the behaviour in time of the [electric] wave field vector … observed at a fixed point in space.

(Azzam & Bashara, 1977)

⇨ **Electric field vector $\vec{e}$ forms an ellipse with time**

Scattering Images L-band

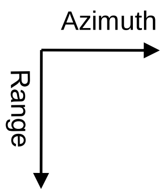

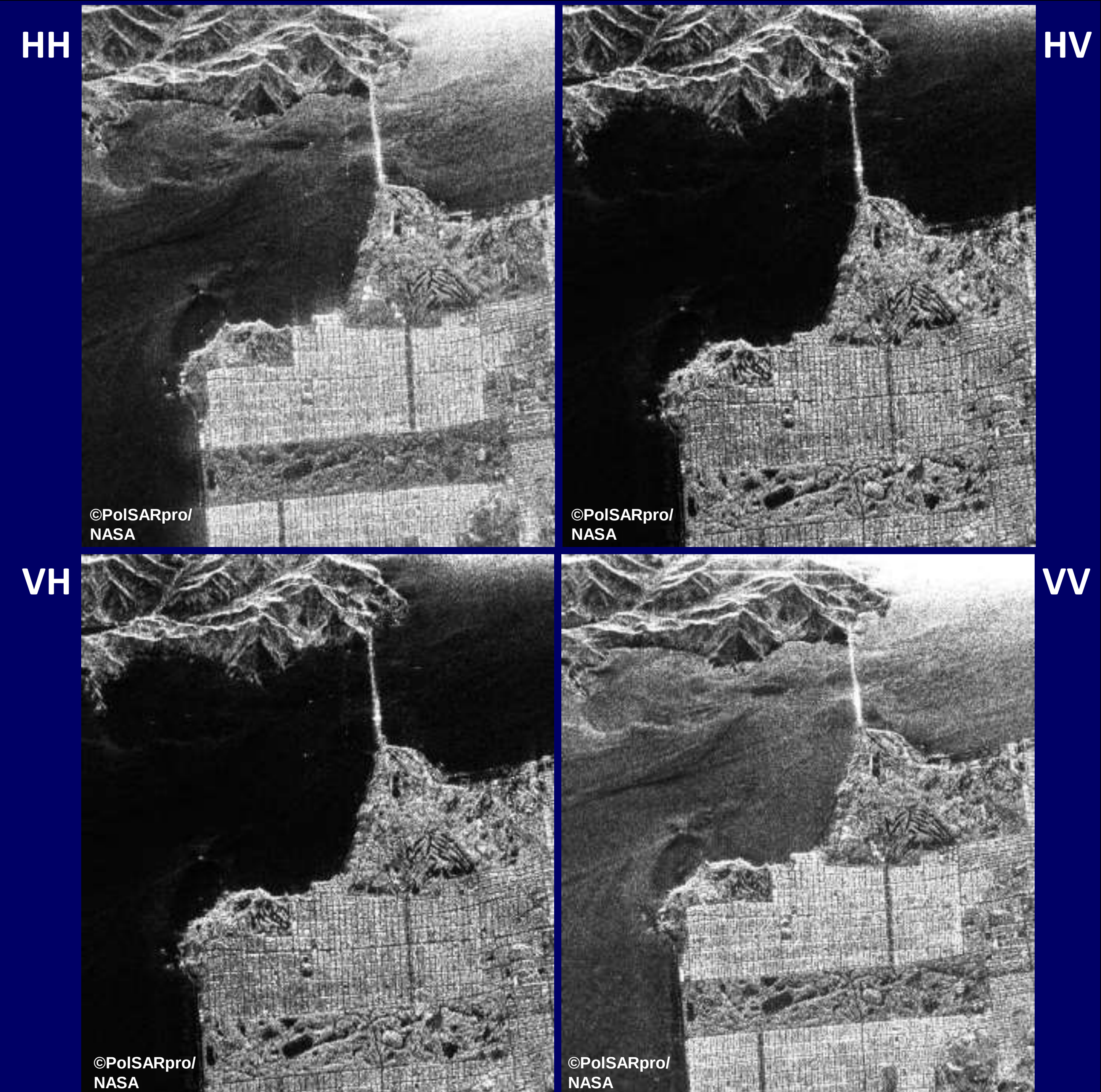

Decomposition Theorems

[S]

Coherent Decomposition

W. Pauli
(1900-1958)

E. Krogager
(1990)

W.L. Cameron
(1990)

[K]

Target Dichtonomy

J.R. Huynen
(1970)

R.M. Barnes
(1988)

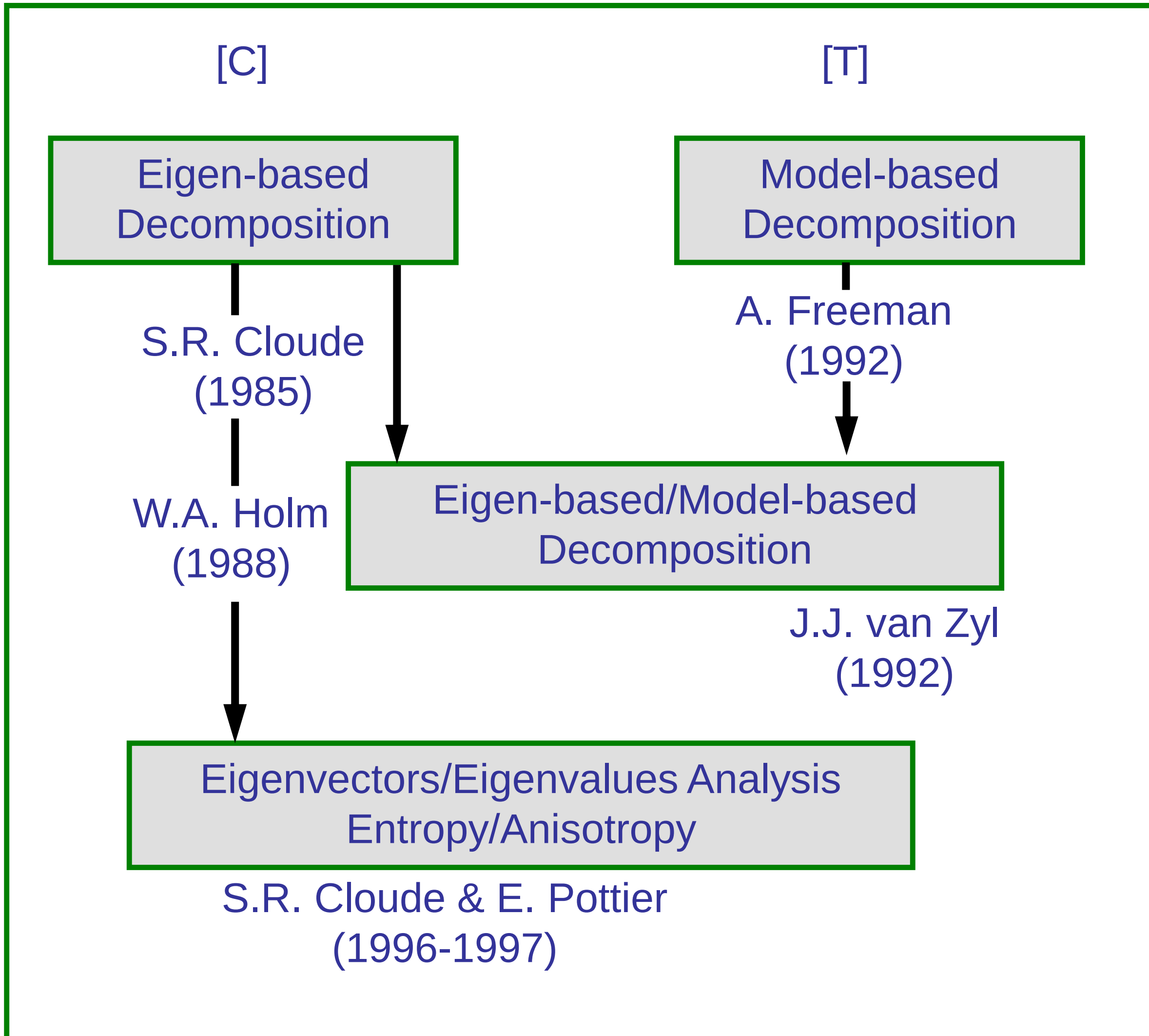

Pauli Decomposition

$$[S]=\begin{bmatrix} S_{HH} & S_{HV} \\ S_{VH} & S_{VV} \end{bmatrix}=\begin{bmatrix} a+b & c-id \\ c+id & a-b \end{bmatrix}$$

$$=\frac{a}{\sqrt{2}}\begin{bmatrix} 1 & 0 \\ 0 & 1 \end{bmatrix}+\frac{b}{\sqrt{2}}\begin{bmatrix} 1 & 0 \\ 0 & -1 \end{bmatrix}+\frac{c}{\sqrt{2}}\begin{bmatrix} 0 & 1 \\ 1 & 0 \end{bmatrix}+\frac{d}{\sqrt{2}}\begin{bmatrix} 0 & -i \\ i & 0 \end{bmatrix}$$

Single or odd-bounce scattering

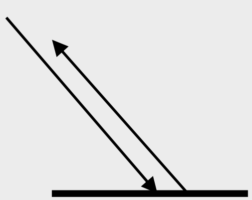

$a = 2^{-0.5} S_{HH} + S_{VV}$

Dihedral or even-bounce scattering

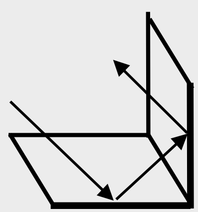

$b = 2^{-0.5} S_{HH} - S_{VV}$

Dihedral or even-bounce scattering rotated by π/4

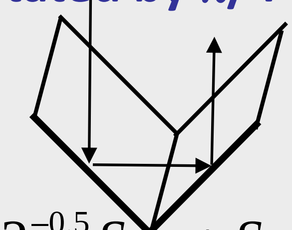

$c = 2^{-0.5} S_{HV} + S_{VH}$

Transformation in orthogonal polarisation state (only in bistatic)

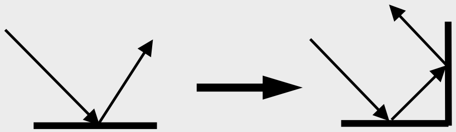

$d = 2^{-0.5} i\left(S_{HV} - S_{VH}\right)$

SAR Techniques: Polarimetry

- Investigation backscatter at different polarisations
- Computation of polarimetric parameters

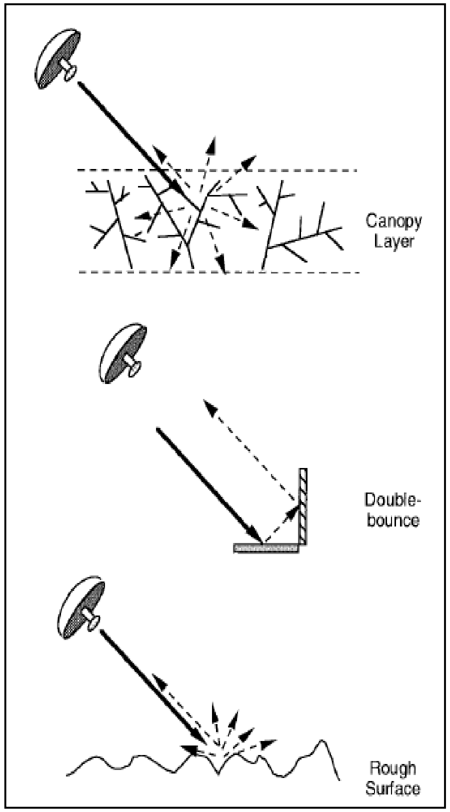

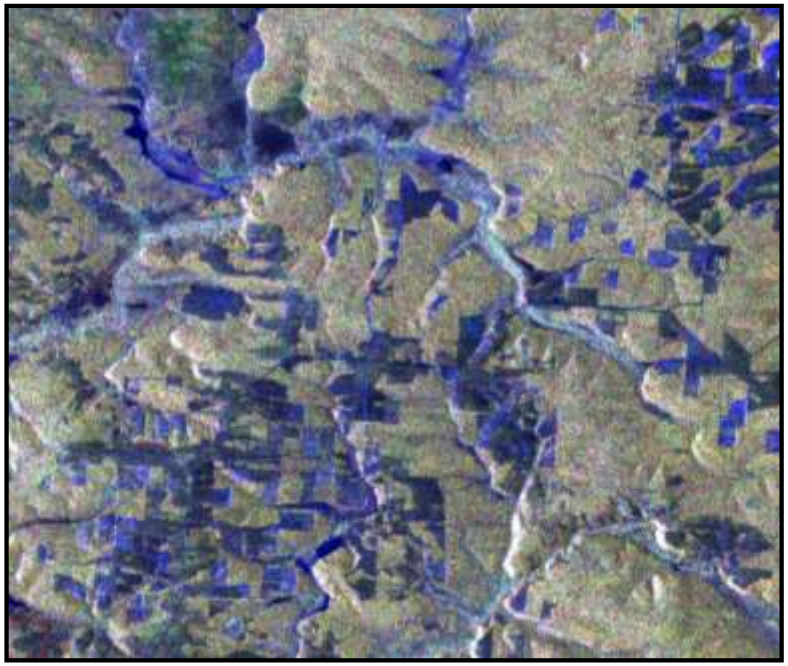

Pauli – Decomposition

$S_{HH} + S_{VV}$	Surface Scattering
$S_{HH} - S_{VV}$	Double Bounce
$2S_{HV}$	Volume Scattering

RGB-Composite of Polarisations to Identify Different Scatterers

Cities

Forests

Rivers

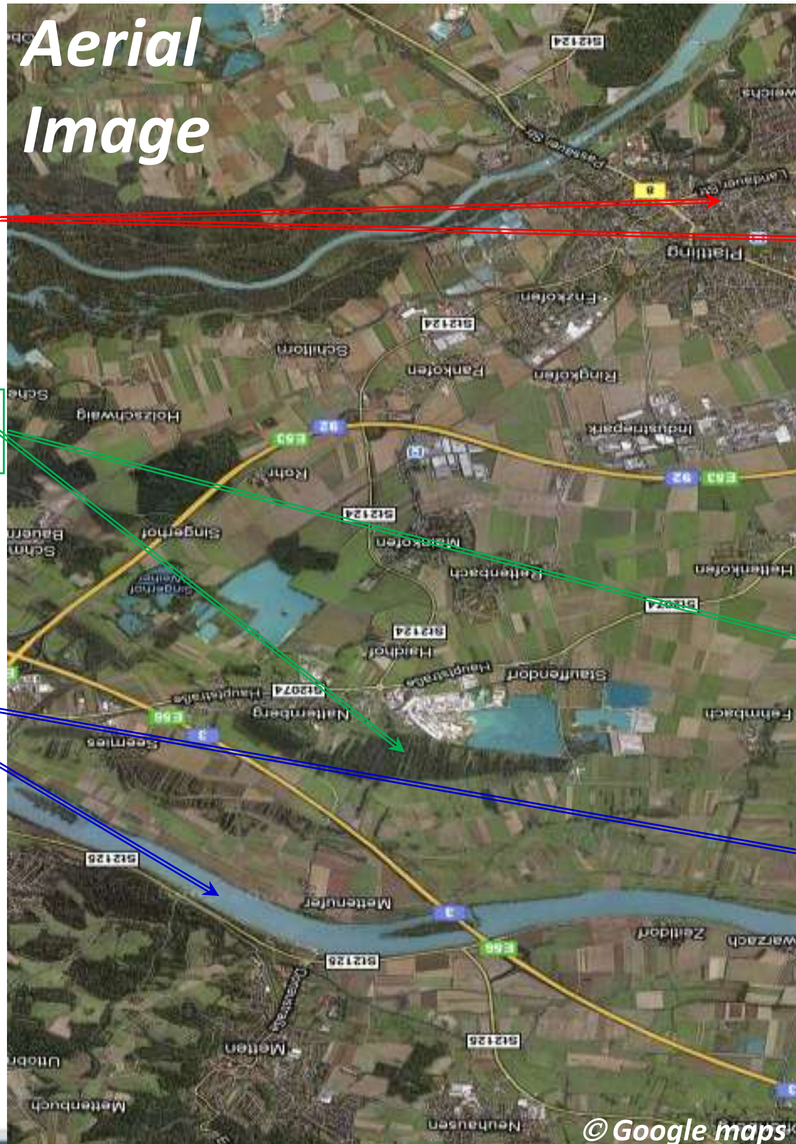

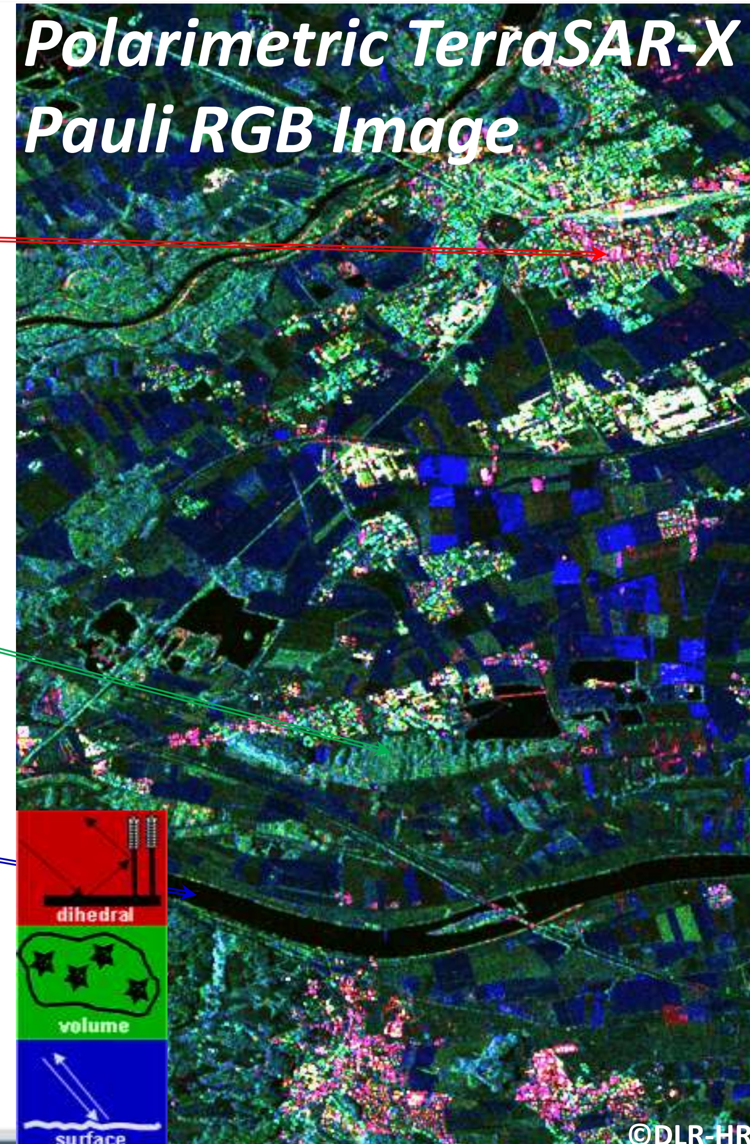

RadarSAT-2 – Fine Quad Pol Mode – San Francisco

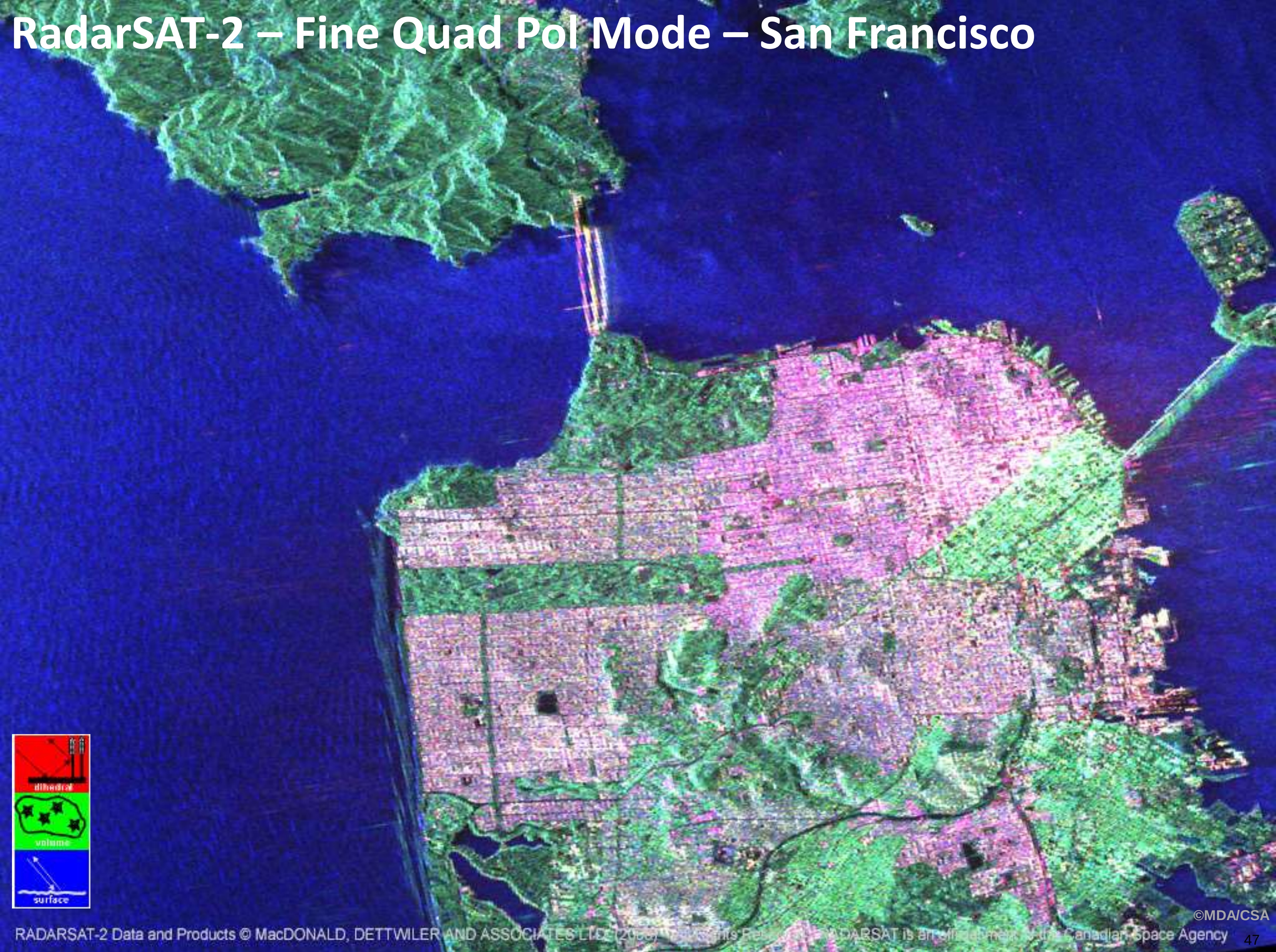

SAR Techniques: Polarimetric Interferometry

- Height localisation of different scattering mechanism
- Requires coherent interferometric pair of polarimetric data

A) Same polarisation – different position

B) Same position – different polarisation

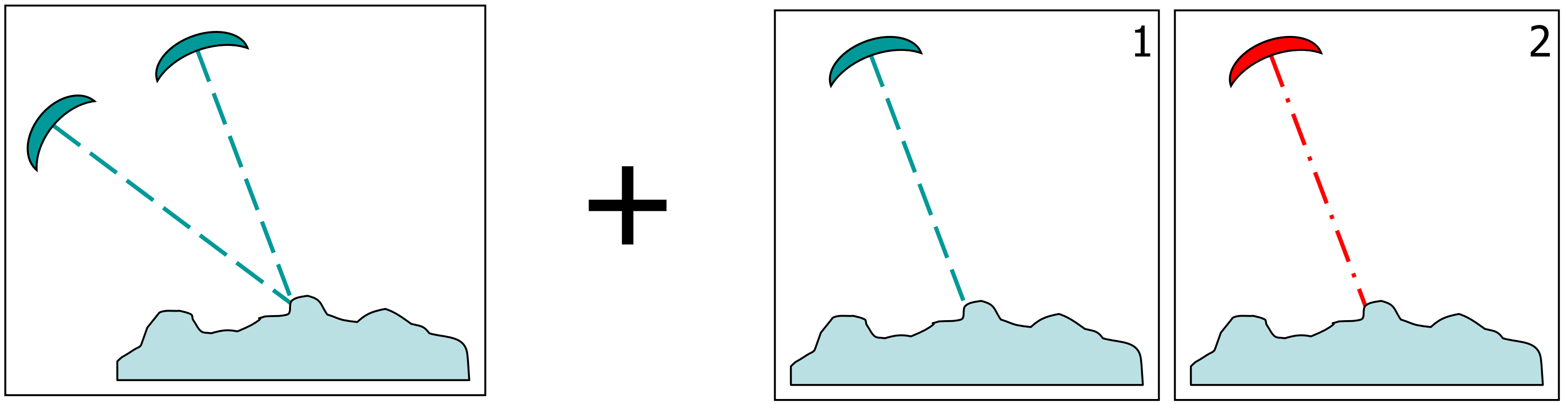

Interferometry

Polarimetry

Tree height from POLINSAR

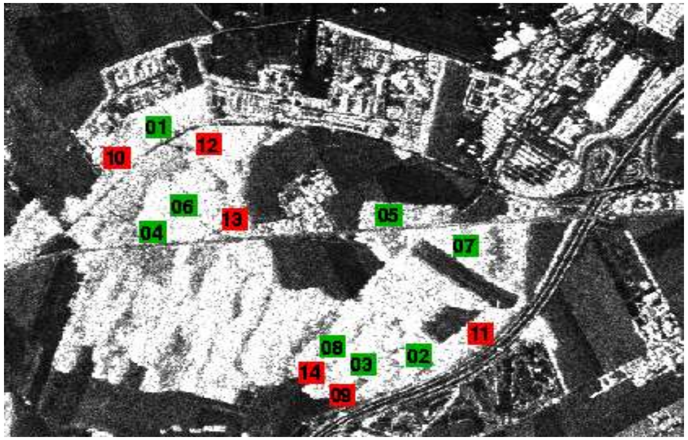

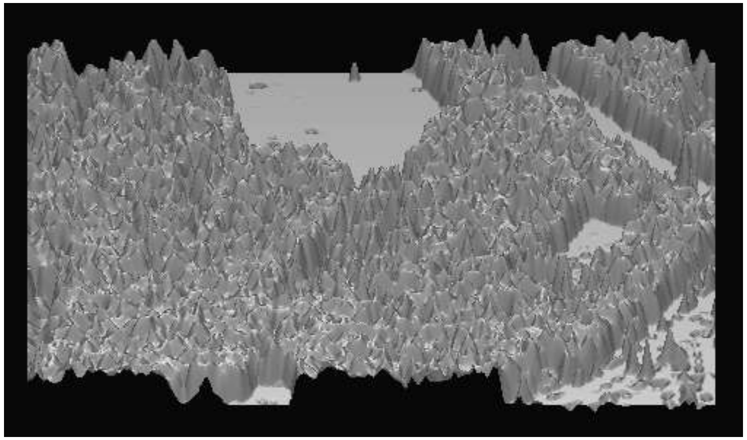

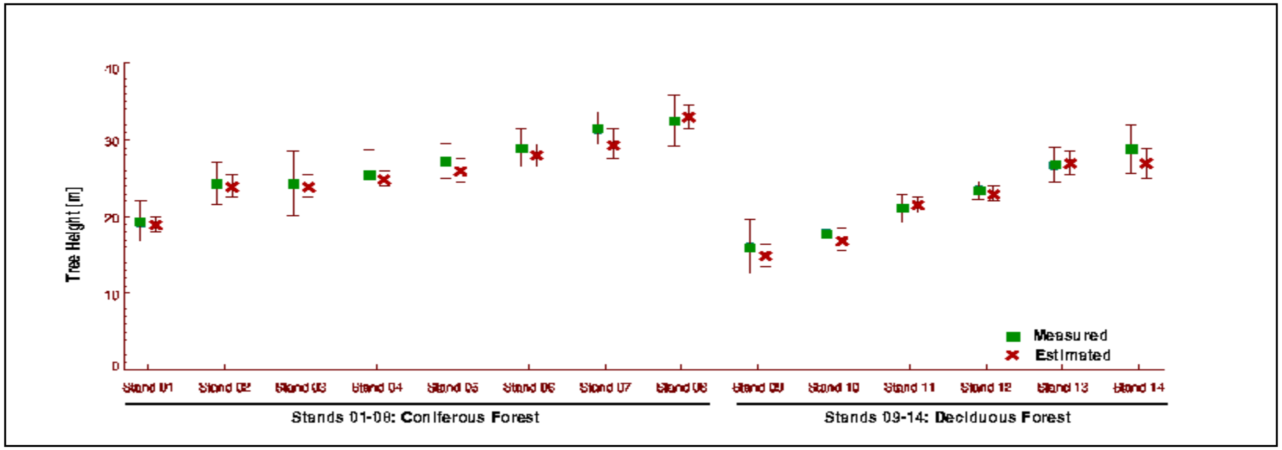

Airfield Oberpfaffenhofen
L-Band pol. InSAR result

Tree height

Konstantinos Papathanassiou et al. (DLR)

Tree height from POLINSAR

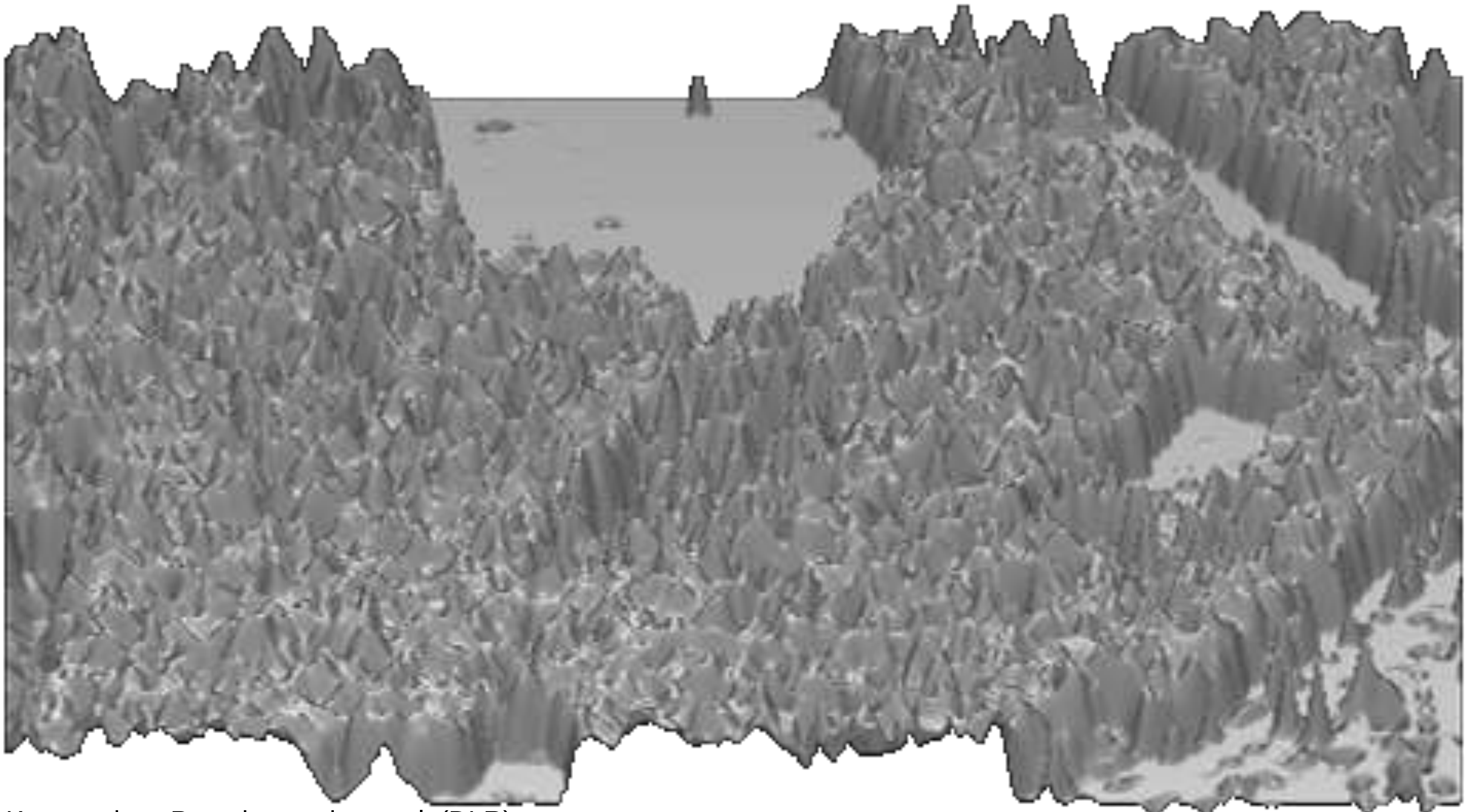

Konstantinos Papathanassiou et al. (DLR)

SAR Techniques: (Polarimetric) SAR Tomography

- Horizontal information on backscatter intensity (and backscattering mechanism)
- Requires many coherent interferometric SAR images

A) Same polarisation – many different positions

B) Same position – different polarisation

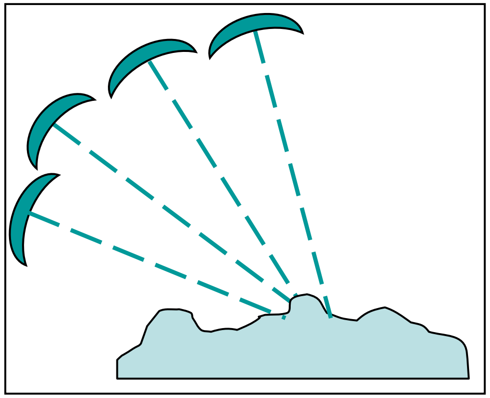

Interferometry

+

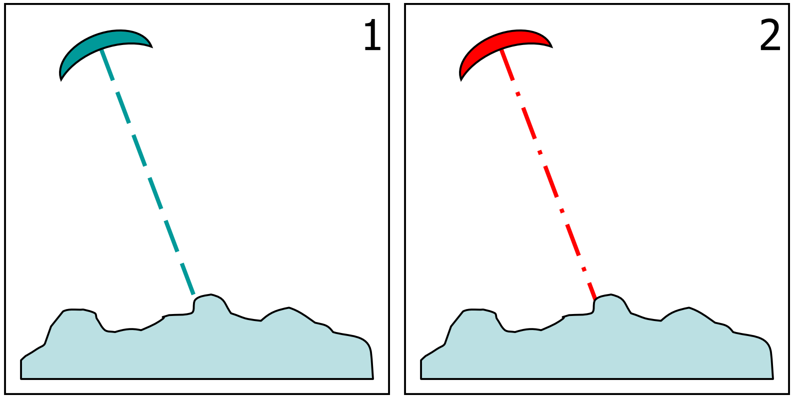

Polarimetry

SAR Polarimetric Tomography

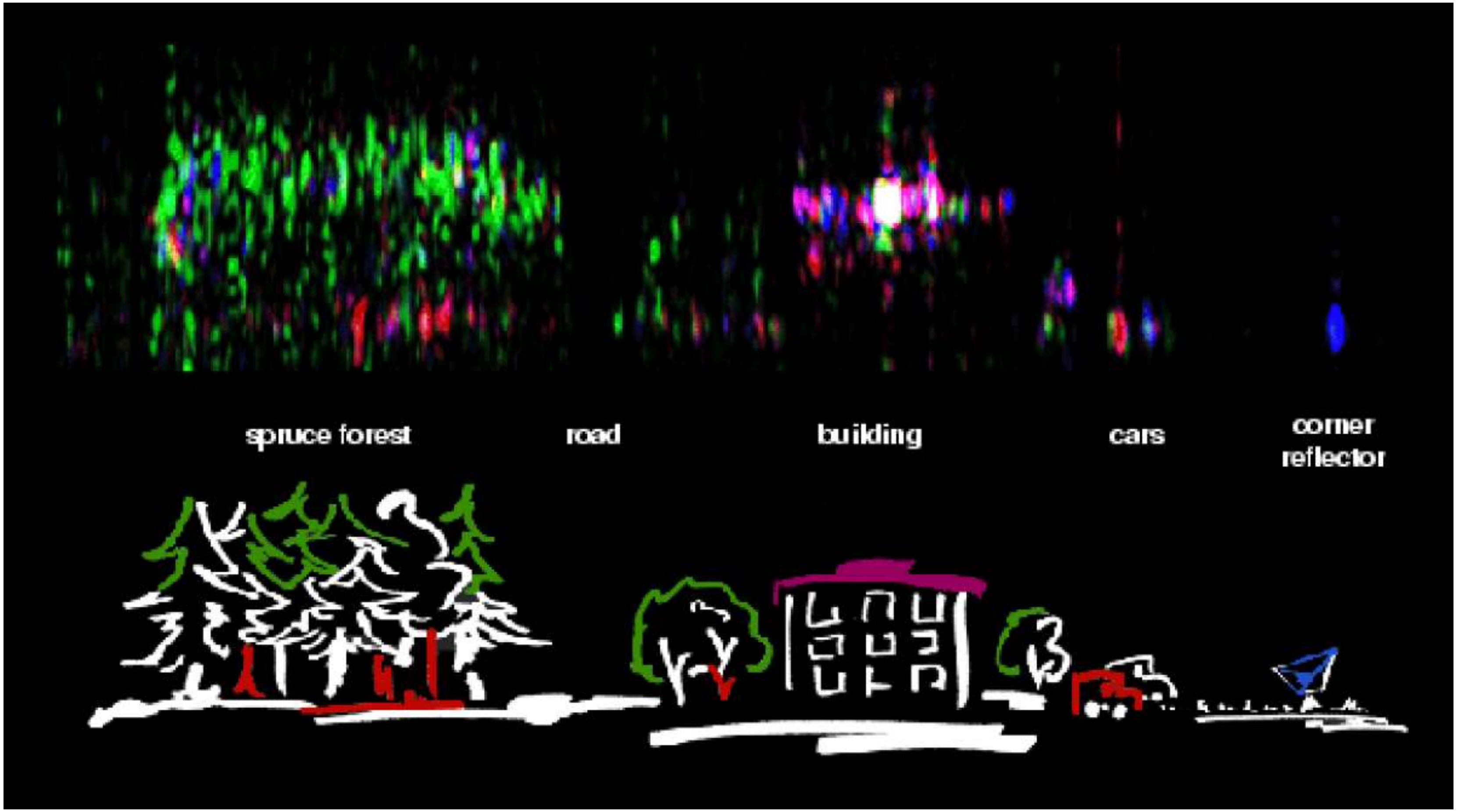

Andreas Reigber - Dissertation

SAR Polarimetric Tomography

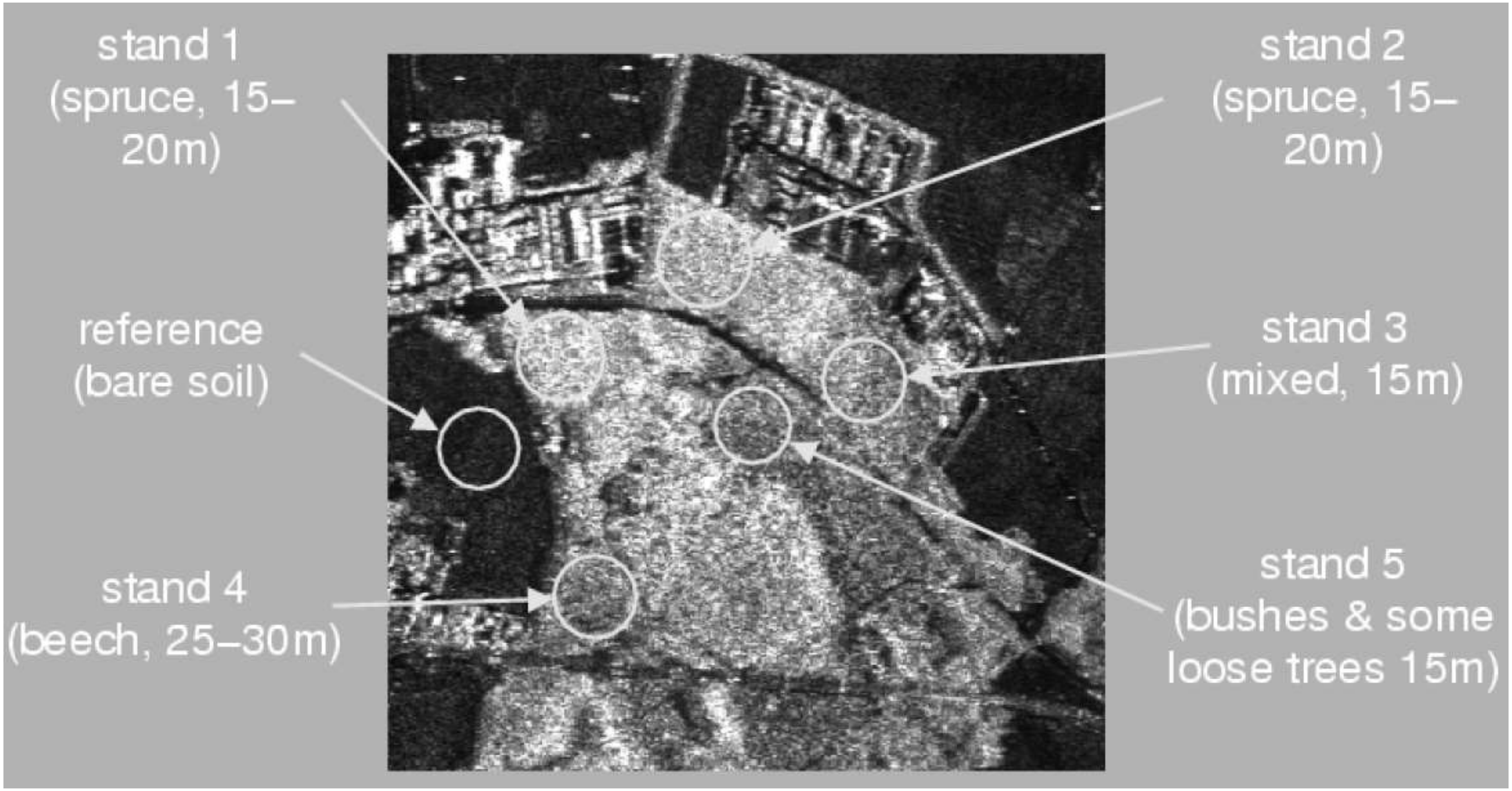

Andreas Reigber - Dissertation

SAR Polarimetric Tomography

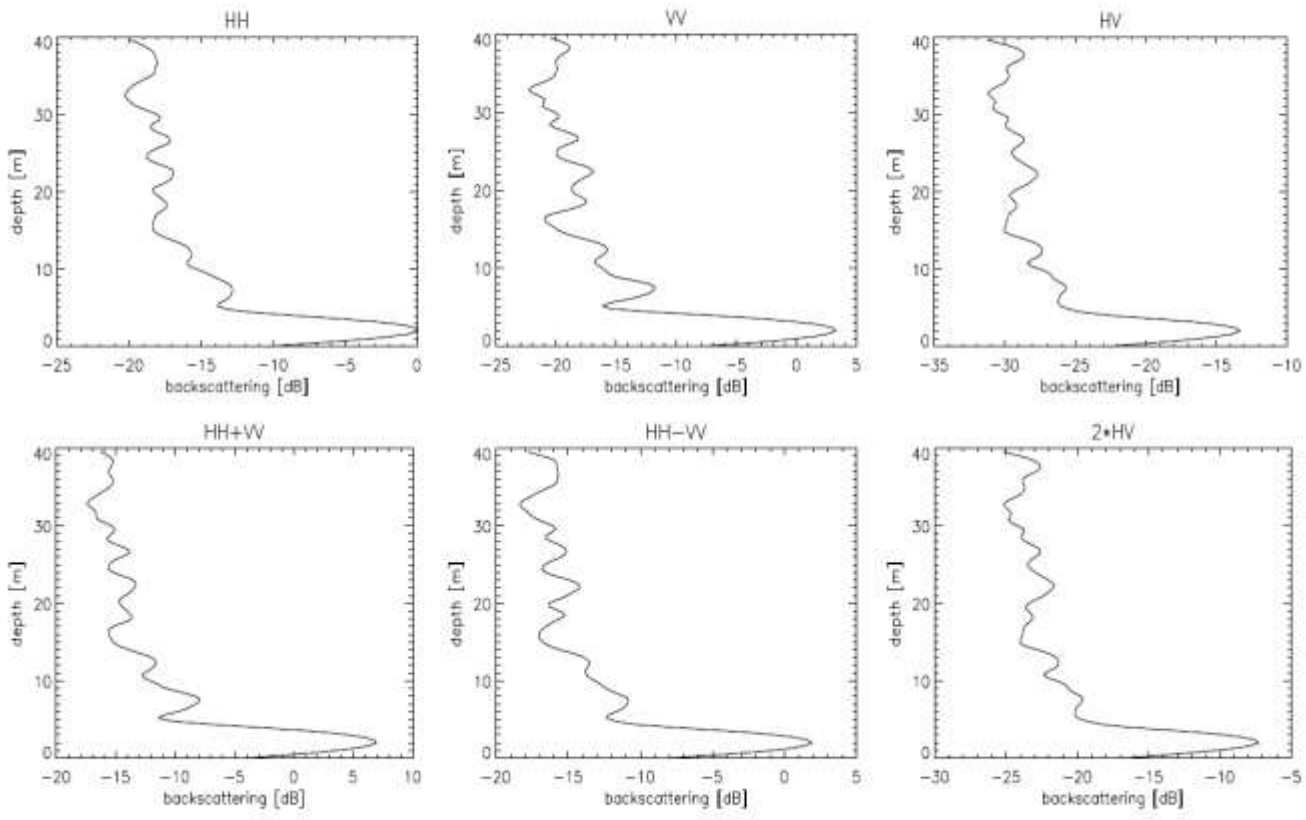

Figure 6.14: Backscattering from reference surface (bare soil with very low vegetation).

Andreas Reigber - Dissertation

SAR Polarimetric Tomography

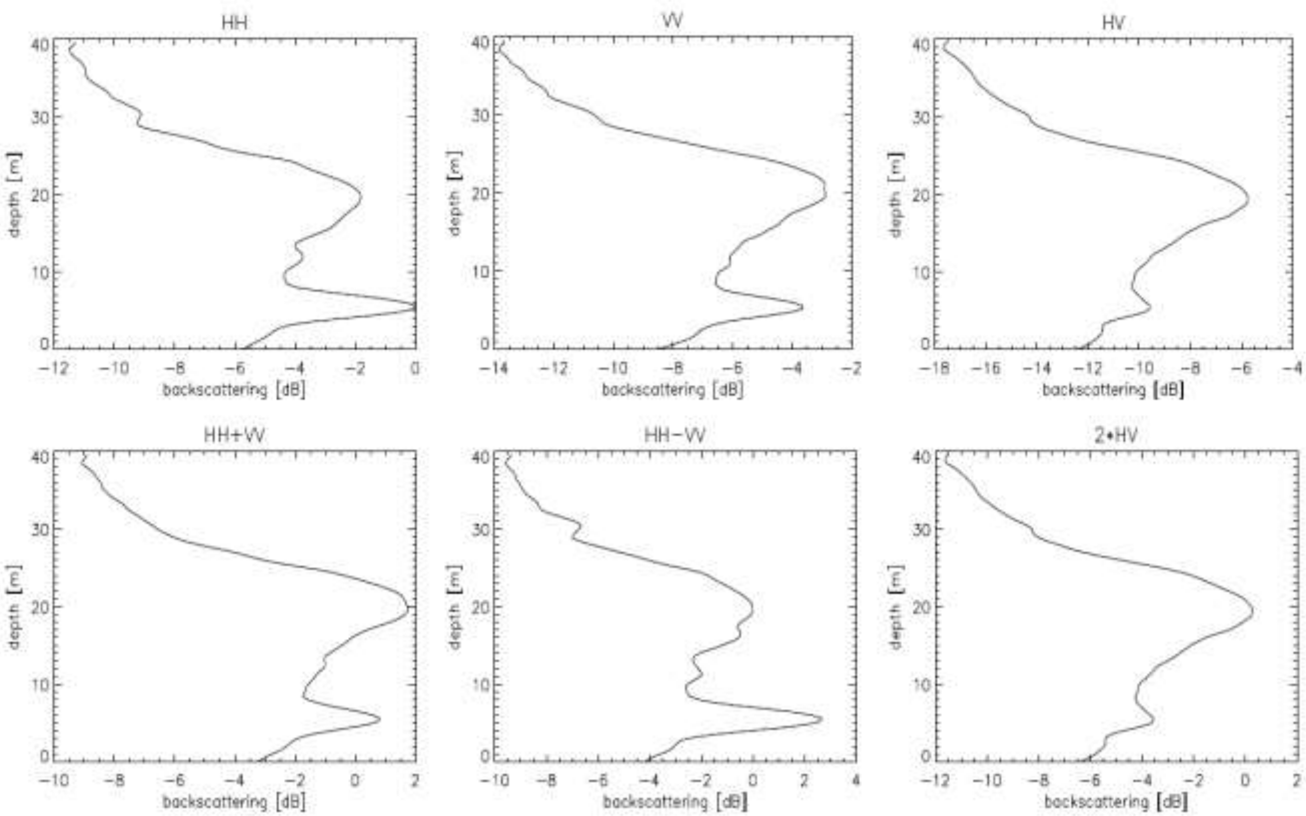

Figure 6.15: Backscattering from forest stand 1 (spruce ~15-20m).

Andreas Reigber - Dissertation

Outline

1. Introduction: Why Forest Observation?
2. SAR Techniques of interest for forestry applications
3. SAR for Forestry Applications – Some Basics
4. Forest Cover and Biomass Mapping – Excurses
    1. BIOMASAR – Hypertemporal C-band Data Assimilation
    2. Forest Cover Mapping Using Backscatter and Coherence
    3. Forest Biomass Mapping Using Backscatter and Coherence
    4. Polarimetry for Forest Cover Mapping
    5. INSAR Phase and Tree Height
    6. Seasonality of C-band Backscatter in Siberia
    7. Seasonality of Coherence in Siberia
    8. X-band coherence over the Thuringian Forest
    9. Mapping of woody cover in KNP using L-band backscatter

Possible Scattering in Forest

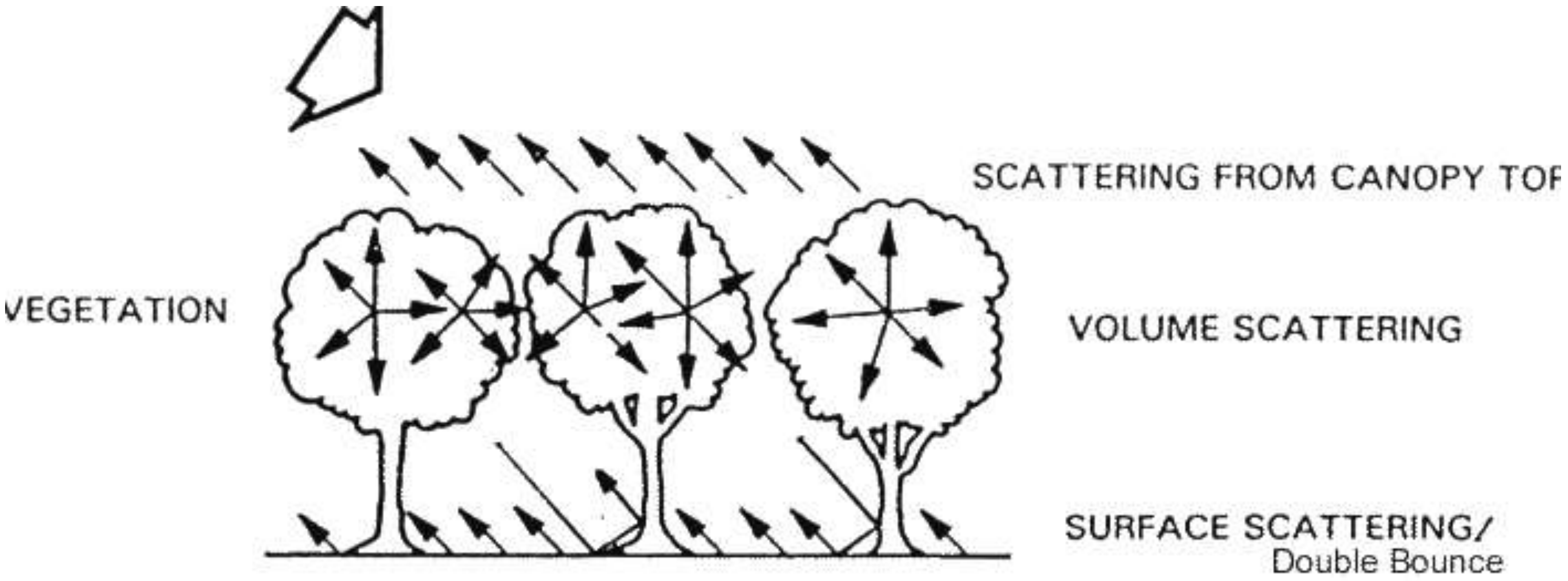

Radar scattering from (boreal) forests

P-band (30-100 cm) L-band (23 cm) C-band (5 cm)

C-band radar backscatter is more sensitive to structural properties of the forest if

1) the radar wave penetrates deeper into the canopy (e.g. frozen or dry conditions) and

2) if the backscatter from the ground is not strong (frozen or dry conditions, smooth soil)

Impact of different frequencies

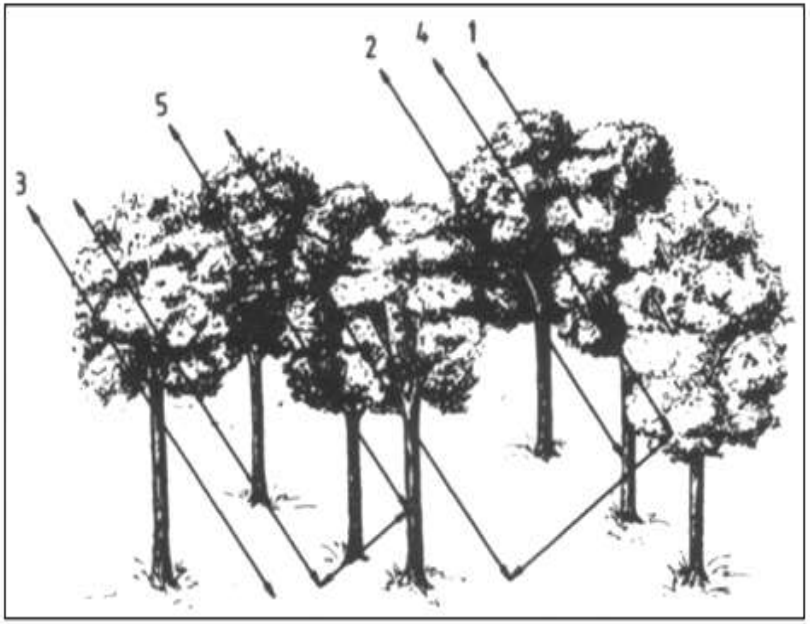

LE TOAN et al. 2001: 4

Frequency band	X	C	L	P	VHF
Main scatterers	Leaves, Twigs	Leaves Small branches	Branches	Branches & Trunk	Trunk

Main Scatterers at different frequencies

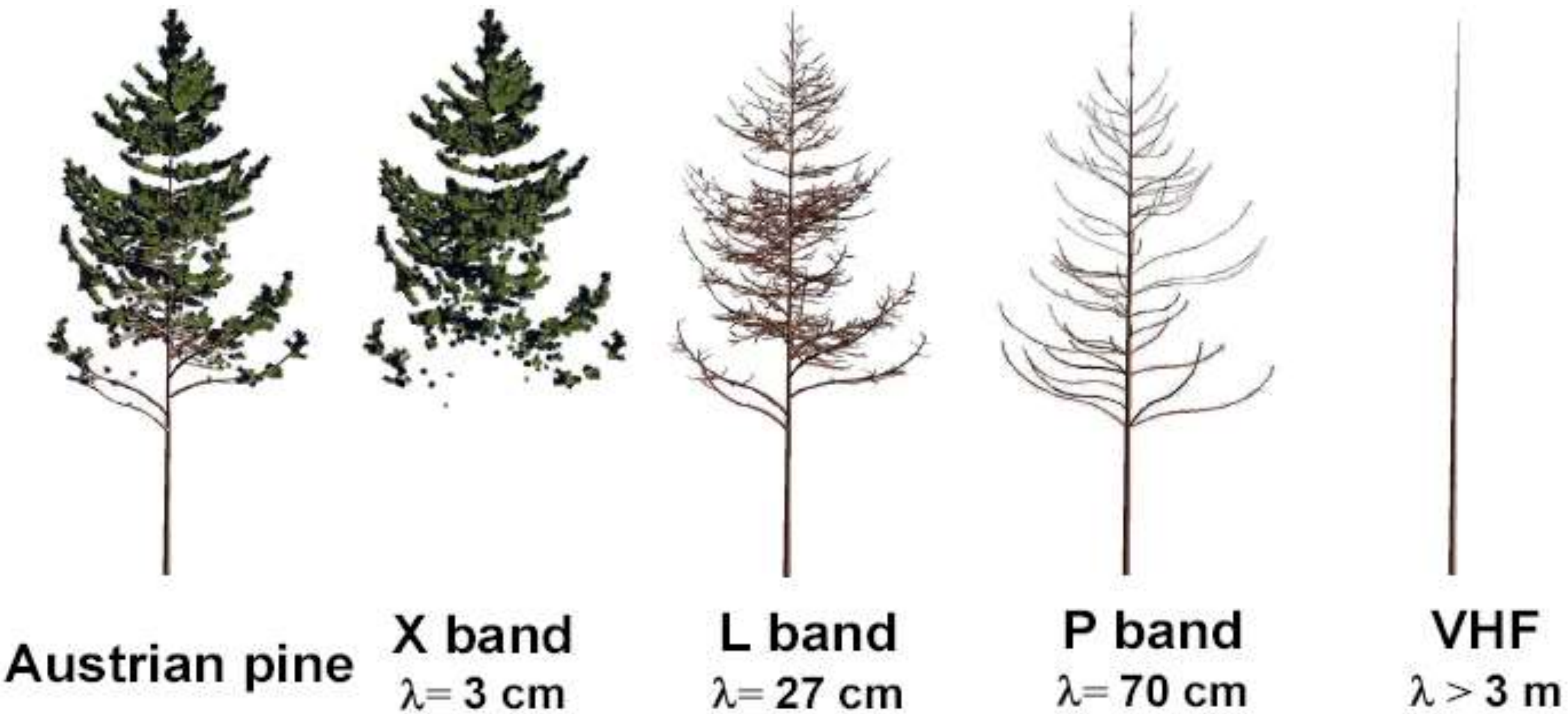

LE TOAN

- AIRSAR (NASA/JPL) polarimetric C-, L- and P-Band with Incidence Angles of 40° and 50°

(mono-temporal acquisitions)

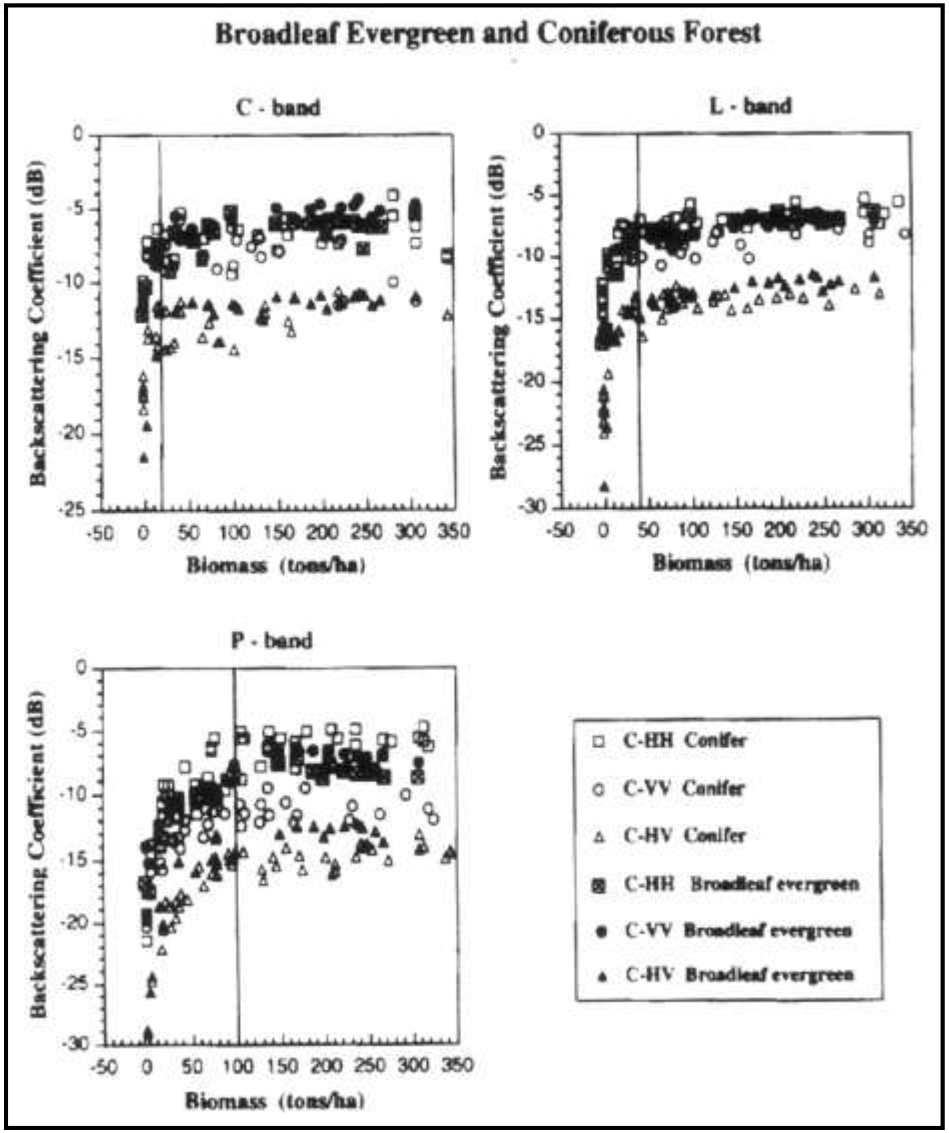

IMHOFF 1995: 514

- AIRSAR (NASA/JPL) polarimetric C-, L- and P-Band with Incidence Angles of 40° and 50°

(mono-temporal acquisitions)

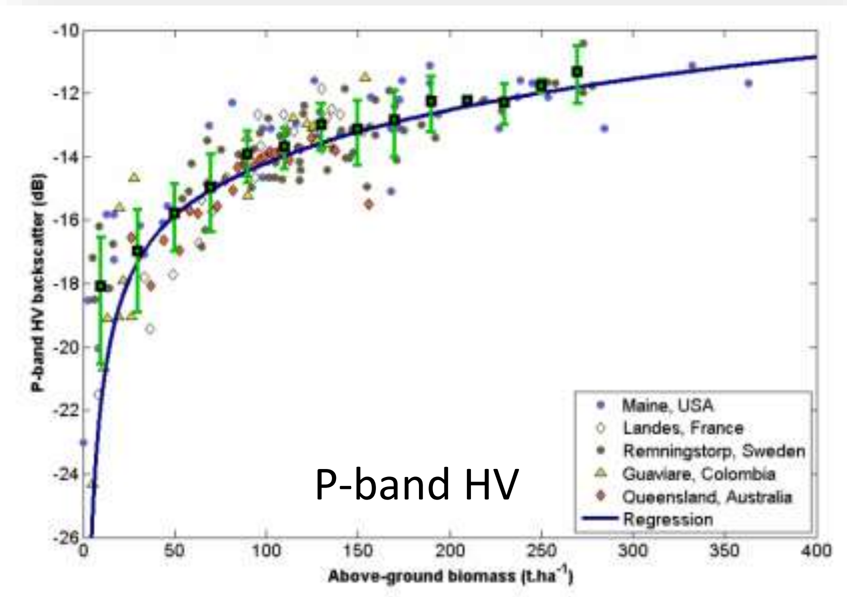

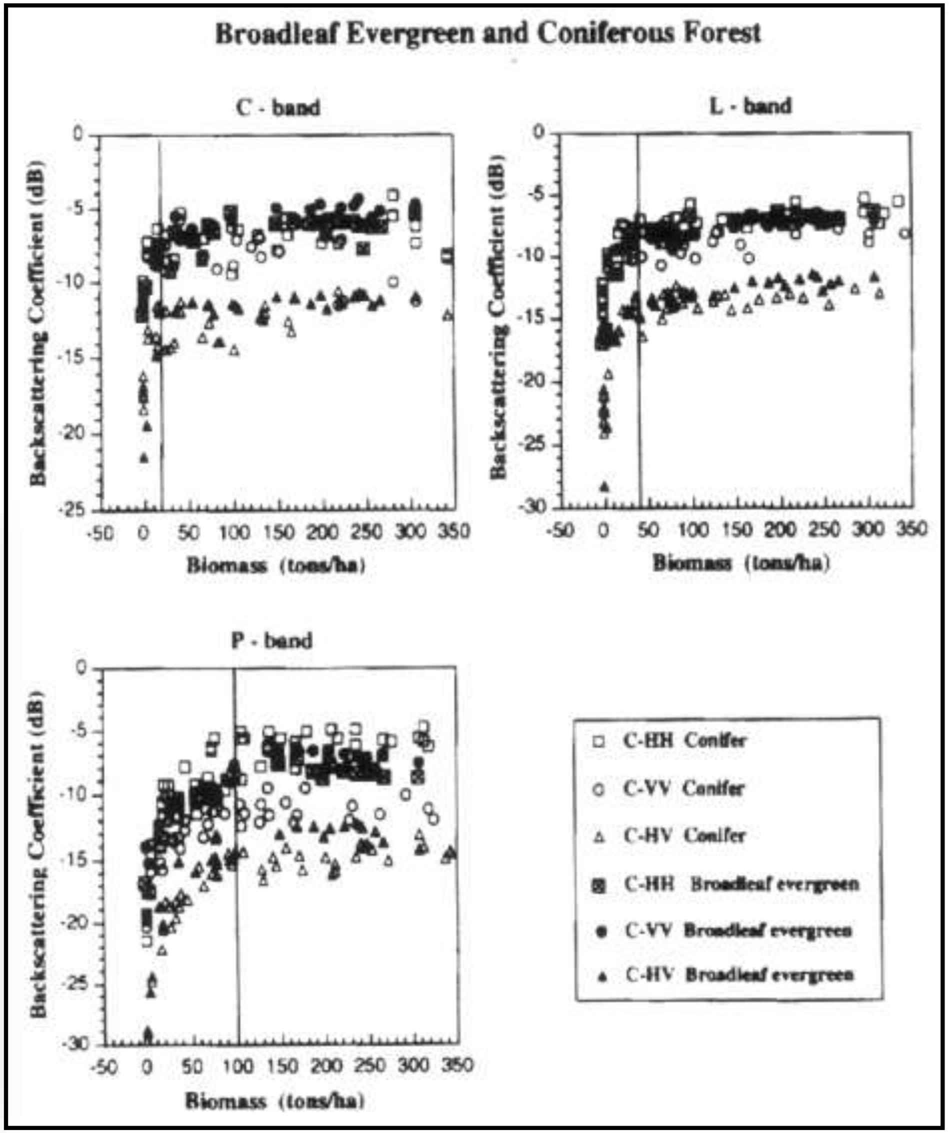

SATURATION PROBLEM

The saturation level of different wavelengths and polarizations depends on:

- ***wavelength*** (i.e. different bands, such as C, L, P)
- ***polarization*** (HV, HH and VV)
- ***object characteristics*** (vegetation stand structure and ground conditions)

Strength of multitemporal data

ERS Tandem Coherence
RMSE: 10 m^3/ha
Relative RMSE: 7 %

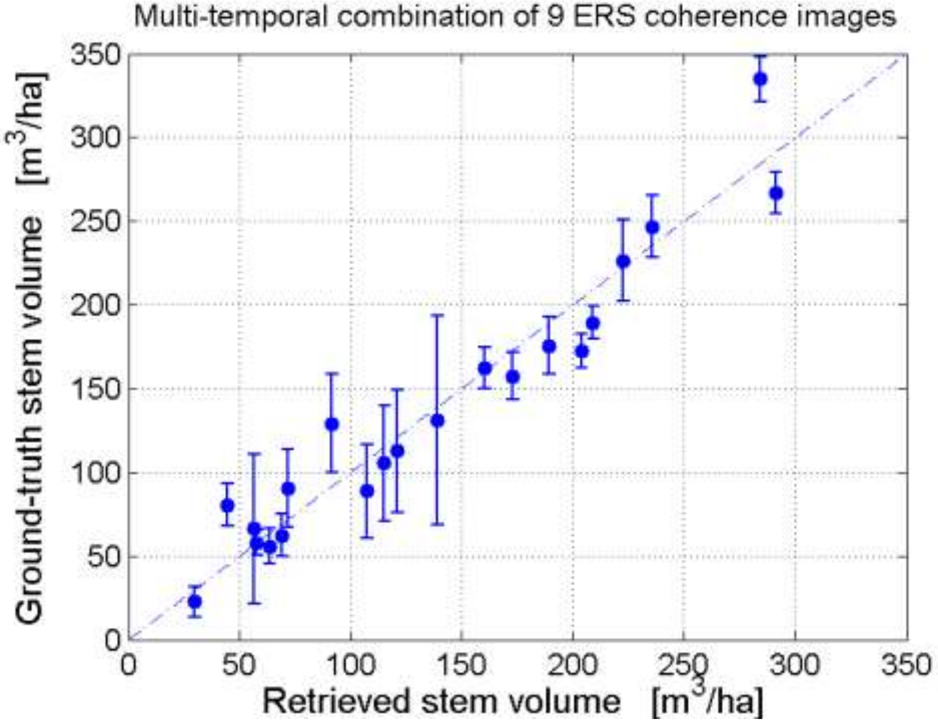

JERS Backscatter
RMSE: 33 m^3/ha,
Relative RMSE: 22 %

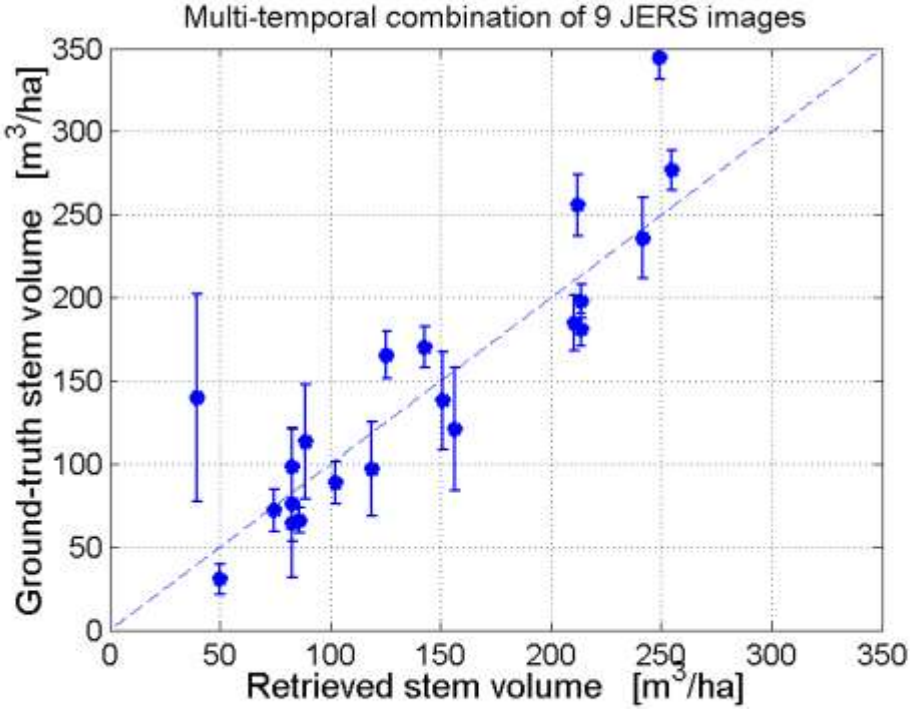

Santoro et al., RSE, 2002

Forest at different frequencies

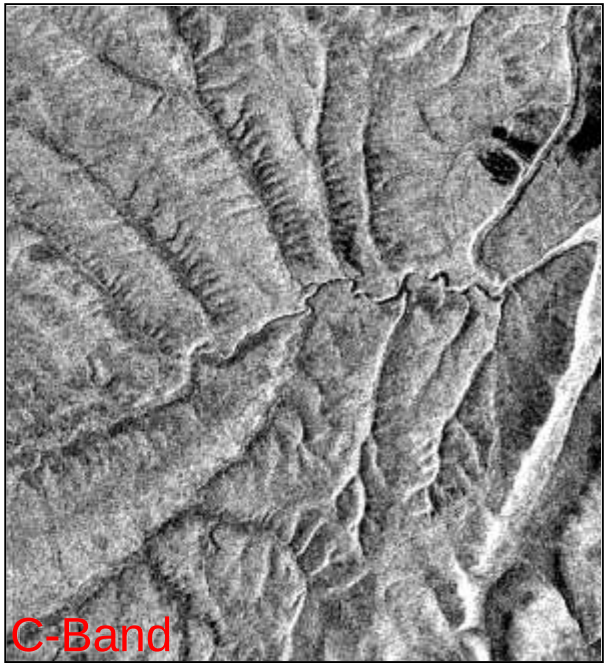

- Small dynamic range
- Variable response to water
- Variable response to open areas
- Can be used as indicator of environmental effects effecting the coherence

- Medium dynamic range
- Stable response to water
- Possible to identify agricultural fields
- Higher frame to frame variations

Forest at different frequencies

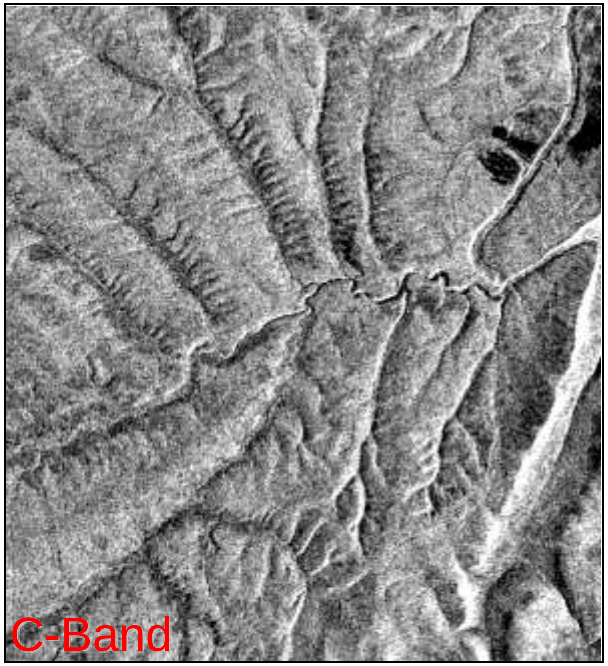

- Small dynamic range
- Variable response to water
- Variable response to open areas
- Can be used as indicator of environmental effects effecting the coherence

- Medium dynamic range
- Stable response to water
- Possible to identify agricultural fields
- Higher frame to frame variations

- Higher contrast between forest/non forest
- Higher sensitivity to forest volume
- Confusion between water and dense forest
- Frame to frame variations

Linking SAR measures and Forest Parameters

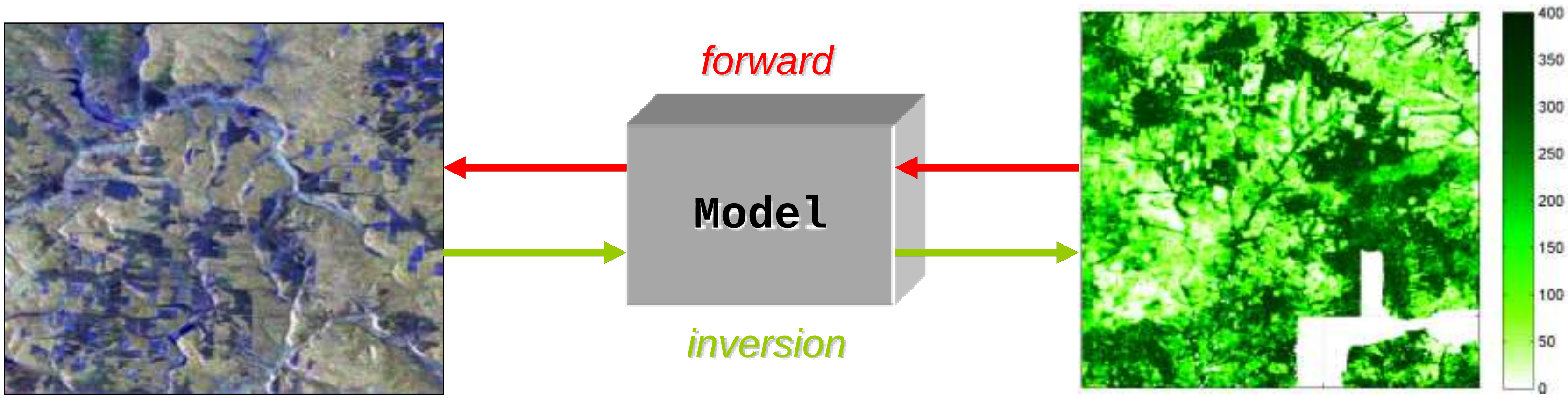

SAR measures

Forest Parameters

Outline

1. Introduction: Why Forest Observation?
2. SAR Techniques of interest for forestry applications
3. SAR for Forestry Applications – Some Basics
4. Forest Cover and Biomass Mapping – Excurses
    1. BIOMASAR – Hypertemporal C-band Data Assimilation
    2. Forest Cover Mapping Using Backscatter and Coherence
    3. Forest Biomass Mapping Using Backscatter and Coherence
    4. Polarimetry for Forest Cover Mapping
    5. INSAR Phase and Tree Height
    6. Seasonality of C-band Backscatter in Siberia
    7. Seasonality of Coherence in Siberia
    8. X-band coherence over the Thuringian Forest
    9. Mapping of woody cover in KNP using L-band backscatter

ENVISAT ASAR Modes – BIOMASAR uses WS & GM

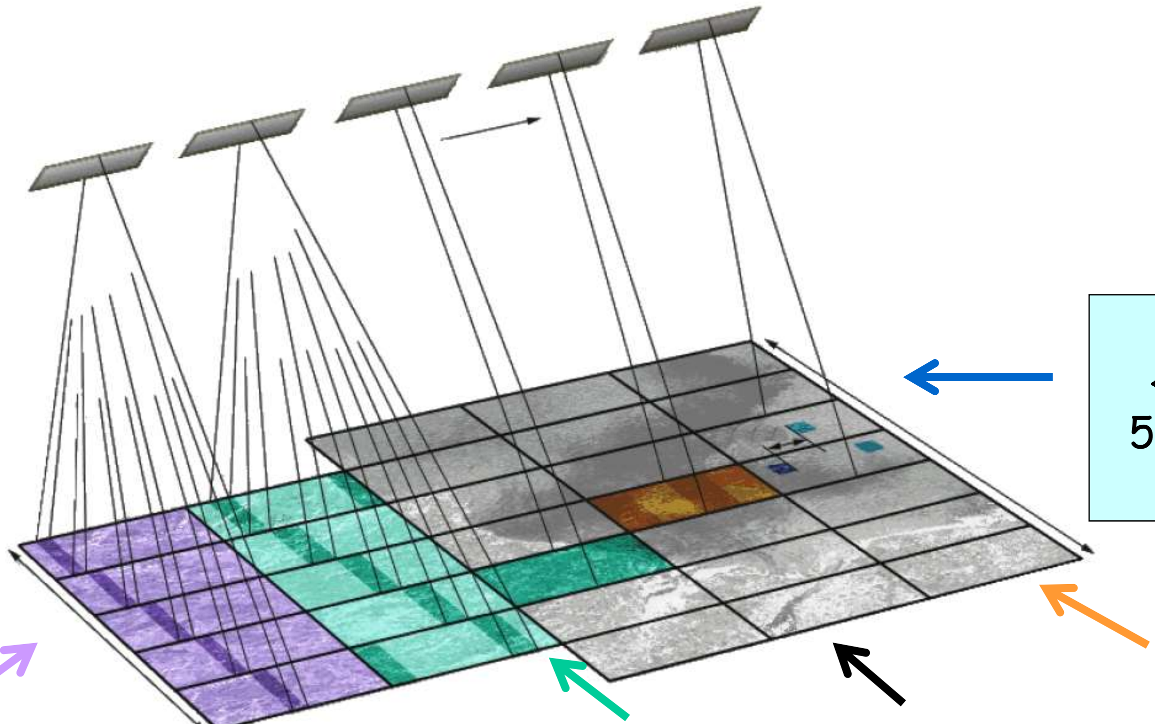

Wave VV or HH
< 10m resolution
5 x 5 km to 10 x 5 km vignettes

Alternating Polarisation
VV/HH or VV/VH or HH/HV
30m resolution
up to 100 km swath

Global Monitoring
VV or HH
1000m resolution
405 km swath width

Wide Swath
VV or HH
150m resolution
405 km swath width

Image VV or HH
< 30m resolution
up to 100 km swath

Envisat ASAR Scansar data availability

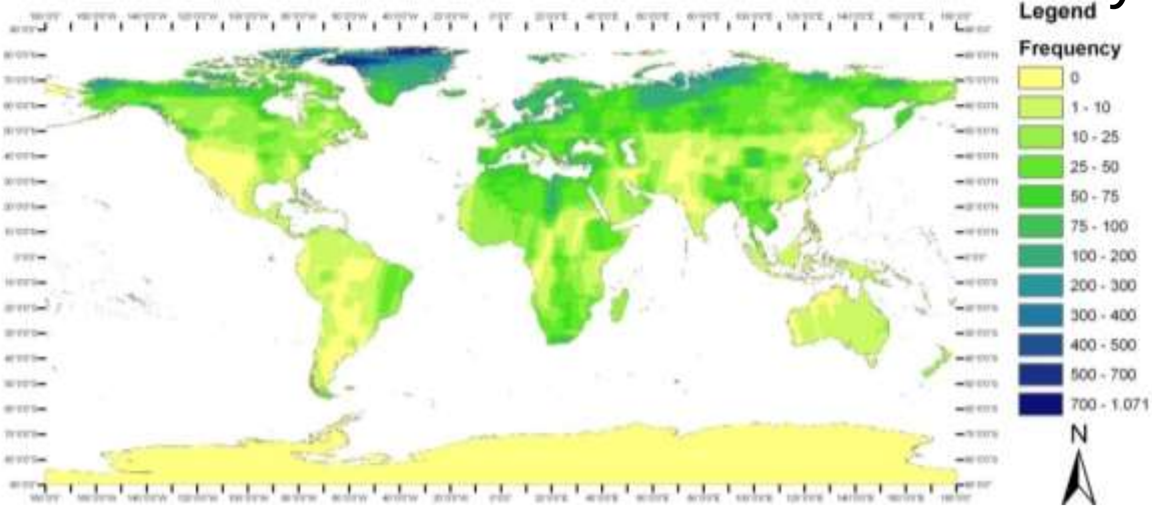

Wide Swath Mode 2007

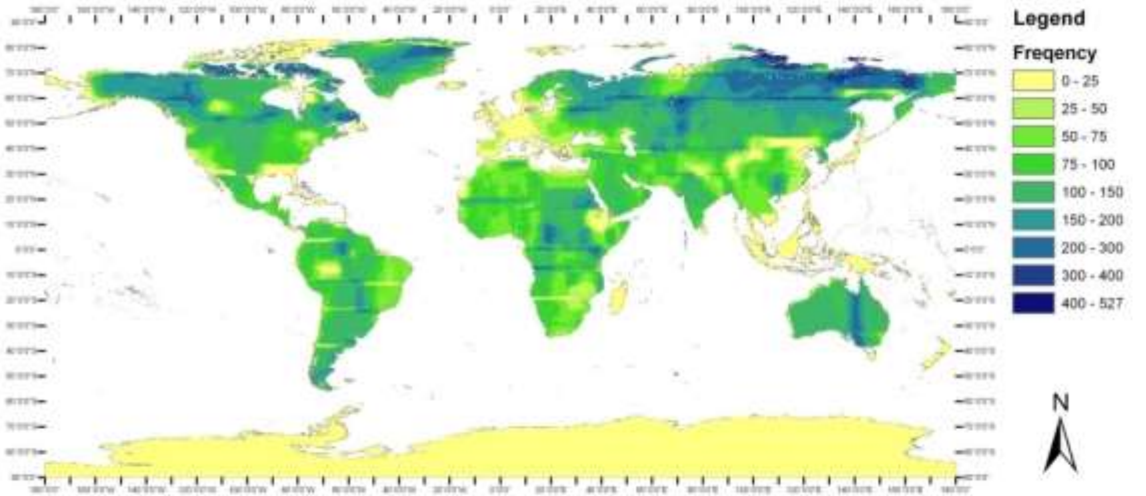

Global Monitoring Mode 2007

ENVISAT ASAR Wide Swath dataset

During 2003 and 2004 ENVISAT ASAR data in Wide Swath mode has been acquired over the study area of the SIBERIA-II Project; Several hundred ASAR scenes have been acquired, with a high degree of overlap between neighboring tracks

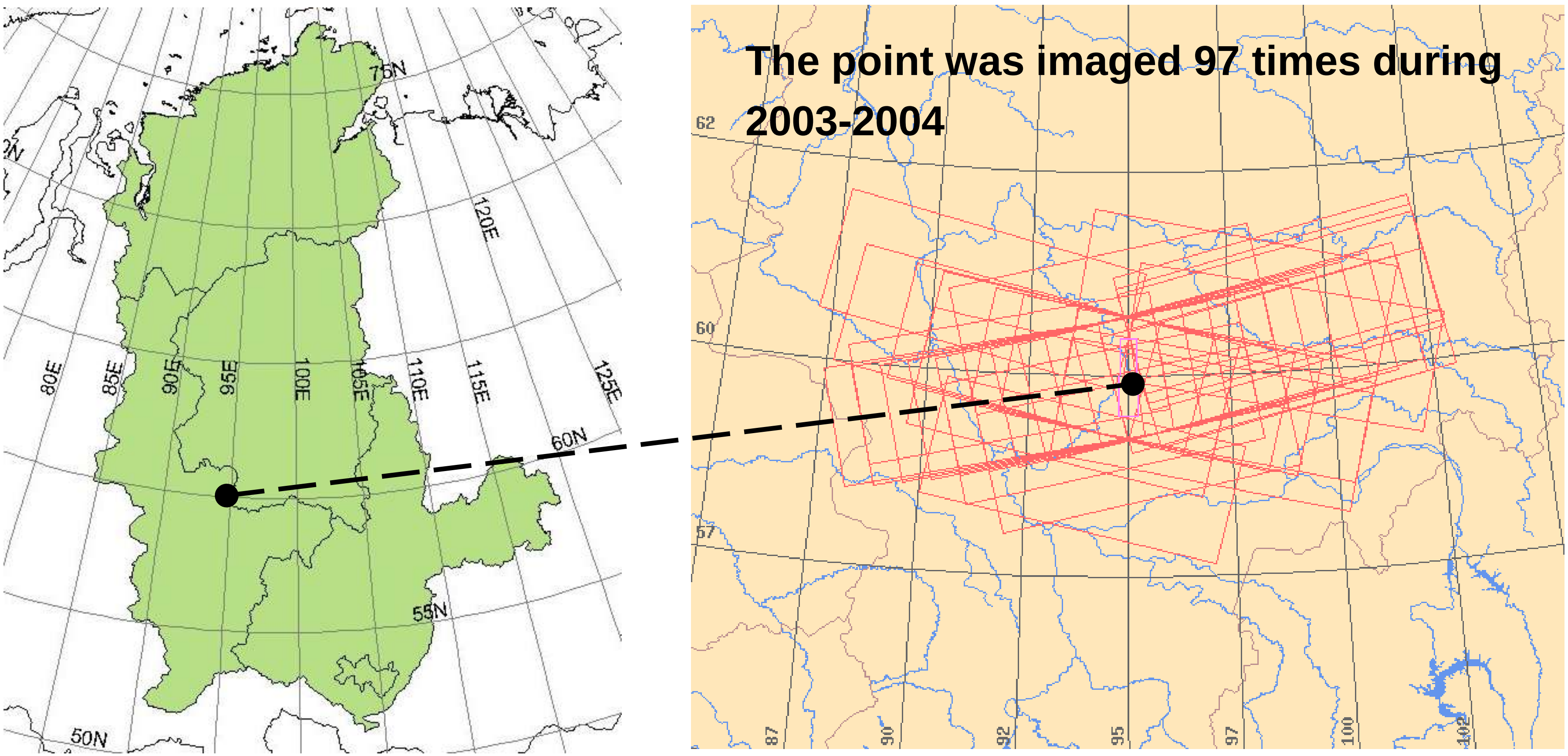

BIOMASAR: ENVISAT ASAR Global Mode

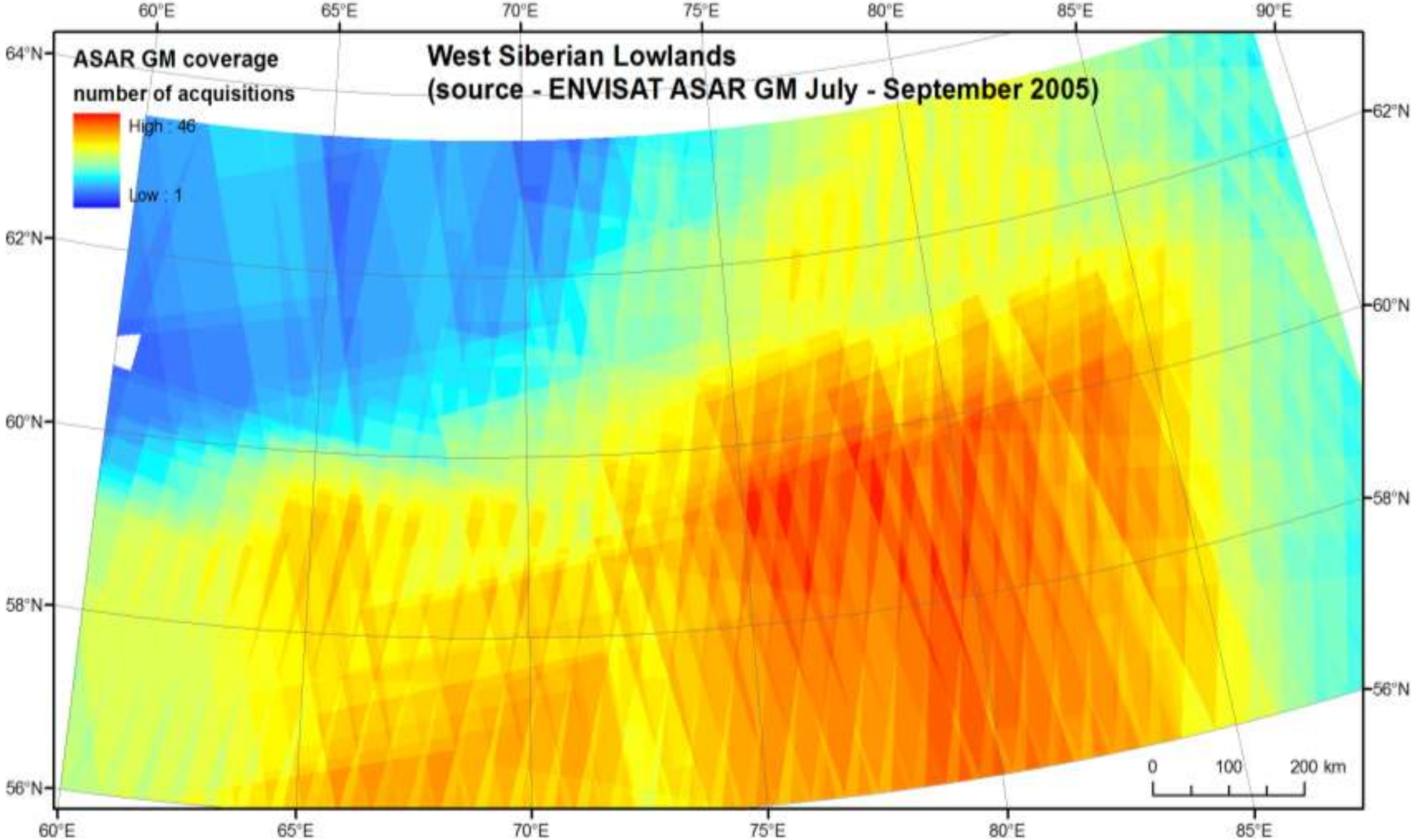

Modeling Example: A Water Cloud-like model

A water cloud with gaps is close to reality and easy to handle

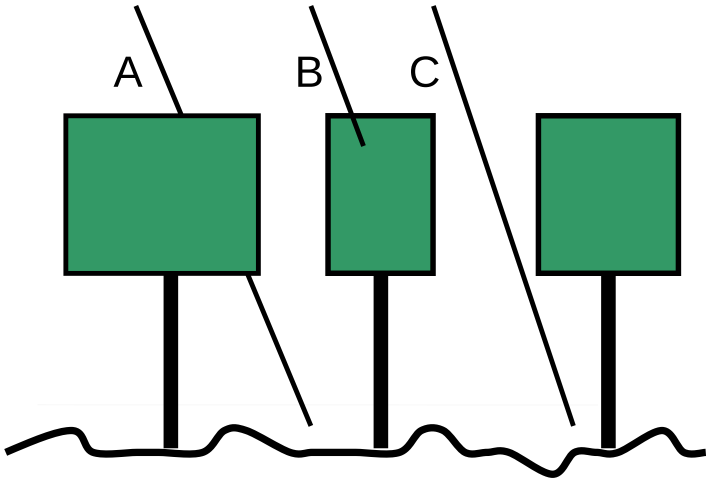

Water cloud with gaps

Modeling Example: A Water Cloud-like model

A water cloud with gaps is close to reality and easy to handle

$$\sigma^{o}_{for} = (1-\eta)\sigma^{o}_{gr} + \eta\sigma^{o}_{gr}T_{tree} + \eta\sigma^{o}_{veg}(1-T_{tree})$$

Canopy cover

tree transmissivity (depends on tree height and signal attenuation)

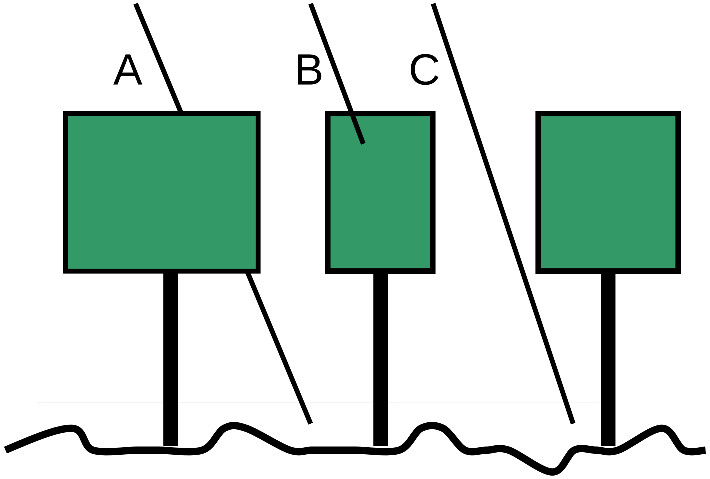

Water cloud with gaps

The model expresses the forest backscatter as function of the area-fill factor η, i.e. the forest canopy cover

For applications it can be written in terms of growing stock volume

Modeling Example: A Water Cloud-like model

A water cloud with gaps is close to reality and easy to handle

$$\sigma^o_{for} = (1-\eta)\sigma^o_{gr} + \eta\sigma^o_{gr} T_{tree} + \eta\sigma^o_{veg}(1-T_{tree})$$

Canopy cover (η)

tree transmissivity (depends on tree height and signal attenuation) (T_{tree})

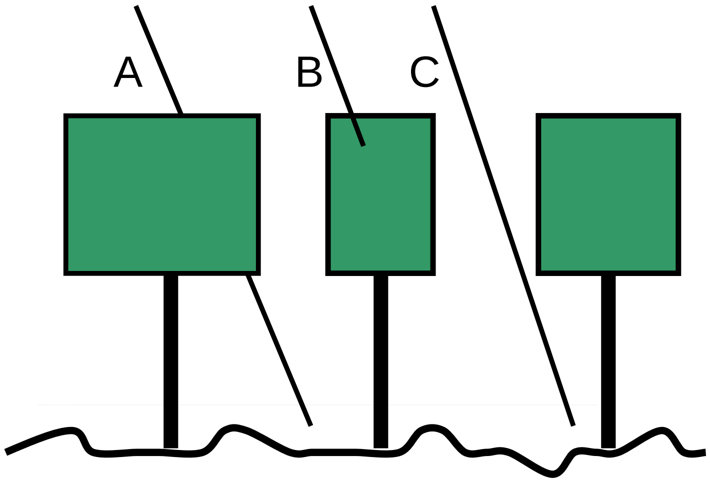

Water cloud with gaps

The model expresses the forest backscatter as function of the area-fill factor η, i.e. the forest canopy cover

For applications it can be written in terms of growing stock volume

$$\sigma^o_{for} = \sigma^o_{veg}\left(1-e^{-\beta V}\right) + \sigma^o_{gr} e^{-\beta V}$$

Unknown: σ^o_{veg}, β, σ^o_{gr}

σ_{gr}	ground backscatter
σ_{veg}	canopy backscatter
β	forest transmissivity coefficient

Multi-temporal combination of single biomass estimates

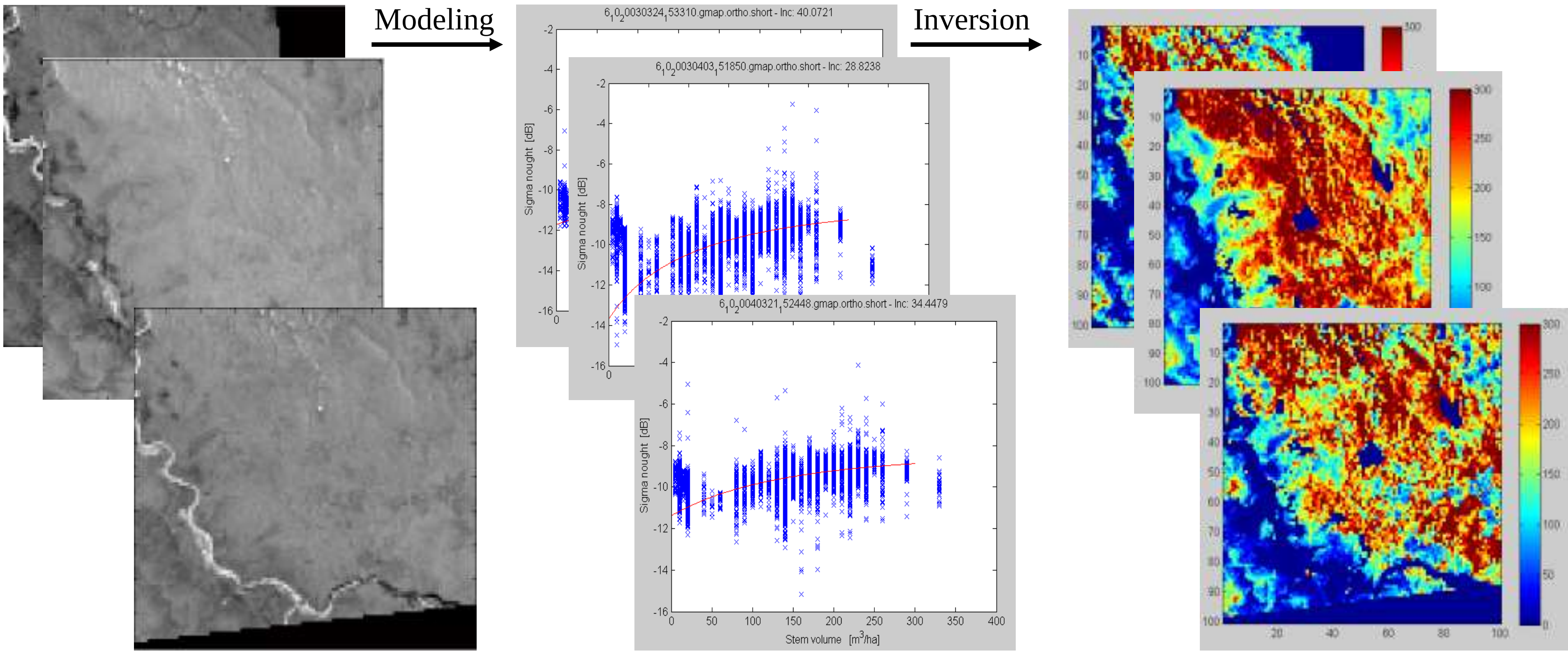

- A multi-temporal combination of single estimates with weights determined by the backscatter contrast σ^0_{veg} - σ^0_{gr} allows obtaining the final estimate

(ESA BIOMASAR Project, Maurizio Santoro, 2007)

Multi-temporal combination of single biomass estimates

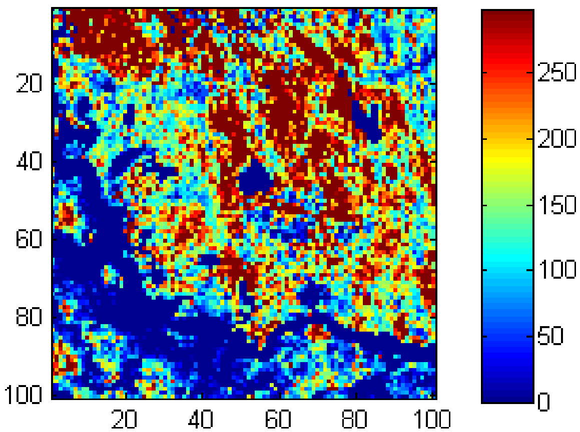

Single-image

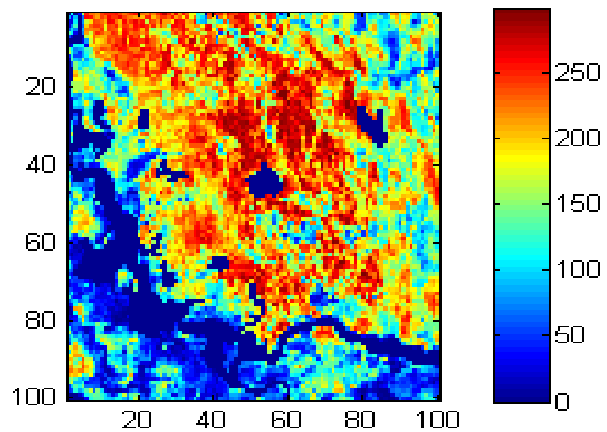

Multi-temporal (29 images)

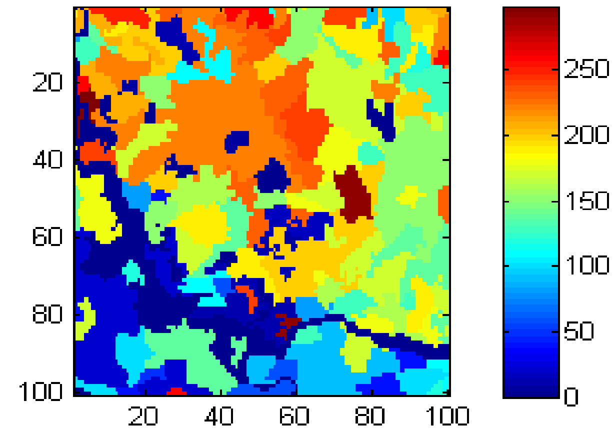

Inventory

- From a single image it is possible to identify sparse/dense forest patterns at most
- From multi-temporal combination it is possible to identify biomass levels

Retrieved GSV Map vs. in-situ data

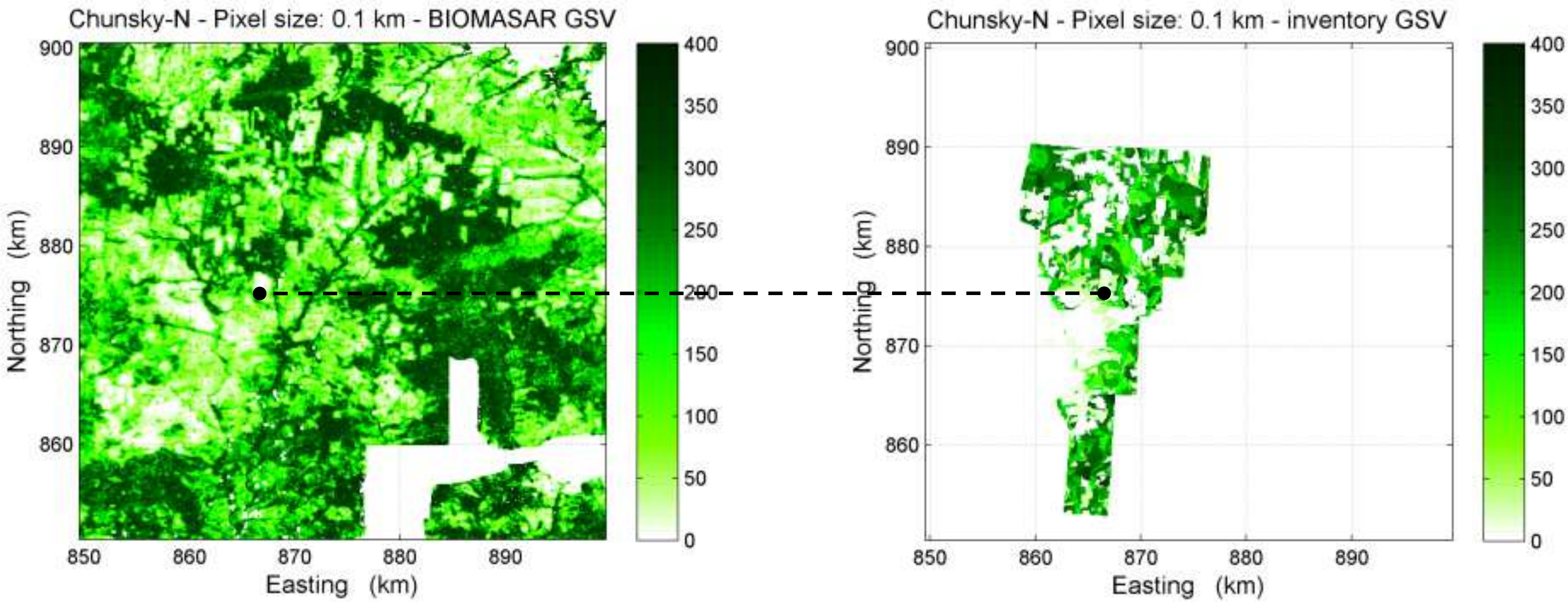

Impact of uncertainty of in situ data

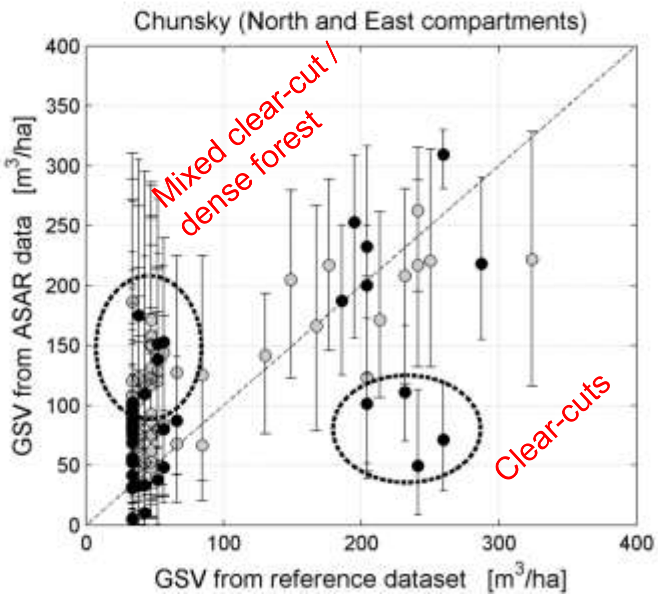

- The quality of the reference data can affect the retrieval statistics
- Cross-comparison with other EO data helped in bailing out extreme cases
- Retrieval statistics at full resolution embed a certain amount of error due to imprecision in the ref. data
- More correct results are obtained when aggregating

BIOMASAR Algorithm Based Stock Volume

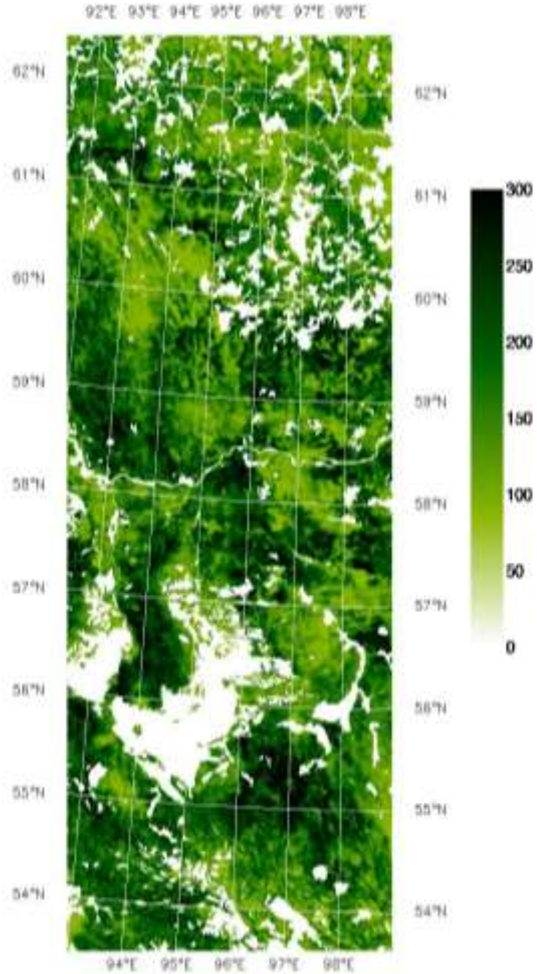

WS-based

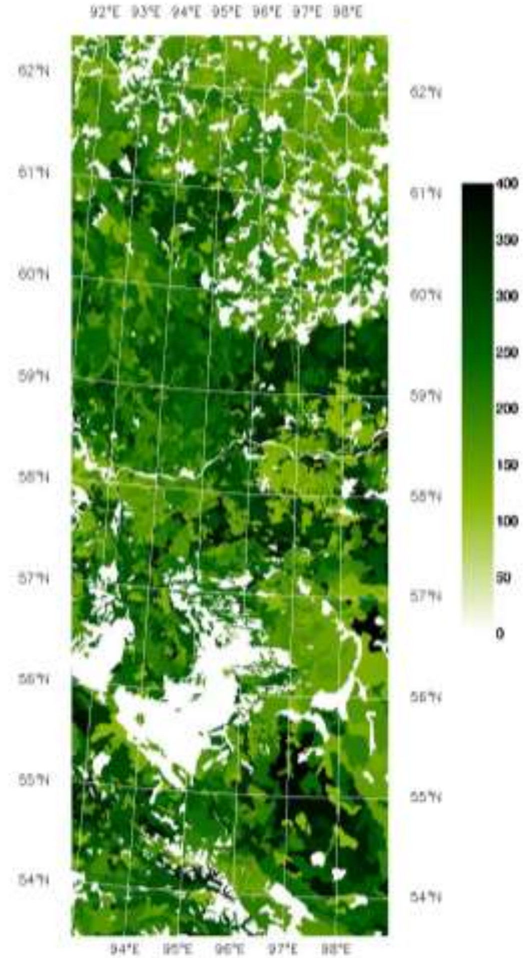

Forest inventory

BIOMASAR GSV map of Central Siberia

- 1 km resolution
- 2,400,000 km^2
- ENVISAT ASAR – Global Monitoring mode (Jan. 2005 – Feb. 2006)
- GLC 2000 land cover used as background

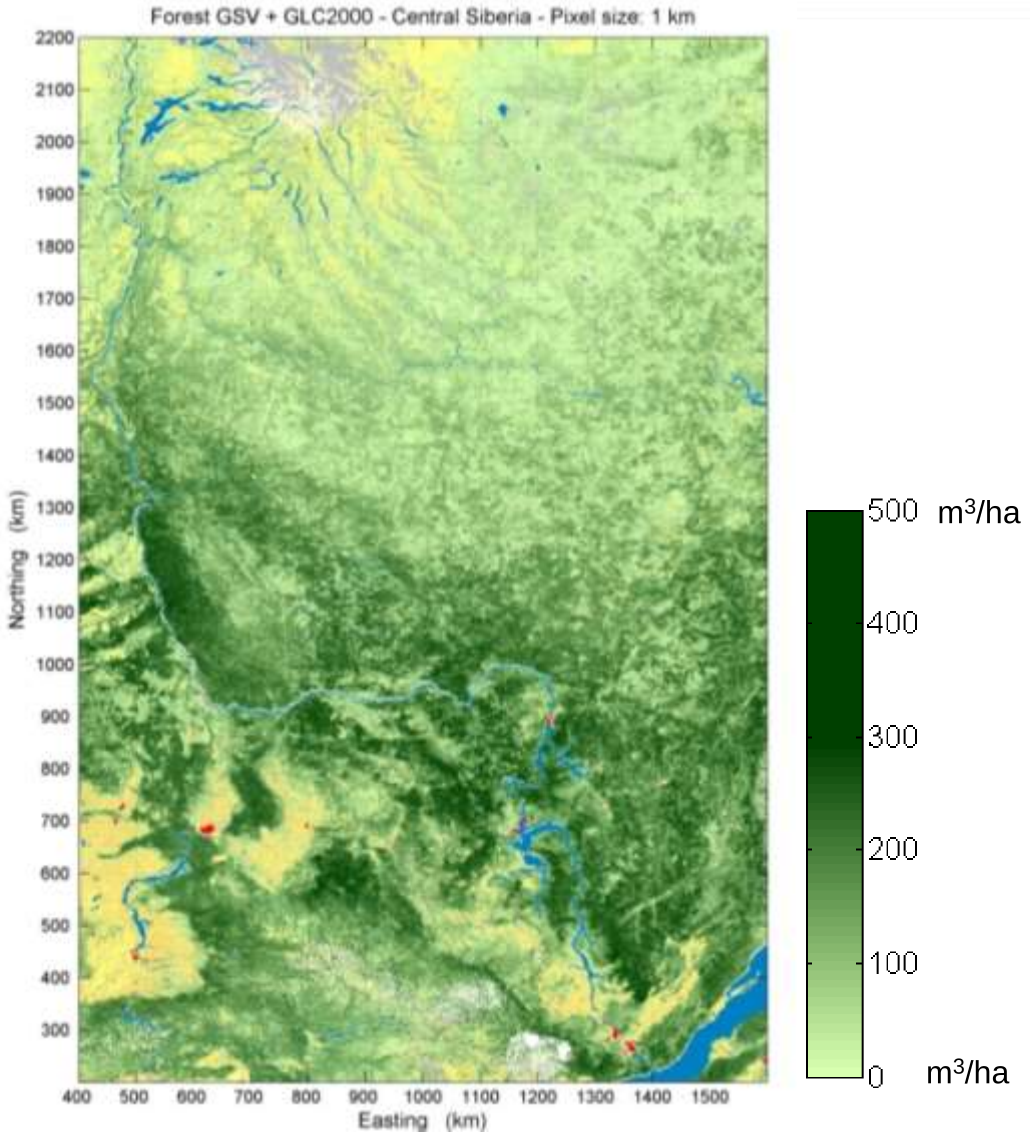

Accuracy for 10 km pixel size

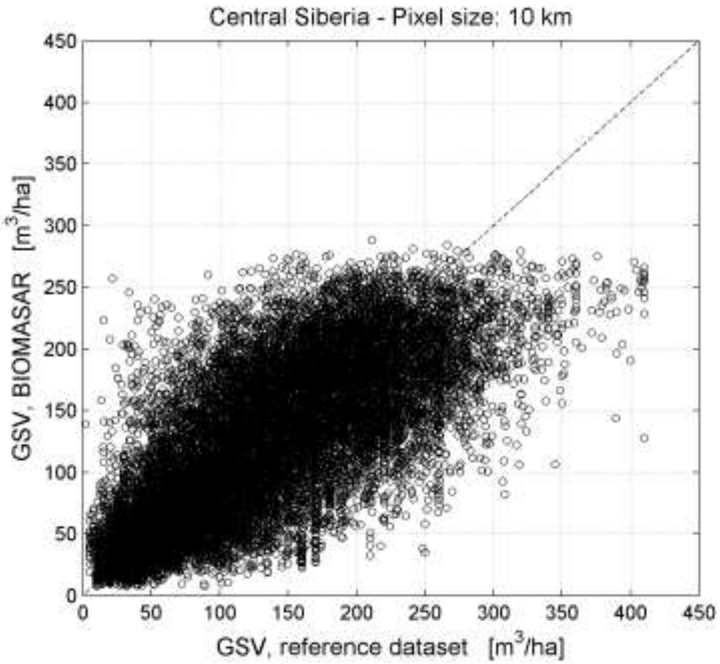

Relative RMSE: 39.6%

Bias: 10.2 m^3/ha

r = 0.73

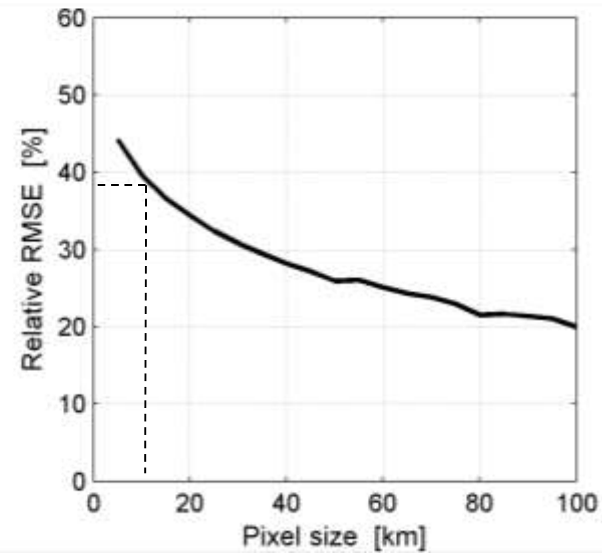

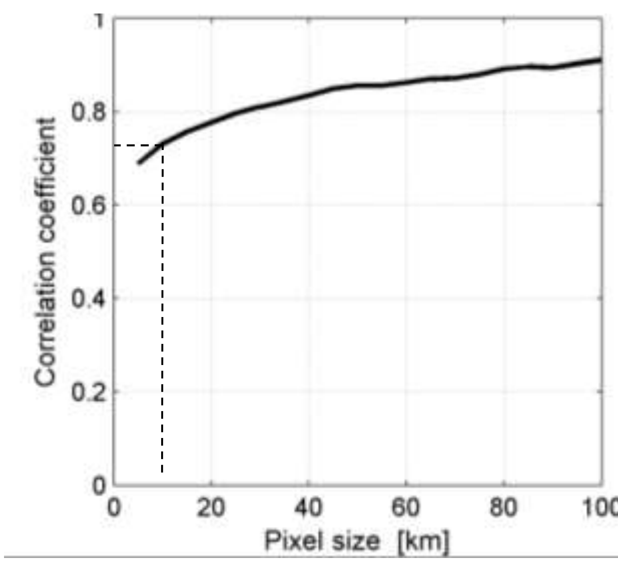

Accuracy for 25 km pixel size

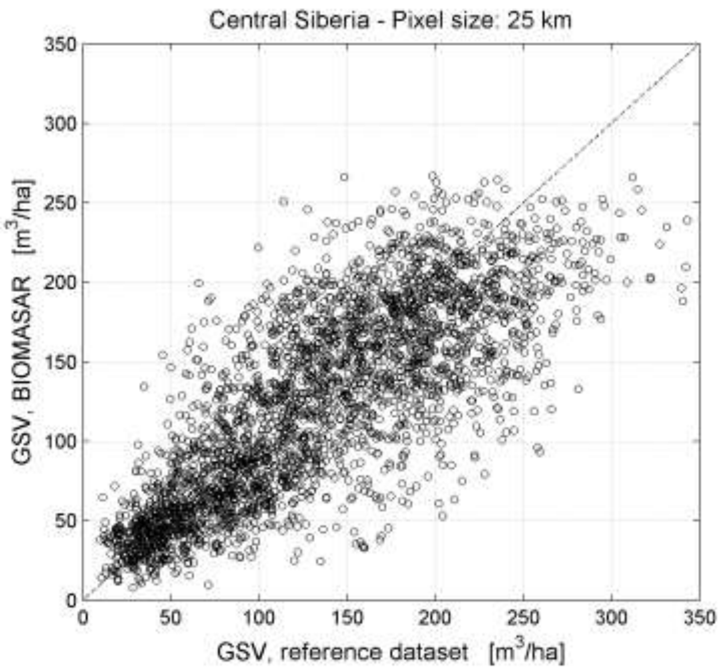

Relative RMSE: 32.3%

Bias: 9.6 m^3/ha

r = 0.80

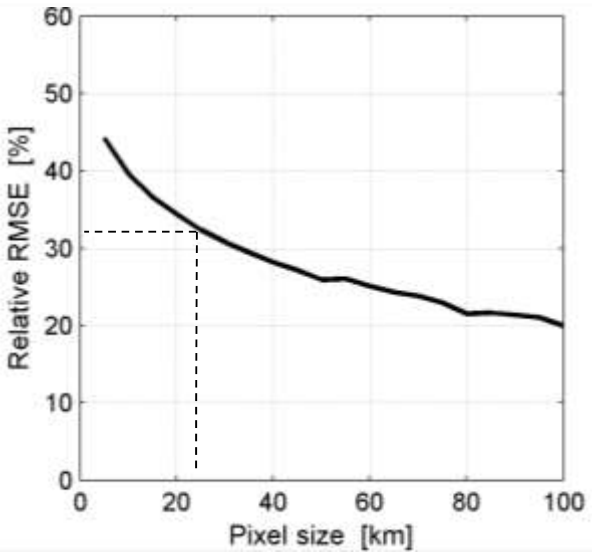

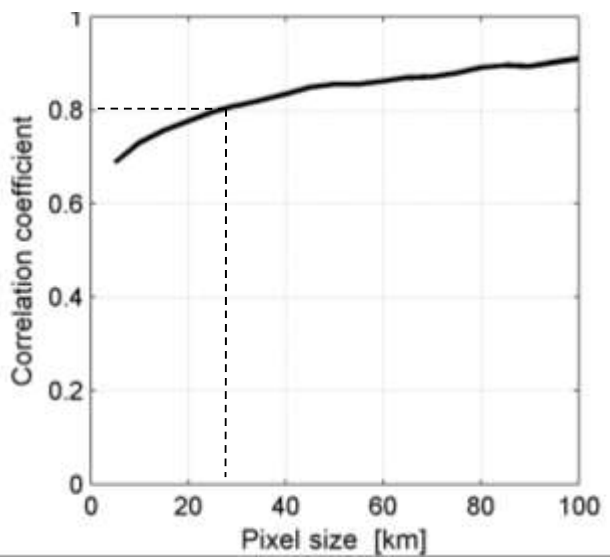

Accuracy for 50 km pixel size

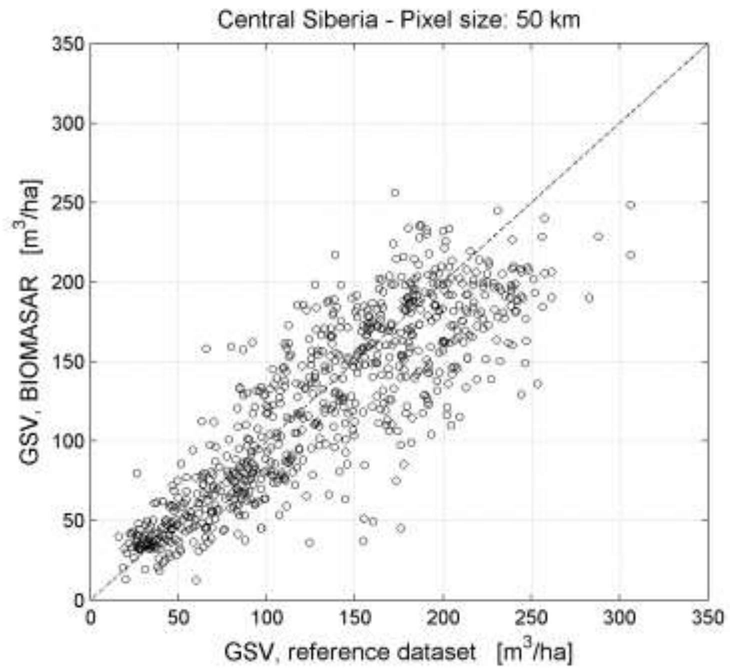

Relative RMSE: 25.9%

Bias: 9.3 m^3/ha

r = 0.86

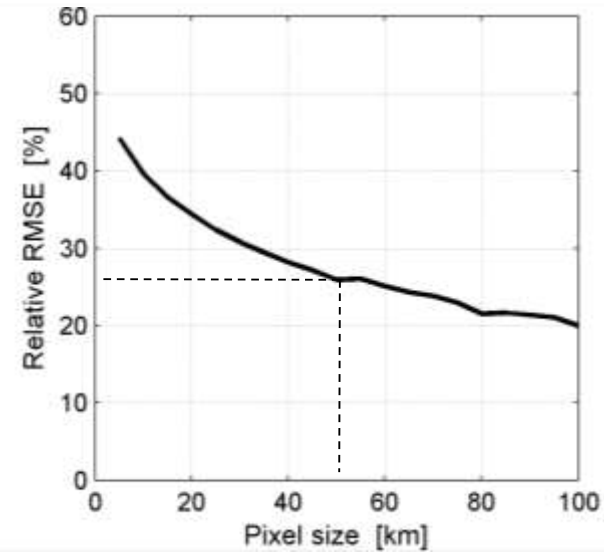

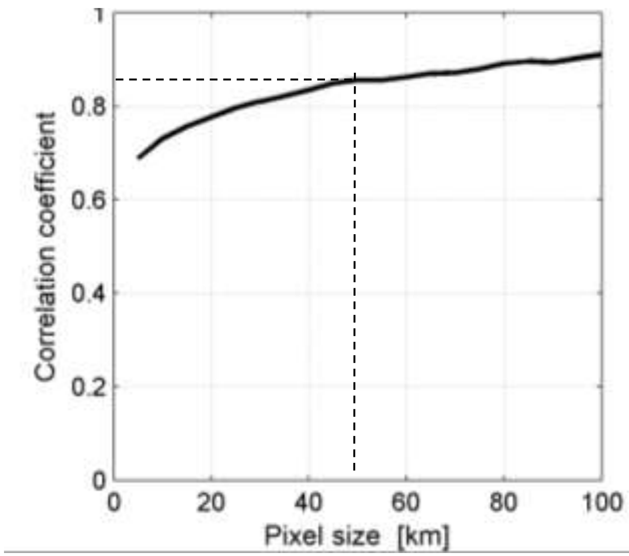

Outline

1. Introduction: Why Forest Observation?
2. SAR Techniques of interest for forestry applications
3. SAR for Forestry Applications – Some Basics
4. Forest Cover and Biomass Mapping – Excurses
    1. BIOMASAR – Hypertemporal C-band Data Assimilation
    2. Forest Cover Mapping Using Backscatter and Coherence
    3. Forest Biomass Mapping Using Backscatter and Coherence
    4. Polarimetry for Forest Cover Mapping
    5. INSAR Phase and Tree Height
    6. Seasonality of C-band Backscatter in Siberia
    7. Seasonality of Coherence in Siberia
    8. X-band coherence over the Thuringian Forest
    9. Mapping of woody cover in KNP using L-band backscatter

Analysis of PALSAR data - FBS

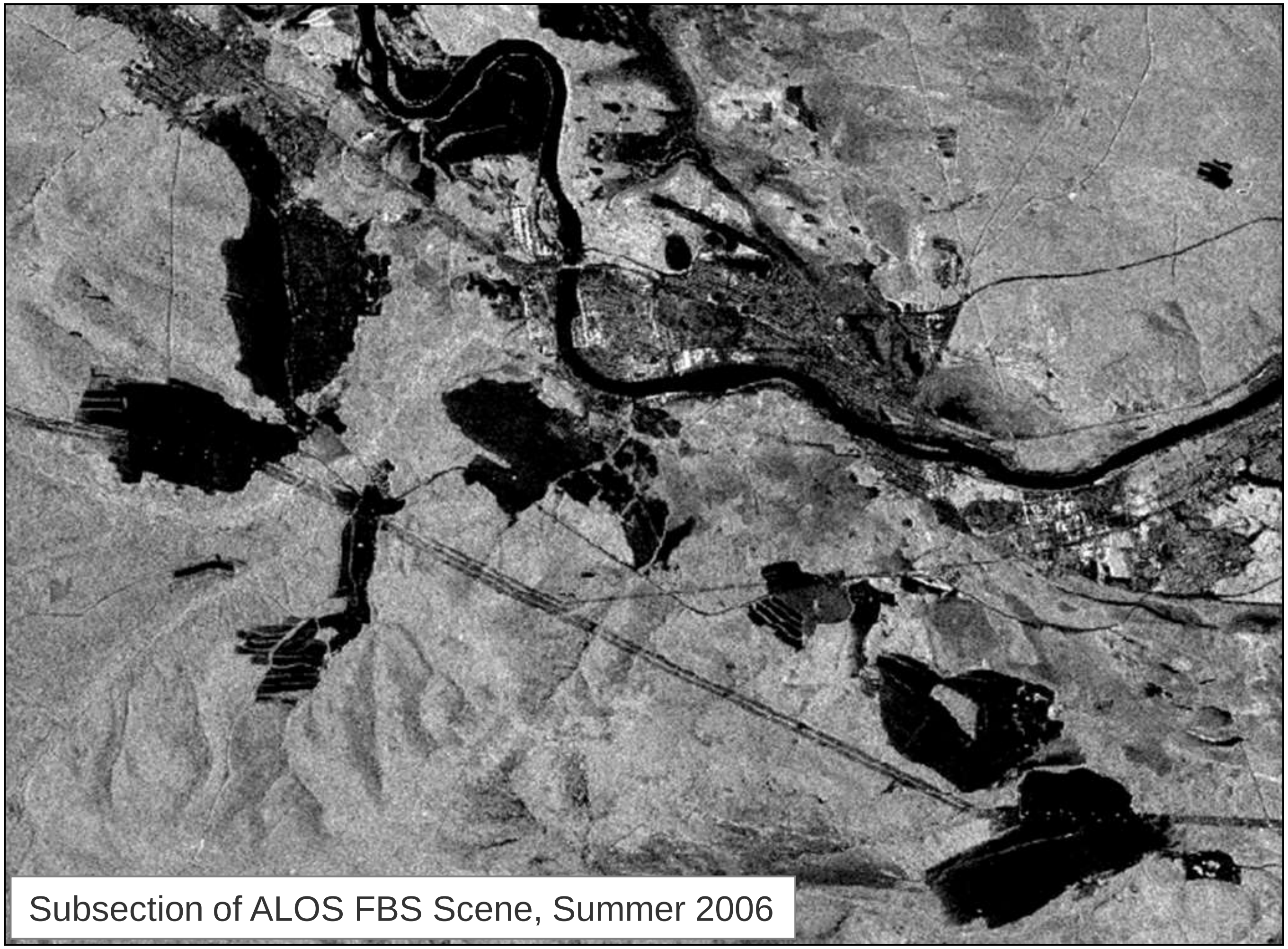

Subsection of ALOS FBS Scene, Summer 2006

Forest Clear-cut separability

date	mode	position		
19MAY06	FBS	54°12’N 99°94’E		
19MAY06	FBS	55°59’N 99°58’E		
19MAY06	FBS	56°08’N 99°46’E		
14AUG06	FBS	54°12’N 101°56’E		
14AUG06	FBS	54°61’N 101°44’E		
27DEC06	FBS	56°84’N 104°16’E		
27DEC06	FBS	57°33’N 103°99’E		
13JAN07	FBS	56°83’N 103°62’E		
13JAN07	FBS	56°83’N 103°62’E		
11FEB07	FBS	56°84’N 104°18’E		
11FEB07	FBS	57°33’N 104°02’E		
28FEB07	FBS	56°84’N 103°64’E		

Forest Clear-cut separability

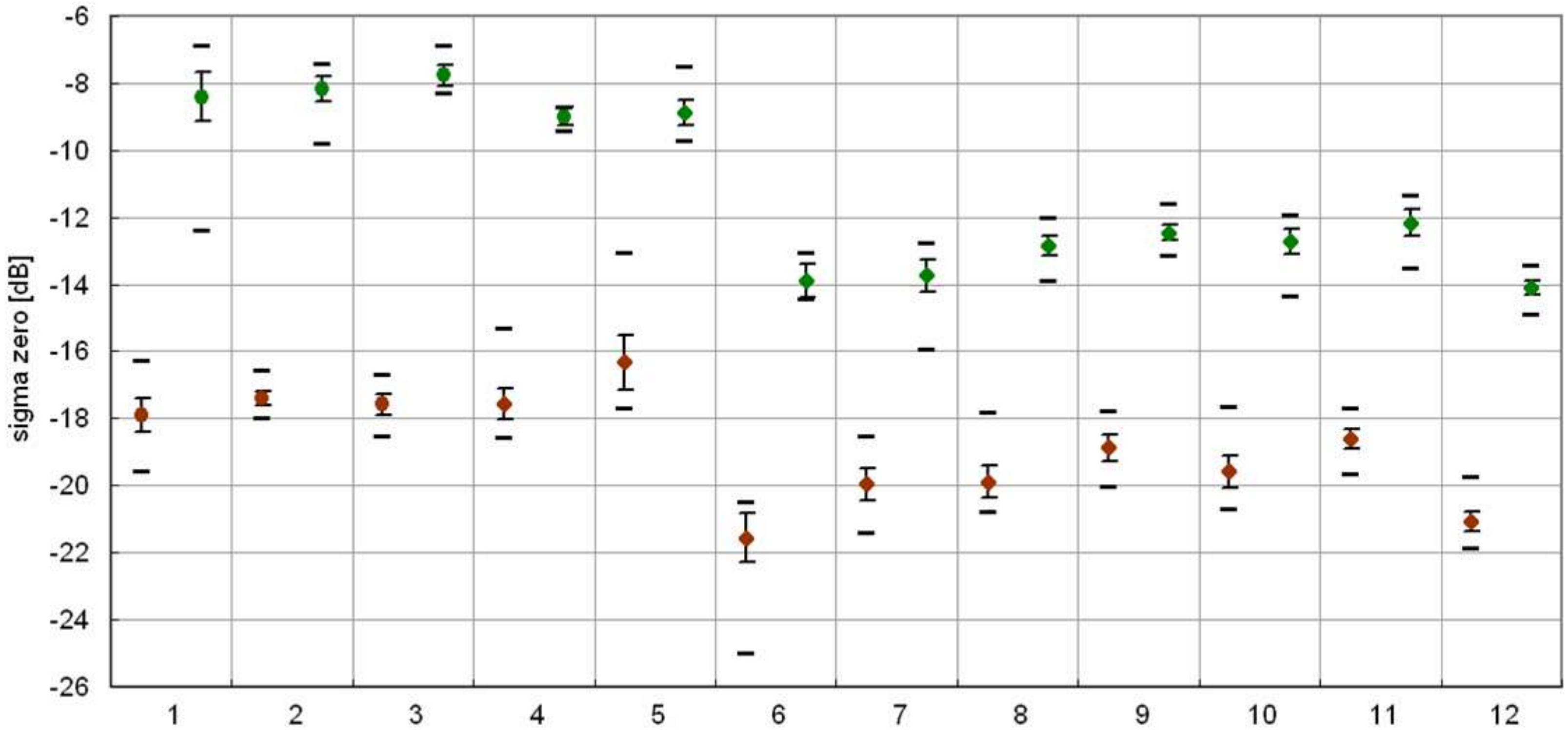

Class signatures basing on image objects including standard deviation and min/max: brown = clear cut (HH), green = forest (HH), X-axis labels test cases

Forest Clear-cut separability

date	mode	position	separability: pixel / object	
19MAY06	FBS	54°12'N 99°94'E	**0.97**	**1.00**
19MAY06	FBS	55°59'N 99°58'E	**0.99**	**1.00**
19MAY06	FBS	56°08'N 99°46'E	**0.99**	**1.00**
14AUG06	FBS	54°12'N 101°56'E	**0.99**	**1.00**
14AUG06	FBS	54°61'N 101°44'E	**0.93**	**1.00**
27DEC06	FBS	56°84'N 104°16'E	**0.94**	**1.00**
27DEC06	FBS	57°33'N 103°99'E	**0.93**	**1.00**
13JAN07	FBS	56°83'N 103°62'E	**0.97**	**1.00**
13JAN07	FBS	56°83'N 103°62'E	**0.94**	**1.00**
11FEB07	FBS	56°84'N 104°18'E	**0.95**	**1.00**
11FEB07	FBS	57°33'N 104°02'E	**0.93**	**1.00**
28FEB07	FBS	56°84'N 103°64'E	**0.96**	**1.00**

Analysis of PALSAR data – PLR

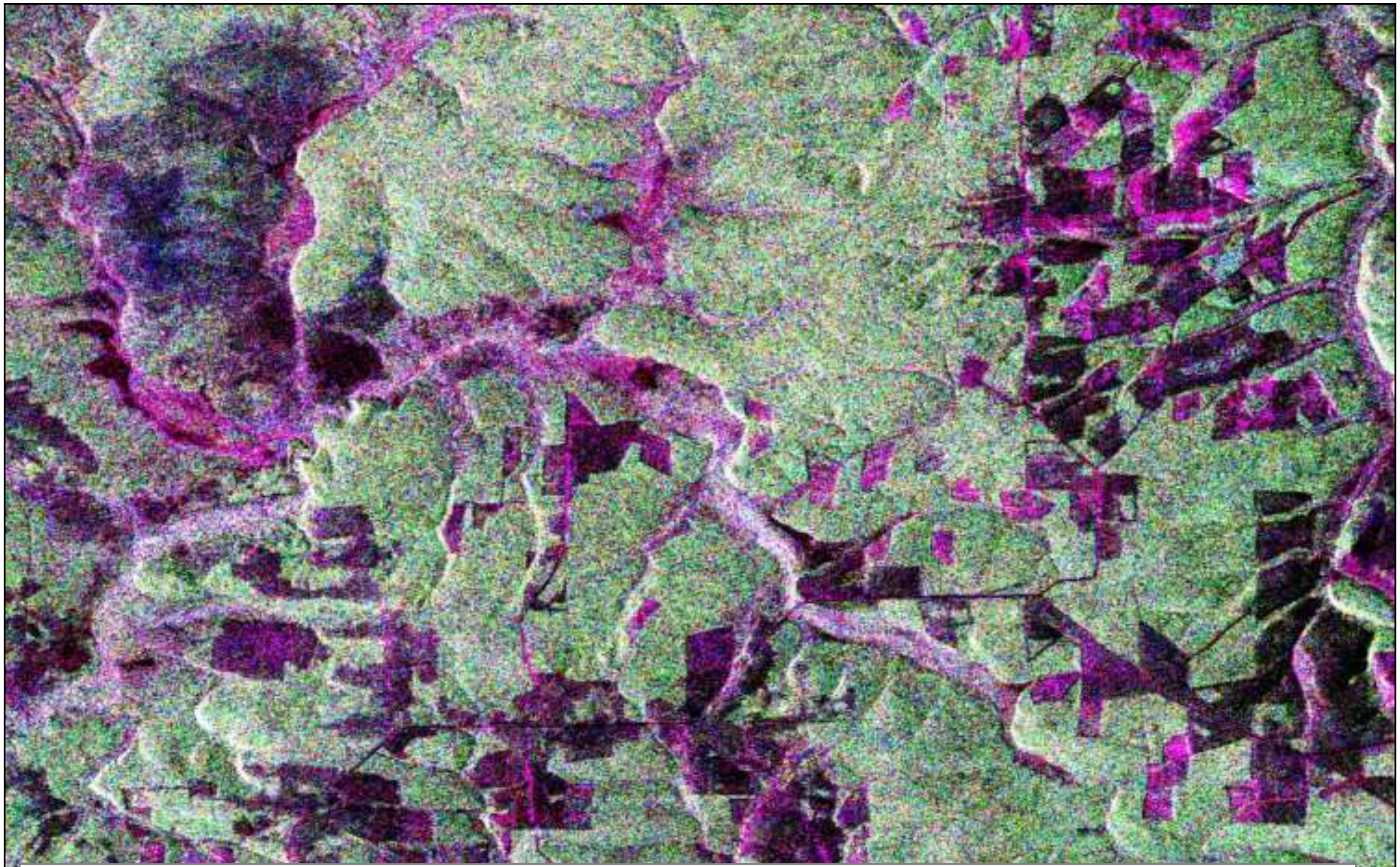

Subsection of ALOS PLR scene (HH/HV/VV RGB) taken over Siberia in August 2006

Analysis of PALSAR data – PLR

date	mode	position		
28AUG06	PLR	56°93’N 99°96’E		
28AUG06	PLR	57°42’N 99°78’E		
14SEP06	PLR	56°44’N 99°63’E		
14SEP06	PLR	54°12’N 101°56’E		
13OCT06	PLR	57°41’N 99°75’E		
17MAR07	PLR	56°45’N 99°67’E		
17MAR07	PLR	57°42’N 99°25’E		

Analysis of PALSAR data – PLR

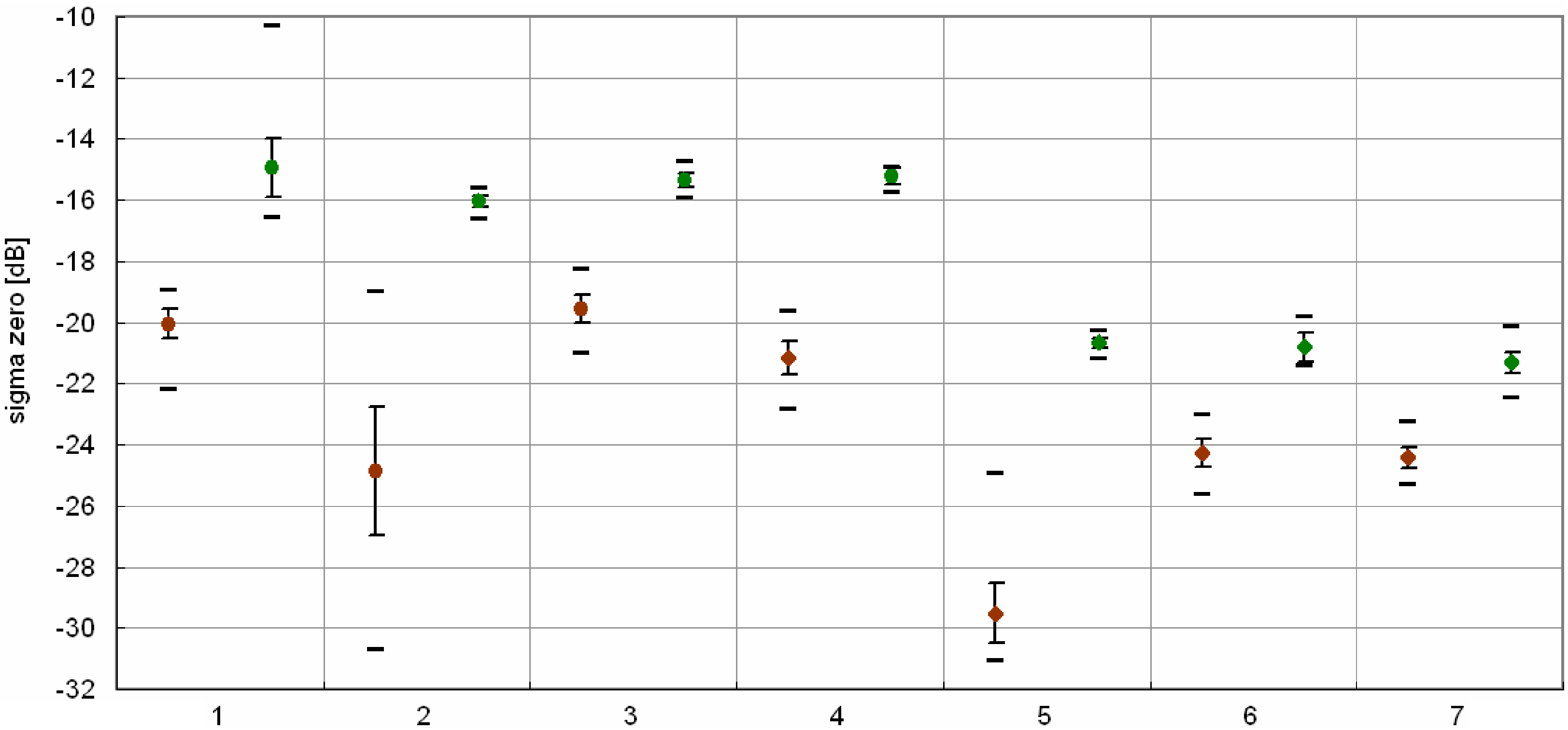

Class signatures basing on image objects including standard deviation and min/max: brown = clear cut (**HV**), green = forest (**HV**), X-axis labels test cases

Analysis of PALSAR data – PLR

date	mode	position	separability: pixel/object	
28AUG06	PLR	56°93'N 99°96'E	0.50 (HH) 0.88 (HV) 0.53 (VV)	1.00 (HH) 1.00 (HV) 1.00 (VV)
28AUG06	PLR	57°42'N 99°78'E	0.51 (HH) 0.93 (HV) 0.43 (VV)	1.00 (HH) 1.00 (HV) 1.00 (VV)
14SEP06	PLR	56°44'N 99°63'E	0.64 (HH) 0.85 (HV) 0.59 (VV)	0.86 (HH) 1.00 (HV) 0.82 (VV)
14SEP06	PLR	54°12'N 101°56'E	0.75 (HH) 0.94 (HV) 0.75 (VV)	1.00 (HH) 1.00 (HV) 1.00 (VV)
13OCT06	PLR	57°41'N 99°75'E	0.65 (HH) 0.99 (HV) 0.39 (VV)	1.00 (HH) 1.00 (HV) 1.00 (VV)
17MAR07	PLR	56°45'N 99°67'E	0.31 (HH) 0.74 (HV) 0.32 (VV)	0.92 (HH) 1.00 (HV) 0.92 (VV)
17MAR07	PLR	57°42'N 99°25'E	0.27 (HH) 0.71 (HV) 0.24 (VV)	0.83 (HH) 1.00 (HV) 0.81 (VV)

Analysis of PALSAR data – FBS Coherence (Winter)

Subsection of PALSAR FBS HH winter coherence, RGB= Coh/Int/Ratio Int.

Analysis of PALSAR data – FBS Coherence (Winter)

date	mode	position		
27DEC06 11FEB07	FBS Coh.	56°84’N 104°16’E		
27DEC06 11FEB07	FBS Coh.	57°33’N 103°99’E		
13JAN07 28FEB07	FBS Coh.	56°84’N 103°62’E		
13JAN07 28FEB07	FBS Coh.	57°33’N 103°45’E		
01JAN07 16FEB07	FBS Coh.	56°35’N 102°69’E		
01JAN07 16FEB07	FBS Coh.	56°84’N 102°54’E		

Analysis of PALSAR data – FBS Coherence (Winter)

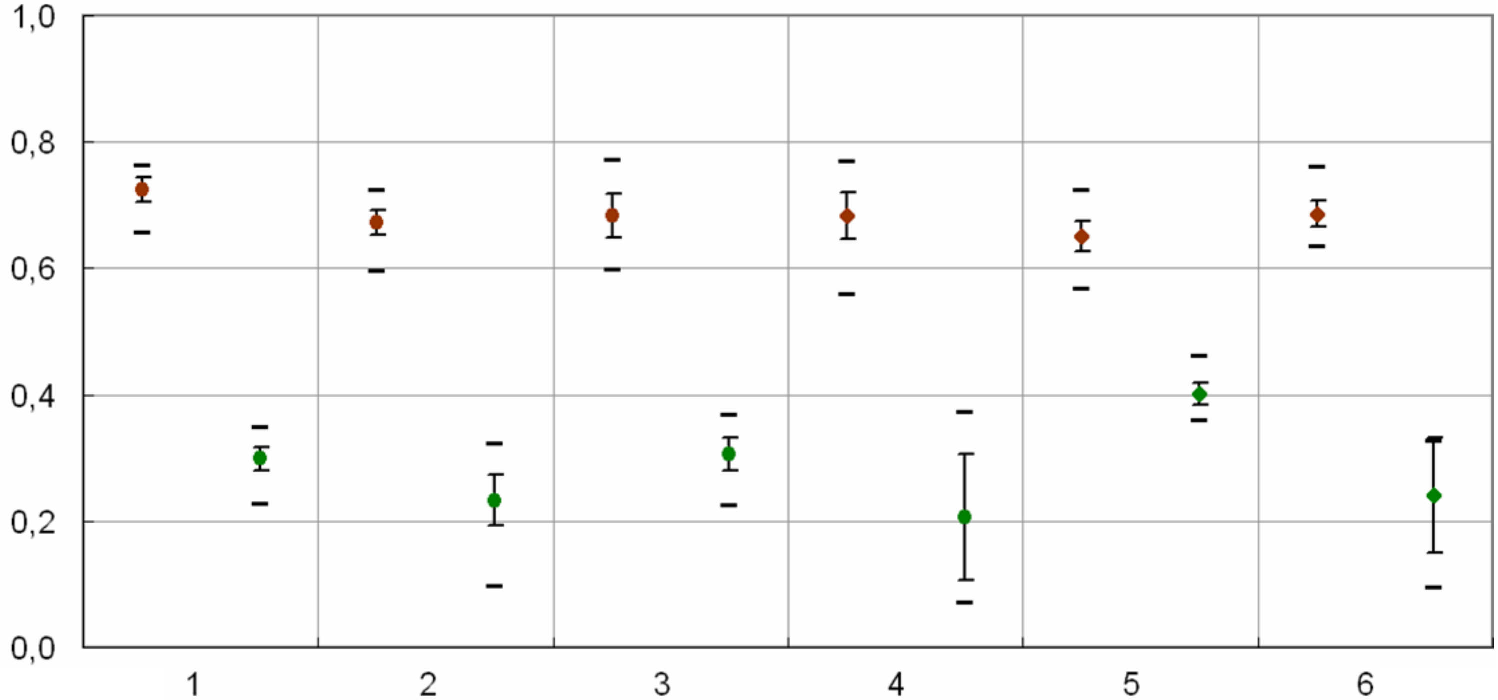

Class signatures basing on image objects including standard deviation and min/max: brown = clear cut (coherence), green = forest (coherence), X-axis labels test cases

Analysis of PALSAR data – FBS Coherence (Winter)

date	mode	position	separability: pixel / object	
27DEC06 11FEB07	FBS Coh.	56°84’N 104°16’E	0.99	1.00
27DEC06 11FEB07	FBS Coh.	57°33’N 103°99’E	0.99	1.00
13JAN07 28FEB07	FBS Coh.	56°84’N 103°62’E	0.98	1.00
13JAN07 28FEB07	FBS Coh.	57°33’N 103°45’E	0.98	1.00
01JAN07 16FEB07	FBS Coh.	56°35’N 102°69’E	0.98	1.00
01JAN07 16FEB07	FBS Coh.	56°84’N 102°54’E	0.99	1.00

Analysis of PALSAR data – FBS Coherence (Winter)

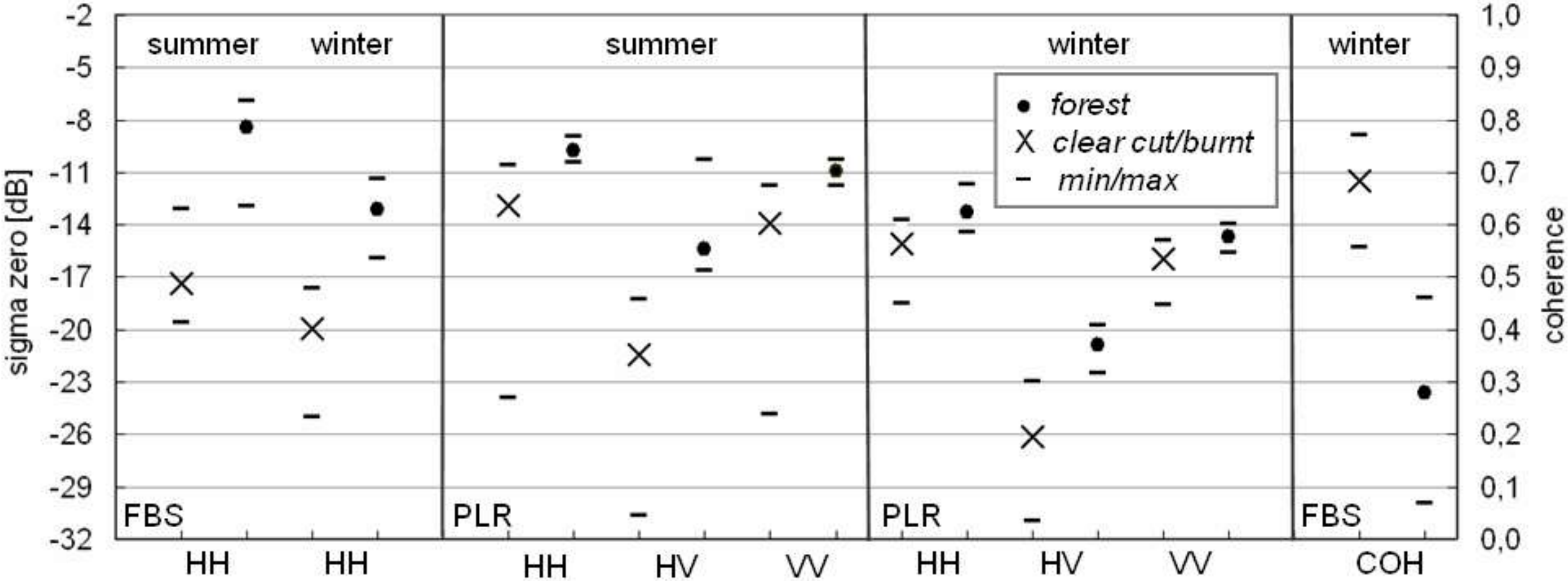

Object based signatures: forest, burnt/clear-cut

- ***Summer intensity seems slightly better suited than winter intensity***
- (Relatively ***poor separability basing on PLR intensity*** is ***owing to the higher noise and speckle effect*** and to the ***reduced resolution***

Value of Coherence

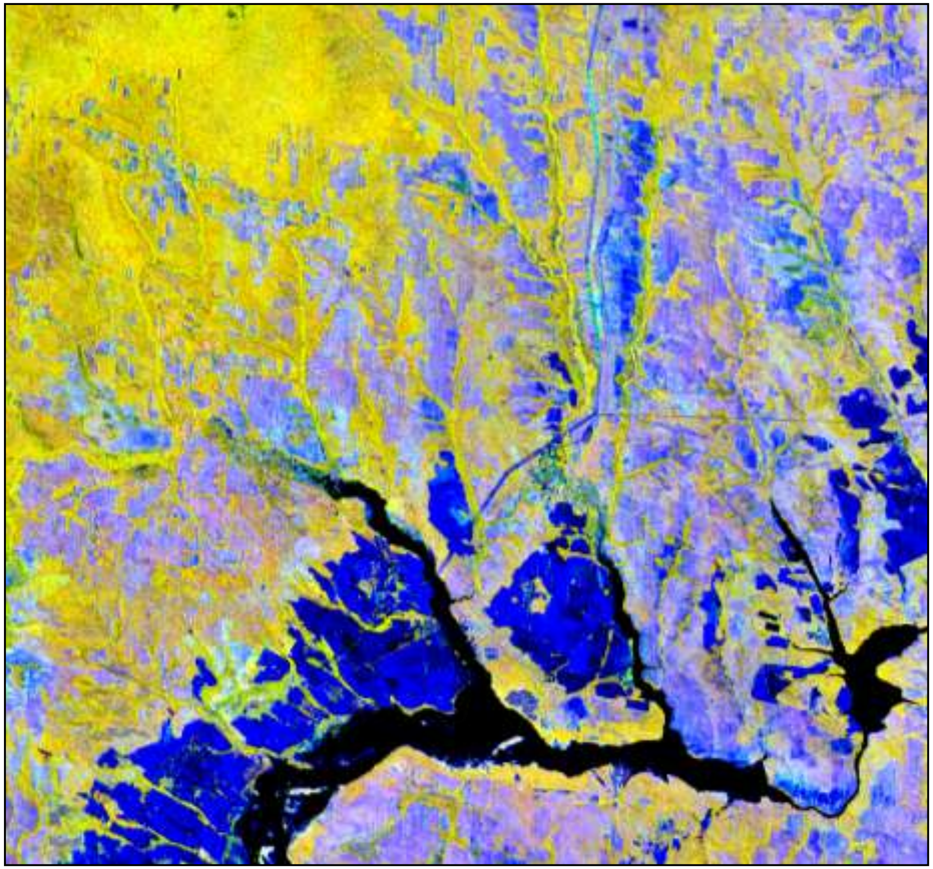

HV / HH / Coherence

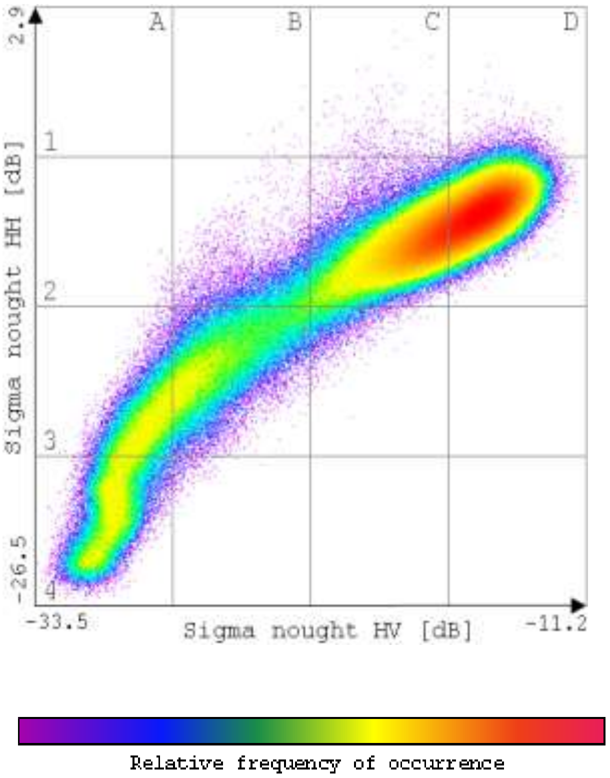

Value of Coherence

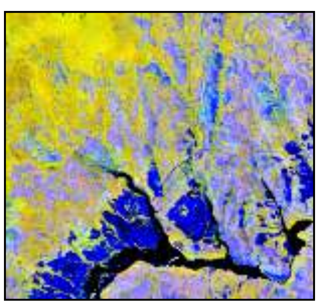

HV / HH / Coherence

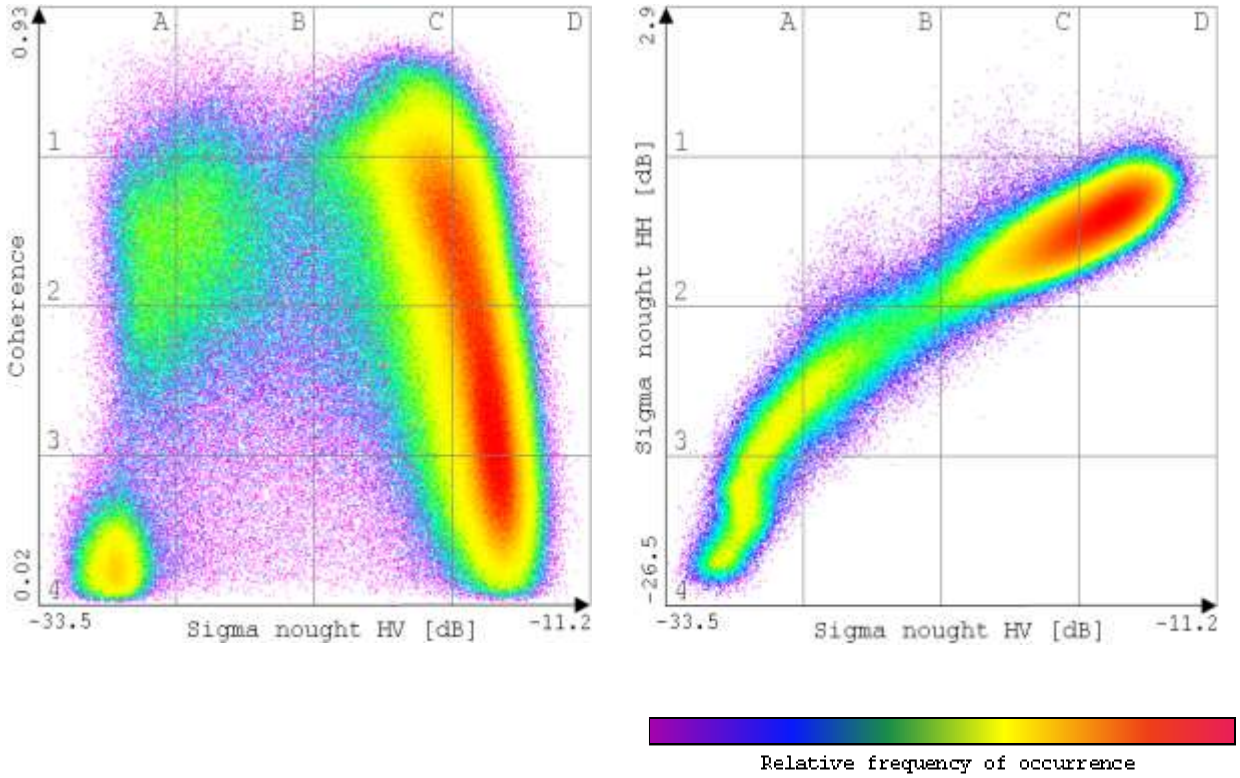

Power of Coherence

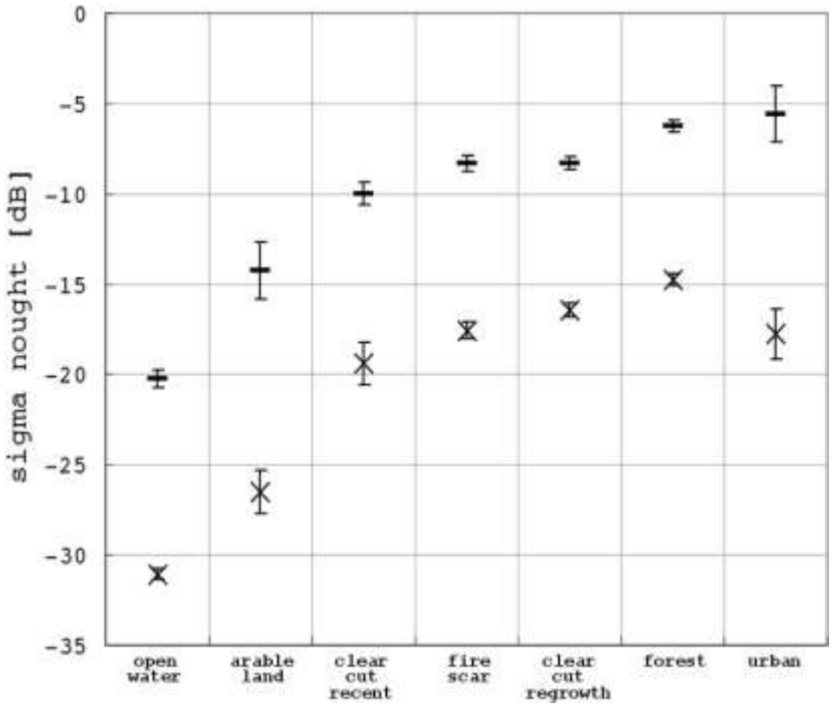

Signature plot for intensities HH (-) and HV (x)

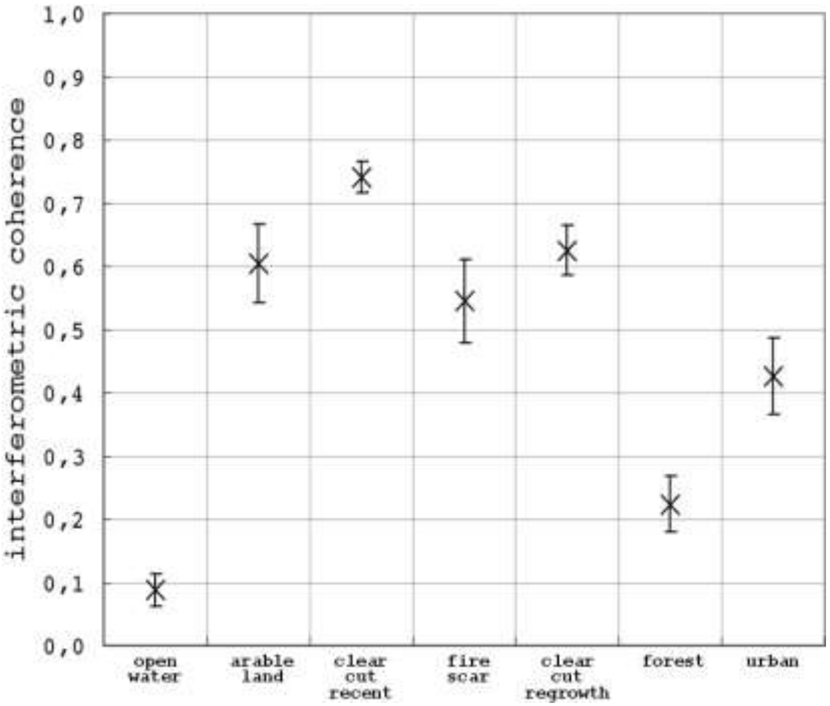

Signature plot for interferometric coherence

Forest Cover Mapping Using Intensity and Coherence

- This initial investigation was carried out in the framework of GSE Forest Monitoring
- Summer intensity and winter coherence images are used

- Intensities (FBD HH/HV) have been acquired during summer 2007 (K&C intensity stripes)

- For coherence estimation standard level 1.1 FBS scenes were applied
- 43 pairs have been acquired during winters 2006/2007 (cycles 8 & 9) and 2007/2008 (cycles 16 & 17)
- Each pair stems from consecutive cycles (46 days temporal baseline)
- During both winters suited weather conditions have been reported

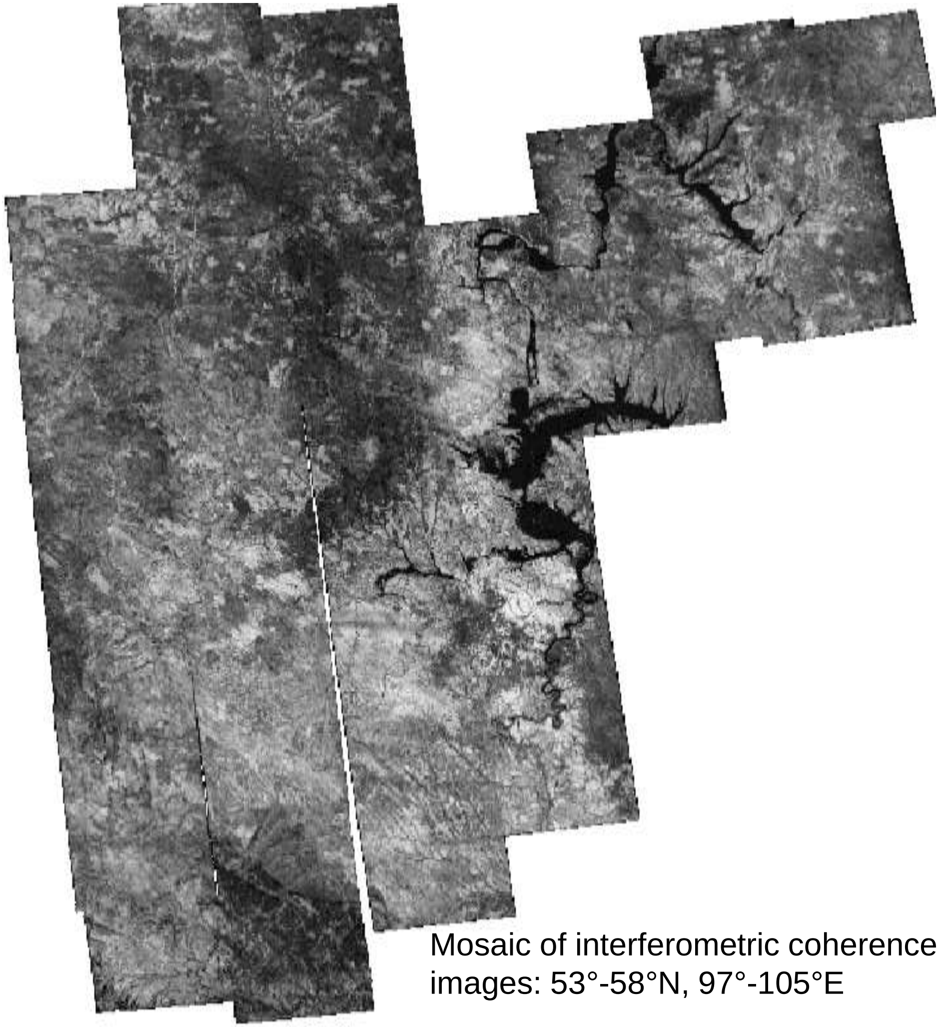

Mosaic of interferometric coherence images: 53°-58°N, 97°-105°E

Forest Cover Mapping Using Intensity and Coherence

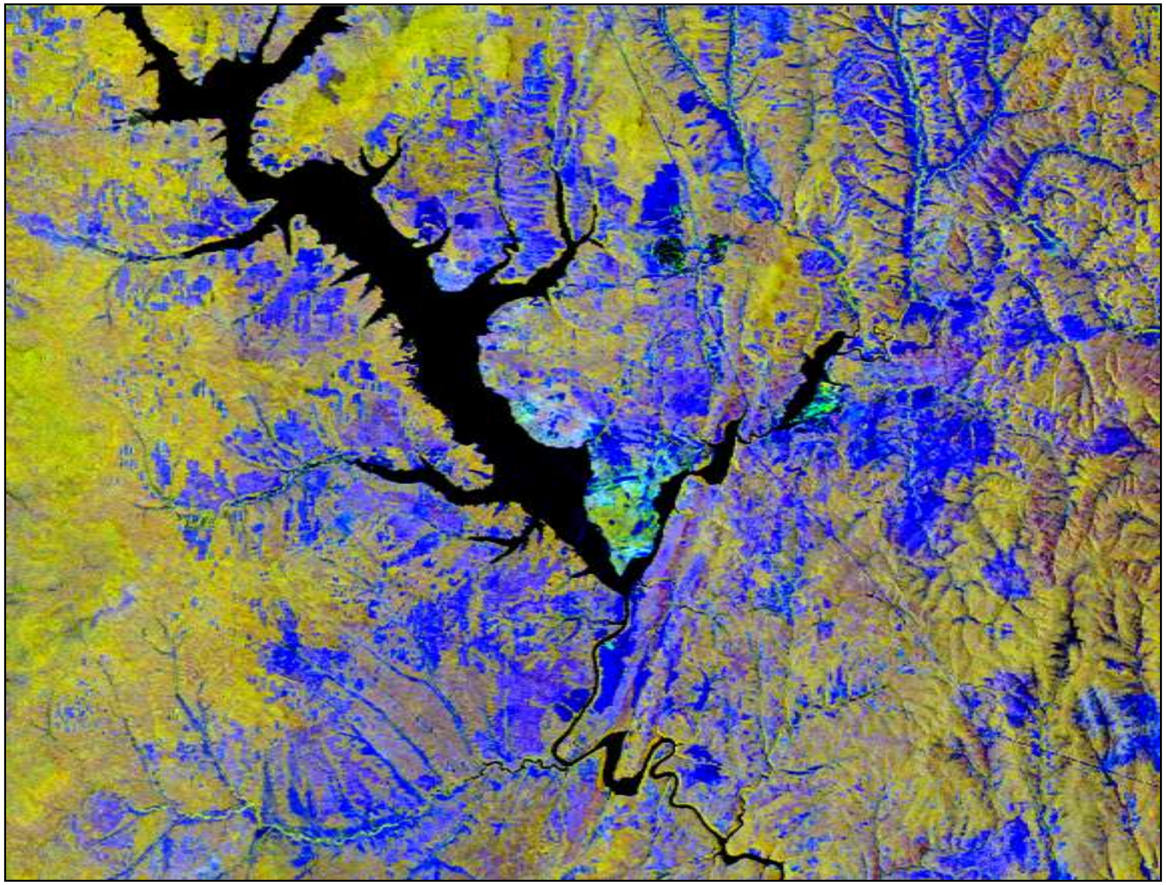

Composite of HV & HH backscatter and winter coherence for a subset of the monitoring area (taken from north-eastern section)

Test area (light green patch, right image) in the centre of the prototype area

Forest Cover Mapping Using Intensity and Coherence

- Classification is based on image segments (multiresolution segmentation algorithm)
- Nearest Neighbor algorithm was used
- Defined target classes: forest, very low biomass forest and non-forest
- For each class 20 samples have been selected

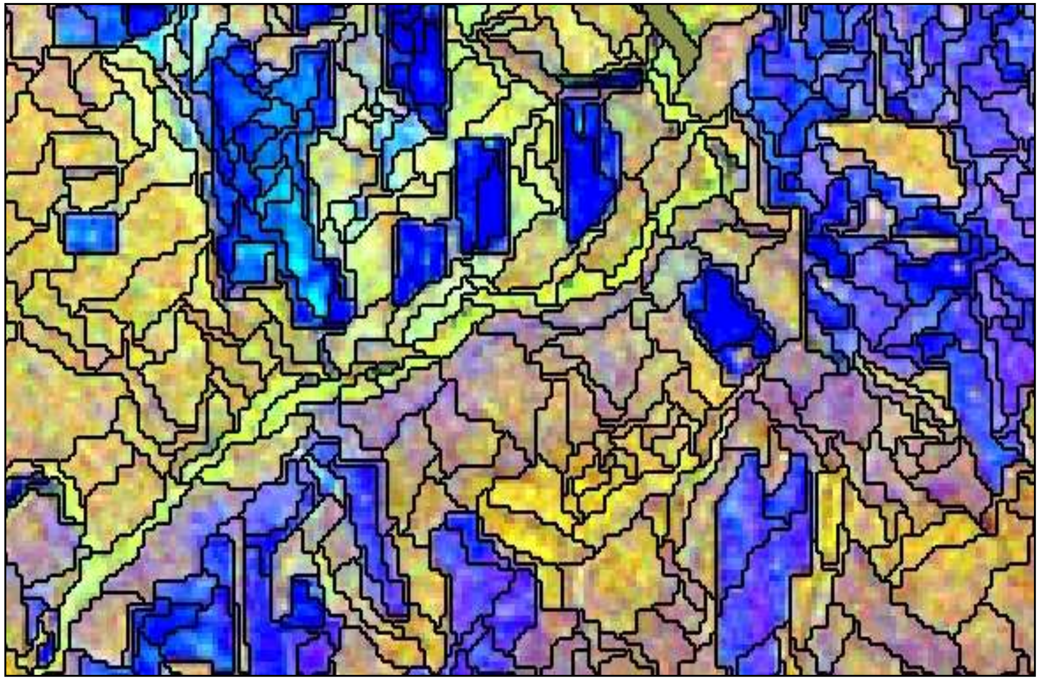

Example of segmented dataset

Forest Cover Mapping Using Intensity and Coherence

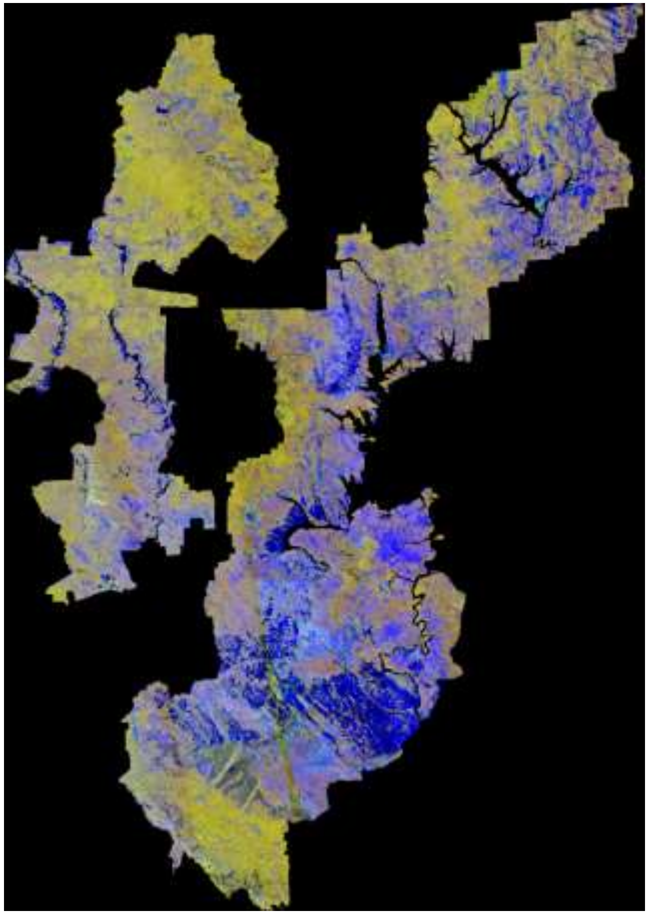

SAR data (HV/HH/Coherence)

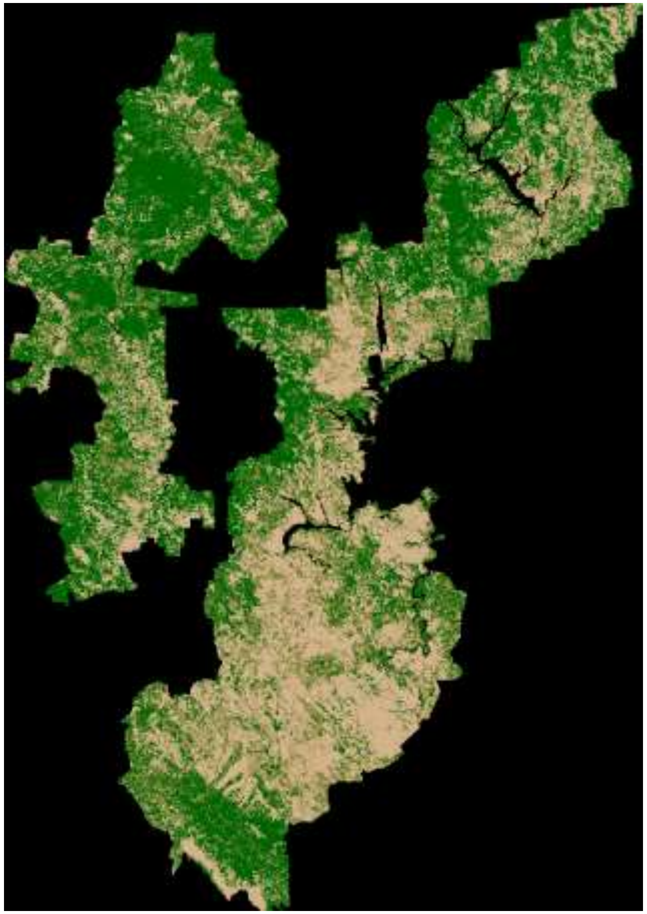

Map (forest: green, very low biomass forest: brownish green, non-forest: light brown)

Forest Cover Mapping Using Intensity and Coherence

- The accuracy assessment for the whole monitoring area is basing on 1,000 point samples
- The random sampling was stratified by class proportion
- Overall accuracy: 90.87%.

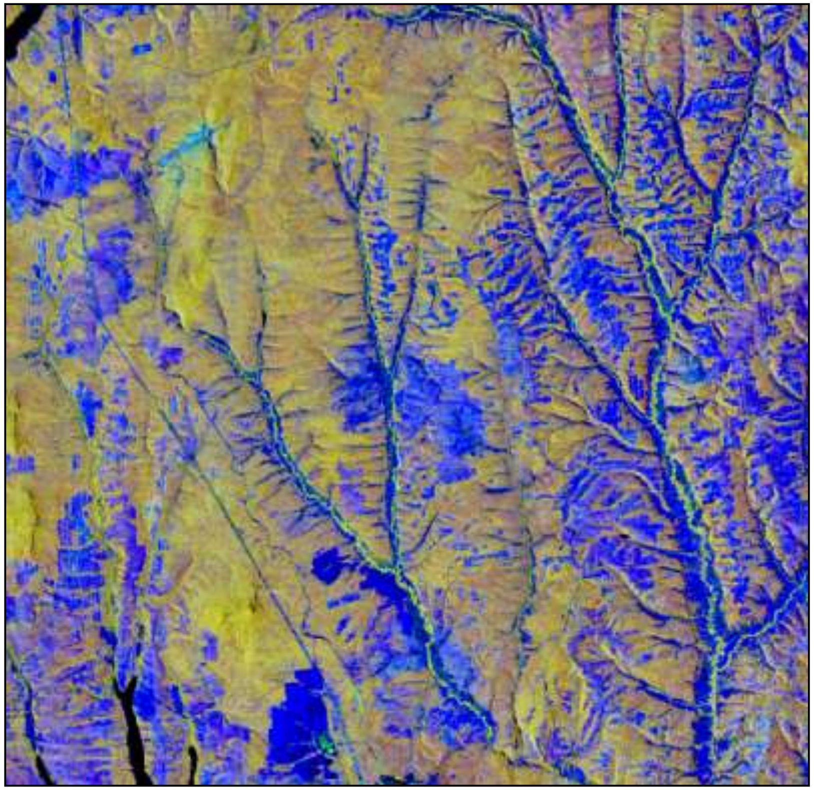

SAR data (HV/HH/Coherence)

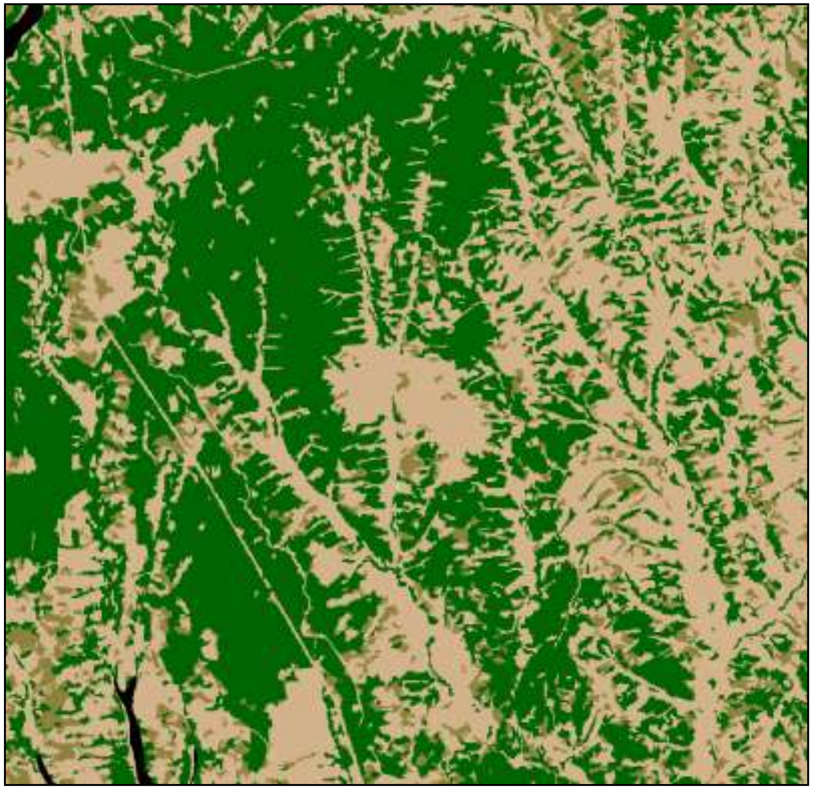

Map (forest: green, very low biomass forest: brownish green, non-forest: light brown)

Forest Cover Mapping using Coherence and Backscatter

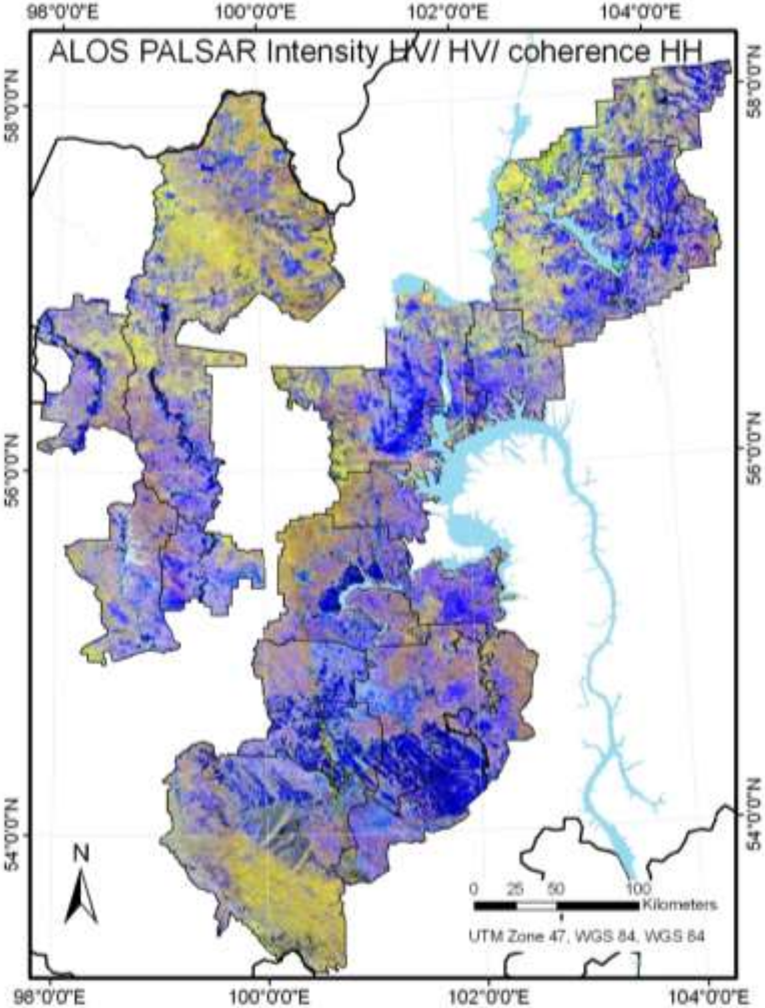

HH/HV/Coherence

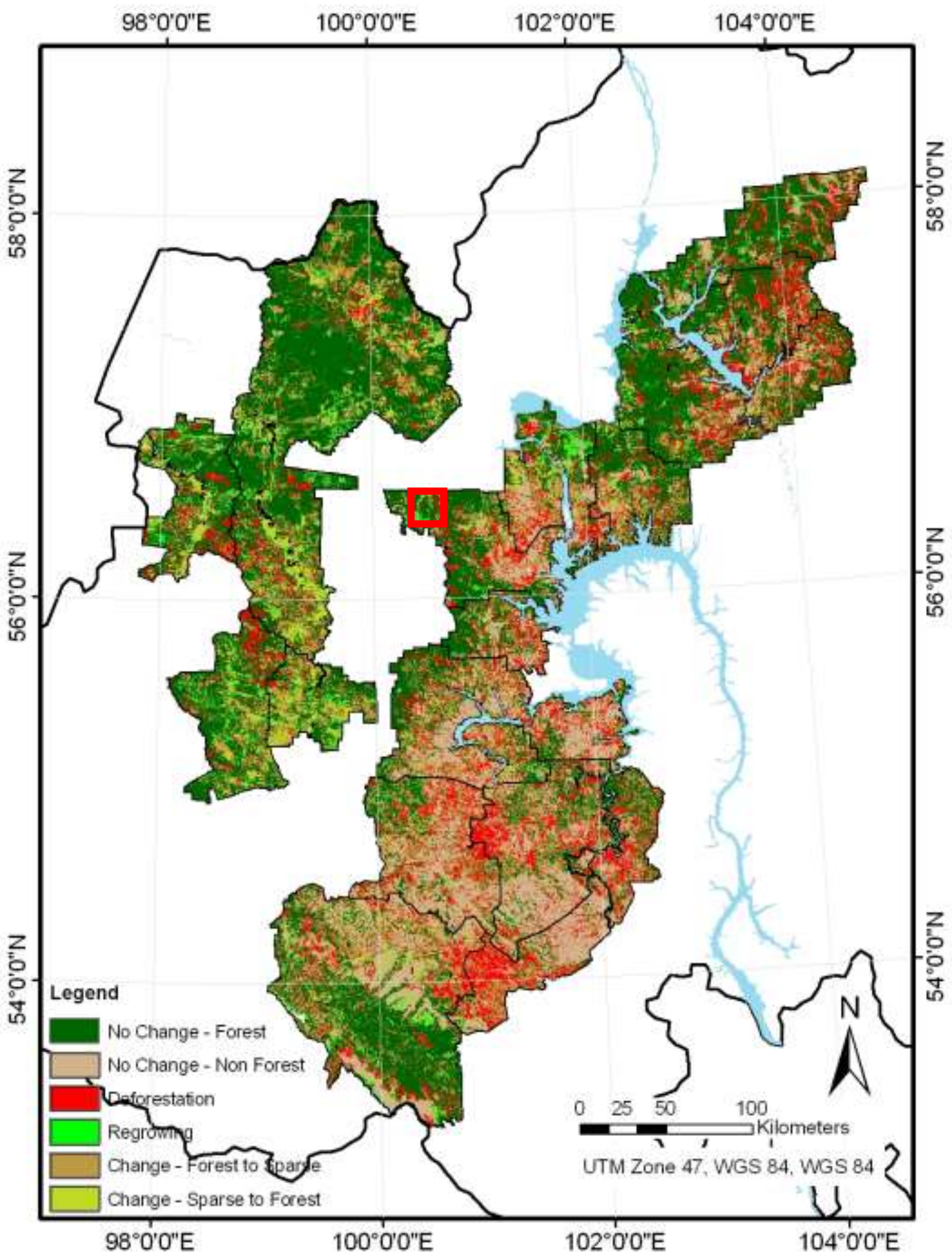

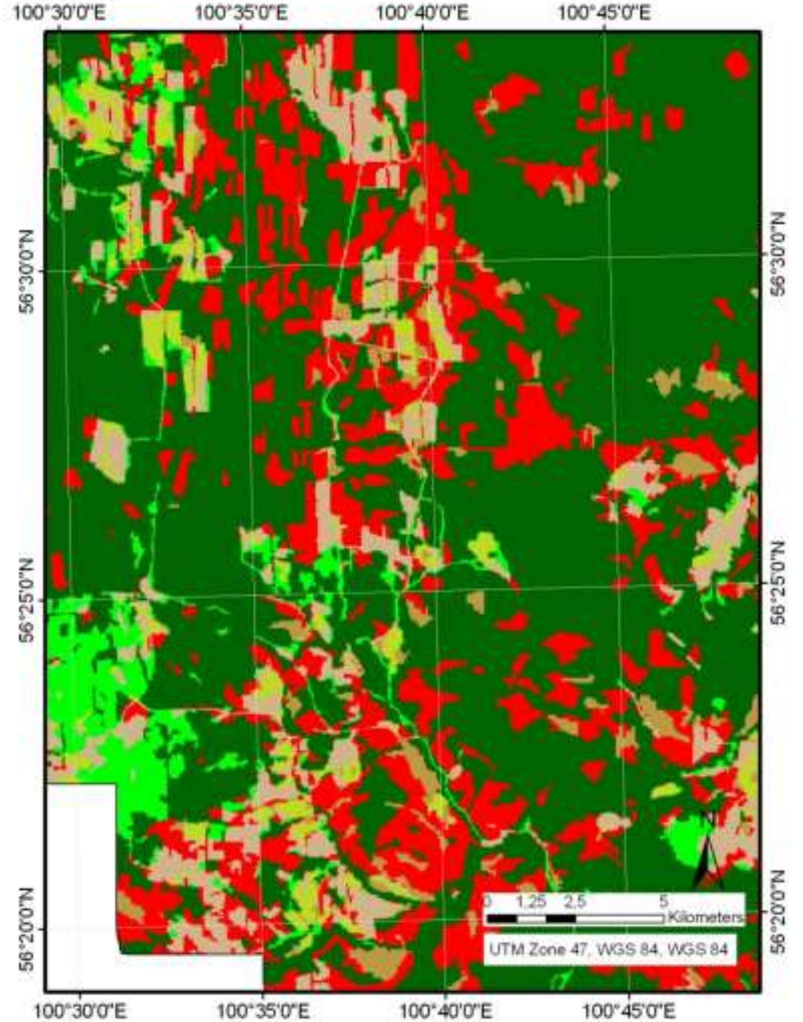

Final Map Product of ESA-Project GSE Forest Monitoring

Is X-band backscatter useful for forest applications?

Is X-band backscatter useful for forest applications?

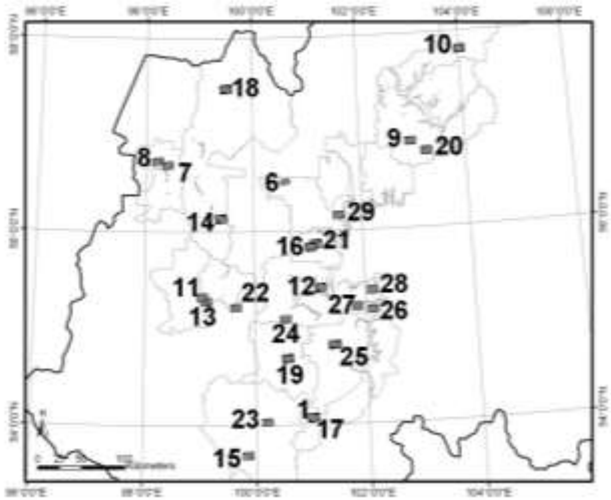

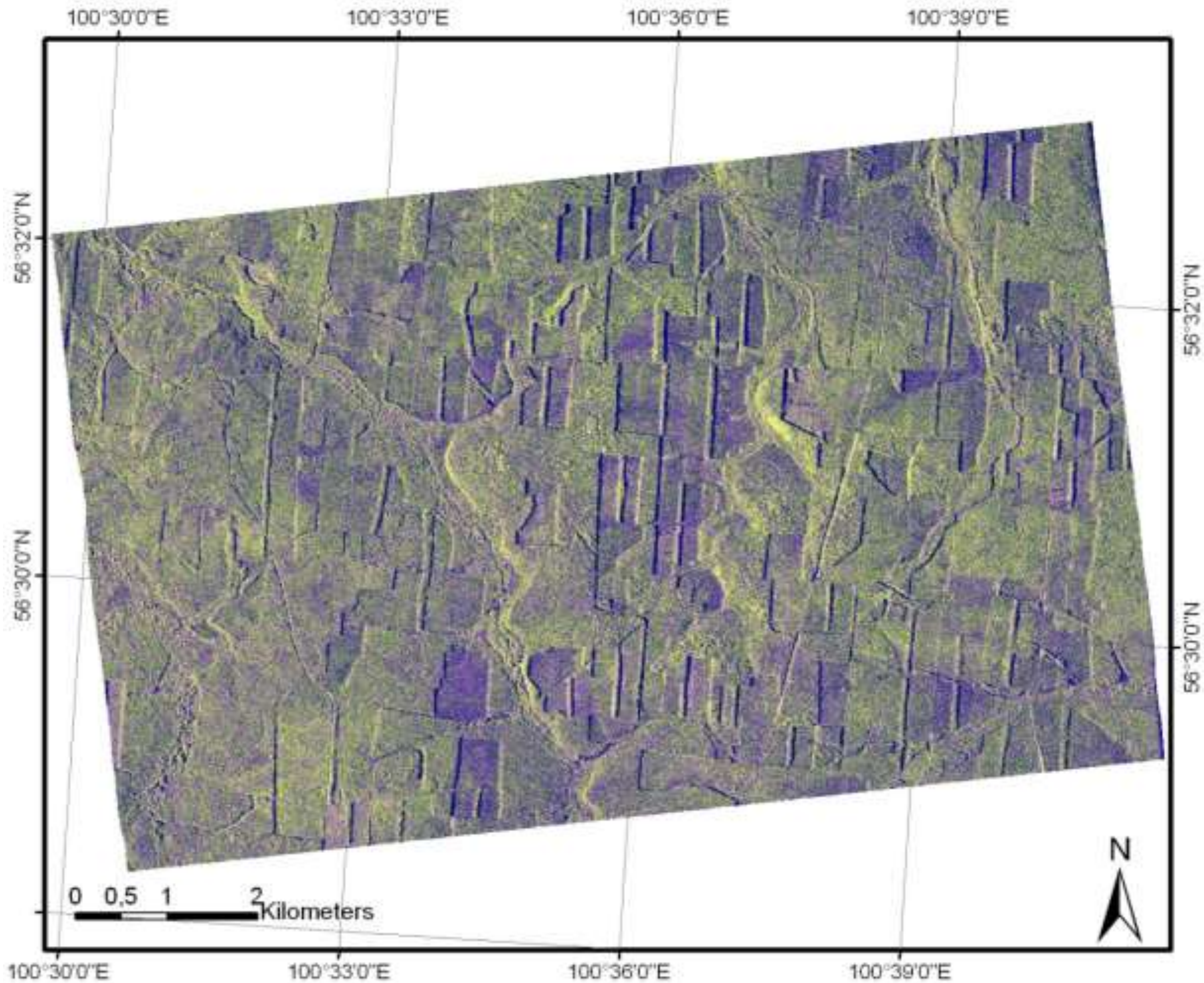

Validation with TerraSAR-X

Is X-band backscatter useful for forest applications?

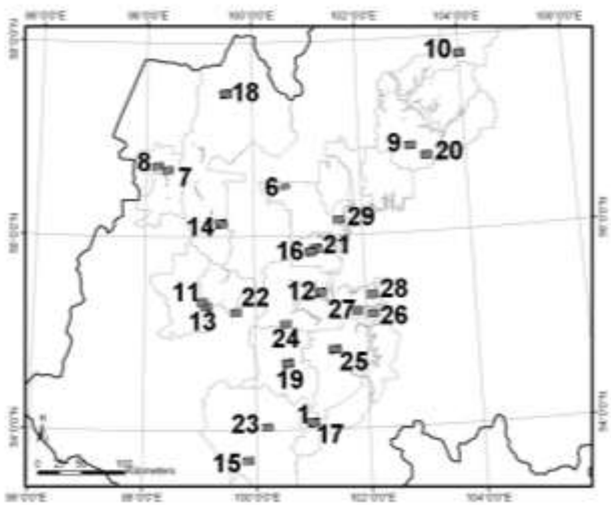

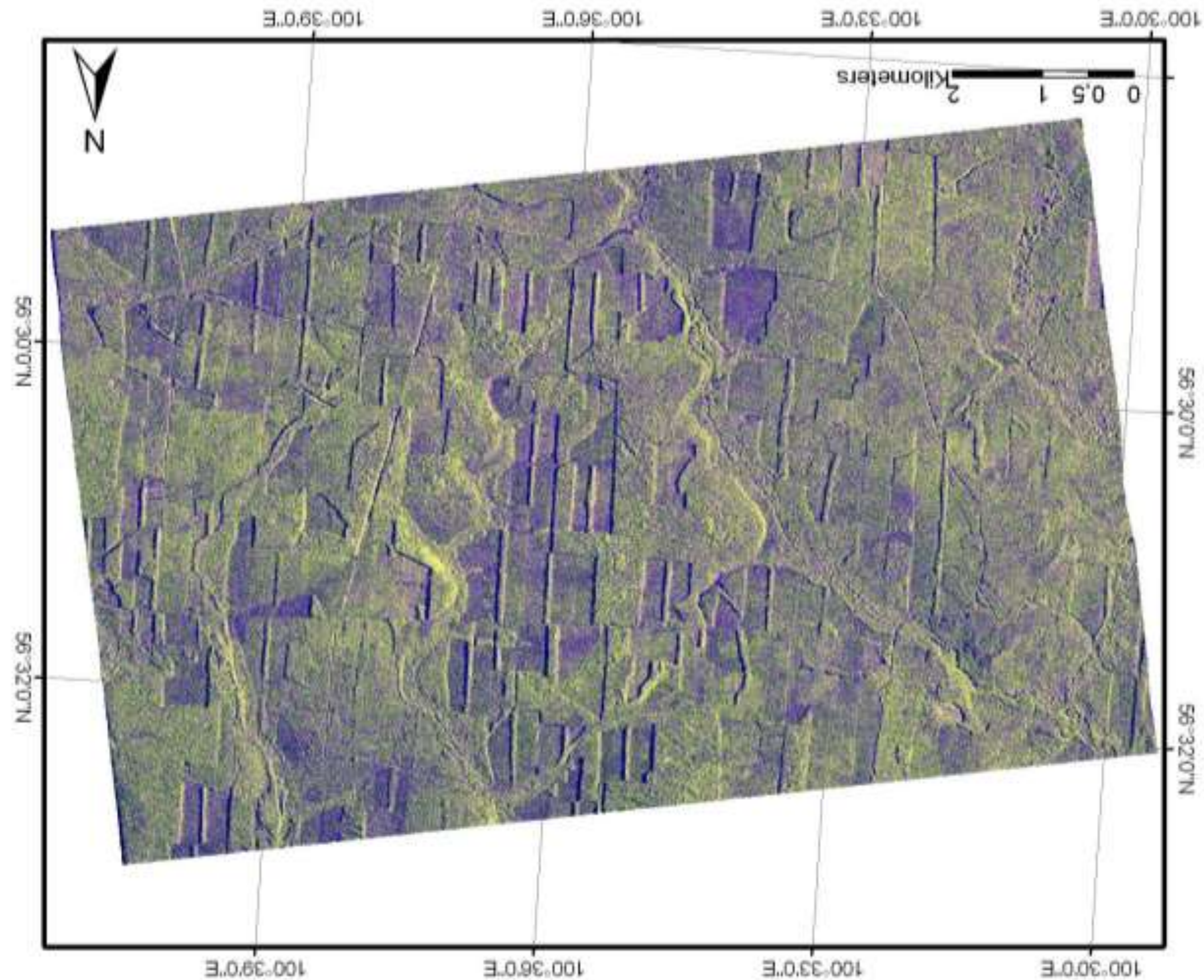

Validation with TerraSAR-X

Is X-band backscatter useful for forest applications?

- Method: Stratified Random Sampling Points
- Reference 25 High Resolution Spotlight TerraSAR-X Data randomly spread over the study area
- Minimum of 5 sampling points per class

	Producers Accuracy [%]	Users Accuracy [%]
Non Forest	***92.6***	***90.9***
Forest	***95.1***	***92.3***
Sparse Forest	***92.6***	***96.6***

Outline

1. Introduction: Why Forest Observation?
2. SAR Techniques of interest for forestry applications
3. SAR for Forestry Applications – Some Basics
4. Forest Cover and Biomass Mapping – Excurses
    1. BIOMASAR – Hypertemporal C-band Data Assimilation
    2. Forest Cover Mapping Using Backscatter and Coherence
    3. Forest Biomass Mapping Using Backscatter and Coherence
    4. Polarimetry for Forest Cover Mapping
    5. INSAR Phase and Tree Height
    6. Seasonality of C-band Backscatter in Siberia
    7. Seasonality of Coherence in Siberia
    8. X-band coherence over the Thuringian Forest
    9. Mapping of woody cover in KNP using L-band backscatter

Demonstrating the Potential of ALOS PALSAR **Backscatter and INSAR Coherence** for Growing Stock Volume Estimation in Central Siberia

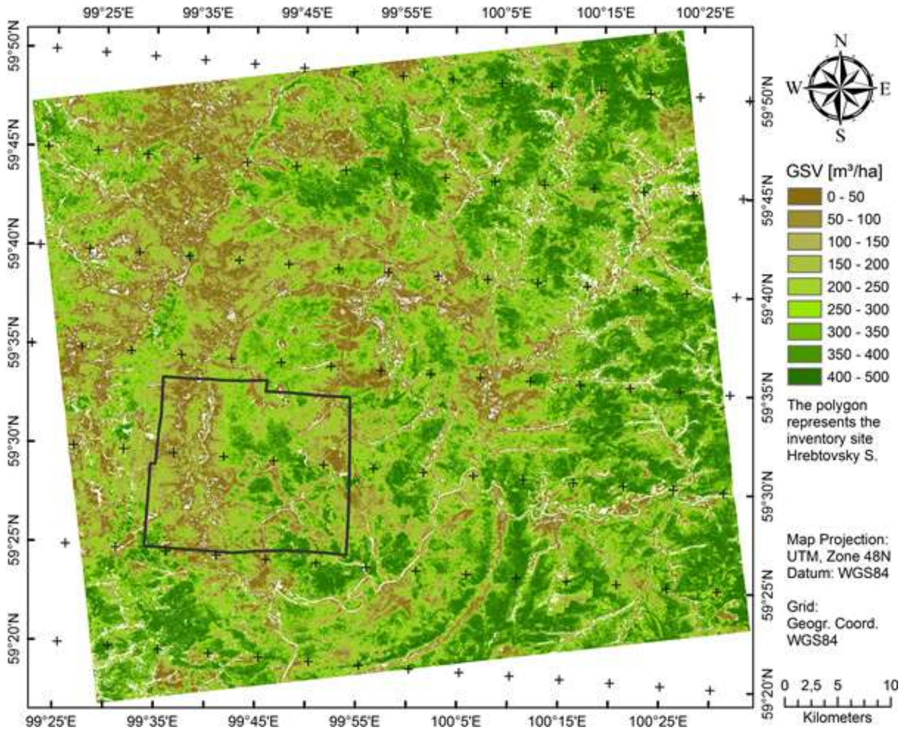

seit 1558

Christian Thiel

Christiane Schmullius

Friedrich-Schiller-University Jena, Germany

Motivation

Backscatter

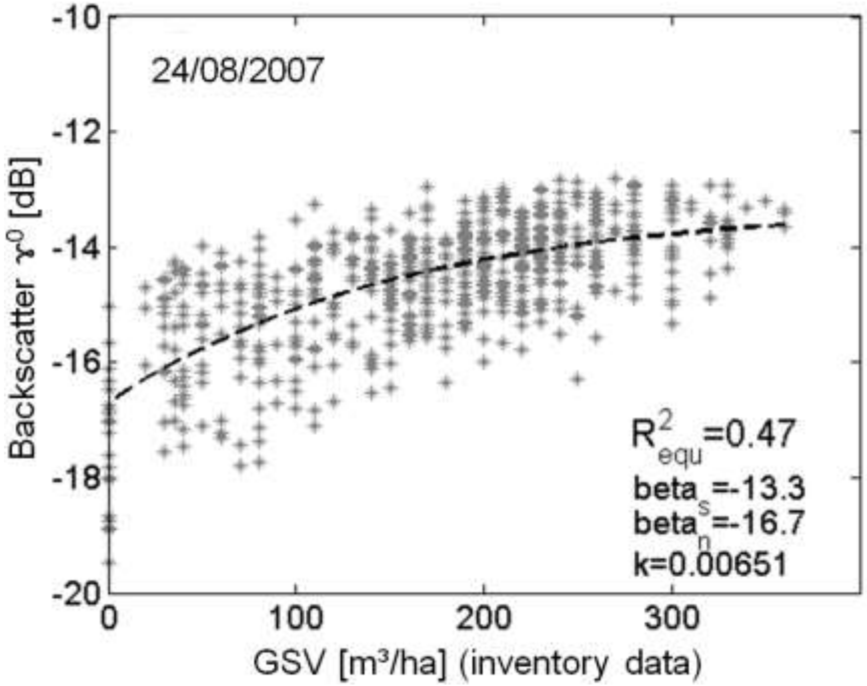

InSAR Coherence

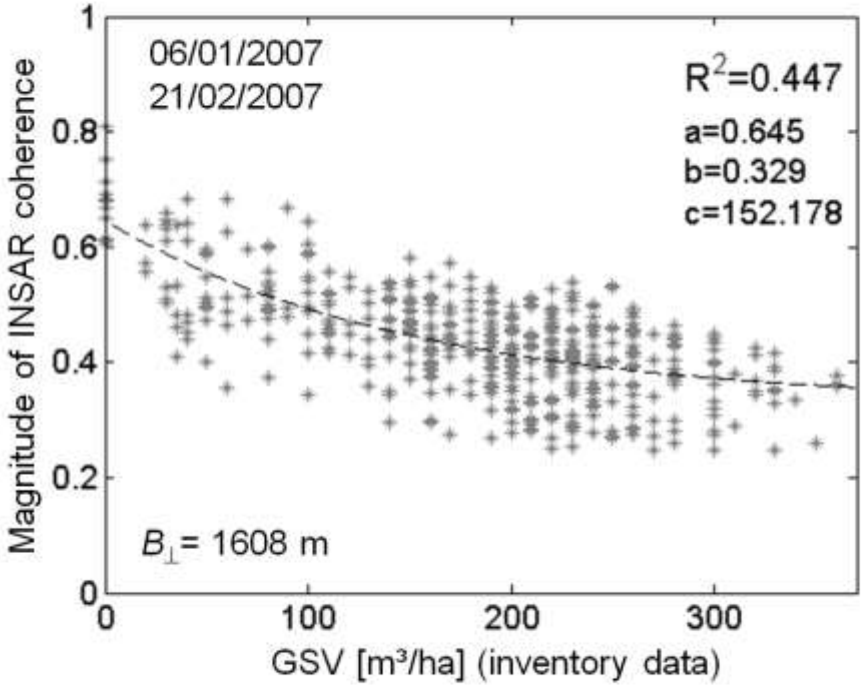

Radar backscatter and coherence as function of GSV for the inventory site Hrebtovsky S. The backscatter image (HV) polarisation was acquired at unfrozen conditions, while the data for the coherence image was acquired at frozen conditions.

Forest Cover Mapping Using Intensity and Coherence

- The accuracy assessment for the whole monitoring area is basing on 1,000 point samples
- The random sampling was stratified by class proportion
- Overall accuracy: 90.87%.

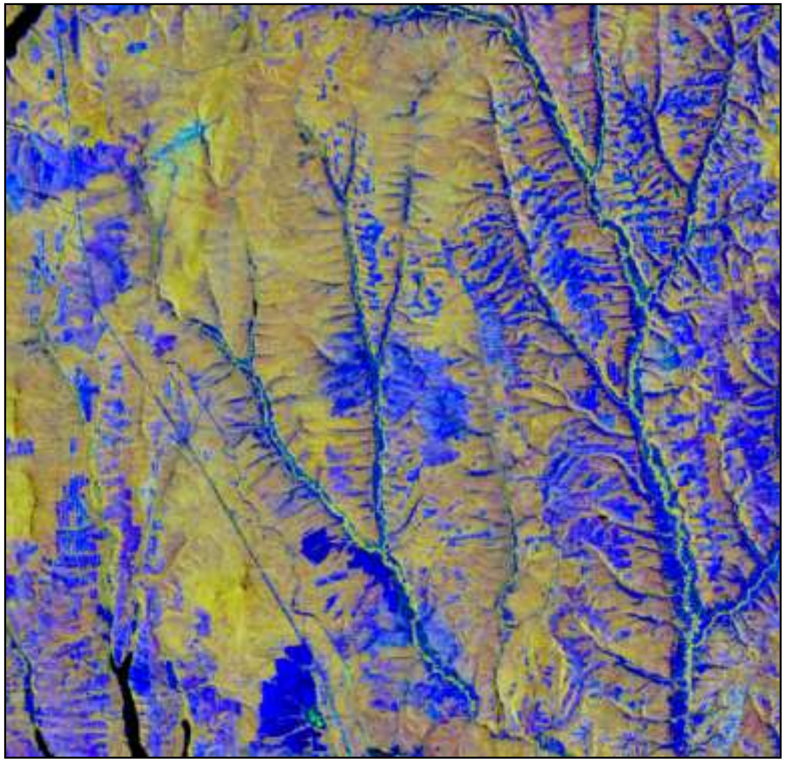

SAR data (HV/HH/Coherence)

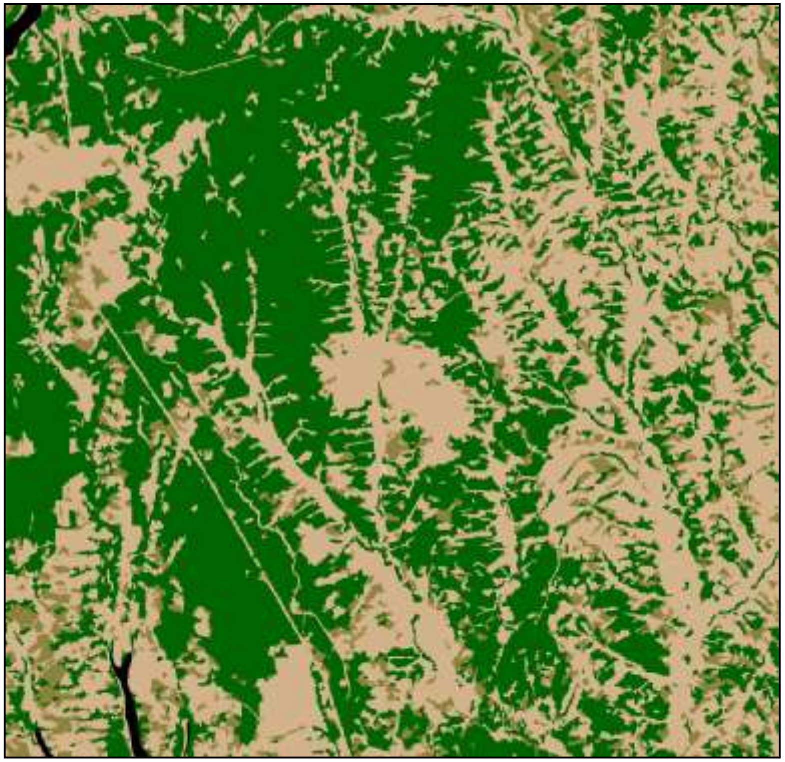

Map (forest, very low biomass forest, non-forest)

Outline

1. Area and test sites
2. PALSAR data
3. Summary of observations
4. Map generation approach
5. Results
6. Conclusions

Test Site

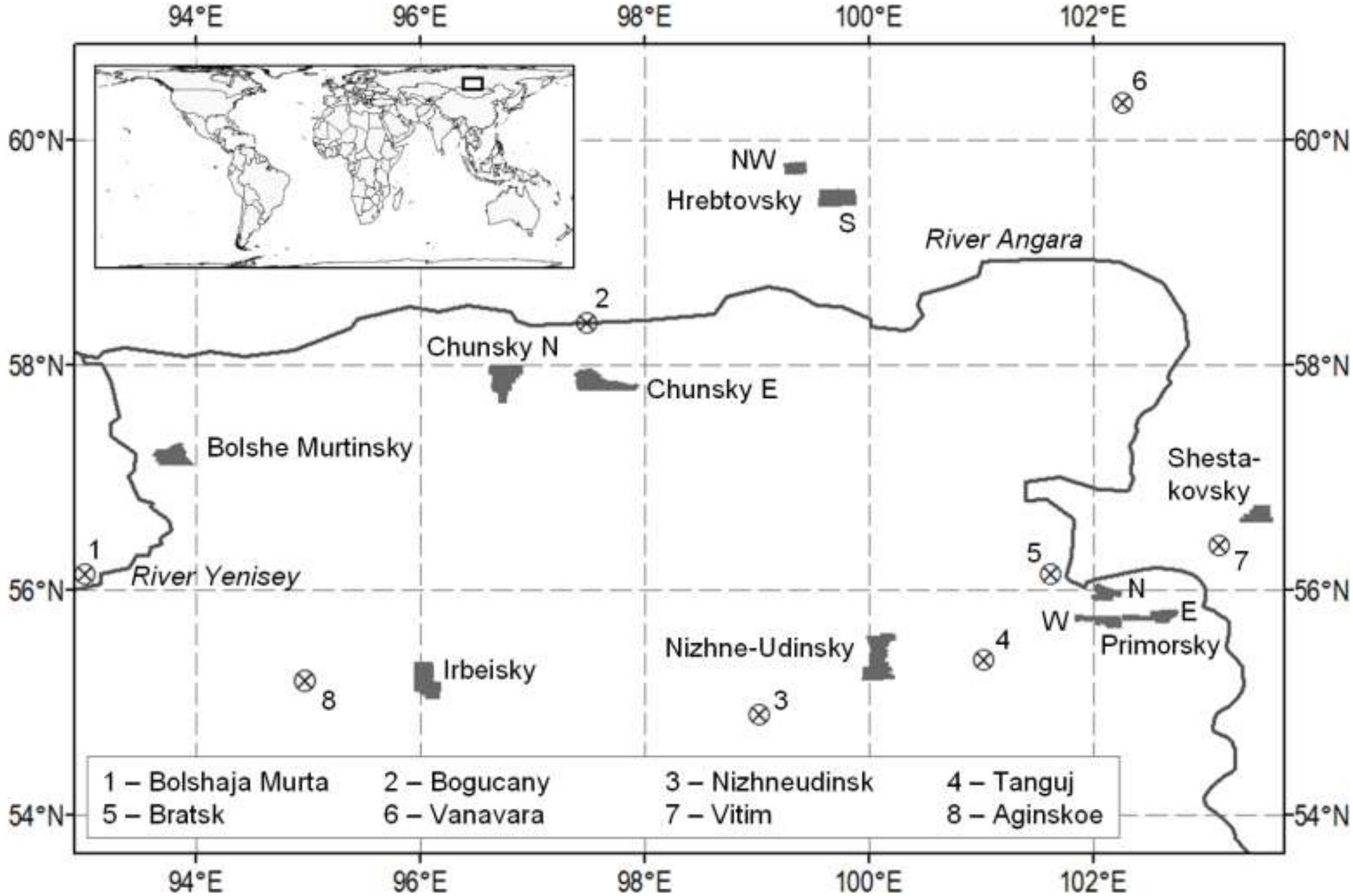
94°E
96°E
98°E
100°E
102°E
60°N
58°N
56°N
54°N
NW
Hrebtovsky
S
River Angara
2
Chunsky N
Chunsky E
Bolshe Murtinsky
Shesta-
kovsky
1
River Yenisey
5
7
6
N
W
E
Primorsky
4
Nizhne-Udinsky
Irbeisky
8
3
1 – Bolshaja Murta
2 – Bogucany
3 – Nizhneudinsk
4 – Tanguj
5 – Bratsk
6 – Vanavara
7 – Vitim
8 – Aginskoe

Site Characteristics

- Middle Siberian Plateau: southern part is dominated by hills up to 1700 m, northern part is plain with heights up to 500 m
- Continental climate, prec. 400-450 mm/y, most of the precipitation occurs in summer
- Territory is characterised by large area changes of forests such as forest fire, insect outbreaks, and intensive human activities
- Characteristic taiga forests (birch, pine, fir, aspen, larch, spruce, cedar) cover about 82% of the region

Site Characteristics

- Middle Siberian Plateau: southern part is dominated by hills up to 1700 m, northern part is plain with heights up to 500 m
- Continental climate, prec. 400-450 mm/y, most of the precipitation occurs in summer
- Territory is characterised by large area changes of forests such as forest fire, insect outbreaks, and intensive human activities
- Characteristic taiga forests (birch, pine, fir, aspen, larch, spruce, cedar) cover about 82% of the region

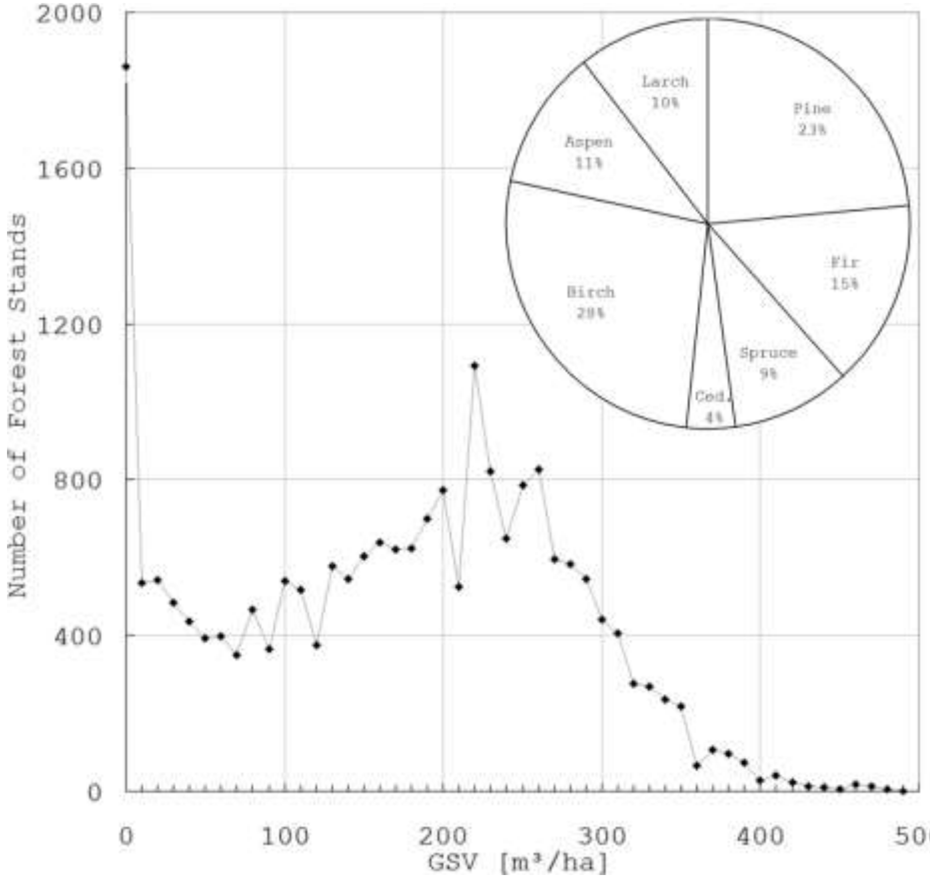

SAR data set

Location	Chunsky N	Chunsky E	Primorsky	Bolshe	Shesta.	Nizhne	Irbeisky	Hrebt.
2006	—	30 Dec	—	28 Dec	—	—	—	—
2007	***20 Jun***	14 Feb	18 Jan	12 Feb	13 Jan	11 Jan	***10 Aug***	6 Jan
	5 Aug	***2 Jul***	5 Mar	***15 Aug***	28 Feb	26 Feb	**10 Nov**	21 Feb
	20 Sep	***17 Aug***	***21 Jul***	***30 Sep***	***16 Jul***	***14 Jul***	26 Dec	***9 Jul***
	5 Nov	***2 Oct***	***5 Sep***	31 Dec	***31 Aug***	***14 Oct***	—	***24 Aug***
	21 Dec	**17 Nov**	***21 Oct***	—	***16 Oct***	—	—	***9 Oct***
2008	5 Feb	2 Jan	21 Jan	15 Feb	16 Jan	29 Feb	10 Feb	9 Jan
	22 Mar	17 Feb	—	***2 Jul***	2 Mar	***16 Jul***	***27 Jun***	24 Feb
	7 May	***4 Jul***	—	***17 Aug***	***17 Apr***	***31 Aug***	***12 Aug***	***11 Jul***
	22 Jun	***19 Aug***	—	—	***18 Jul***	—	28 Dec	***26 Aug***
	7 Aug	—	—	—	***2 Sep***	—	—	—
2009	—	4 Jan	—	2 Jan	18 Jan	16 Jan	12 Feb	11 Jan
	—	19 Feb	—	17 Feb	5 Mar	3 Mar	***30 Jun***	26 Feb
	—	—	—	—	***21 Jul***	—	***15 Aug***	***14 Jul***
	—	—	—	—	***5 Sep***	—	***30 Sep***	***29 Aug***
	—	—	—	—	***21 Oct***	—	—	***14 Oct***

- PALSAR L-band (1,27 GHz) data
- 87 acquisitions, mode: FBS ***FBD***
- Approx. 300 interferograms
- FBS: HH (28 MHz), FBD; HH/HV (14 MHz)
- Repetition rate: 46 days

Outline

1. Area and test sites
2. PALSAR data
3. Summary of observations
4. Map generation approach
5. Results
6. Conclusions

Experimental data – Summary

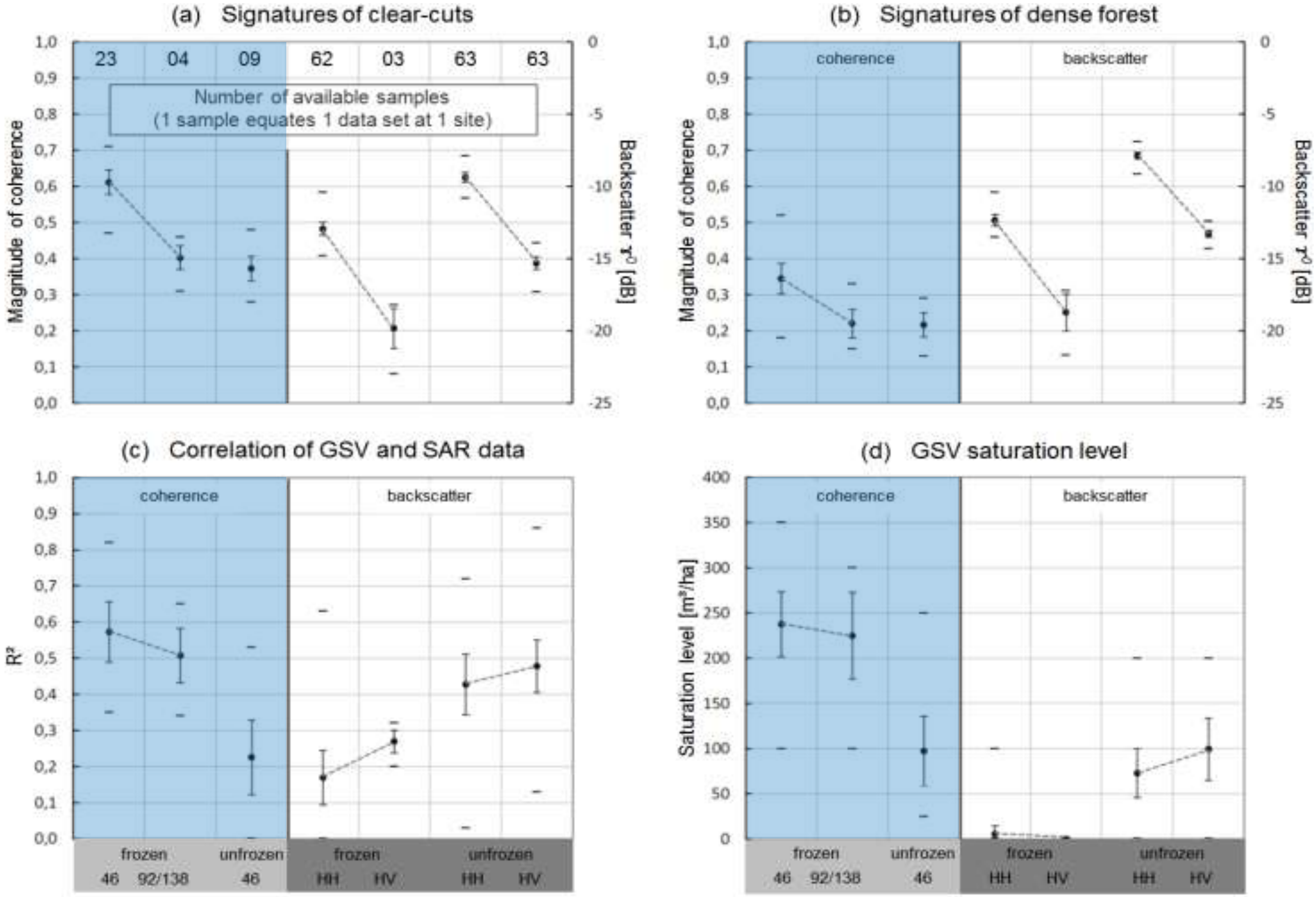

• = average; ⌶ = standard deviation; ‾ _ = minimum/maximum; 46, 92,138 = temporal baseline [d]

Experimental data – Summary

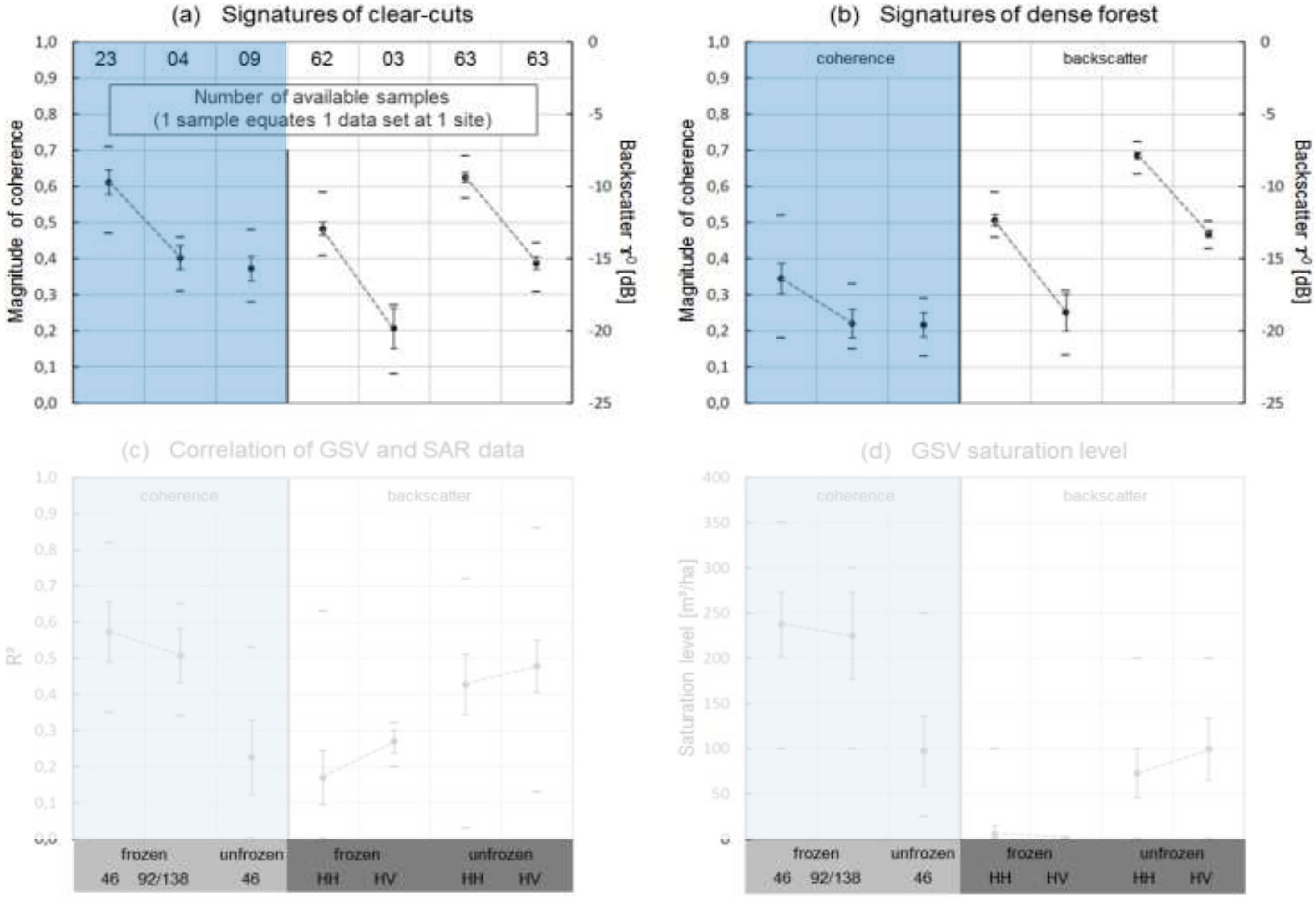

• = average; I = standard deviation; ‾ = minimum/maximum; 46, 92,138 = temporal baseline [d]

Experimental data – Summary

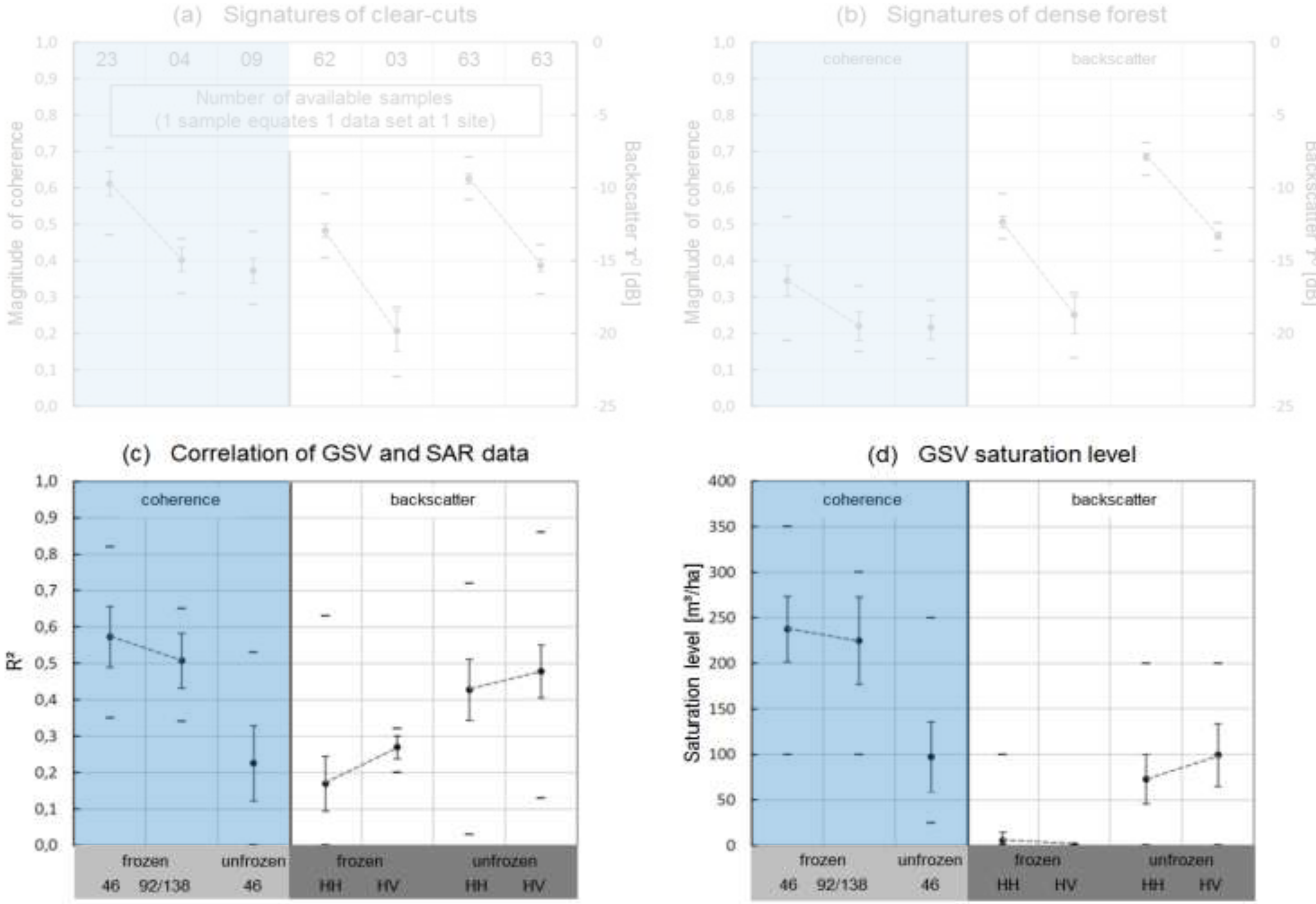

• = average; I = standard deviation; ‾ _ = minimum/maximum; 46, 92,138 = temporal baseline [d]

Outline

1. Area and test sites
2. PALSAR data
3. Summary of observations
4. Map generation approach
5. Results
6. Conclusions

Delineation of GSV Maps

- Random training data selection (20% of the forest inventory data)
- Training of empirical exponential model
- Pixel based model inversion
- Averaging intermediate *GSV* maps resulting in one backscatter based and in one coherence based *GSV* map
- Merging coherence and backscatter based *GSV* map
- Elimination of pixels with a GSV difference > 100 m^3/ha (floodplains, change, water, urban etc.)
- Setting all negative *GSV* values to zero
- Assessing accuracy using the remaining 80% of the reference data

Outline

1. Area and test sites
2. PALSAR data
3. Summary of observations
4. Map generation approach
5. Results
6. Conclusions

Example for delineation of GSV Map (Hrebtovsky site)

Data:

- 3 coherence images (frozen conditions)
- 6 HV backscatter images (unfrozen conditions)
- R^2 between coherence and GSV: 0.44 (average)
- R^2 between backscatter and GSV: 0.48 (average)
- Coherence saturation level: 250 m^3/ha (average)
- Backscatter saturation level: 200 m^3/ha (average)

Example for delineation of GSV Map (Hrebtovsky site)

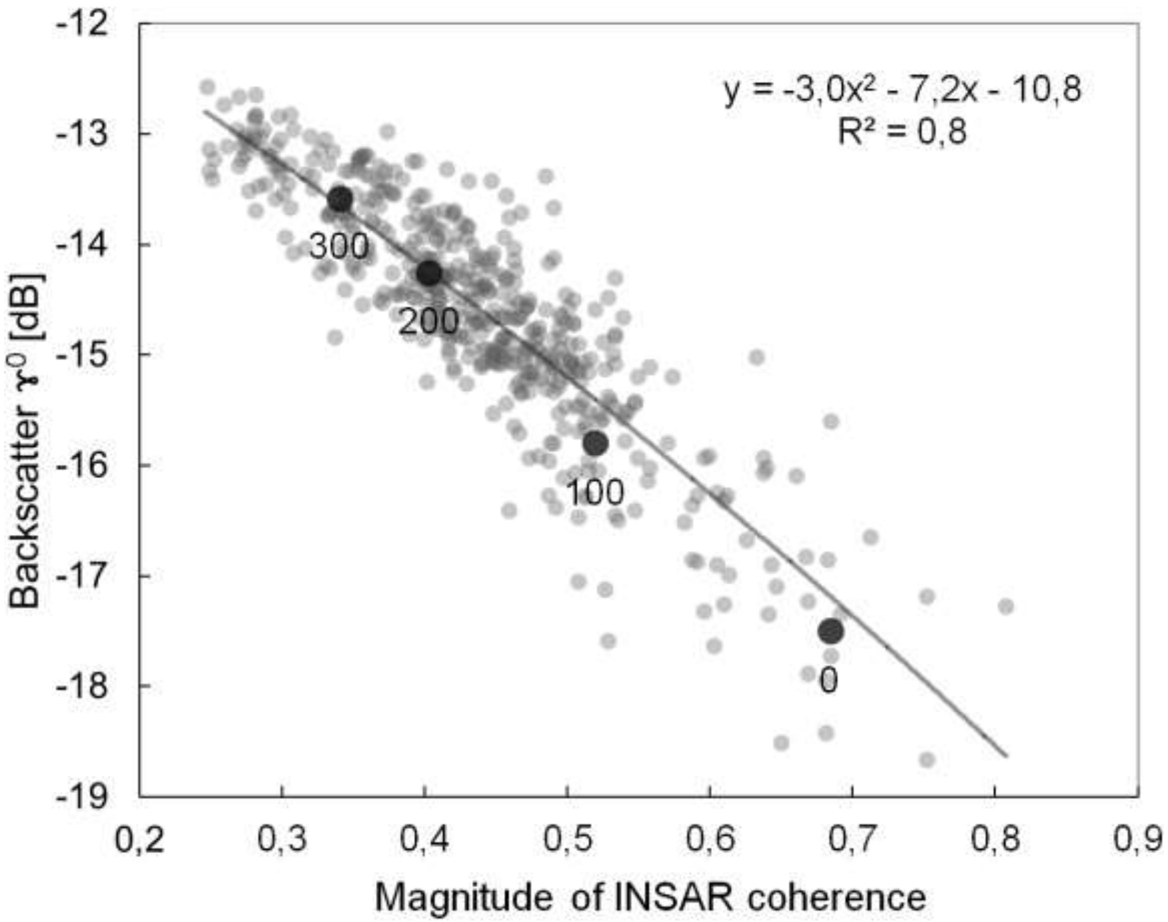

Example for delineation of GSV Map (Hrebtovsky site)

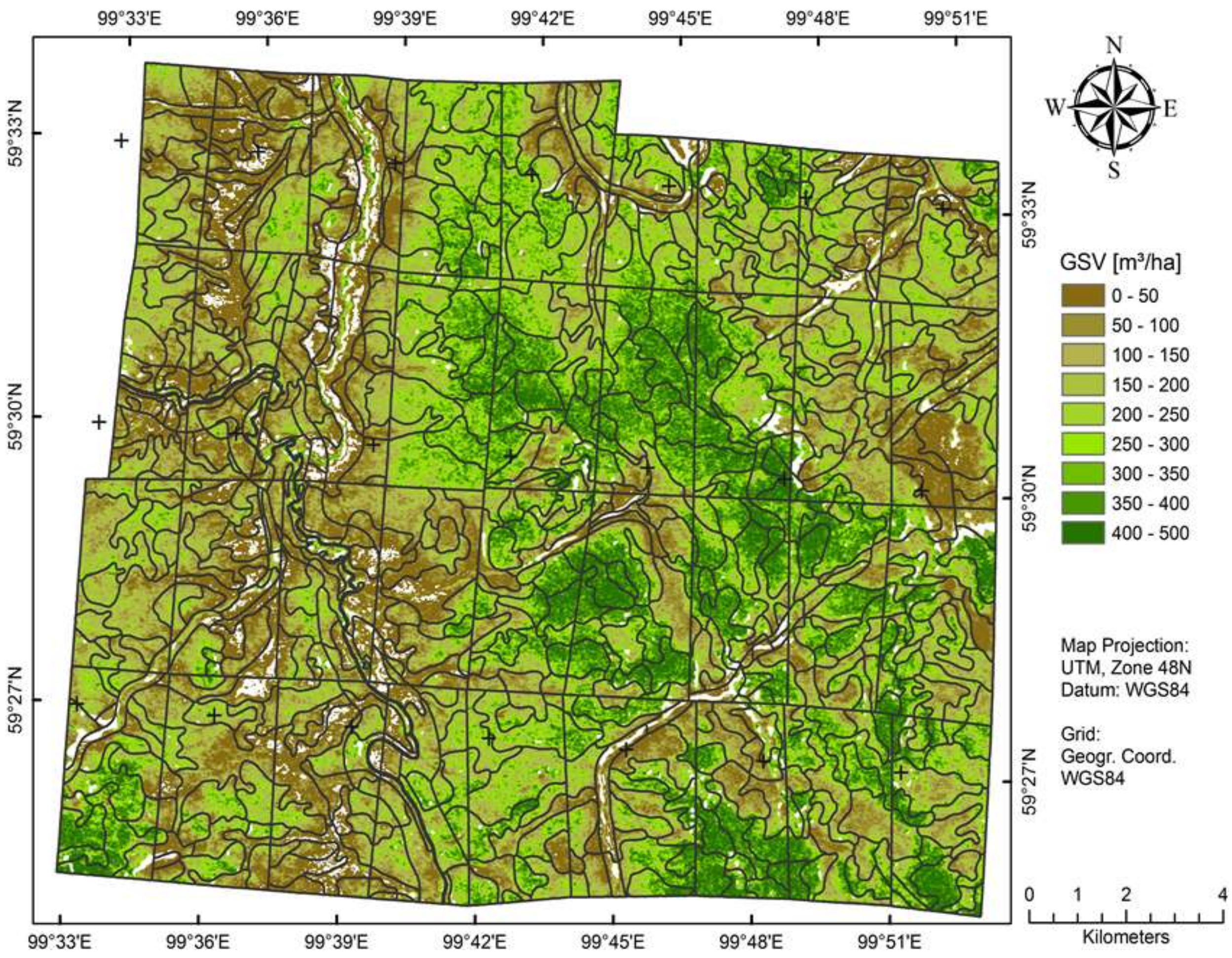

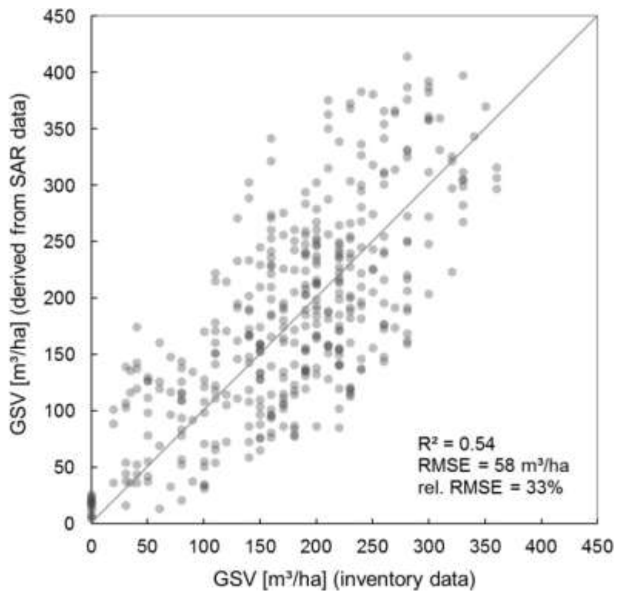

Example for delineation of GSV Map (Hrebtovsky site)

Backscatter vs. coherence

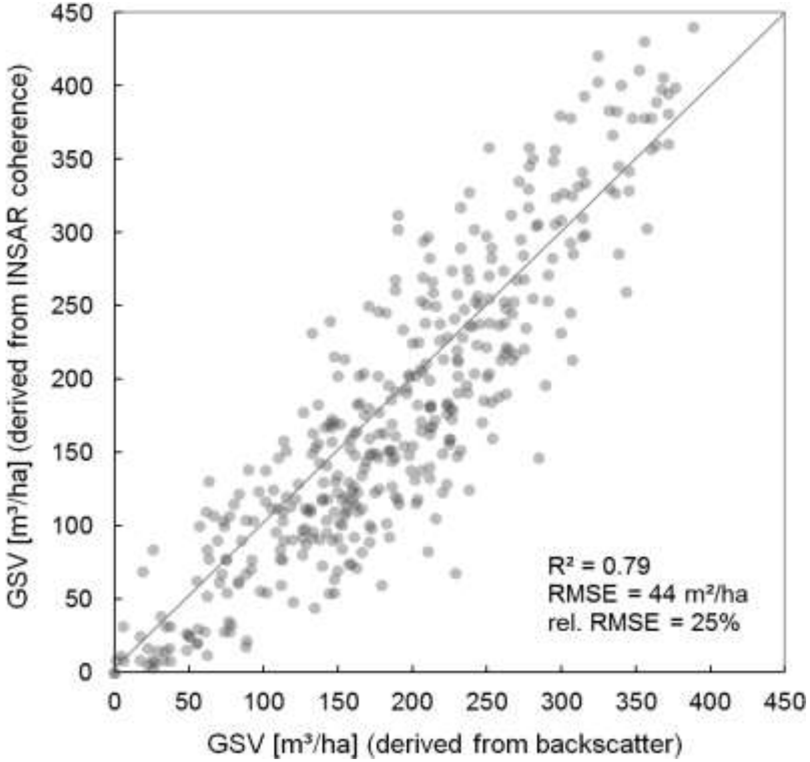

SAR vs. inventory

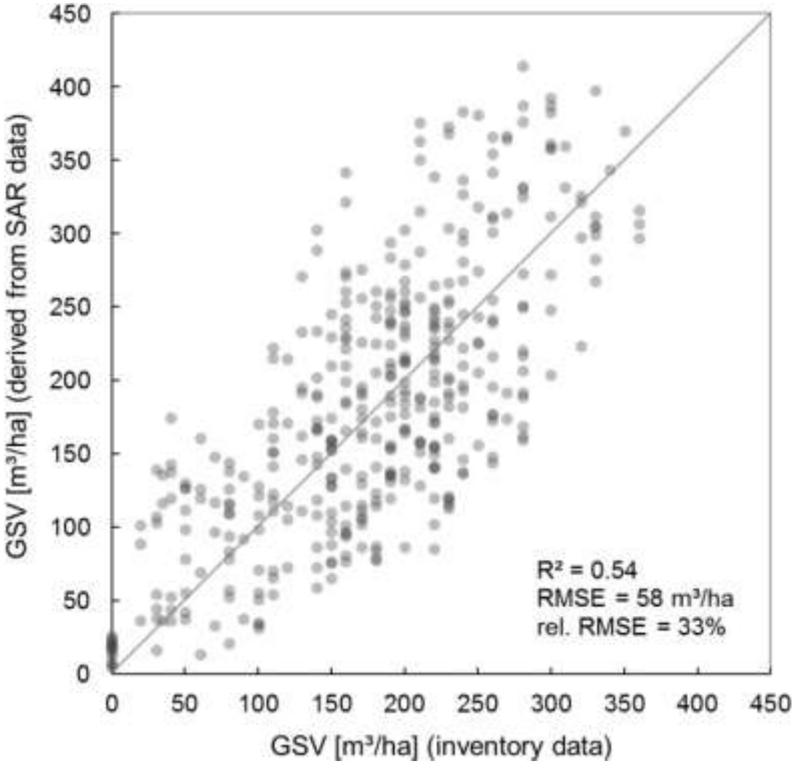

Forest stand level based comparison of two SAR data based *GSV* maps for Hrebtovsky S

Results for the other sites

	Chunsky E	Chunsky N	Shesta	Hrebt S	Nishni
R^2 coh + int	**0.79**	**0.79**	**0.54**	**0.57**	**0.83**
R^2 coh	0.80	0.78	0.37	0.55	0.82
R^2 int	0.67	0.70	0.56	0.50	0.82
RMSE [m^3/ha] coh + int	**56.6**	**41.2**	**50.4**	**57.4**	**48.9**
RMSE [m^3/ha] coh	56.4	42.4	52.7	61.9	50.7
RMSE [m^3/ha] int	71.1	50.3	56.2	59.1	56.1

Rel. RMSE approximately 25% for all sites

Outline

1. Area and test sites
2. PALSAR data
3. Summary of observations
4. Map generation approach
5. Results
6. Conclusions

Conclusions

- Coherence at frozen conditions offers the largest potential for *GSV* estimation
  - Saturation at 230 m³/ha, R^2 between coherence and *GSV* is 0.58
  - Comparable results were found in other studies using ERS-1/2 Tandem data
- Backscatter less sensitive
  - Saturation at 75-100 m³/ha, R^2 between backscatter and *GSV* 0.42 (HH) - 0.48 (HV)

Conclusions

- Coherence at frozen conditions offers the largest potential for *GSV* estimation
    - Saturation at 230 m³/ha, R^2 between coherence and *GSV* is 0.58
    - Comparable results were found in other studies using ERS-1/2 Tandem data
- Backscatter less sensitive
    - Saturation at 75-100 m³/ha, R^2 between backscatter and *GSV* 0.42 (HH) - 0.48 (HV)
- Combination of backscatter and coherence led to improvement of *GSV* estimation, in particular exclusion of areas with contradictory *GSV* (coherence vs. backscatter) helpful

Conclusions

- Coherence at frozen conditions offers the largest potential for *GSV* estimation
    - Saturation at 230 m³/ha, R^2 between coherence and *GSV* is 0.58
    - Comparable results were found in other studies using ERS-1/2 Tandem data
- Backscatter less sensitive
    - Saturation at 75-100 m³/ha, R^2 between backscatter and *GSV* 0.42 (HH) - 0.48 (HV)
- Combination of backscatter and coherence led to improvement of *GSV* estimation, in particular exclusion of areas with contradictory *GSV* (coherence vs. backscatter) helpful
- Demonstrated: Potential of ALOS PALSAR to map the *GSV* of the Siberian forest with a precision close to the accuracy of the conventional forest inventory data (relative RMSE approx. 25%)
- Data availability: At each region in Siberia in average 4 coherence images (temporal baseline 46 days) acquired at frozen conditions and 6 FBD backscatter images acquired at unfrozen conditions are available

Outline

SAR Techniques: Polarimetry

- Investigation backscatter at different polarisations
- Computation of polarimetric parameters

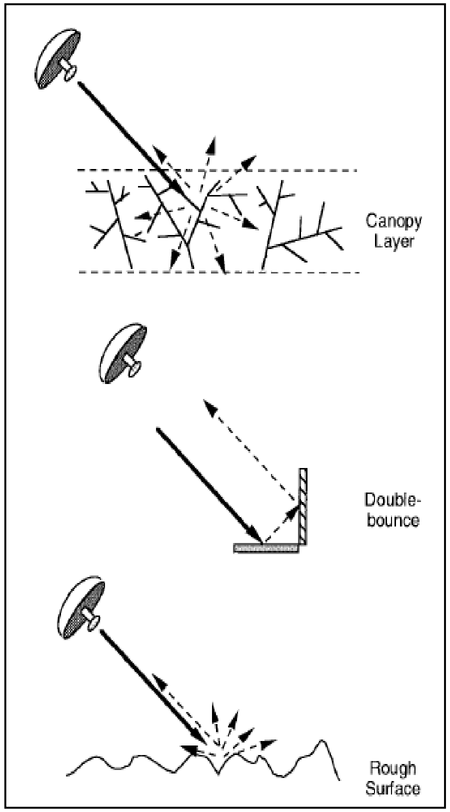

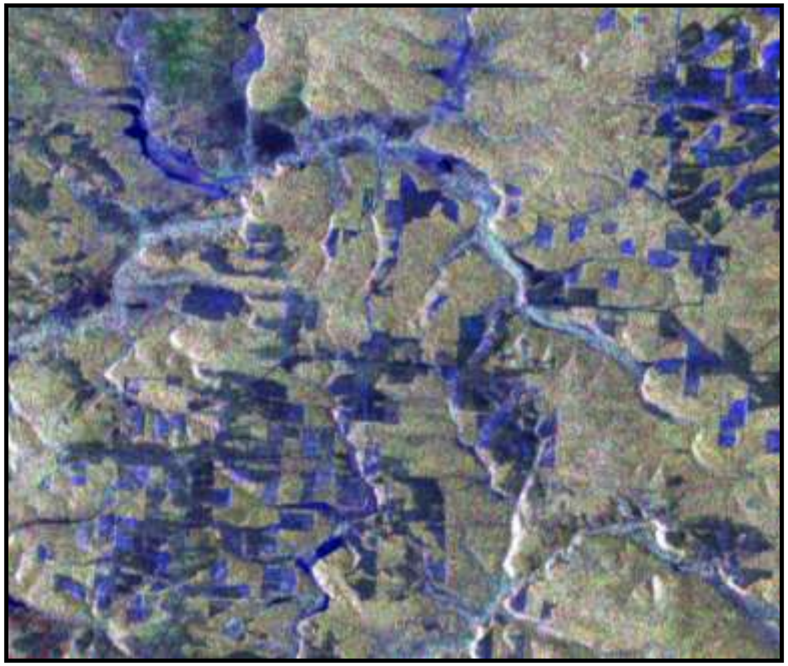

Pauli – Decomposition

$S_{HH} + S_{VV}$	Surface Scattering
$S_{HH} - S_{VV}$	Double Bounce
$2S_{HV}$	Volume Scattering

Analysis of Polarimetric Parameters

1. Intensities
2. Polarimetric HHVV Coherence
3. Cloude decomposition parameters
4. Freeman decomposition parameters
5. Krogager decomposition parameters

} Class signature analysis

6. Summary of separability measures

Intensities – Overview

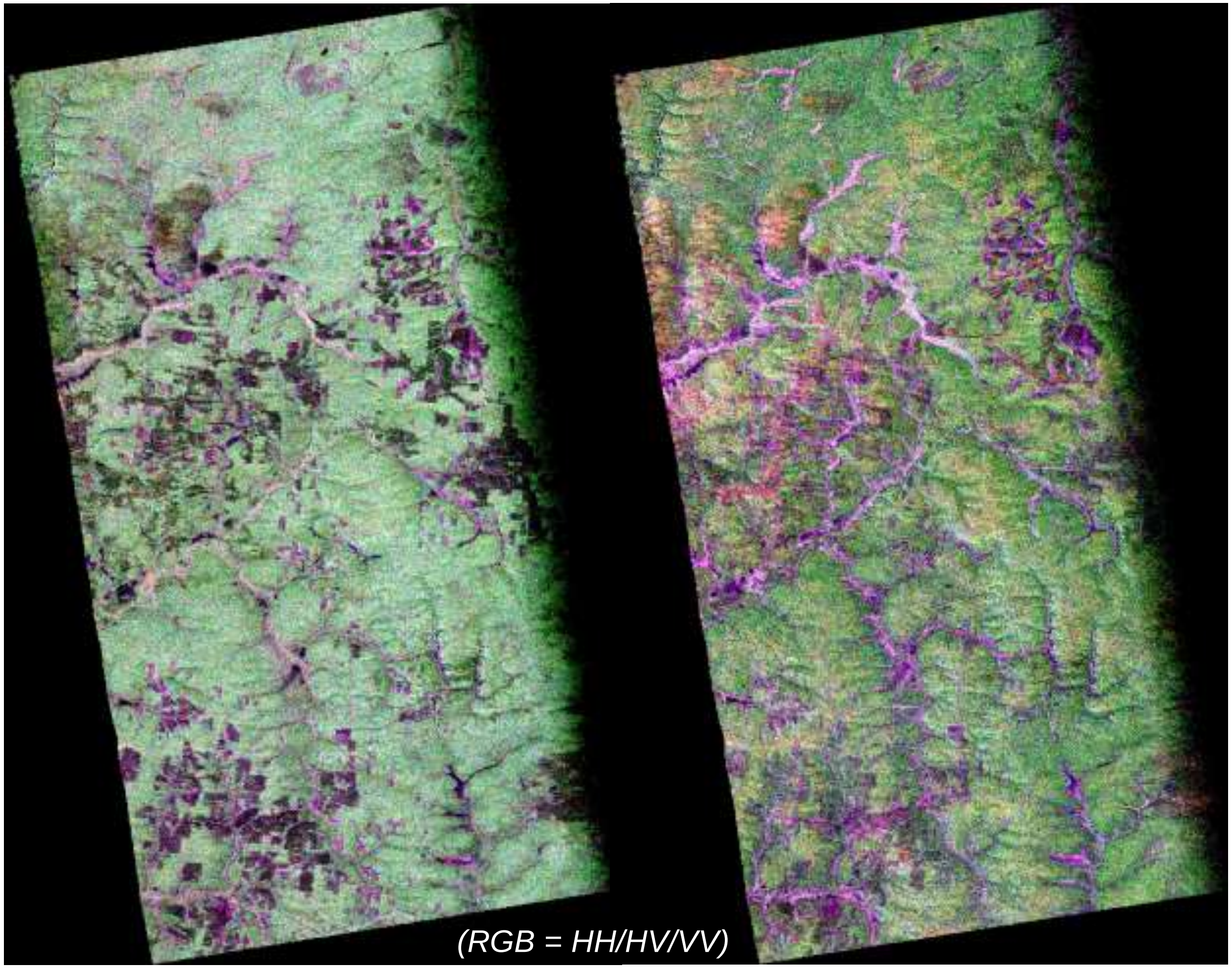

- LEFT: Summer conditions (28th August 2006)
- RIGHT: Autumn/Early winter conditions – beginning of freezing, leaves off (13th October 2006)

Intensities – Overview

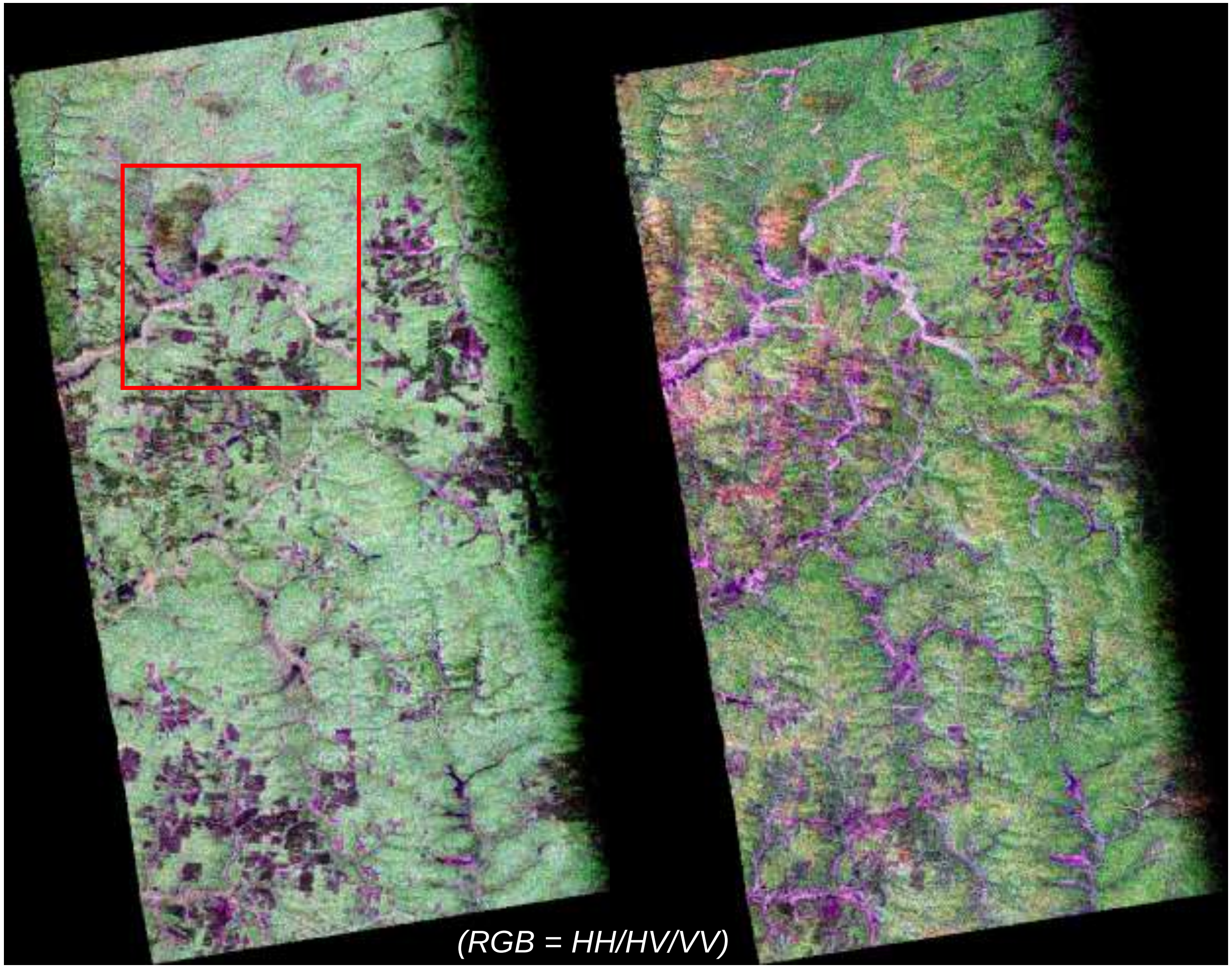

- LEFT: Summer conditions (28th August 2006)
- RIGHT: Autumn/Early winter conditions – beginning of freezing, leaves off (13th October 2006)

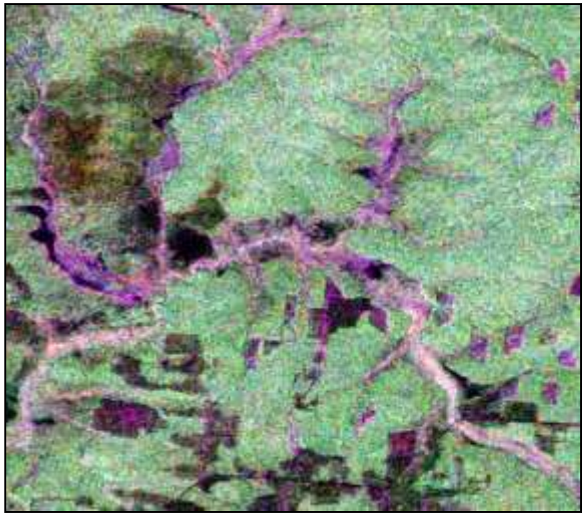

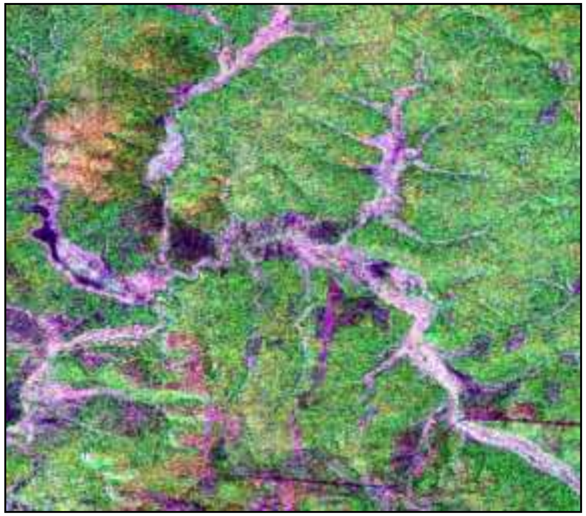

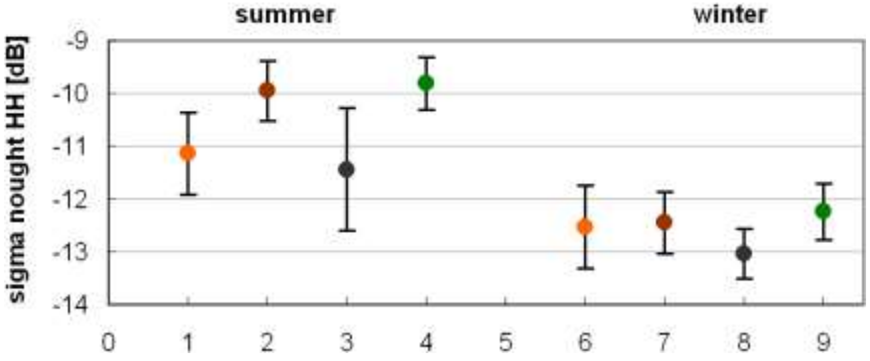

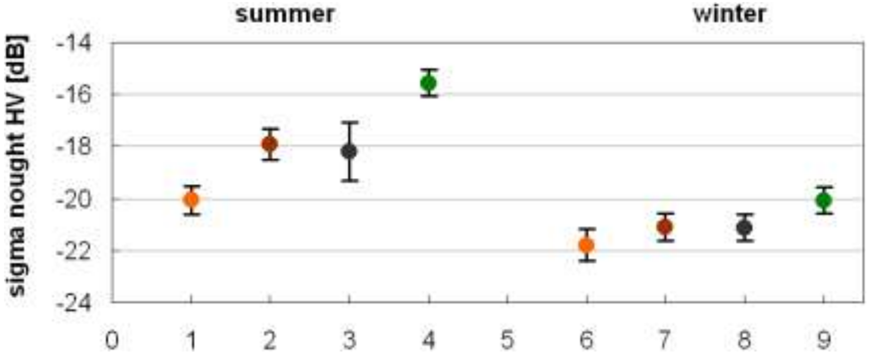

Signature plot of HV & HH intensity
1 & 6 = recent clear-cut
2 & 7 = former clear-cut
3 & 8 = fire scar
4 & 9 = forest

Intensities

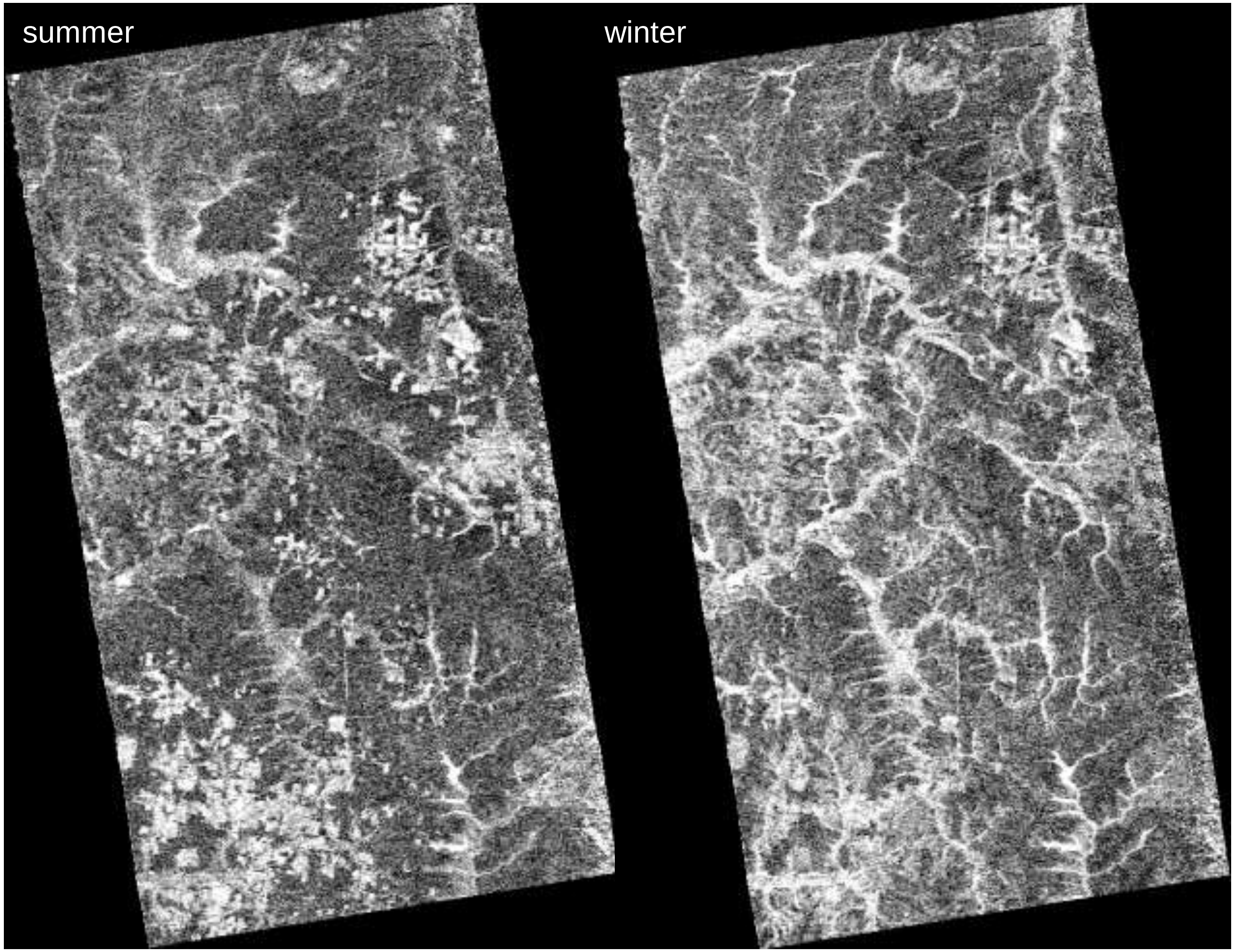

- Displayed: Magnitude of HHVV Coherence
- Provides information on the scattering process
- Surface scattering creates high coherence, multiple scattering low values

$$\rho_{HHVV} = \left\langle \frac{S_{HH} S_{VV}^*}{\sqrt{\langle S_{HH} S_{HH}^* \rangle \langle S_{VV} S_{VV}^* \rangle}} \right\rangle$$

HHVV Coh.

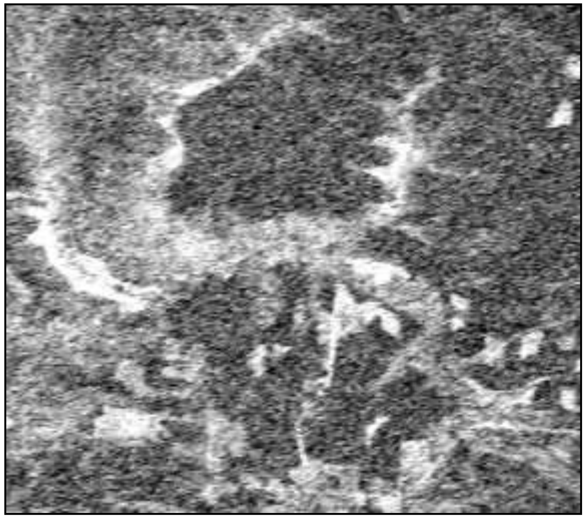

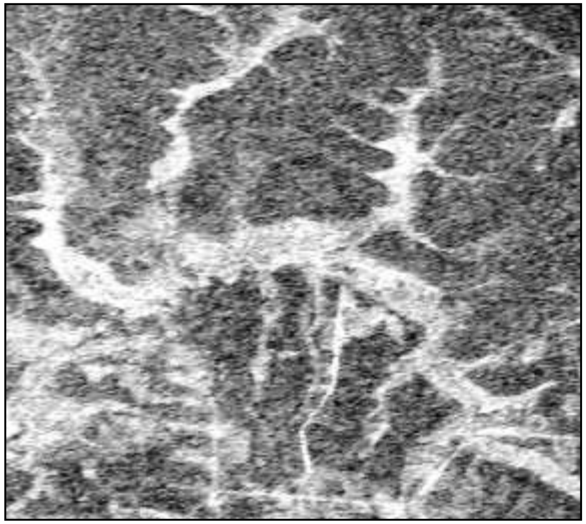

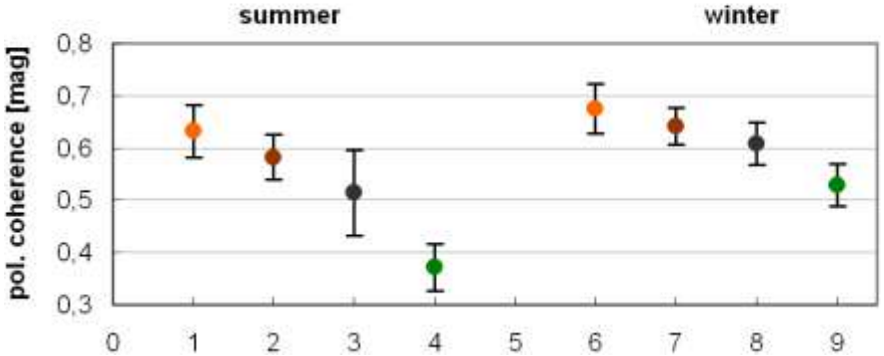

1 & 6 = recent clear-cut
2 & 7 = former clear-cut
3 & 8 = fire scar
4 & 9 = forest

HHVV Coh.

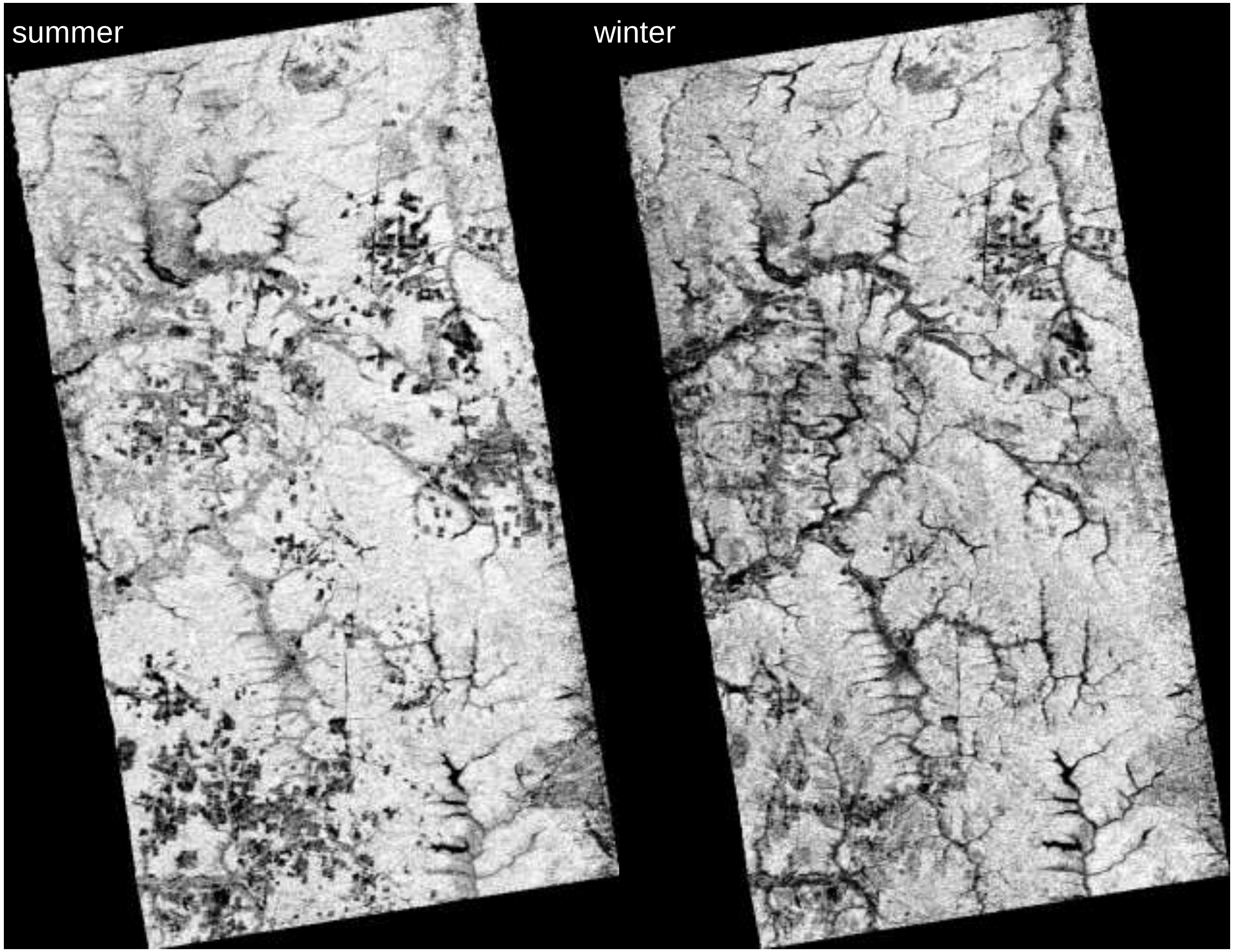

- Roll invariant Eigenvector-Eigenvalue based decomposition of the coherency matrix
- Physical interpretability of concluding parameters
- **Alpha** indicates type of mean scattering mechanism
- **Entropy** and **Anisotropy** specify distribution of the scattering mechanisms
- Displayed: Entropy

Cloude

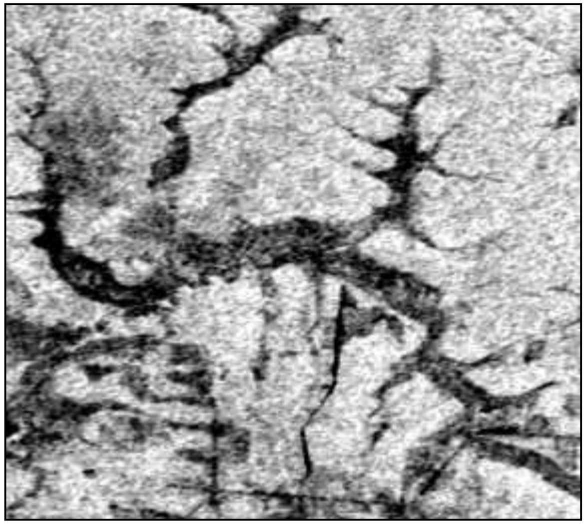

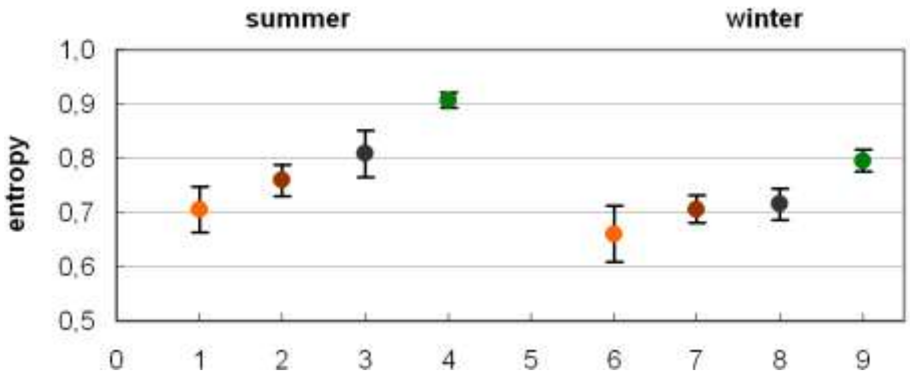

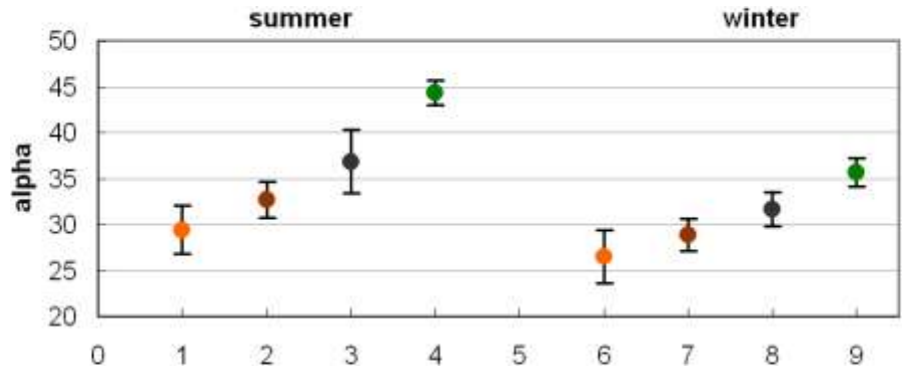

1 & 6 = recent clear-cut
2 & 7 = former clear-cut
3 & 8 = fire scar
4 & 9 = forest

Cloude

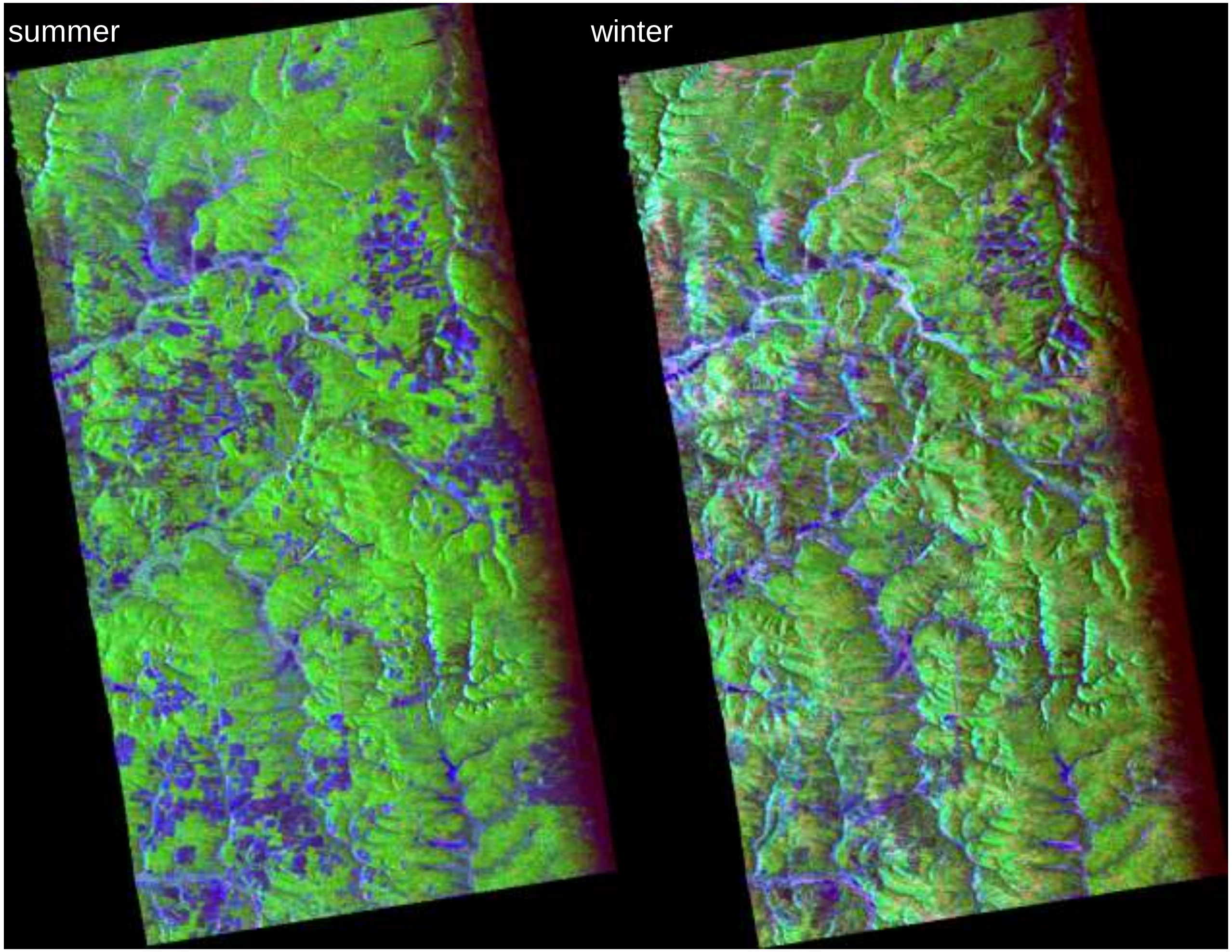

- Separates backscattered power with a modelled covariance matrix into three fractions: **Volume scattering** (Pv), **double bounce** (Pd) and **surface scattering** (Ps)
- Not roll invariant and topography can affect the fractioning
- Displayed: Pd/ Pv/ Ps

Freeman

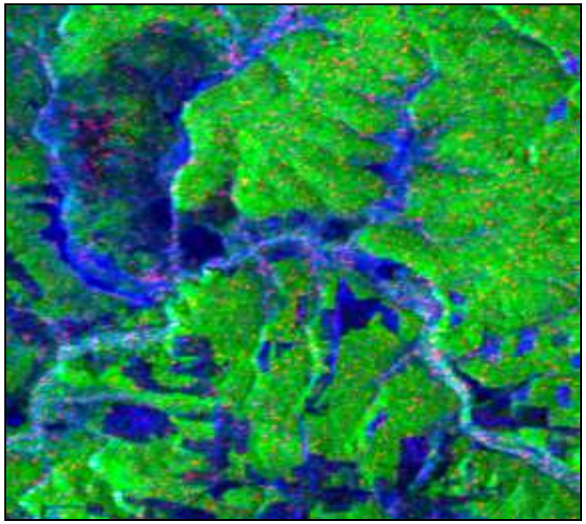

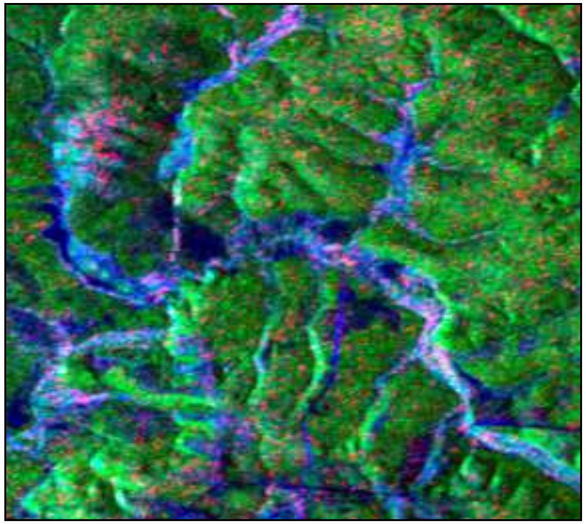

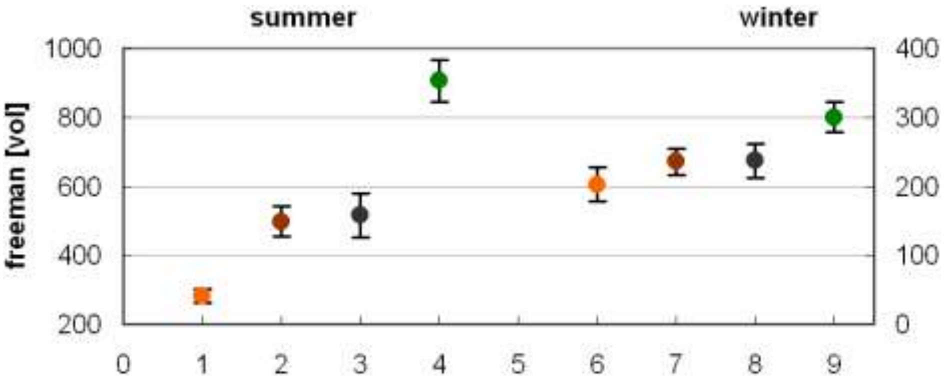

Signature plot of Pv (volume scattering)
1 & 6 = recent clear-cut
2 & 7 = former clear-cut
3 & 8 = fire scar
4 & 9 = forest

Freeman

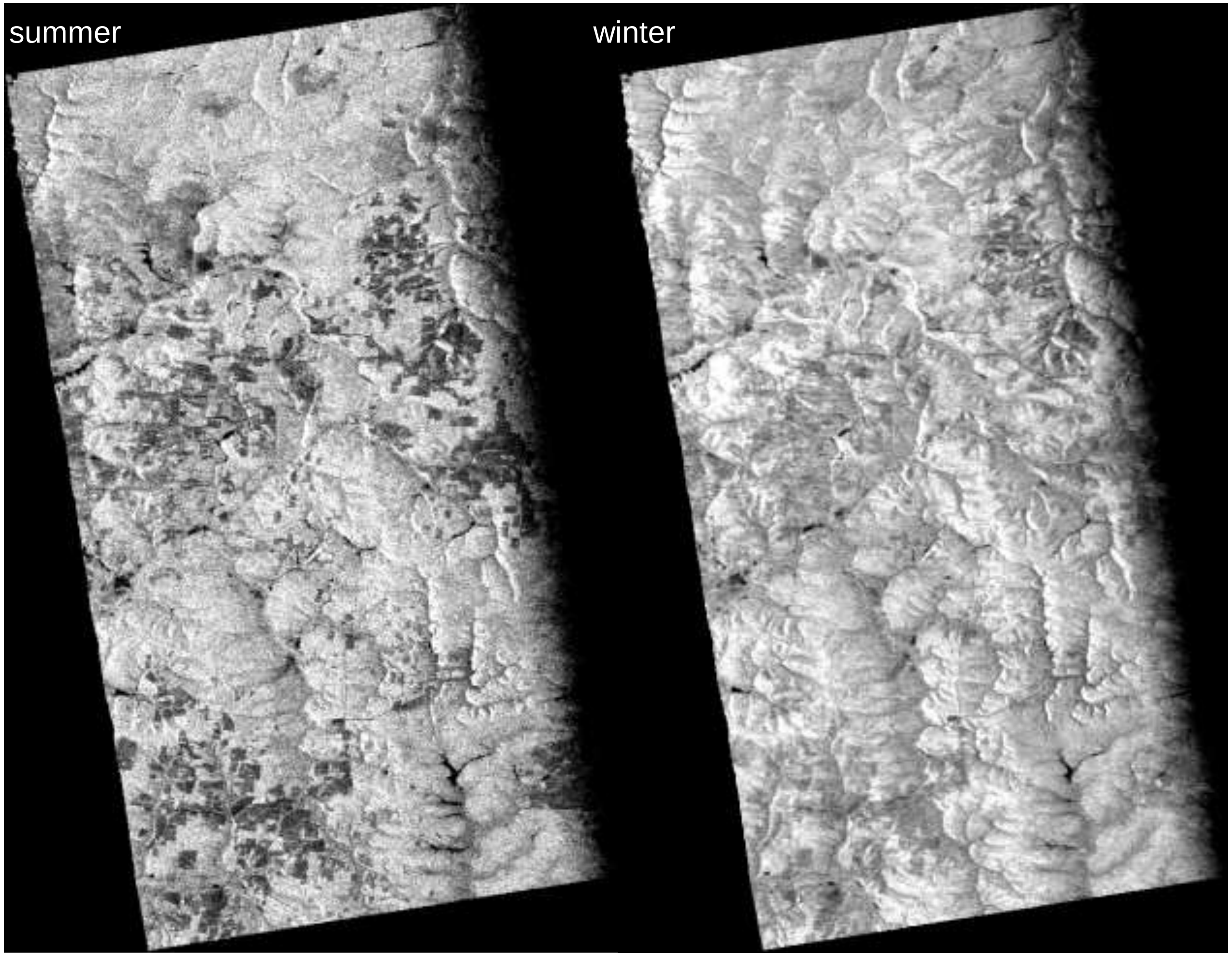

- Coherent decomposition
- Factorises the scattering matrix as combination of three responses: sphere, helix and diplane
- Power scattered by each of these responses is given by $|ks|^2$, $|kh|^2$ and $|kd|^2$
- Displayed: $|kd|^2$

Krogager

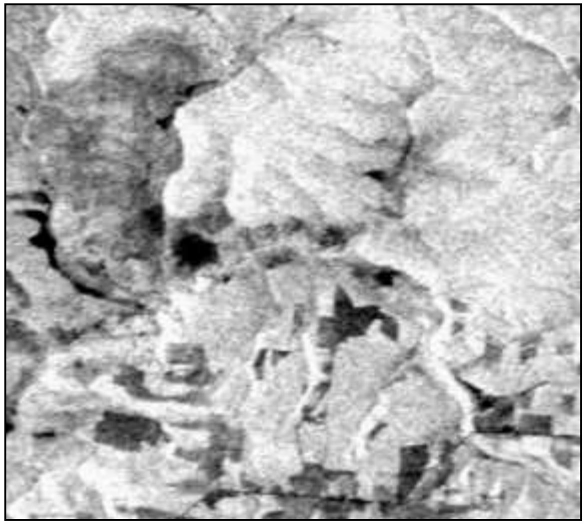

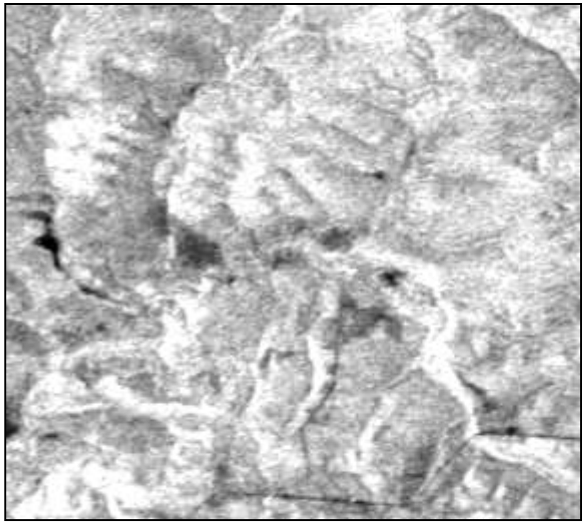

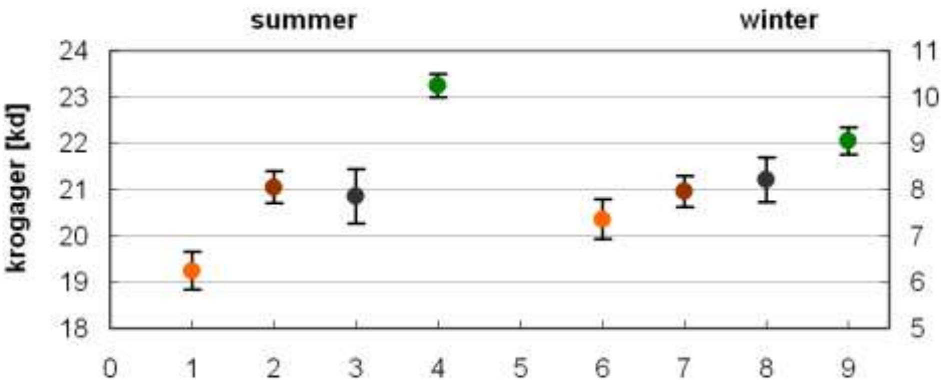

Signature plot of |kd|² (diplane response)
1 & 6 = recent clear-cut
2 & 7 = former clear-cut
3 & 8 = fire scar
4 & 9 = forest

Krogager

Summary of separability measures

Summary of separability measures

	1 - 2	1-3	1 -4	2 - 3	2 - 4	3 – 4
σ^0 HH	0,34	0,20	0,40	0,23	0,08	0,29
σ^0 HV	0,49	0,45	**0,91**	0,07	0,69	0,74
σ^0 VV	0,32	0,13	0,41	0,32	0,11	0,42
$\lvert\rho_{HHVV}\rvert$	0,20	0,44	0,78	0,28	0,72	0,54
Alpha	0,27	0,57	**0,91**	0,38	**0,88**	0,72
Entropy	0,32	0,58	0,89	0,35	**0,88**	0,80
Pv	**0,71**	0,65	**0,99**	0,15	**0,91**	**0,95**
$\lvert kd\rvert^2$	**0,72**	**0,70**	**0,99**	0,13	**0,90**	**0,95**

1 = recent clear-cut, 2 = former clear-cut
3 = fire scar, 4 = forest

Normalised Jefferies-Matusita distance
(1.0 = signatures separable; 0.0 = signatures inseparable)

Summary of separability measures

	1 - 2	1-3	1 -4	2 - 3	2 - 4	3 – 4
σ^0 HH	0,34	0,20	0,40	0,23	0,08	0,29
σ^0 HV	0,49	0,45	**0,91**	0,07	0,69	0,74
σ^0 VV	0,32	0,13	0,41	0,32	0,11	0,42
$\lvert\rho_{HHVV}\rvert$	0,20	0,44	0,78	0,28	0,72	0,54
Alpha	0,27	0,57	**0,91**	0,38	**0,88**	0,72
Entropy	0,32	0,58	0,89	0,35	**0,88**	0,80
Pv	**0,71**	0,65	**0,99**	0,15	**0,91**	**0,95**
$\lvert kd\rvert^2$	**0,72**	**0,70**	**0,99**	0,13	**0,90**	**0,95**

1 = recent clear-cut, 2 = former clear-cut
3 = fire scar, 4 = forest

Normalised Jefferies-Matusita distance
(1.0 = signatures separable; 0.0 = signatures inseparable)

Outline

1. Introduction: Why Forest Observation?
2. SAR Techniques of interest for forestry applications
3. SAR for Forestry Applications – Some Basics
4. Forest Cover and Biomass Mapping – Excursus
    1. BIOMASAR – Hypertemporal C-band Data Assimilation
    2. Forest Cover Mapping Using Backscatter and Coherence
    3. Forest Biomass Mapping Using Backscatter and Coherence
    4. Polarimetry for Forest Cover Mapping
    5. INSAR Phase and Tree Height
    6. Seasonality of C-band Backscatter in Siberia
    7. Seasonality of Coherence in Siberia
    8. X-band coherence over the Thuringian Forest
    9. Mapping of woody cover in KNP using L-band backscatter

Vegetation height estimation from SRTM

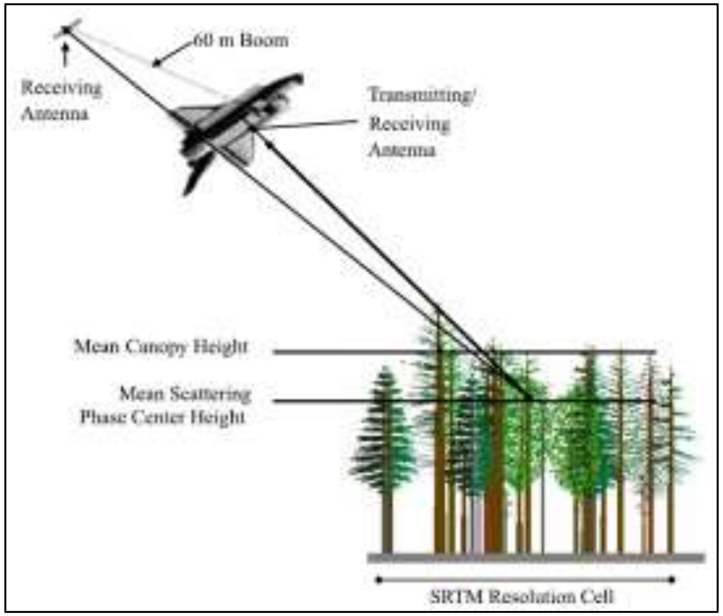

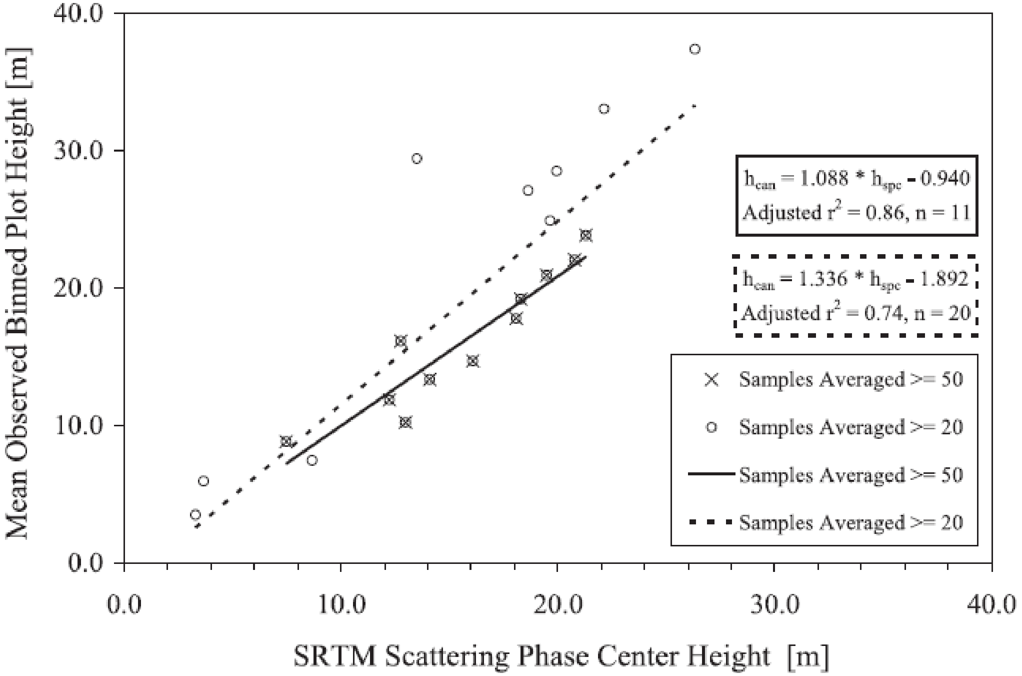

J. Kellndorfer et al. / Remote Sensing of Environment 93 (2004) 339–358

SRTM X-SAR
Topographic Map

Site:	Sibiria
Acquisition Date:	19-Feb-2000
Datatake ID:	121 020
Scene Center:	52.11 E 106.95 N
Approx. Area Size:	45 X 170 km

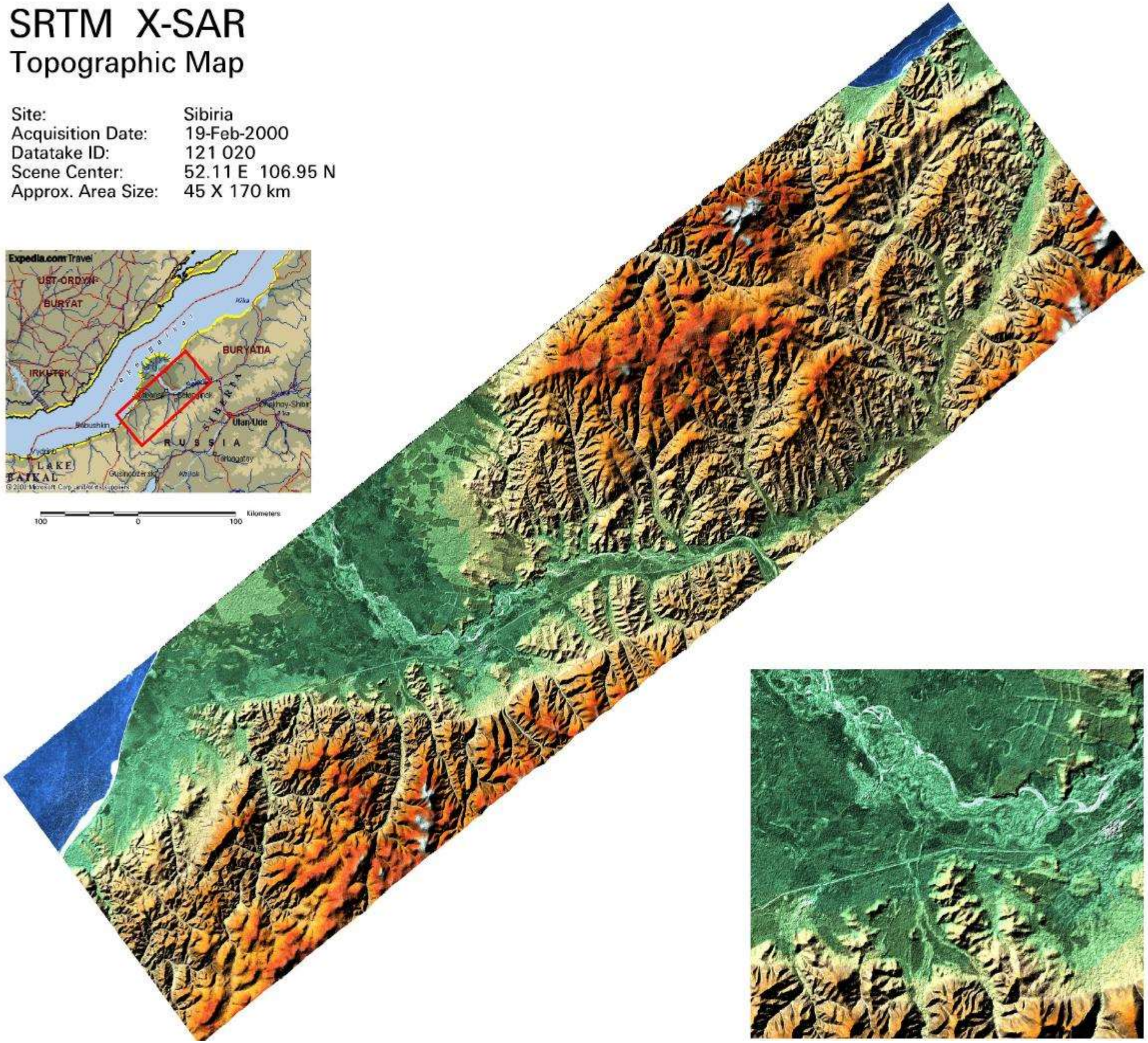

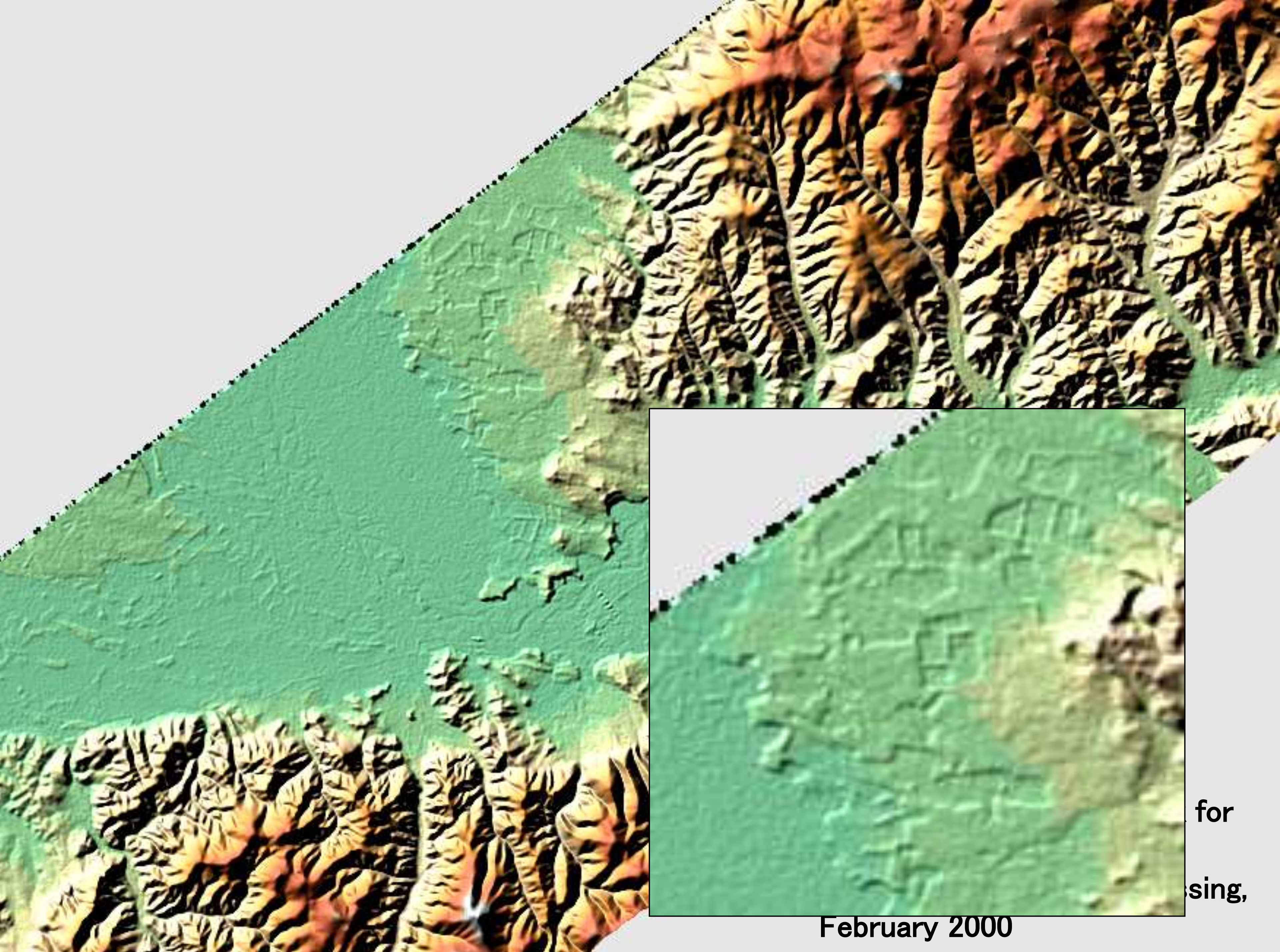

for

ssing,

February 2000

Vegetation height estimation from E-SAR Data

Specifications of INSAR-DHM

Geometric Resolution: 5 x 5 m
Height Accuracy: 1 m

X-Band

1. DHM contains height of buildings and trees

2. Errors were backscatter is little

DHM vs. DEM

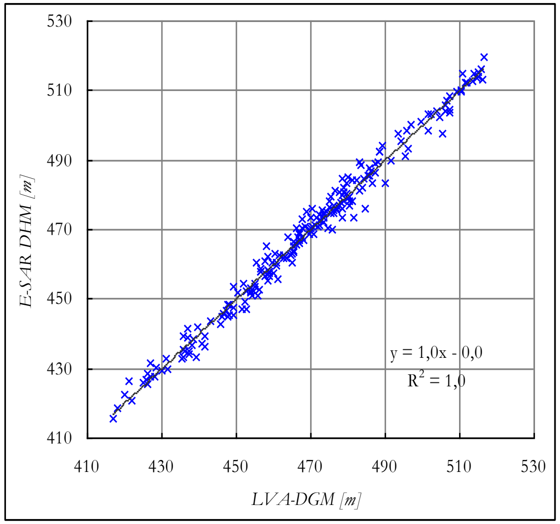

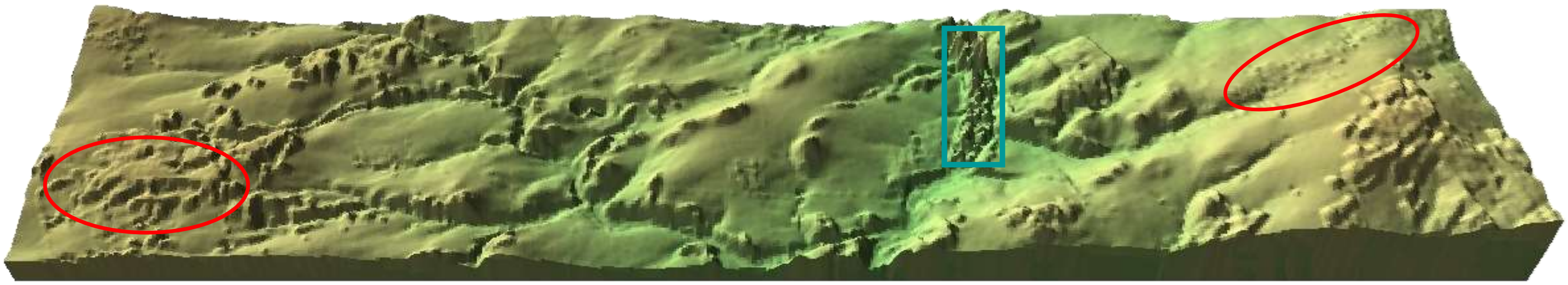

Vegetation (and building) height estimation from E-SAR Data

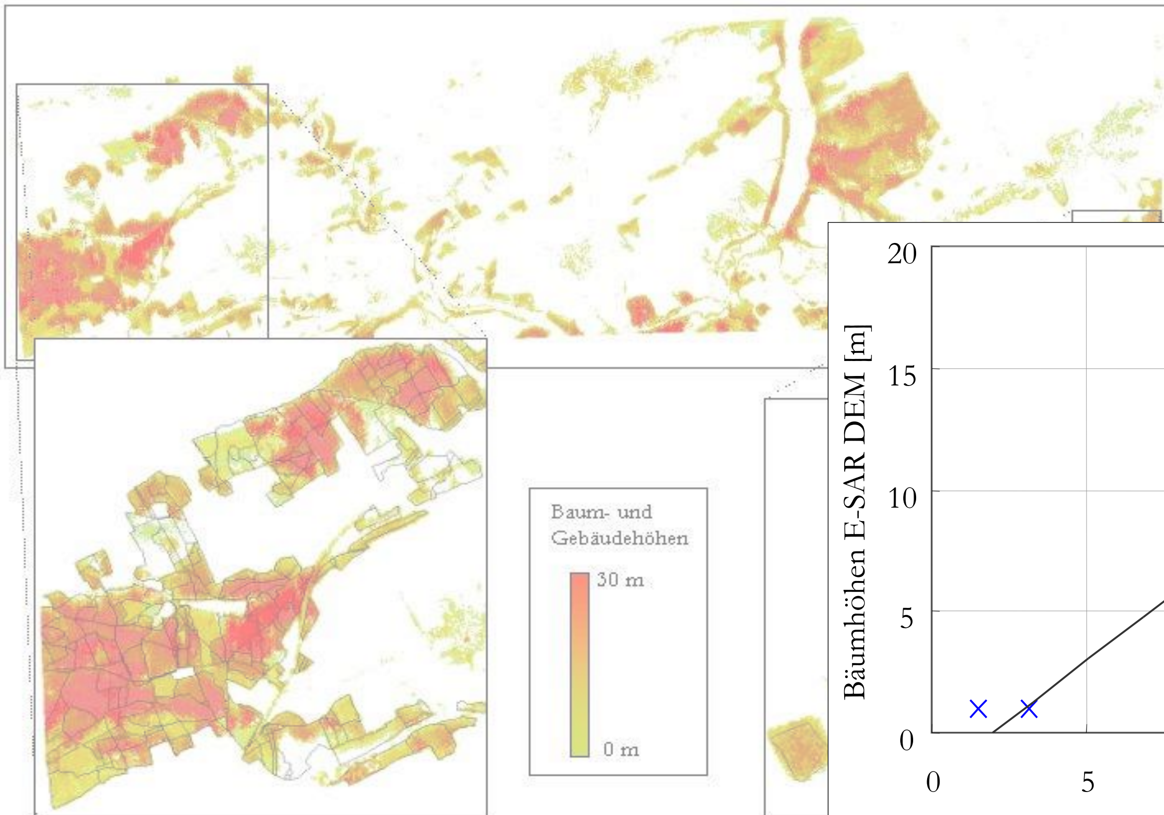

Validation with in-situ data

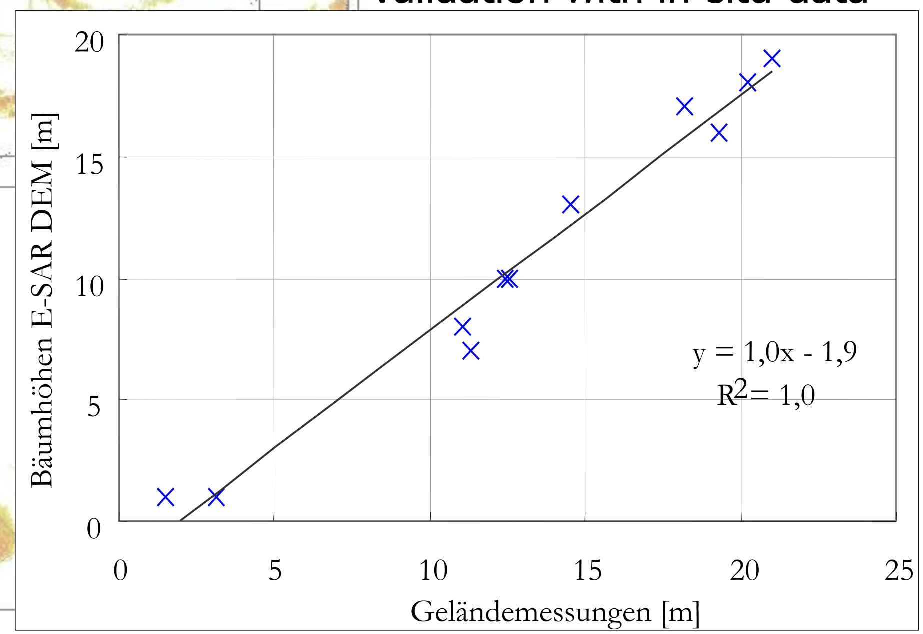

Trees acquired at superhigh resolution (X-band)

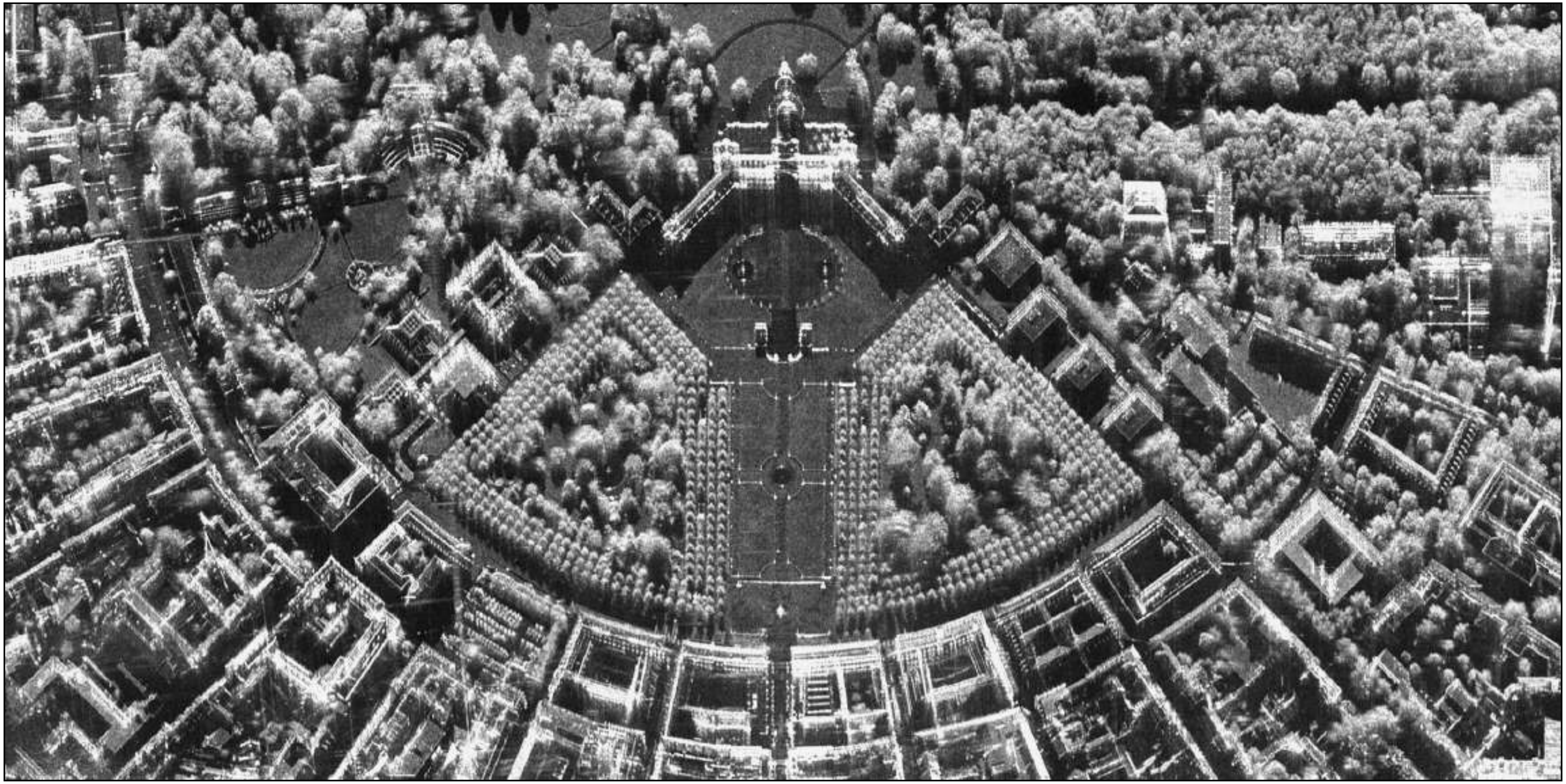

Andreas R. Brenner and Ludwig Roessing, Radar Imaging of Urban Areas by Means of Very High-Resolution SAR and Interferometric SAR, IEEE TRANSACTIONS ON GEOSCIENCE AND REMOTE SENSING, VOL. 46, NO. 10, OCTOBER 2008

Trees acquired at superhigh resolution (X-band)

CURRENT SYSTEM PARAMETERS OF PAMIR

center frequency	9.45 GHz (X-band)
bandwidth (rel.)	1.82 GHz (20%)
resolution	< 0.1 m x 0.1 m
range	up to 35 km
no. of receive channels	5
transmit power	240 W
azimuthal scan angle	±45°
polarization	VV

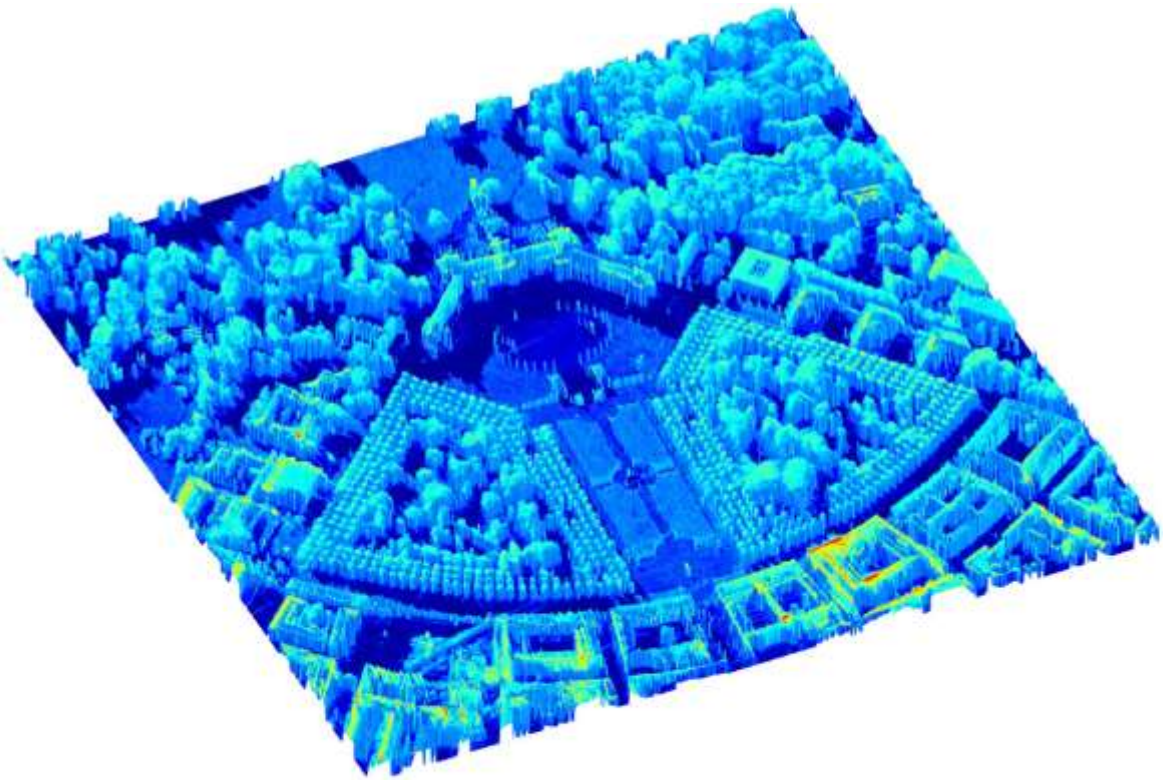

Andreas R. Brenner and Ludwig Roessing, Radar Imaging of Urban Areas by Means of Very High-Resolution SAR and Interferometric SAR, IEEE TRANSACTIONS ON GEOSCIENCE AND REMOTE SENSING, VOL. 46, NO. 10, OCTOBER 2008

Trees acquired at high resolution (L-band)

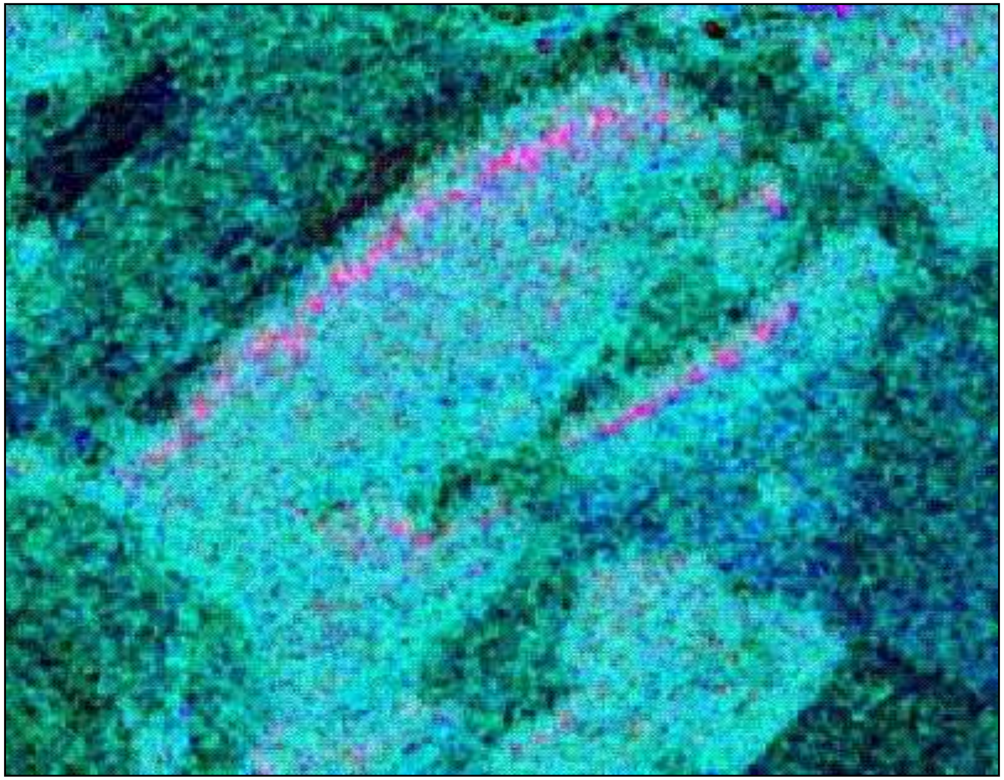

Forest Edge in L-Band

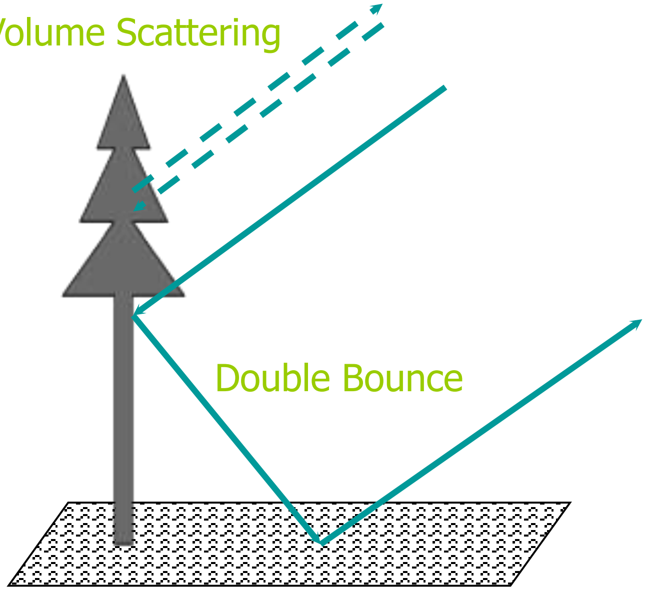

Outline

1. Introduction: Why Forest Observation?
2. SAR Techniques of interest for forestry applications
3. SAR for Forestry Applications – Some Basics
4. Forest Cover and Biomass Mapping – Excurses
    1. BIOMASAR – Hypertemporal C-band Data Assimilation
    2. Forest Cover Mapping Using Backscatter and Coherence
    3. Forest Biomass Mapping Using Backscatter and Coherence
    4. Polarimetry for Forest Cover Mapping
    5. INSAR Phase and Tree Height
    6. Seasonality of C-band Backscatter in Siberia
    7. Seasonality of Coherence in Siberia
    8. X-band coherence over the Thuringian Forest
    9. Mapping of woody cover in KNP using L-band backscatter

Seasonal behaviour of C-Band Backscatter in Siberian Forests

Climate data for year 2006

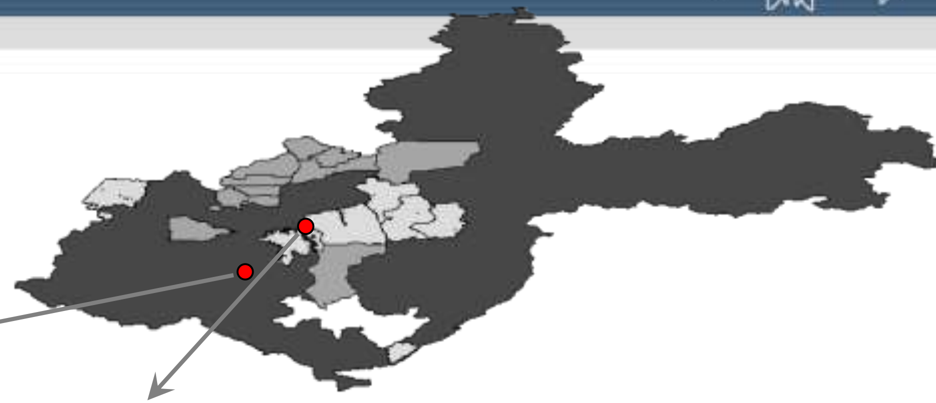

Tulun (100,5°E / 54,5°N, altitude 522 m)

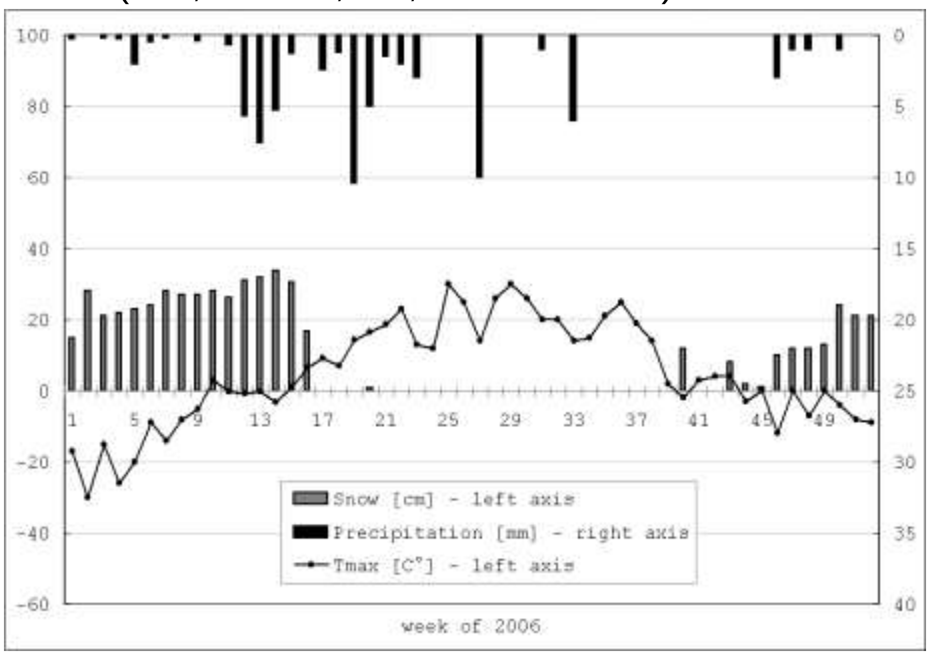

Vitim (103,1°E / 56,3°N, altitude 190 m)

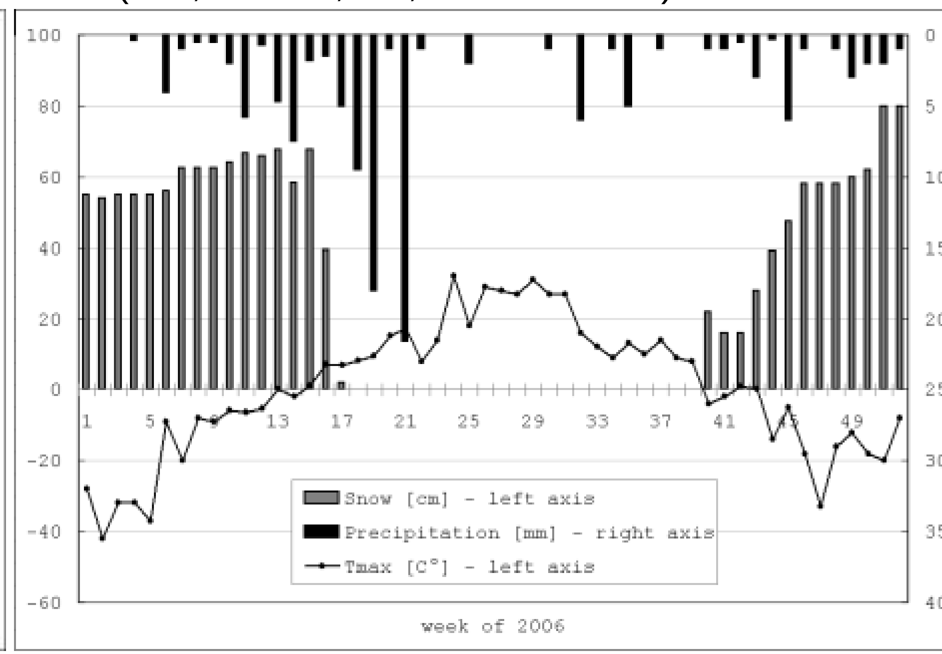

Weekly averages for T_{max} and snow depth, weekly sum for precipitation

ASAR Data: APP (HH/HV) I7

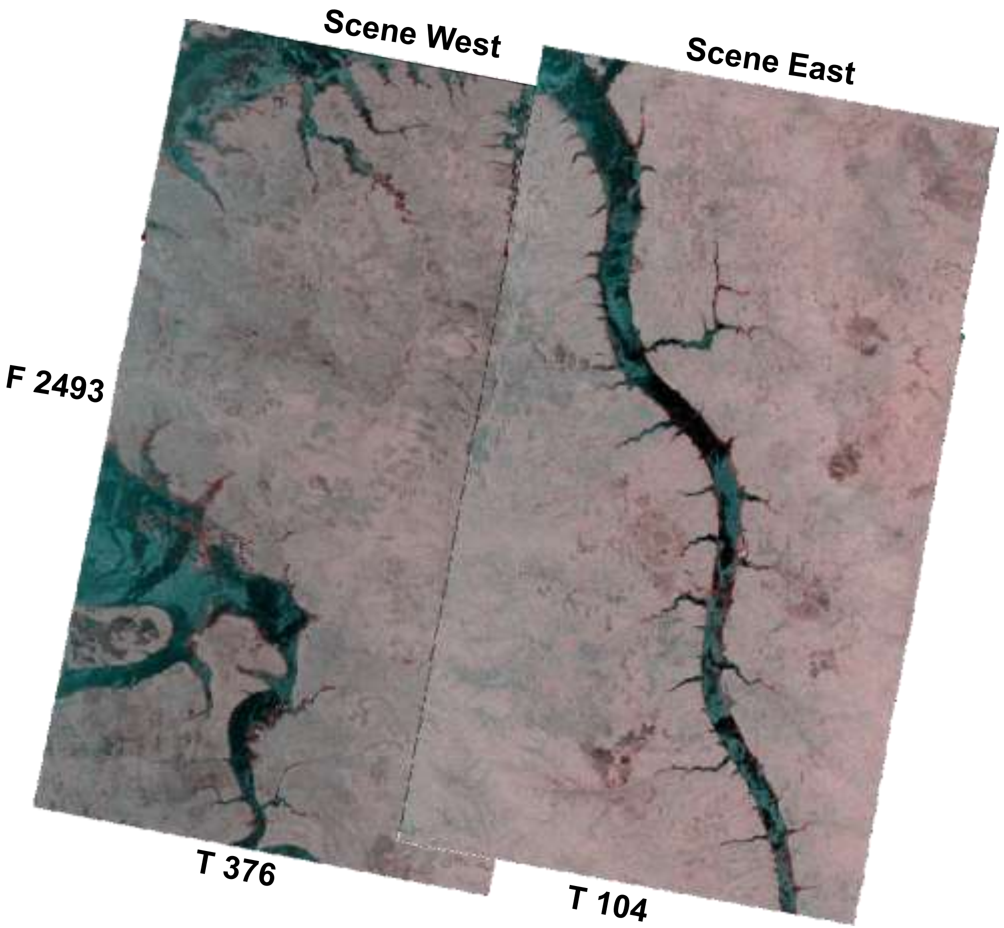

March data depicted (RGB = HH-HV-HV)

Data available for time series:

	West	East
February	-	14.02.2006
March	05.03.2006	21.03.2006
April	-	25.04.2006
May	14.05.2006	-
June	18.06.2006	-
July	23.07.2006	04.07.2006
August	27.08.2006	-
September	-	12.09.2006
October	-	-
November	05.11.2006	21.11.2006

- = no acquisition

Seasonal behaviour of C-Band Backscatter in Siberian Forests

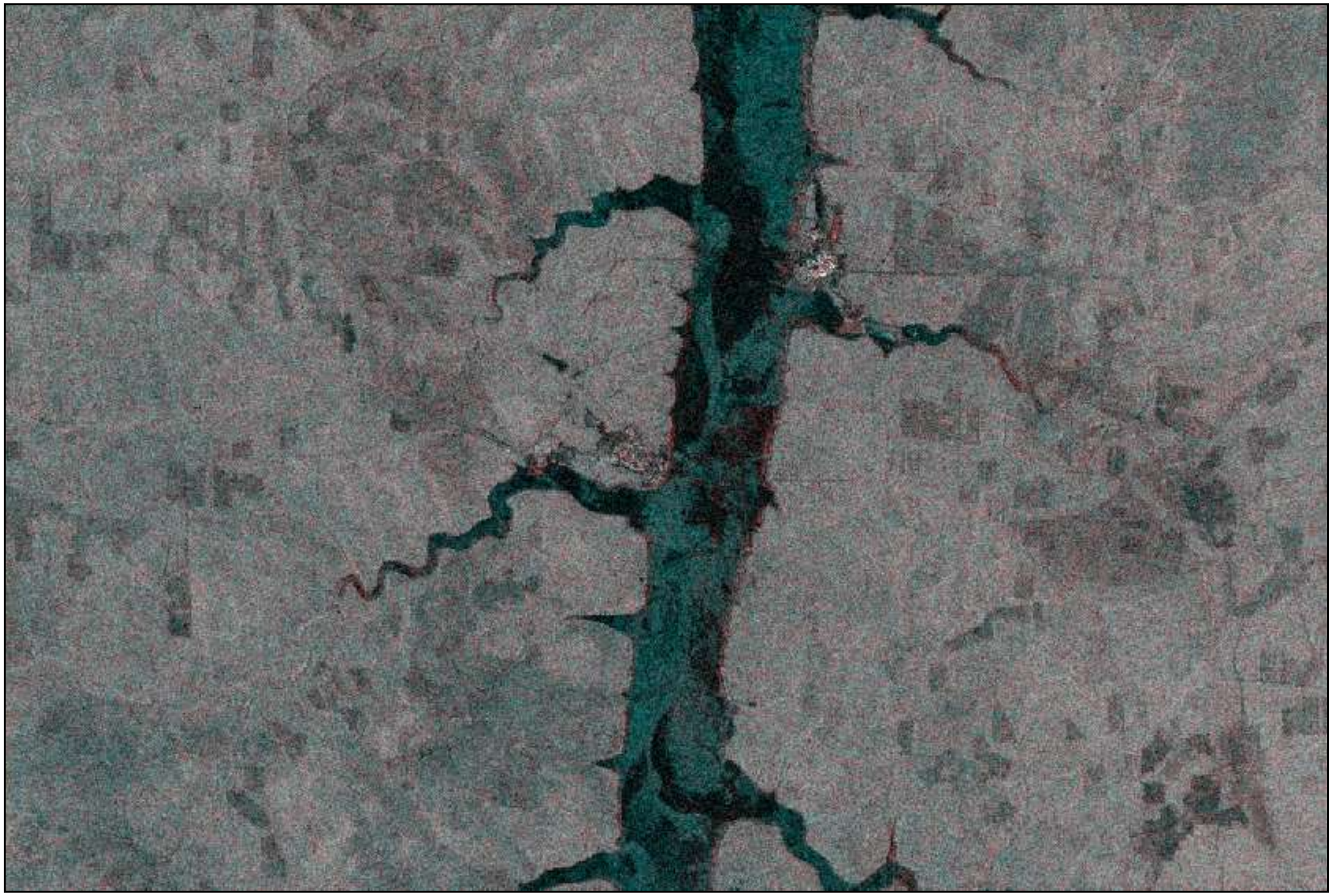

(RGB = HH-HV-HV)

East
14.02.2006
21.03.2006
25.04.2006
-
-
04.07.2006
-
12.09.2006
-
21.11.2006

Seasonal behaviour of C-Band Backscatter in Siberian Forests

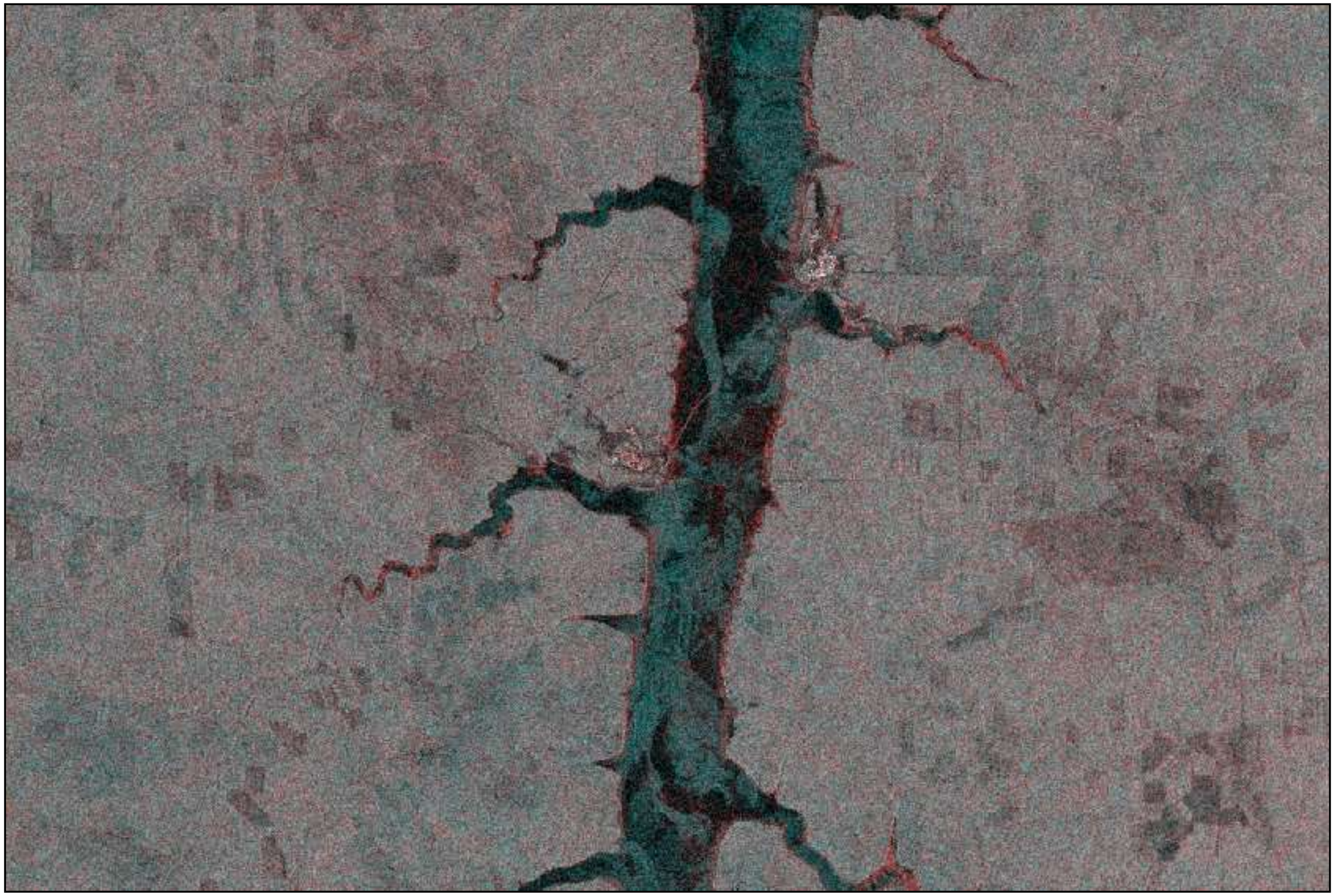

(RGB = HH-HV-HV)

East
14.02.2006
21.03.2006
25.04.2006
-
-
04.07.2006
-
12.09.2006
-
21.11.2006

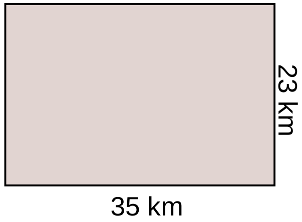

Seasonal behaviour of C-Band Backscatter in Siberian Forests

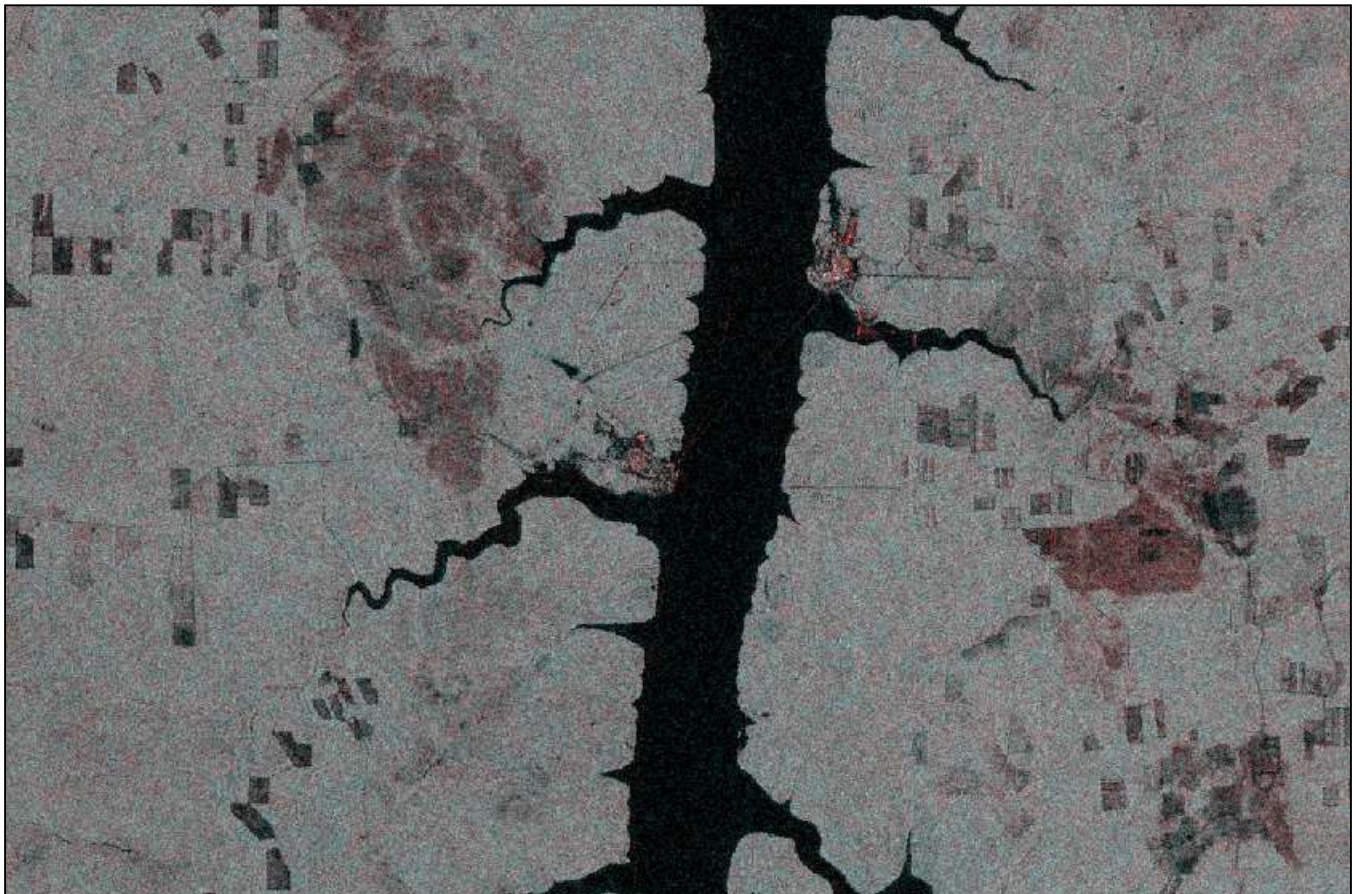

(RGB = HH-HV-HV)

East
14.02.2006
21.03.2006
25.04.2006
-
-
04.07.2006
-
12.09.2006
-
21.11.2006

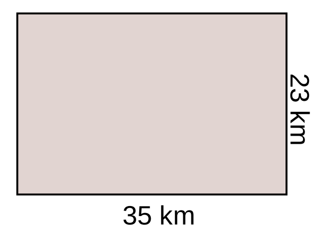

Seasonal behaviour of C-Band Backscatter in Siberian Forests

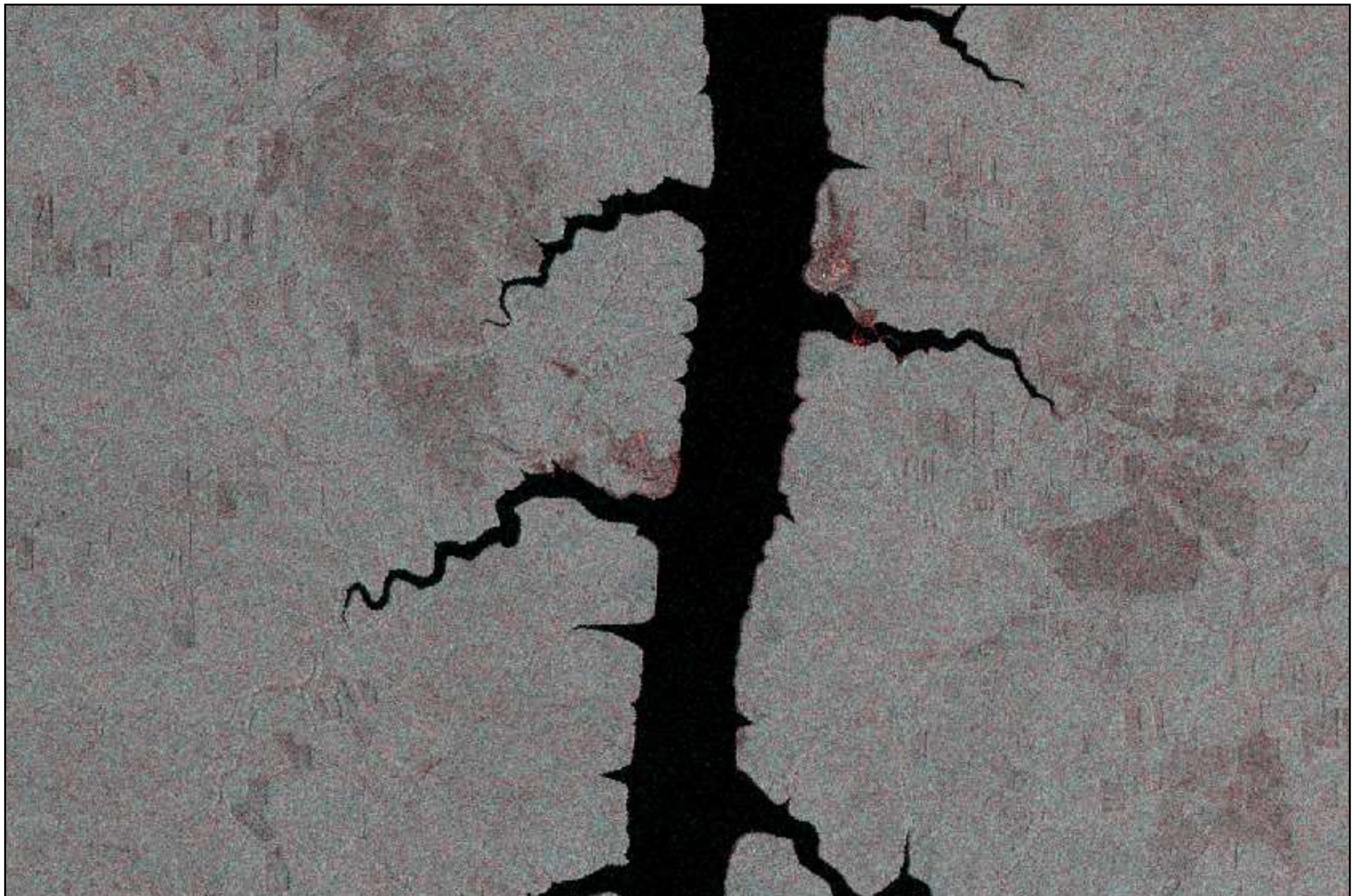

(RGB = HH-HV-HV)

East
14.02.2006
21.03.2006
25.04.2006
-
-
04.07.2006
-
12.09.2006
-
21.11.2006

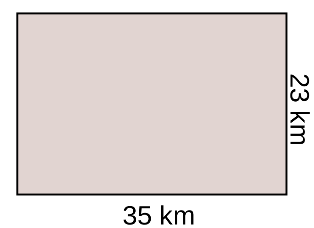

Seasonal behaviour of C-Band Backscatter in Siberian Forests

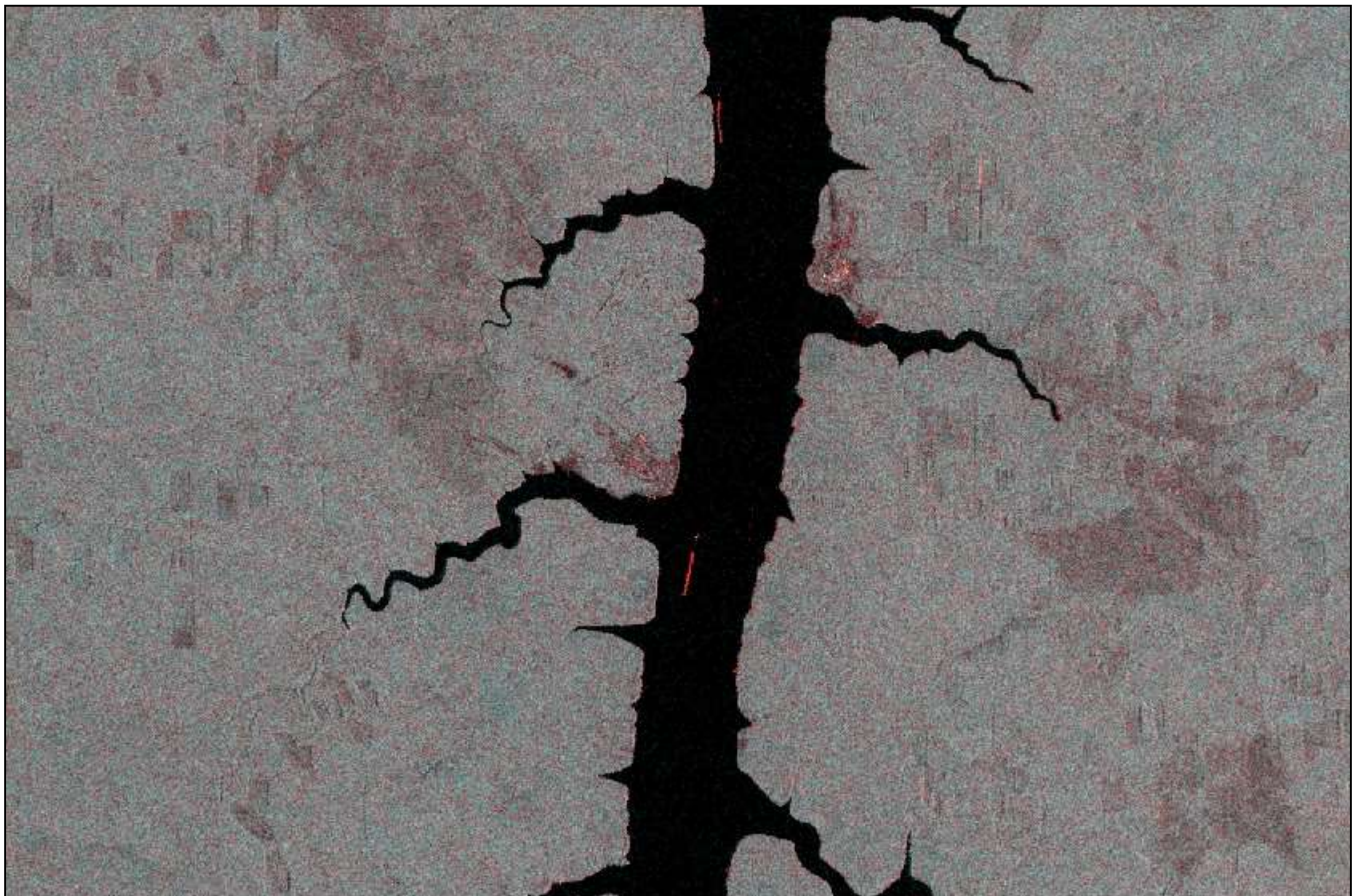

(RGB = HH-HV-HV)

East
14.02.2006
21.03.2006
25.04.2006
-
-
04.07.2006
-
12.09.2006
-
21.11.2006

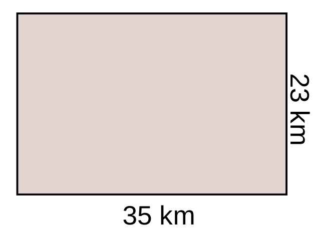

Seasonal behaviour of C-Band Backscatter in Siberian Forests

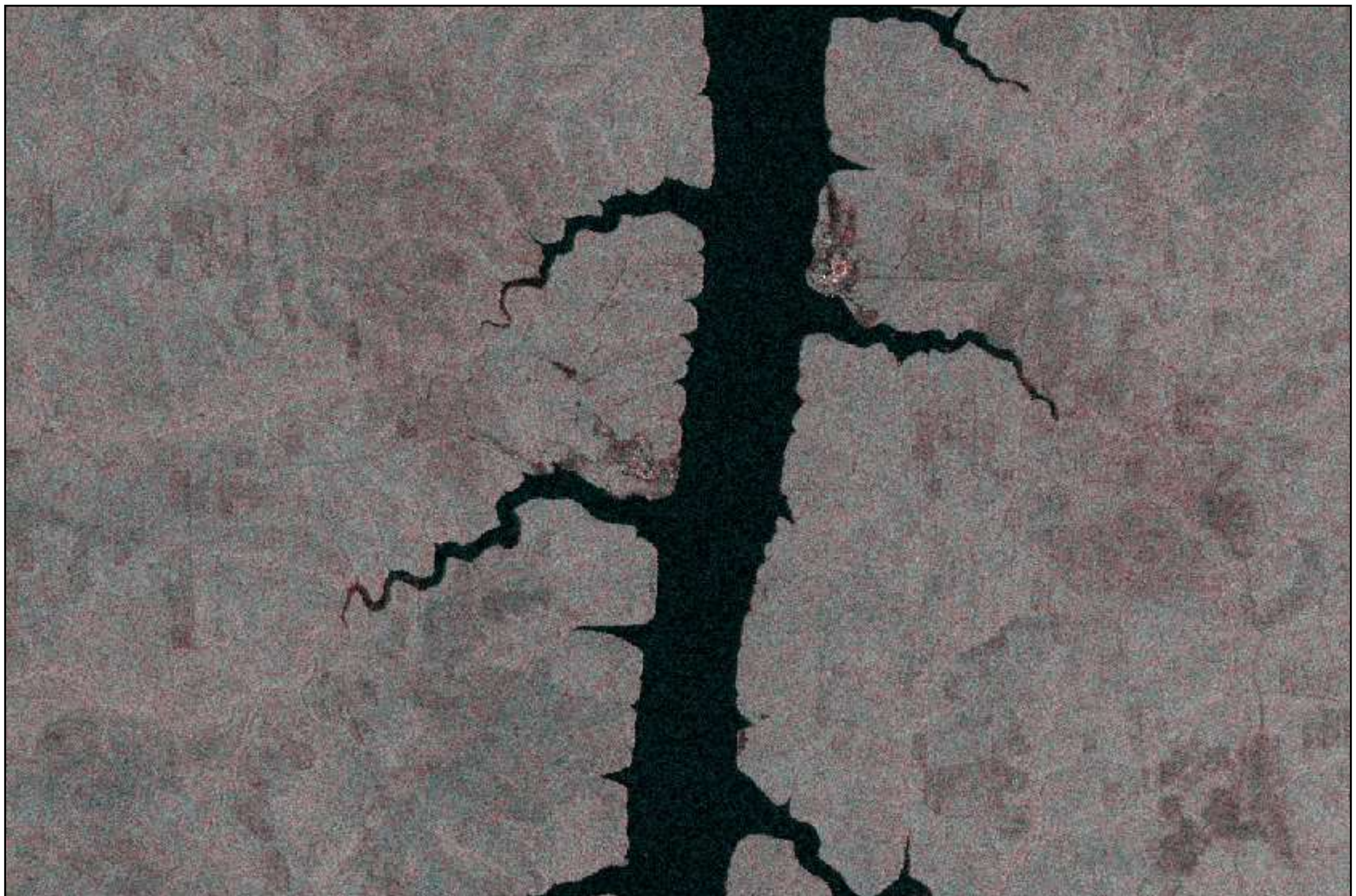

(RGB = HH-HV-HV)

East
14.02.2006
21.03.2006
25.04.2006
-
-
04.07.2006
-
12.09.2006
-
21.11.2006

23 km

35 km

Seasonal behaviour of C-Band Backscatter in Siberian Forests

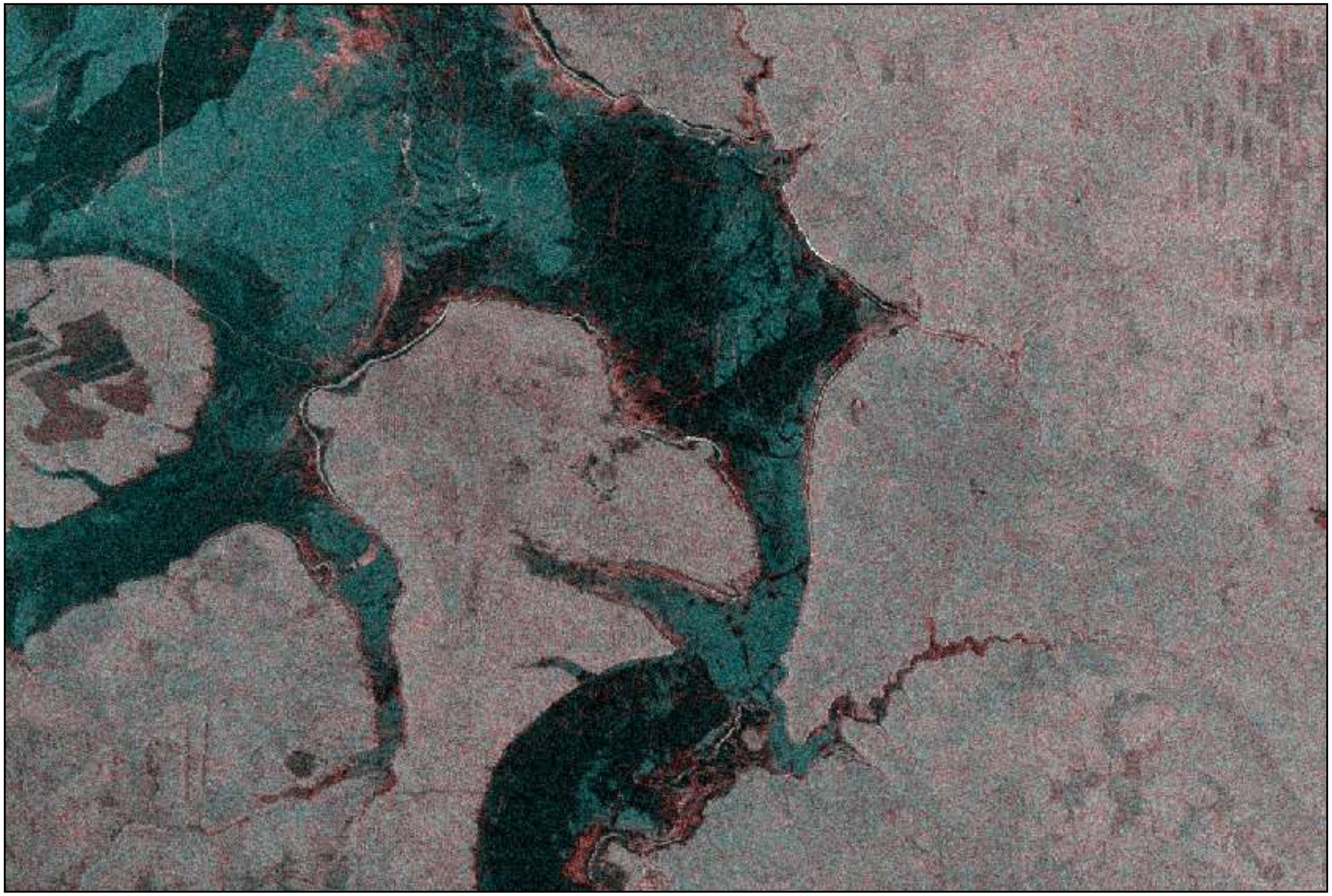

(RGB = HH-HV-HV)

West
-
05.03.2006
-
14.05.2006
18.06.2006
23.07.2006
27.08.2006
-
-
05.11.2006

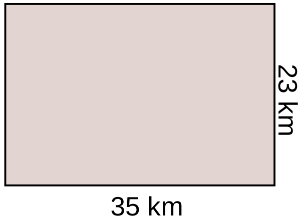

Seasonal behaviour of C-Band Backscatter in Siberian Forests

(RGB = HH-HV-HV)

West
-
05.03.2006
-
14.05.2006
18.06.2006
23.07.2006
27.08.2006
-
-
05.11.2006

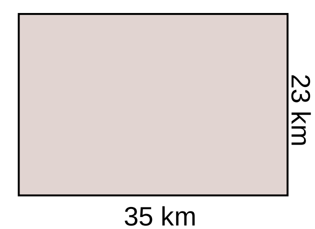

Seasonal behaviour of C-Band Backscatter in Siberian Forests

(RGB = HH-HV-HV)

West
-
05.03.2006
-
14.05.2006
18.06.2006
23.07.2006
27.08.2006
-
-
05.11.2006

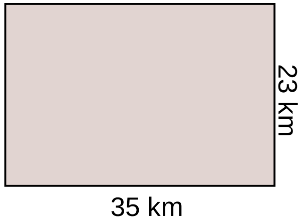

Seasonal behaviour of C-Band Backscatter in Siberian Forests

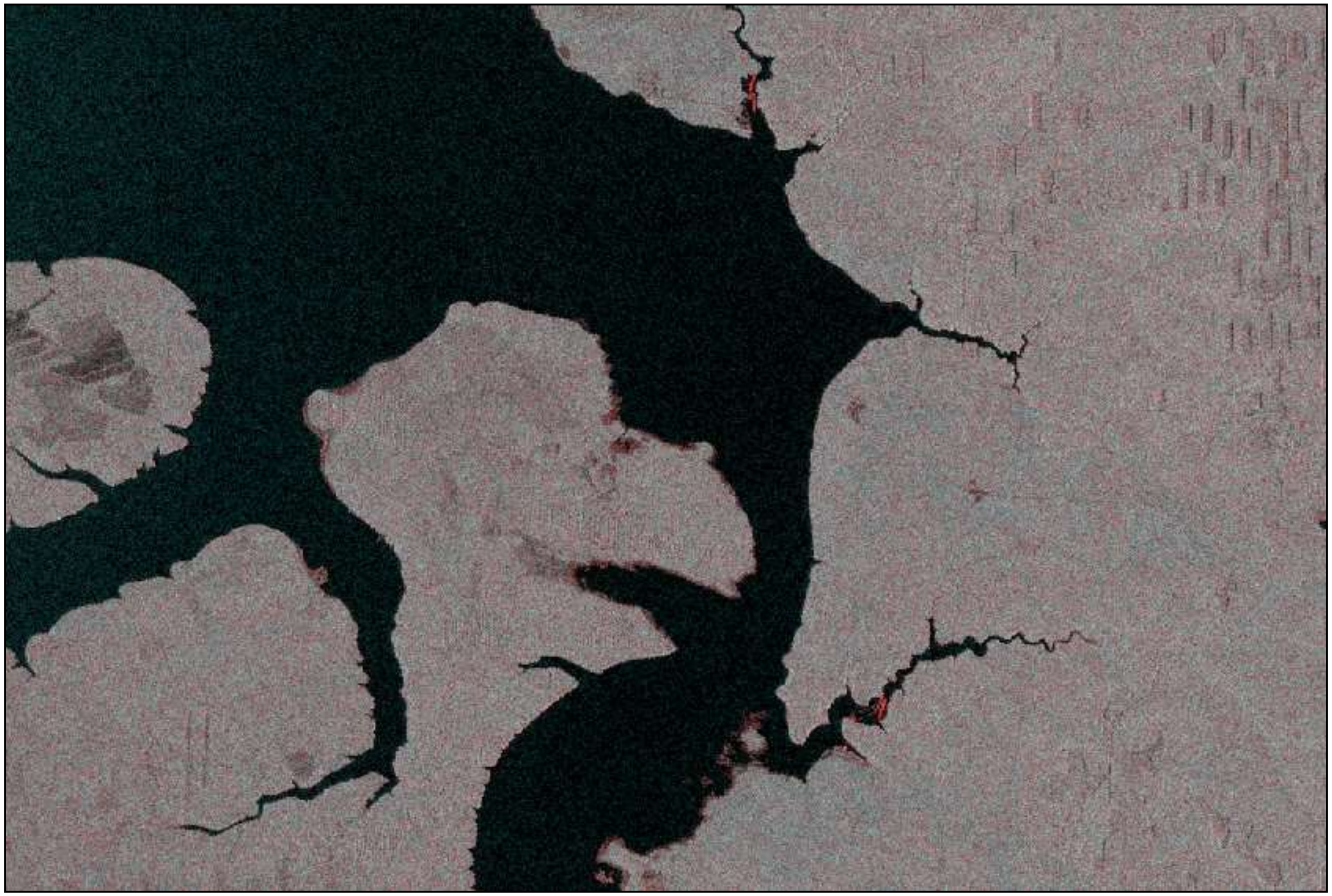

(RGB = HH-HV-HV)

West
-
05.03.2006
-
14.05.2006
18.06.2006
23.07.2006
27.08.2006
-
-
05.11.2006

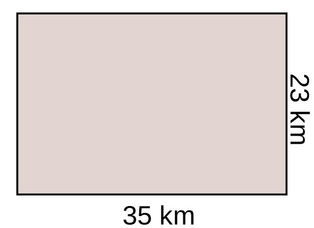

Seasonal behaviour of C-Band Backscatter in Siberian Forests

(RGB = HH-HV-HV)

West
-
05.03.2006
-
14.05.2006
18.06.2006
23.07.2006
27.08.2006
-
-
05.11.2006

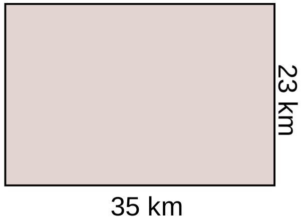

Seasonal behaviour of C-Band Backscatter in Siberian Forests

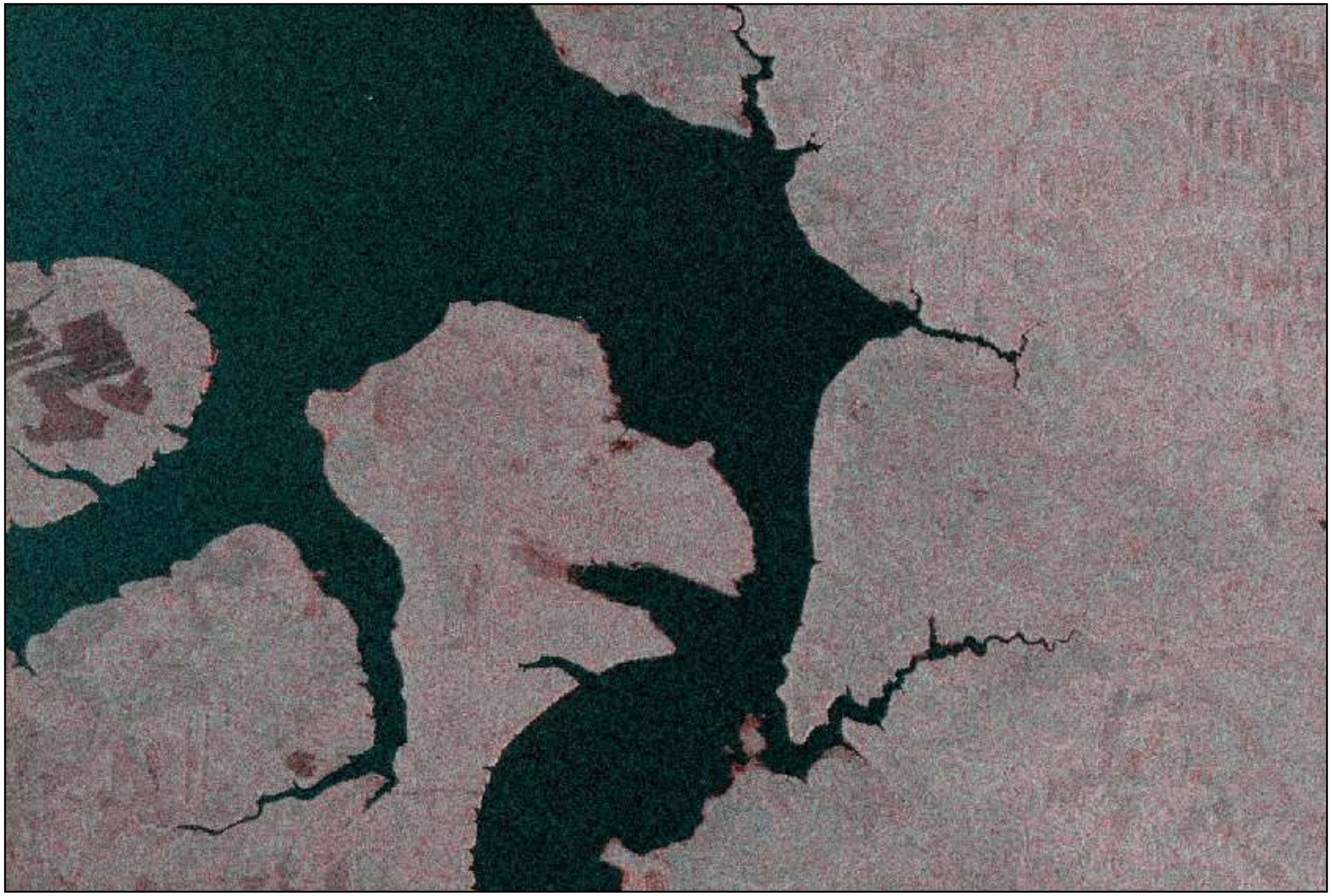

(RGB = HH-HV-HV)

West
-
05.03.2006
-
14.05.2006
18.06.2006
23.07.2006
27.08.2006
-
-
05.11.2006

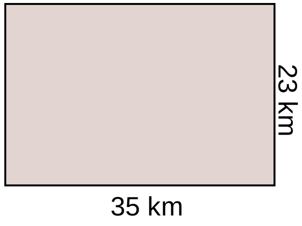

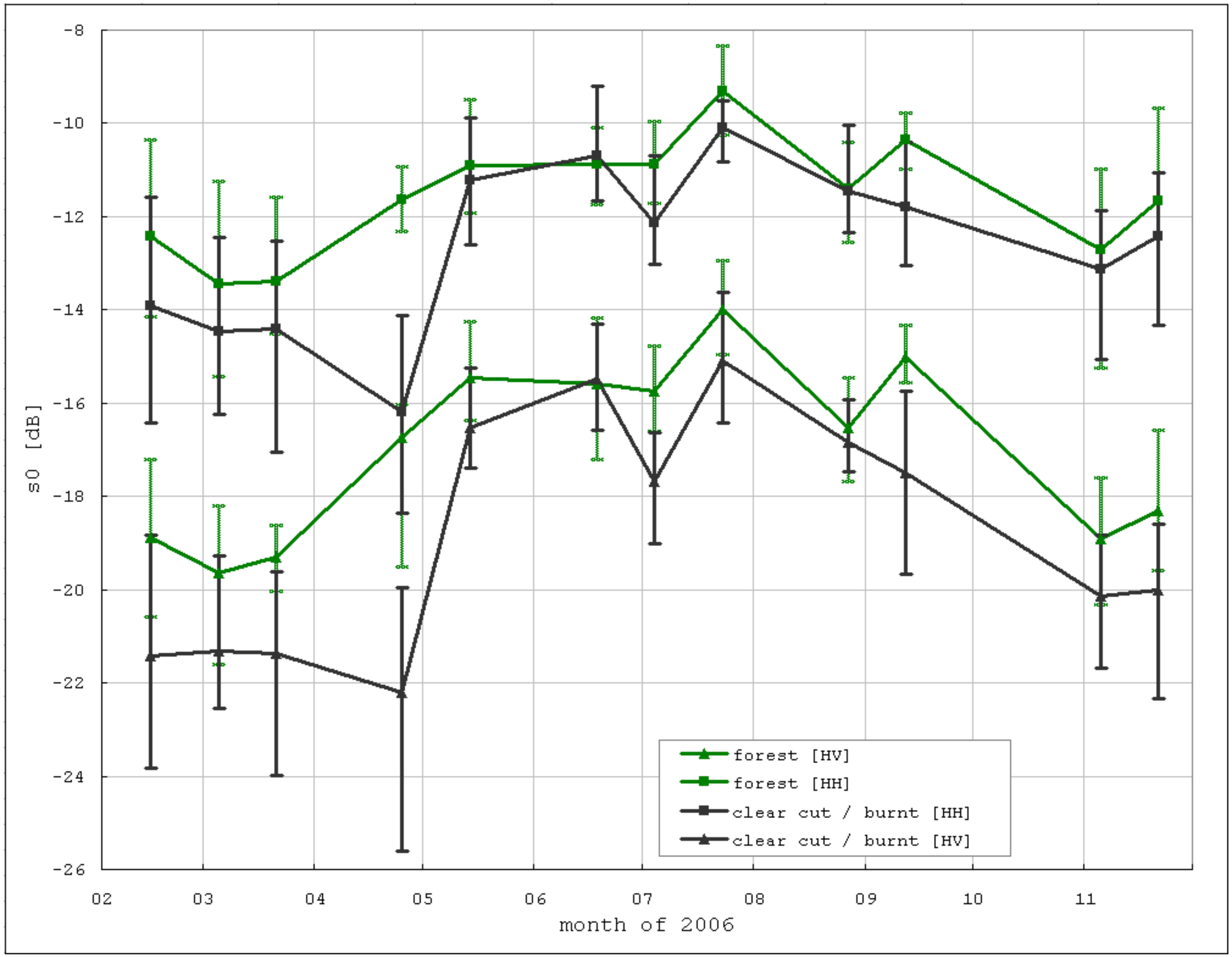

Eastern & Western Scene – combined signature plot:

Mean backscatter for forest and non-forest (signatures merged from previous 3 forest and 2 non-forest classes)

Bars denote min and max respectively

Separability analysis

	burnt/clear-cut vs. forest
14.02.2006	0,38
05.03.2006	0,49
21.03.2006	0,34
25.04.2006	0,78
14.05.2006	0,23
18.06.2006	0,11
04.07.2006	0,36
23.07.2006	0,24
27.08.2006	0,11
12.09.2006	0,46
05.11.2006	0,38
21.11.2006	0,27

Eastern & Western Scene: Normalised Jefferies-Matusita distances

Separability analysis performed on pixel level

1.0 = signatures separable
0.0 = signatures inseparable

Mean separability for forest and non-forest (signatures merged from previous 3 forest and 2 non-forest classes)

Best overall separability: 25th April

Separability analysis

- High separability of forest/non-forest at late April / early May is also evident for other scenes (were no complete time series was available) – next slide
- Where available, late April / early May scenes were utilised for map production, if not available less suited acquisition dates had to be applied

Weather and snow conditions in late April

Tulun (100,5°E / 54,5°N, altitude 522 m)

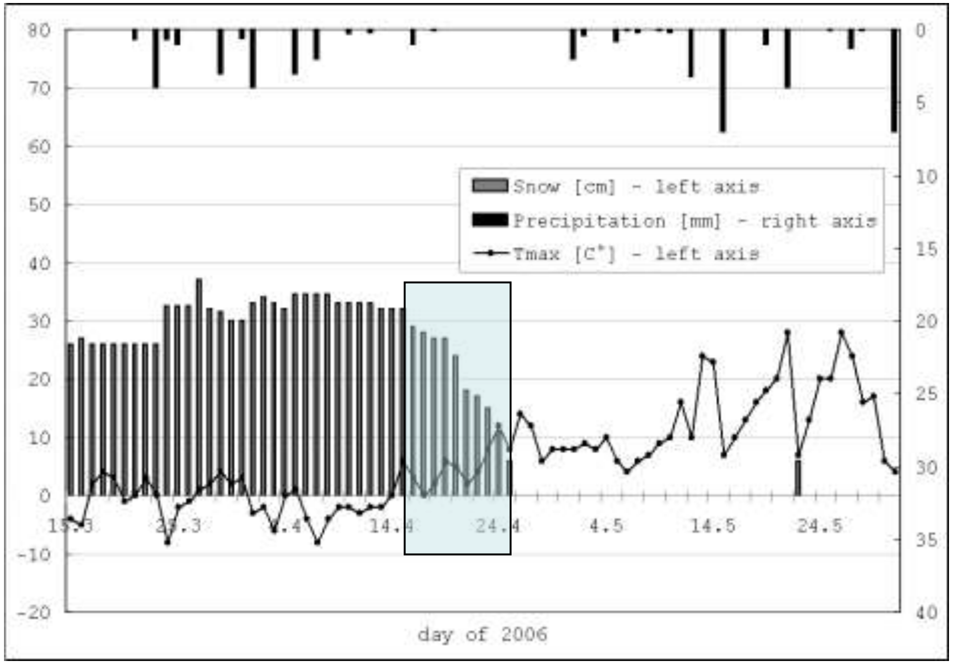

Vitim (103,1°E / 56,3°N, altitude 190 m)

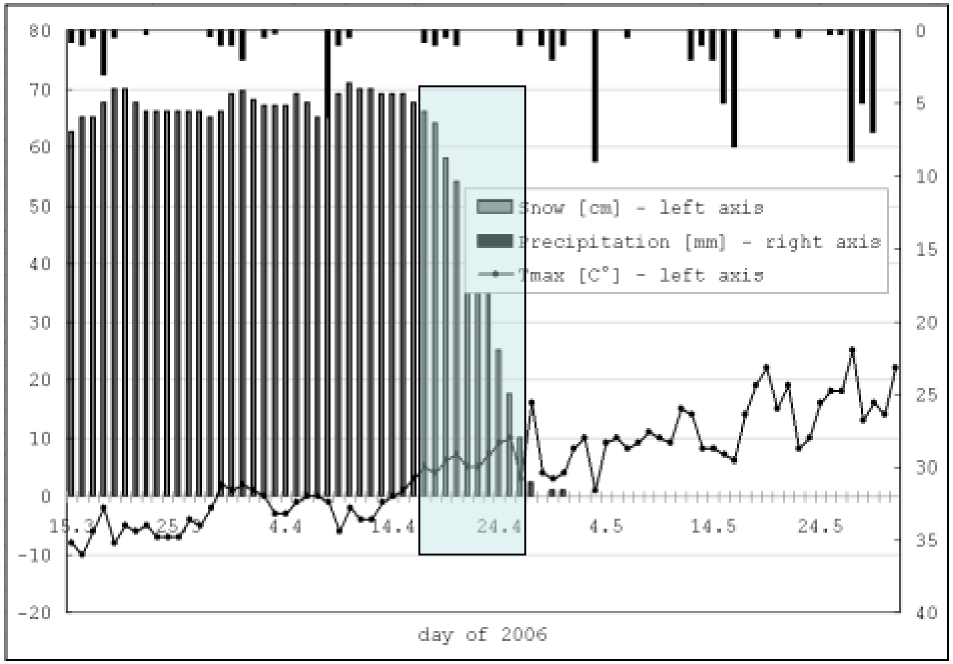

Daily values

C-band scattering processes in late April

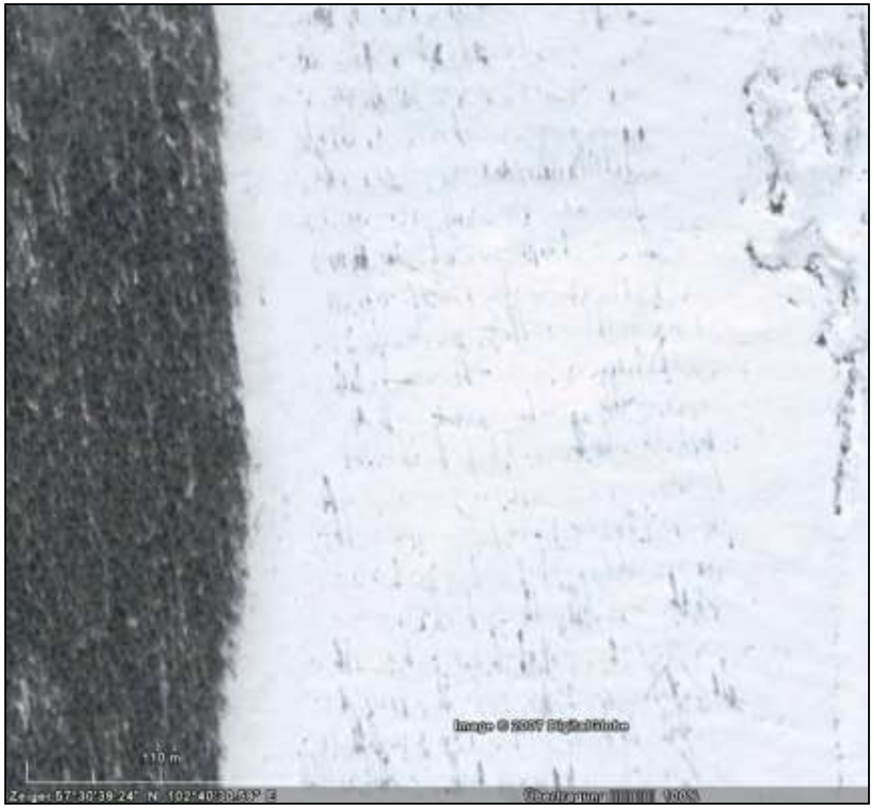

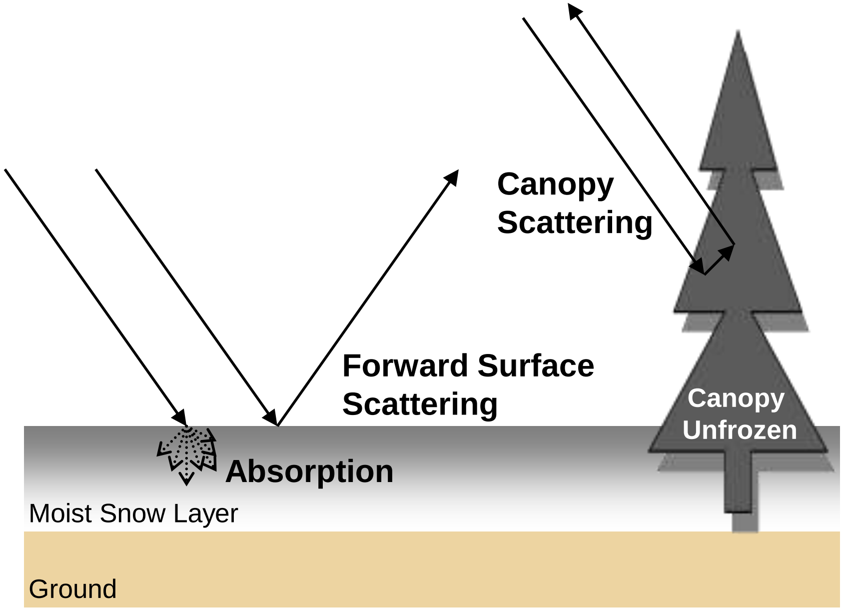

Outline

Background

The boreal zone (in particular Siberia) is characterised by unique environmental conditions

Winter:

- Trees are frozen, almost transparent, backscatter significantly reduced, environmental conditions are very stable
- Snow hardly impacts the scattering
- Soil is also frozen, changes in soil moisture do not appear
- Very low temporal decorrelation, great potential for forest biomass estimation

Thawing “season”:

- Wet snow cover
- High level of heterogeneity in space and time (snow cover, moisture, state of forest)
- Most unsuitable time

Summer:

- Temporal decorrelation (rainfall, changing soil moisture and interception water, wind)
- Repeat pass coherence for forest is assumed being in general much smaller compared to mid-winter
- However, not much is known about L-band mid-summer coherence (some work by Eriksson)

Site Characteristics

- Central Siberia in Russia (Irkutsk Oblast, Krasnoyarsk Kray)
- Middle Siberian Plateau: southern part is dominated by hills up to 1700 m, northern part is plain with heights up to 500 m
- Characteristic taiga forests (spruce, birch, larch, pine, aspen etc.) cover about 82% of the region
- Territory is characterised by large area changes of forests such as forest fire, and intensive human activities
- Continental climate, prec. ca. 400-450 mm/y

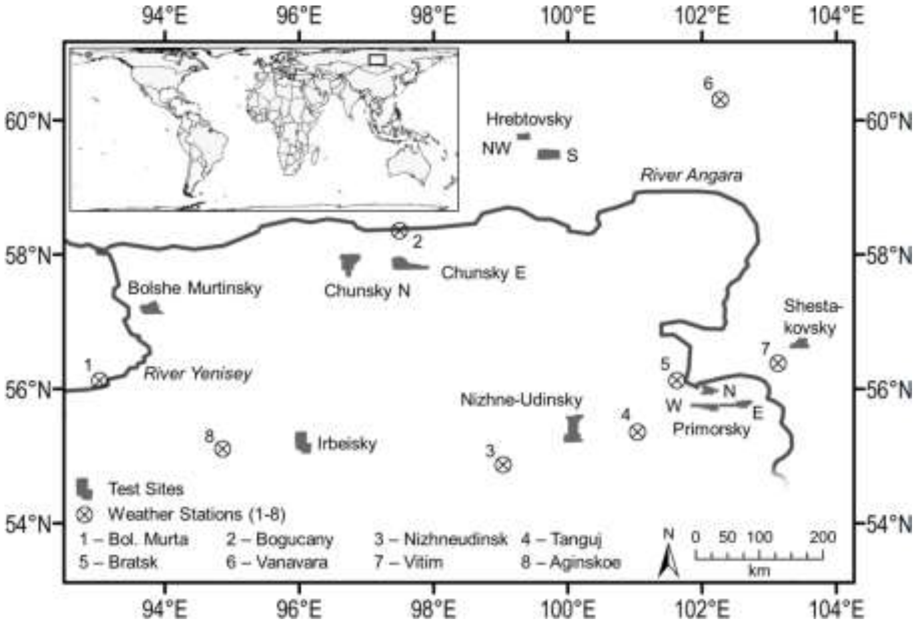

Methodology of Investigation – Overview

1. Generation of subsets from original frames covering forest inventory data
2. Computation of mean coherence per forest stand – new entity: forest stand
3. Computation of various statistical parameters
4. Fit of empirical exponential model (compare Askne & Santoro, 2005)
5. Creation of plots: stem volume vs. coherence
6. Check of perpendicular baseline → rejection of coherence data with baseline > ½ of critical baseline
7. Check of weather conditions

$$\gamma_{vol} = a e^{\frac{-vol}{c}} + b\left(1 - e^{\frac{-vol}{c}}\right)$$

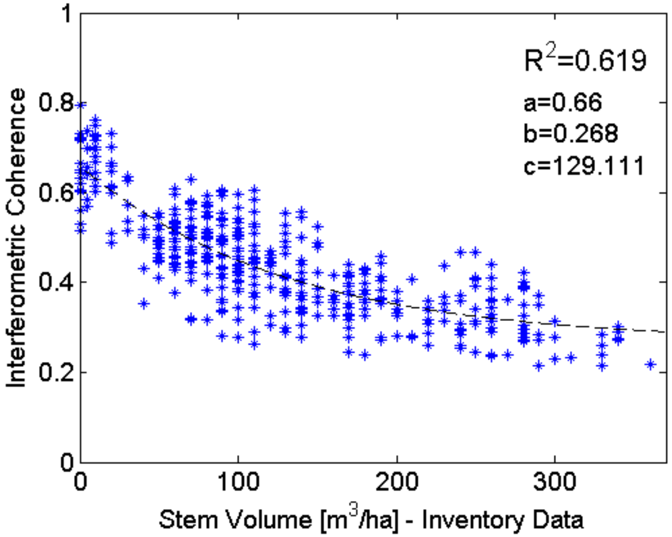

PALSAR Data

Location	Chunsky N	Chunsky E	Primorsky	Bolshe Murtinsky	Shesta-kovsky	Nizhne Udinsky	Irbeisky	Hrebtovsky
Track	T475	T473	T466	T481	T0463	T0471	T0478	T0468
Frame	F1150	F1150	F1110	F1140	F1130	F1100	F1100	F1190
Date		30 Dec 06	18 Jan 07	28 Dec 06	13 Jan 07	11 Jan 07		6 Jan 07
		14 Feb 07	5 Mar 07	12 Feb 07	28 Feb 07	26 Feb 07		21 Feb 07
	20 Jun 07	***2 Jul 07***	***21 Jul 07***	***15 Aug 07***	***16 Jul 07***	***14 Jul 07***		***9 Jul 07***
	5 Aug 07	***17 Aug 07***	***5 Sep 07***	***30 Sep 07***	***31 Aug 07***		***10 Aug 07***	***24 Aug 07***
	20 Sep 07	***2 Oct 07***	***21 Oct 07***		***16 Oct 07***	***14 Oct 07***		***9 Oct 07***
		17 Nov 07			16 Jan 08		**10 Nov 07**	9 Jan 08
	5 Nov 07				2 Mar 08	29 Feb 08	26 Dec 07	24 Feb 08
	21 Dec 07			31 Dec 07	***17 Apr 08***		10 Feb 08	***11 Jul 08***
	5 Feb 08	2 Jan 08	21 Jan 08	15 Feb 08	***18 Jul 08***	***16 Jul 08***	***27 Jun 08***	***26 Aug 08***
	22 Mar 08	17 Feb 08			***2 Sep 08***	***31 Aug 08***	***12 Aug 08***	
	7 May 08				18 Jan 09	16 Jan 09	28 Dec 08	11 Jan 09
	22 Jun 08	***4 Jul 08***		***2 Jul 08***	5 Mar 09	3 Mar 09	12 Feb 09	26 Feb 09
	7 Aug 08	***19 Aug 08***		***17 Aug 08***	***21 Jul 09***		***30 Jun 09***	***14 Jul 09***
		4 Jan 09		2 Jan 09	***5 Sep 09***		***15 Aug 09***	***29 Aug 09***
		19 Feb 09		17 Feb 09	***21 Oct 09***		***30 Sep 09***	***14 Oct 09***

Coherence Images – Examples Chunsky N – Winter-Winter (Temporal Baseline 46 d)

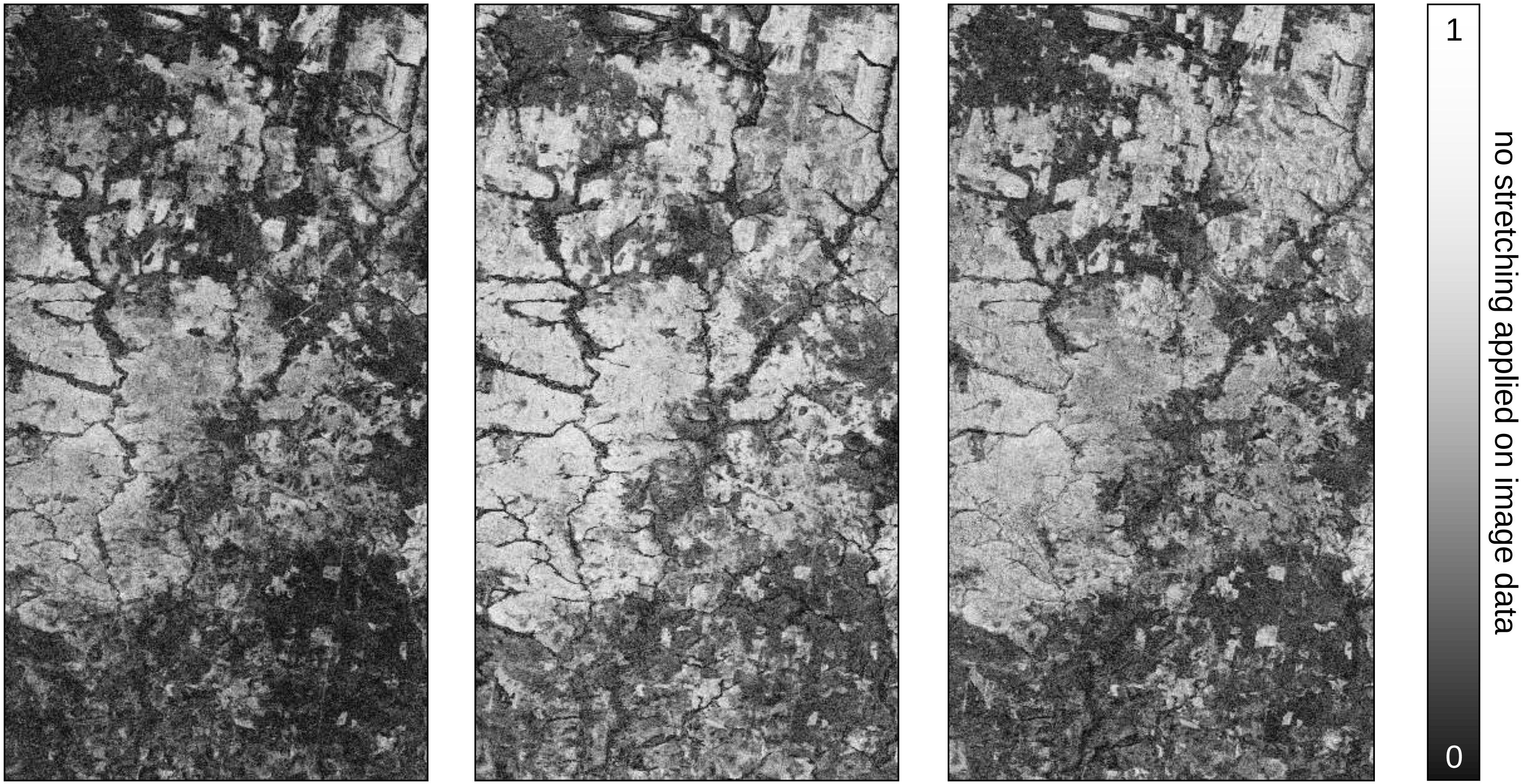

05nov07_21dec07 | 21dec07_05feb08 | 05feb08_22mar08

Coherence Images – Examples Chunsky N – Winter-Winter (Temporal Baseline 46 d)

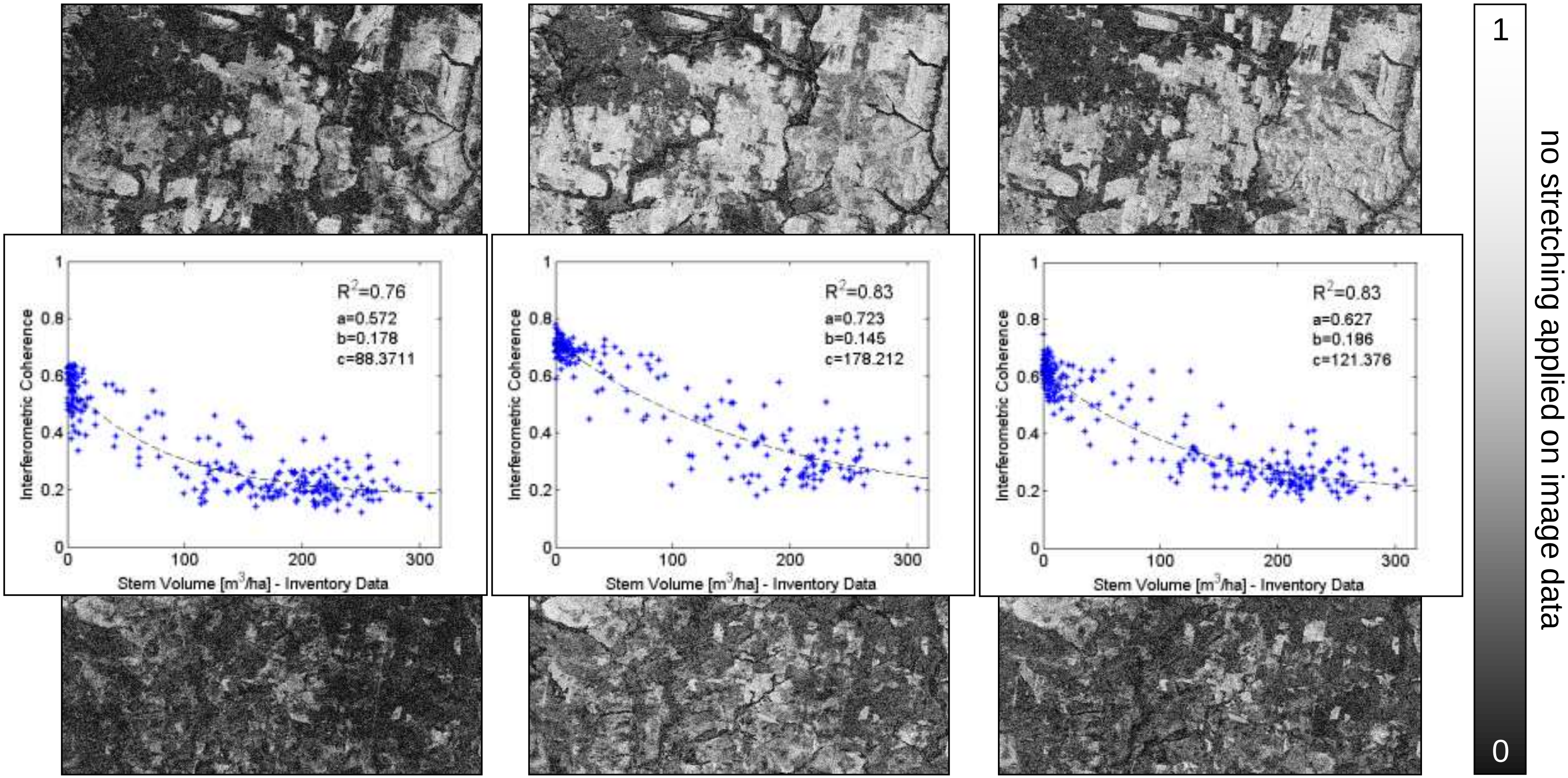

05nov07_21dec07 | 21dec07_05feb08 | 05feb08_22mar08

Coherence Images – Examples Chunsky N – Winter-Summer


05feb08_20jun07

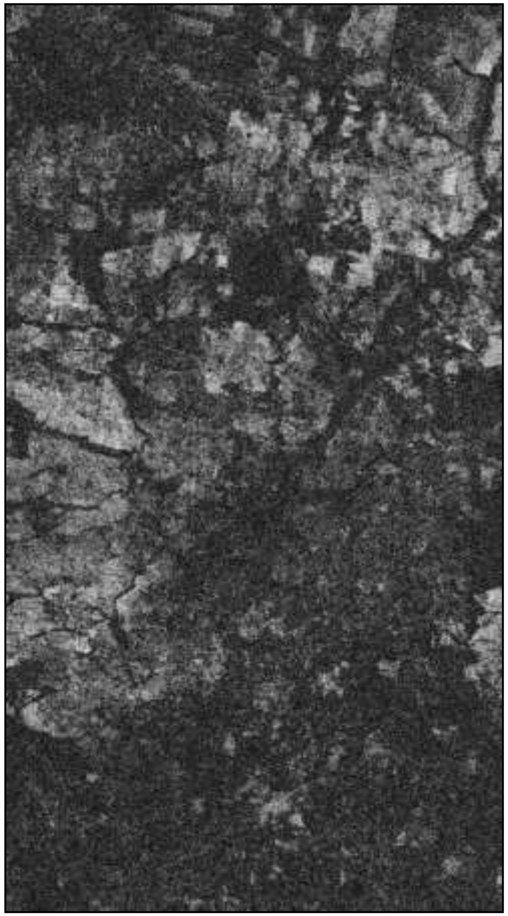
05nov07_20jun07

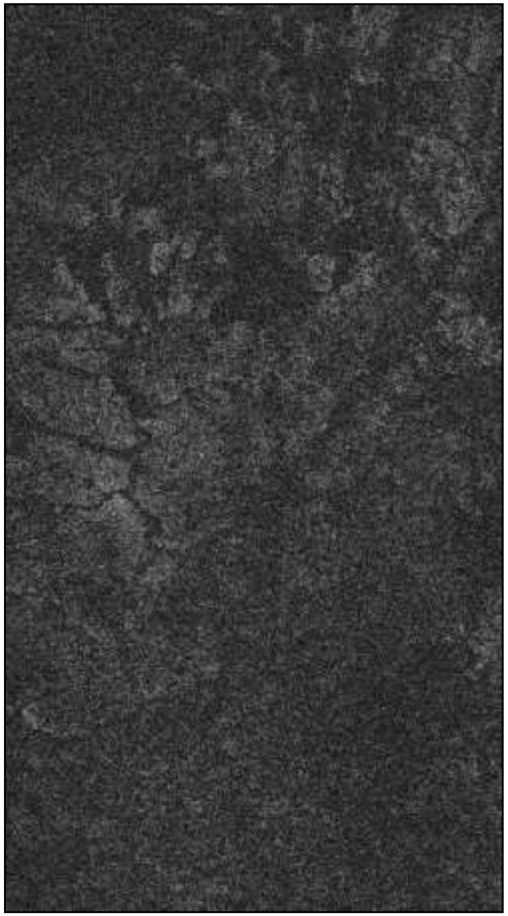
22mar08_20sep07

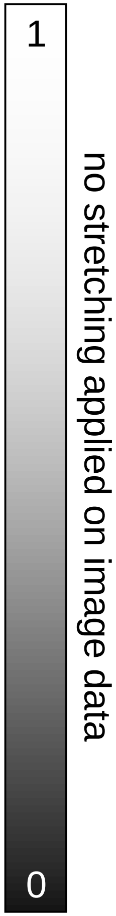

Coherence Images – Examples Chunsky N – Winter-Summer

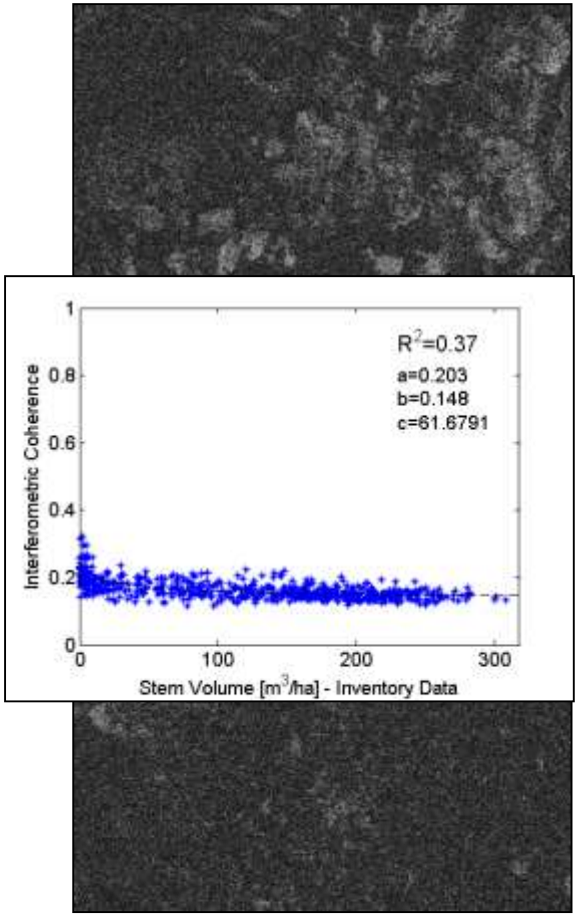

05feb08_20jun07

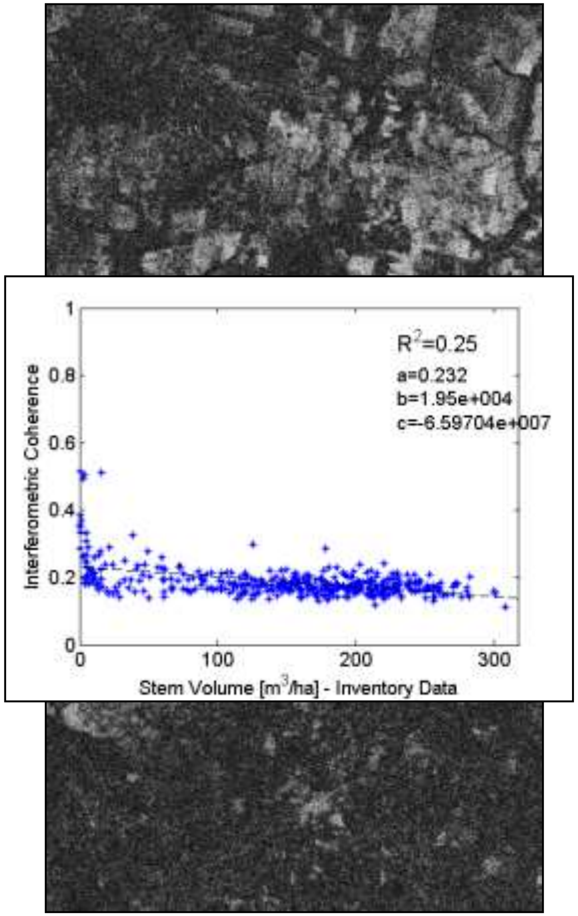

05nov07_20jun07

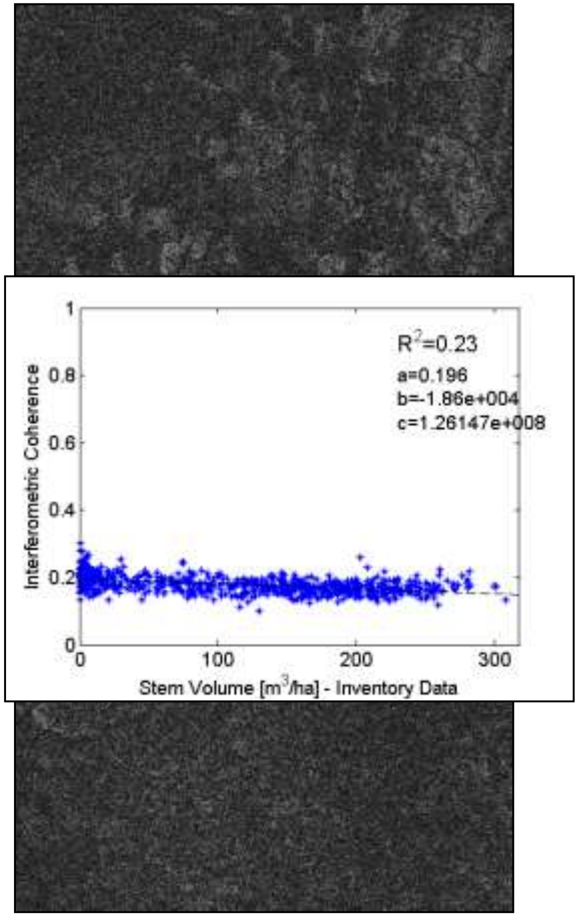

22mar08_20sep07

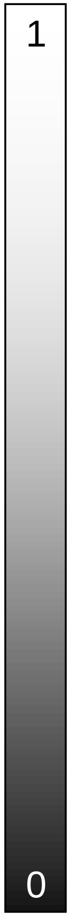

no stretching applied on image data

Coherence Images – Examples Chunsky N – Summer-Summer (Temp. Baseline 46 d)

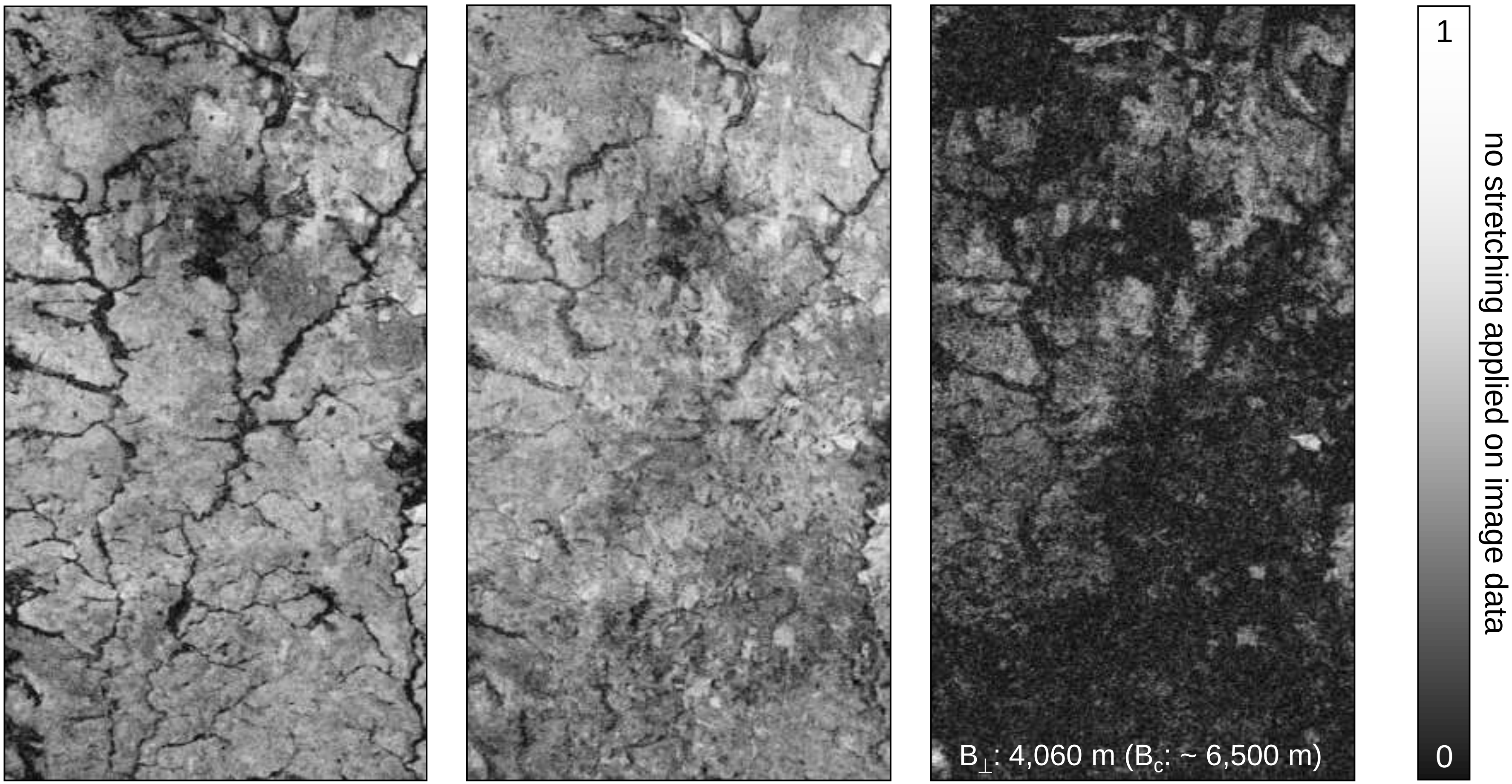

20jun07_05aug07 | 05aug07_20sep07 | 22jun08_07aug08

Coherence Images – Examples Chunsky N – Summer-Summer (Temp. Baseline 46 d)

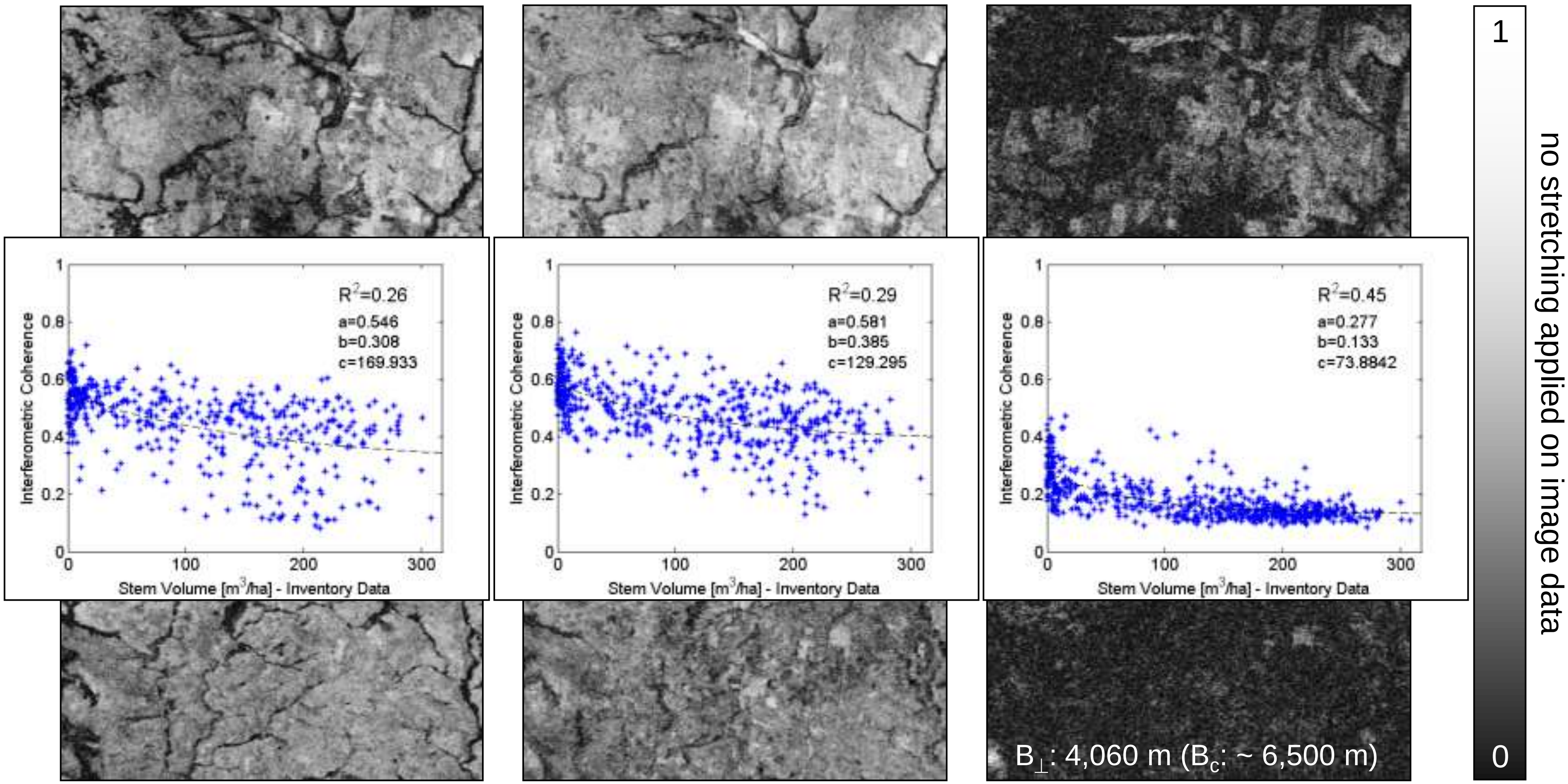

20jun07_05aug07 | 05aug07_20sep07 | 22jun08_07aug08

Scatter Plots – Representative Examples: Observed impact of GSV on |γ|

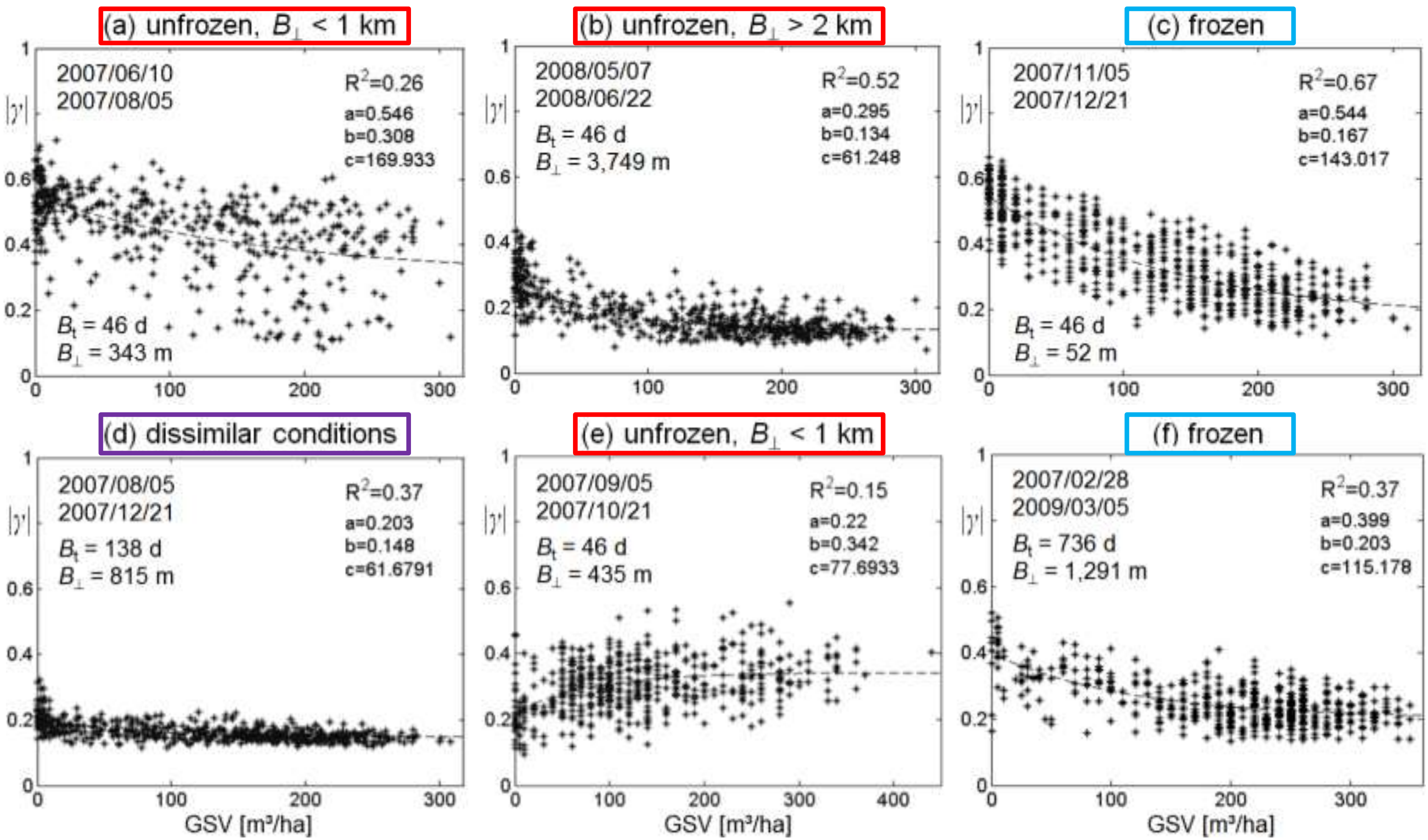

Impact of $B_\perp$ on |γ| (unfrozen conditions)

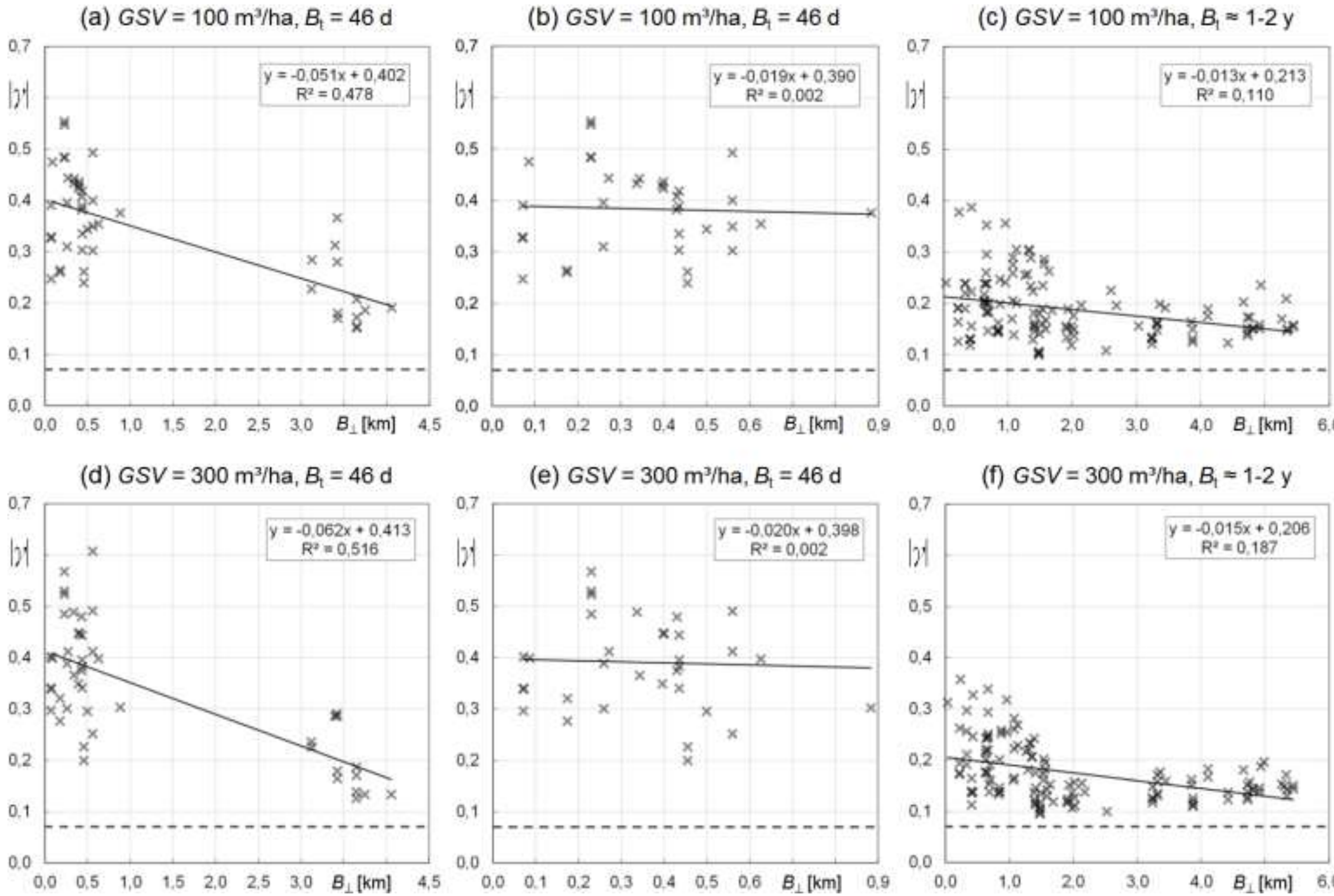

Impact of $B_\perp$ on |γ| (frozen conditions)

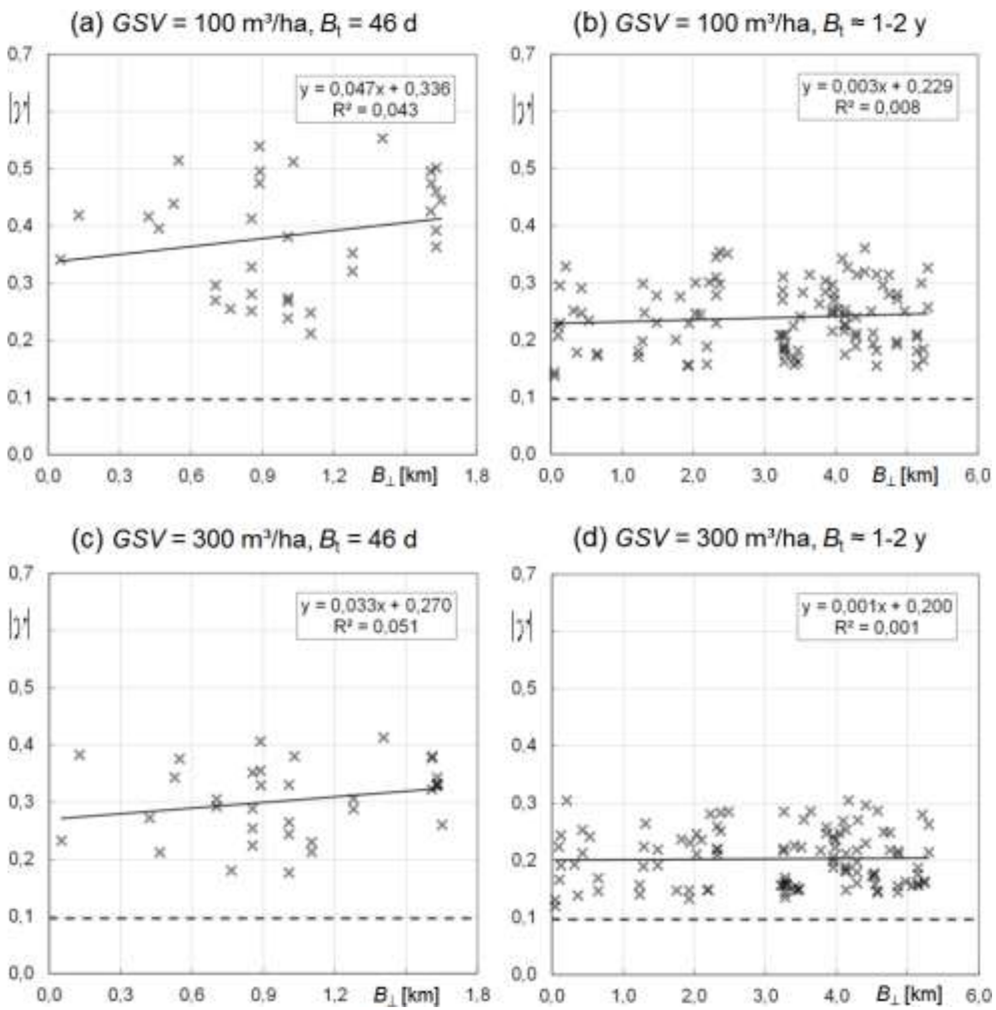

Summary of all PALSAR Observations

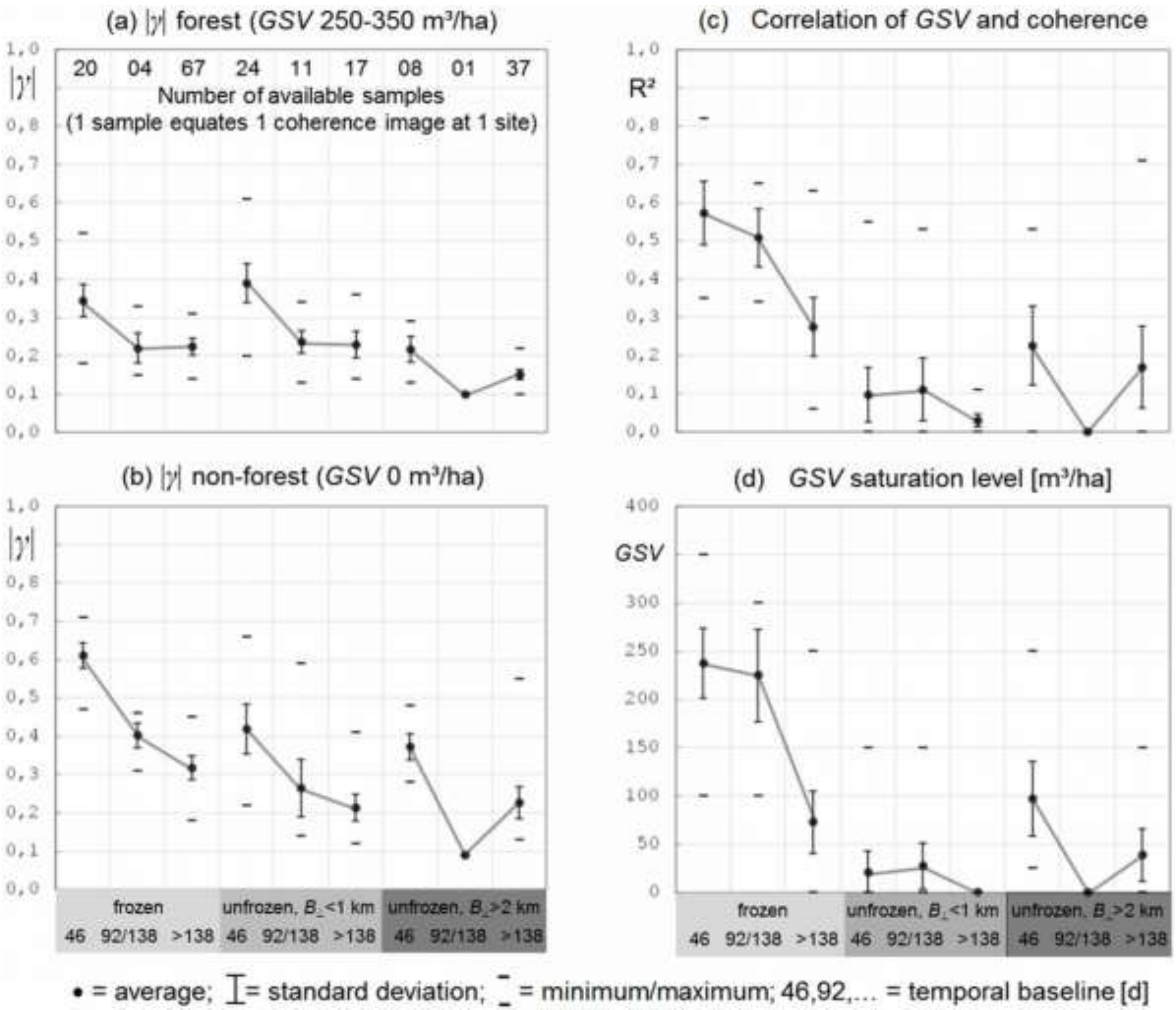

Outline

X-band coherence over the Thuringian Forest

Nicolas Ackermann

Introduction

- Context:
  - The **monitoring of forested areas** represents a great **challenge** in the context of the actual climate change and the development of the wood industry activities.
  - Cosmo-SkyMed, with a **constellation of 4 satellites,** constitutes a promising instruments for the retrieval of **forest biophysical parameters**.

Introduction

- Context:
  - The **monitoring of forested areas** represents a great **challenge** in the context of the actual climate change and the development of the wood industry activities.
  - Cosmo-SkyMed, with a **constellation of 4 satellites,** constitutes a promising instruments for the retrieval of **forest biophysical parameters**.

- Objectives:
  - Can **X-band** data be useful for forest **biomass assessment**?
  - Investigate the X-band **backscatter intensity** and **interferometric coherence**.




Test site & data

Test site

- Thuringian Forest (Germany)
  - 110 km x 50 km
  - Moderate topography
  - Tree species composition
    - Scots Pine
    - Norway Spruce
    - European Beech
  - Climate
    - cool and rainy
    - frequently clouded
  - Peculiarities
    - logging for forest exploitation
    - Kyrill storm (February 2007)

Test site

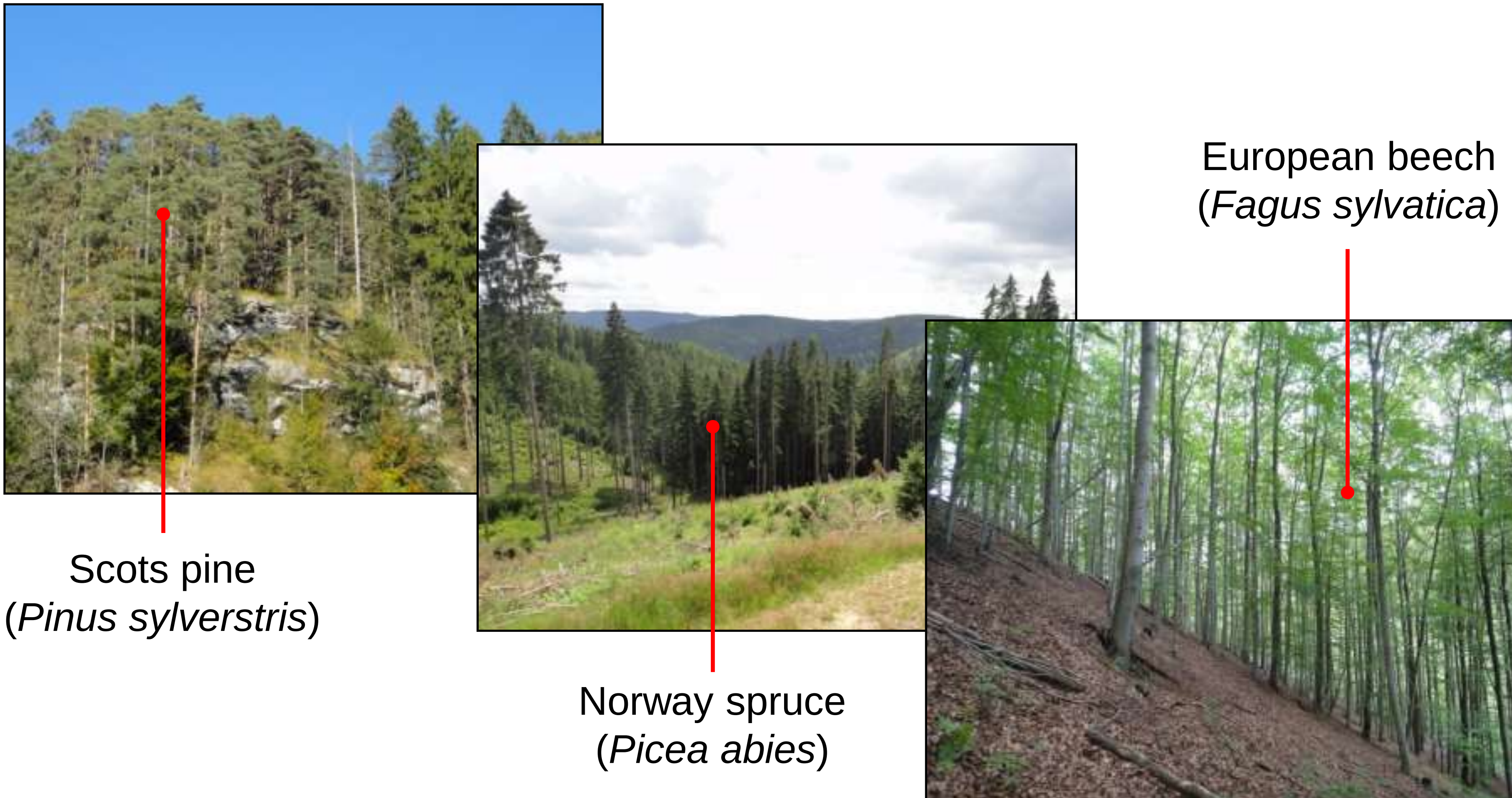
Scots pine
(*Pinus sylverstris*)
Norway spruce
(*Picea abies*)
European beech
(*Fagus sylvatica*)

Differentation of conifers and broadleaves

X-band backscatter

- Visual interpretations

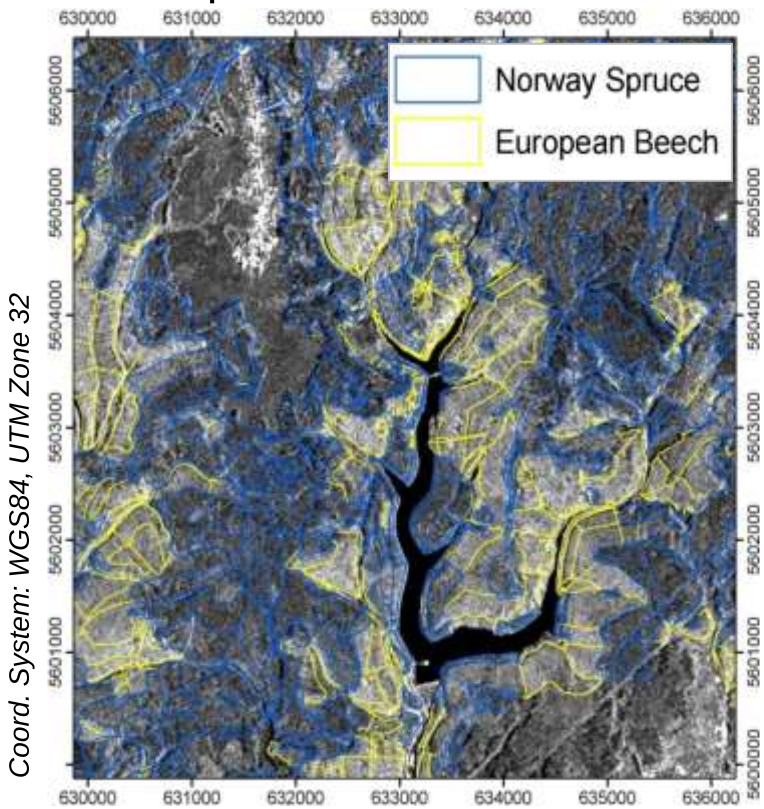

CSK 34˚ HH, 41˚, Desc. 23nov10

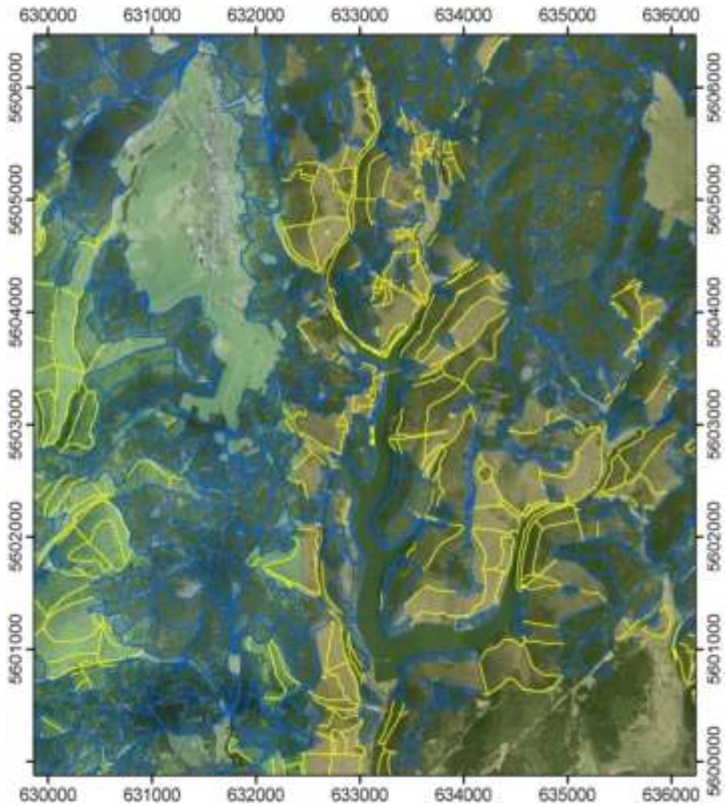

Digital orthophoto, 28apr08

X-band backscatter

- Phenologies

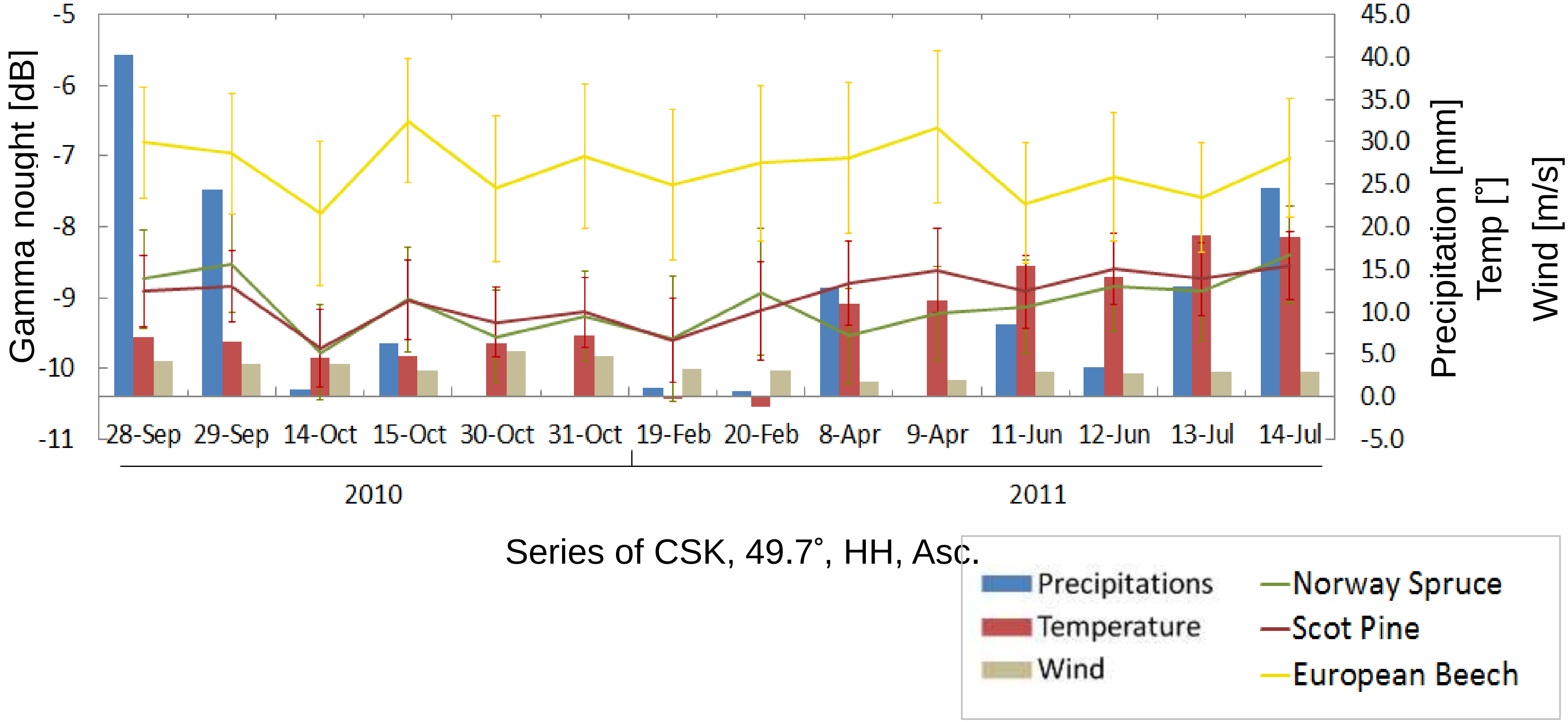

Series of CSK, 49.7˚, HH, Asc.

Conifers discrimination to broadleaves improved during leaf-off period.

Signal relatively stable

X-band backscatter

- Phenologies

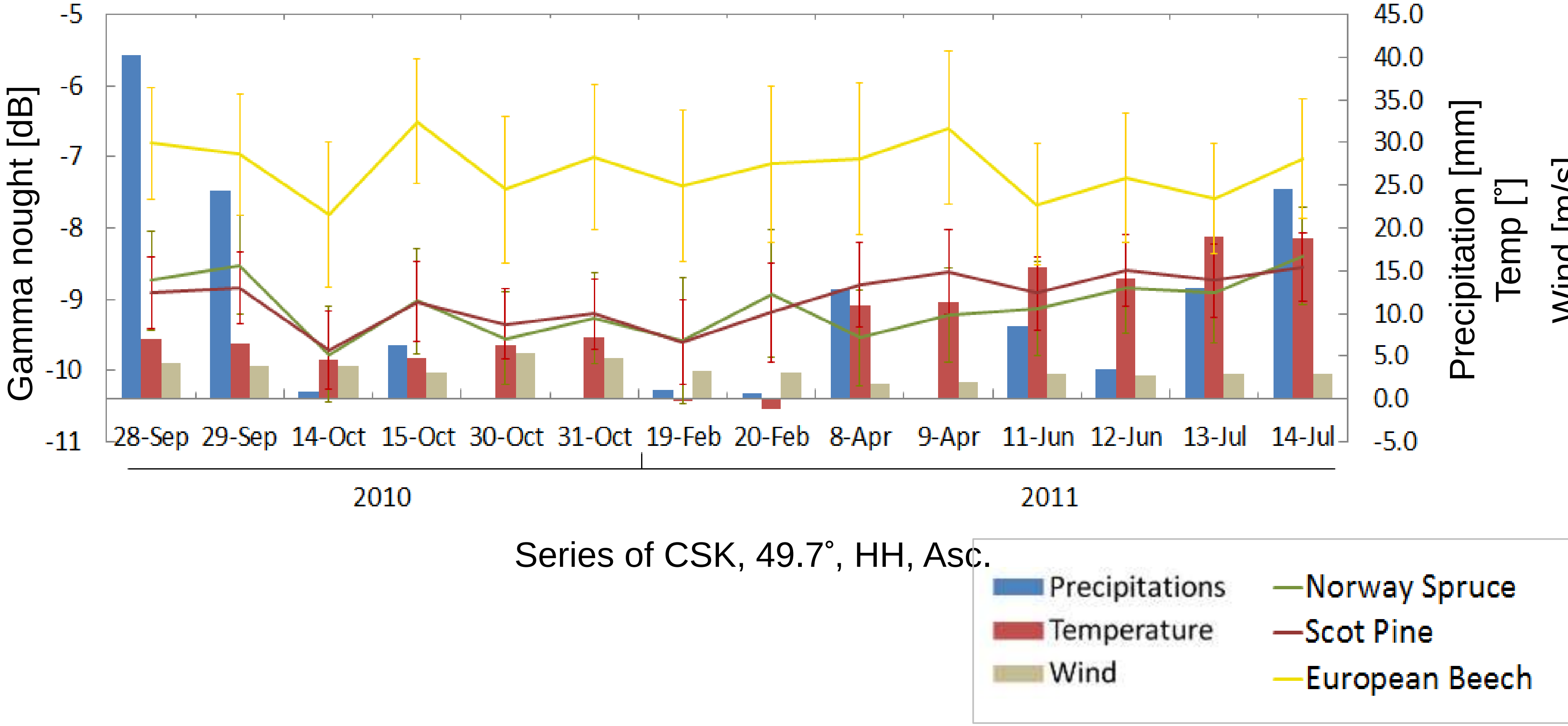

Series of CSK, 49.7˚, HH, Asc.

X-band InSAR coherence

X-band InSAR coherence

Forested areas:

TDX – low decorrelation
CSK – high decorrelation
TSX – complete decorr.

- Visual interpretations

RapidEye RGB – 13jun09

TDX SM 30aug10
Single pass
B_n=259 m

CSK Himage 30oct10 – 31oct10
1 day repeat pass
B_n=296 m

TSX HS 05jul09 – 16jul09
11 days repeat pass
B_n=209 m

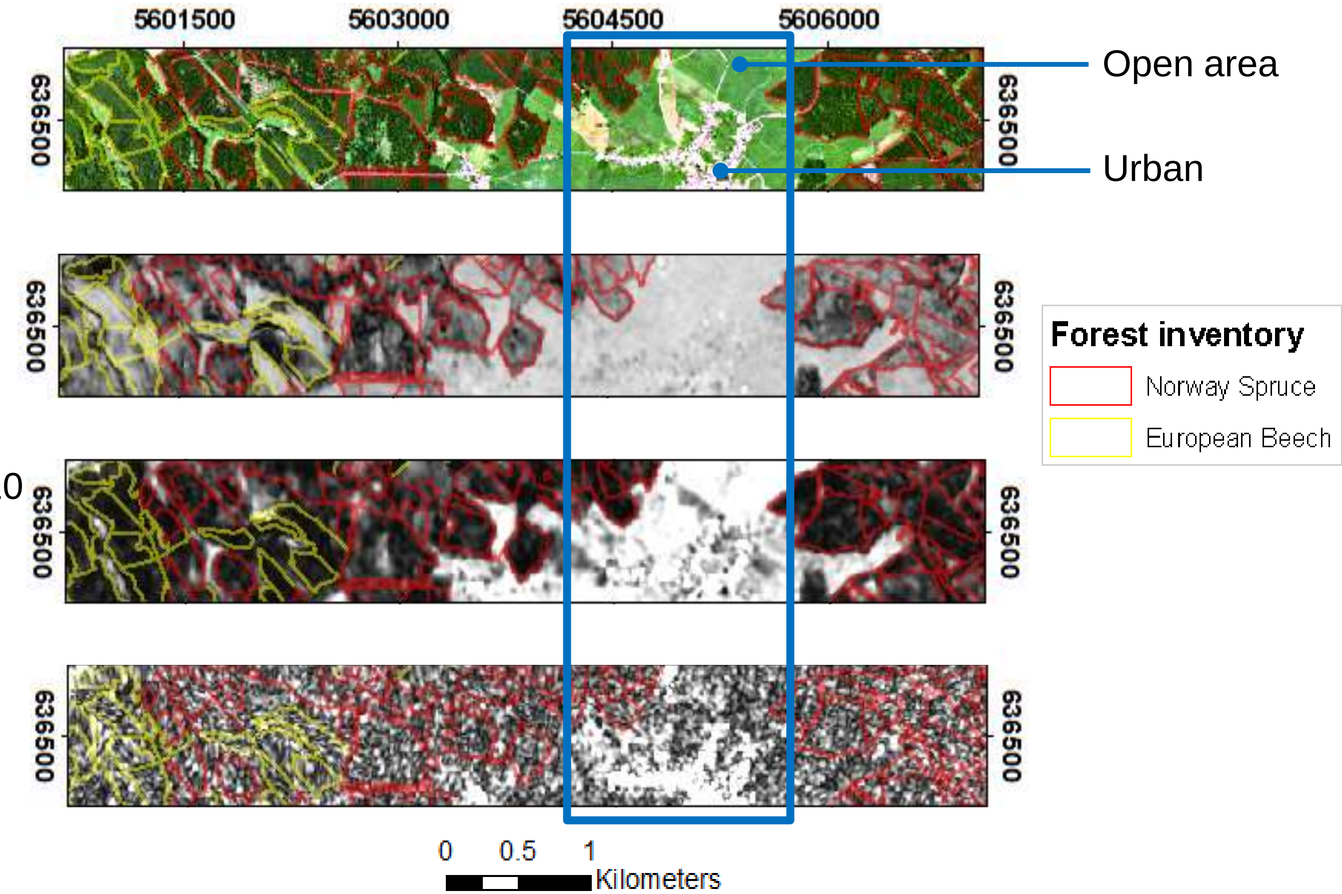

X-band InSAR coherence

- Temporal decorrelation: Boxplot – **open area (grass)**

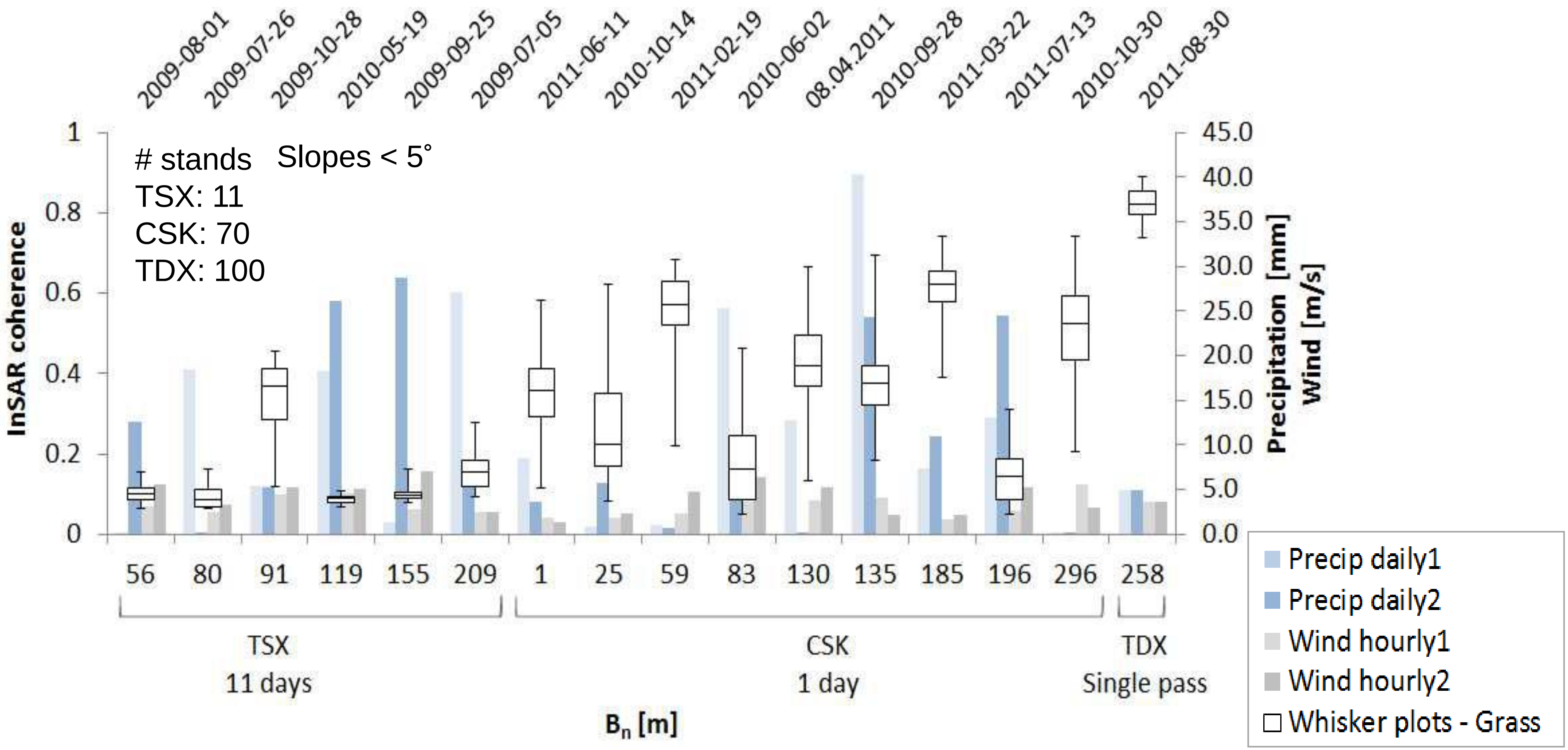

X-band InSAR coherence

- Volume/Temporal decorrelation: Boxplot – **forest (spruce)**

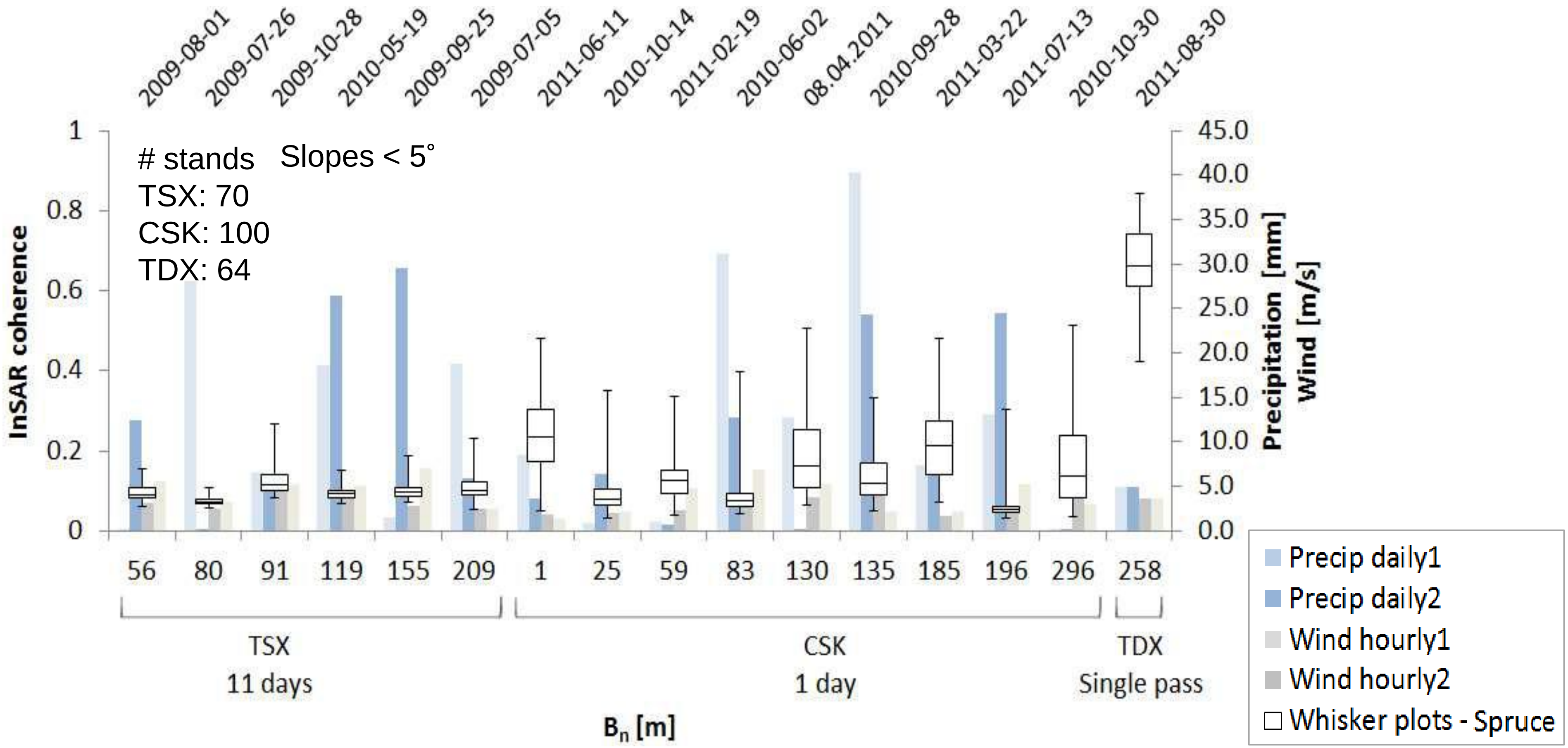

X-band InSAR coherence

- Volume/Temporal decorrelation: Boxplot – **forest (spruce)**

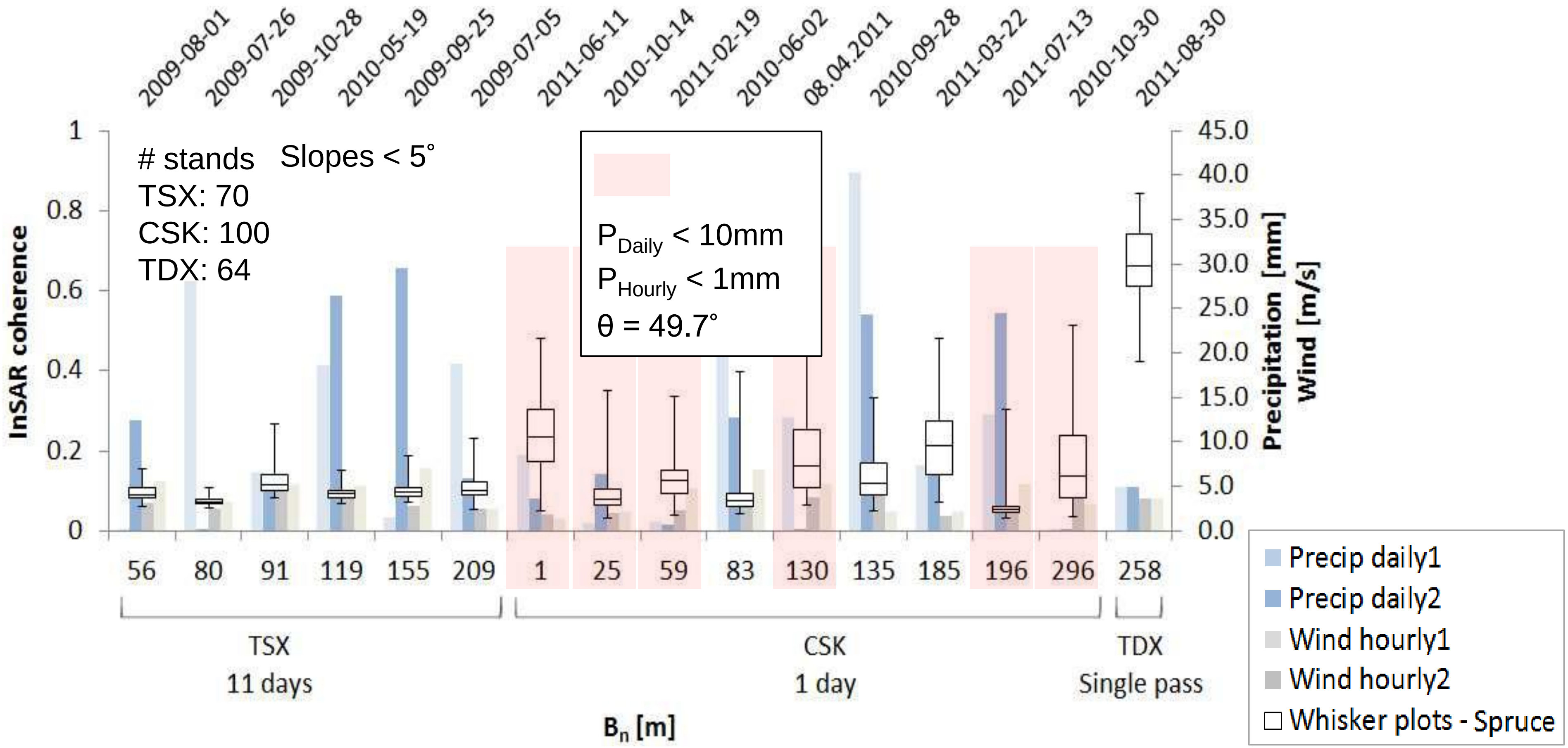

X-band InSAR coherence

- Volume decorrelation: Boxplot – **forest (spruce)**

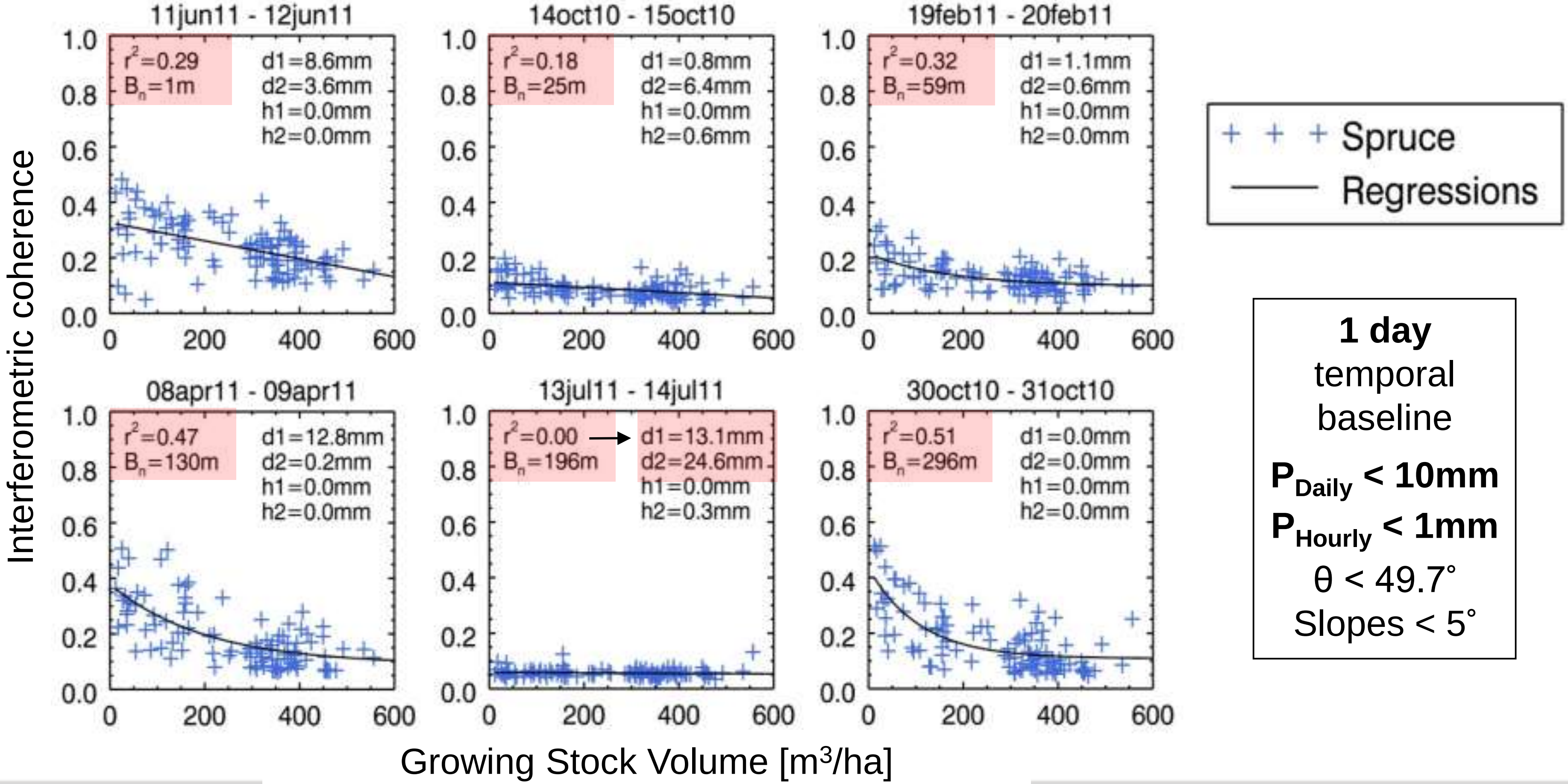

1 day temporal baseline

P_{Daily} < 10mm

P_{Hourly} < 1mm

θ < 49.7°

Slopes < 5°

X-band InSAR coherence

- Volume decorrelation: Boxplot – **forest (spruce)**

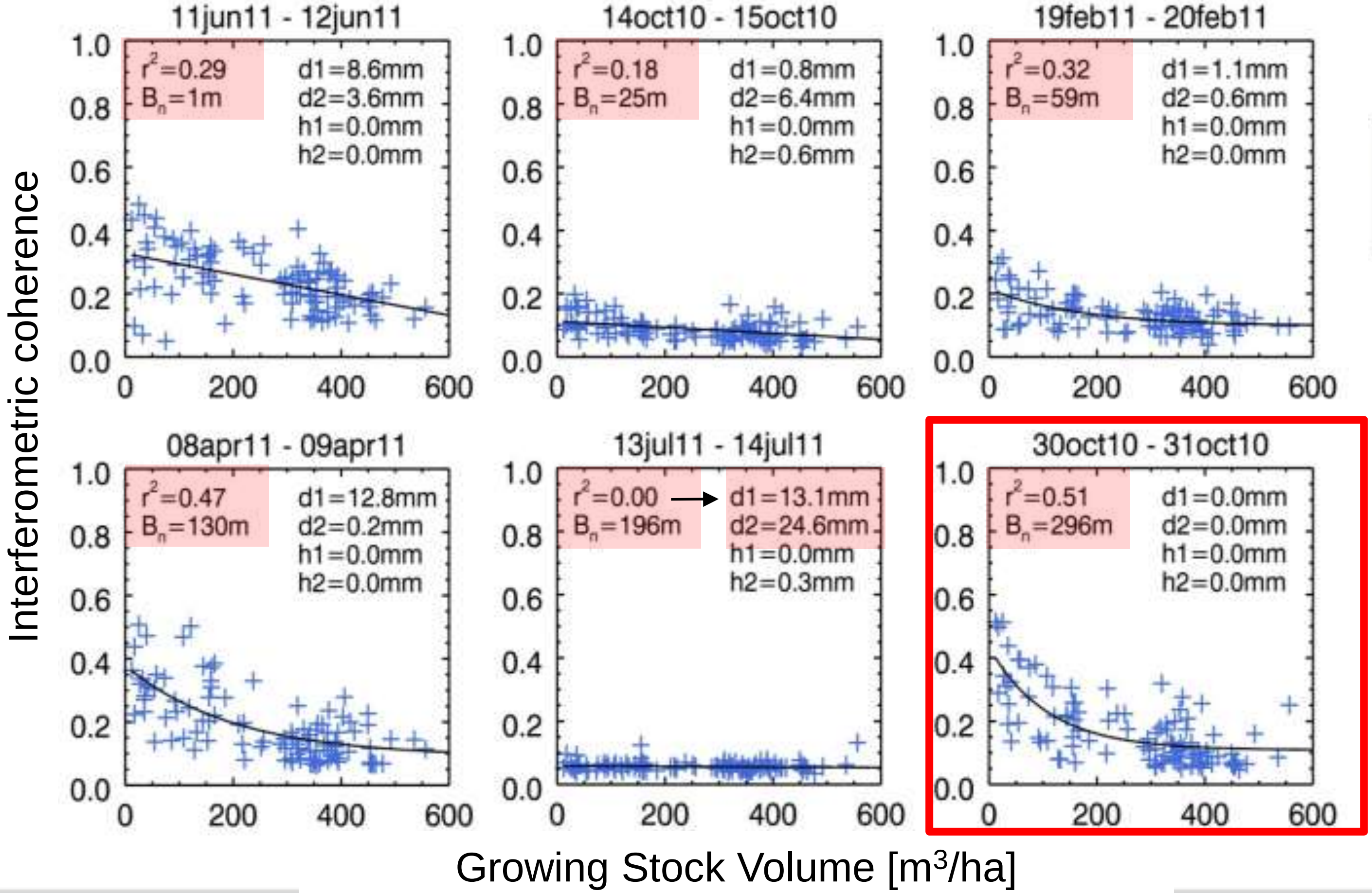

1 day
temporal
baseline

P_{Daily} < 10mm
P_{Hourly} < 1mm
$\theta < 49.7°$
Slopes < 5°

X-band InSAR coherence

- InSAR Coherence versus Stem Volume

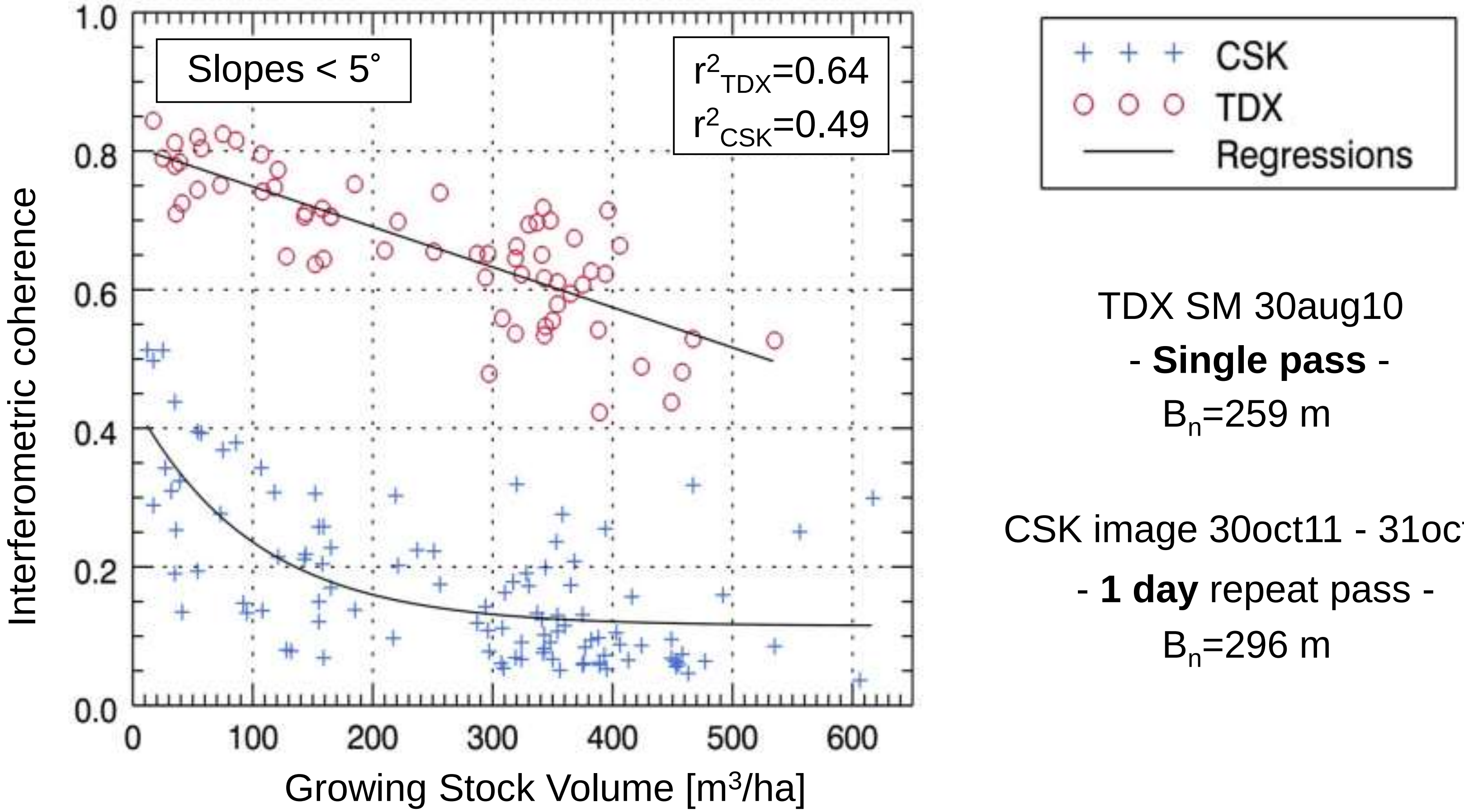

TDX SM 30aug10

- **Single pass** -

B_n=259 m

CSK image 30oct11 - 31oct11

- **1 day** repeat pass -

B_n=296 m

Conclusions

- Investigations of the **CSK, TSX and TDX** backscatter intensity and interferometric coherence have been conducted.

- Conifers and Broadleaves amplitude signal can be separated with CSK HH.

- **High temporal decorrelation** in X-band repeat pass acquisitions (even with 1 day).

- X-band single pass coherence show **potential for estimating biomass**

Outline

Mapping of fractional woody cover using ALOS PALSAR L-band backscatter in southern African savannas

M. URBAZAEV, C.J. THIEL, C.C. SCHMULLIUS, *FSU Jena, Germany*
R. MATHIEU, L. NAIDOO, *CSIR Pretoria, SA*
S. R. LEVICK, *MPI for Biogeochemistry Jena, Germany*
I. P. J. SMIT, *Sientific Services, SANParks, Skukuza, SA*
G. P. ASNER, *Carnegie Institution for Science, USA*

1. Simultaneous occurrence of patches of trees, shrubs and grasses
2. Pronounced seasonal variations (e.g. dry and rainy seasons)

→ savannas are very heterogeneous, dynamic and sensitive ecosystems

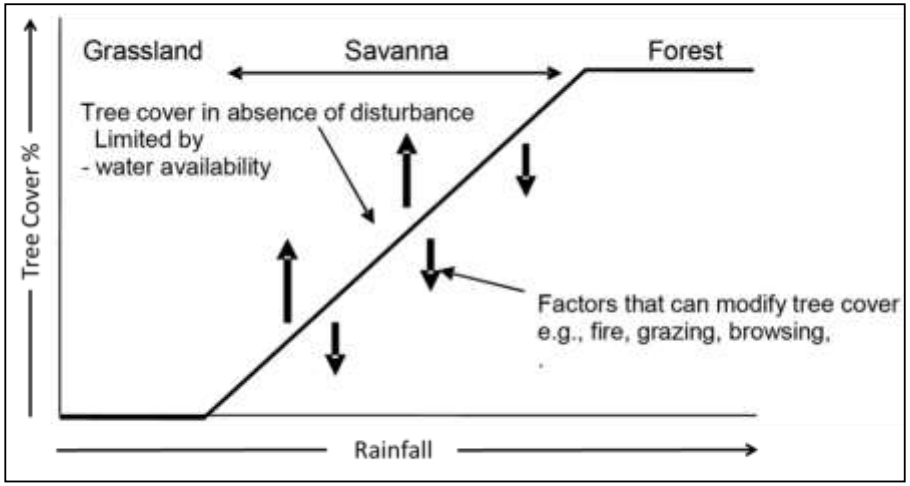

Fig. 1: Predicted tree-grass ratios across rainfall gradients (SANKARAN et al. 2004: 482)

hanspeternarjes.de

3. Status of savannas and their temporal dynamics (e.g. vegetation height, woody cover, AGB)
4. Woody cover affects the carbon and water cycles, fire regimes, nutrient cycling and soil erosion

Study area / Data

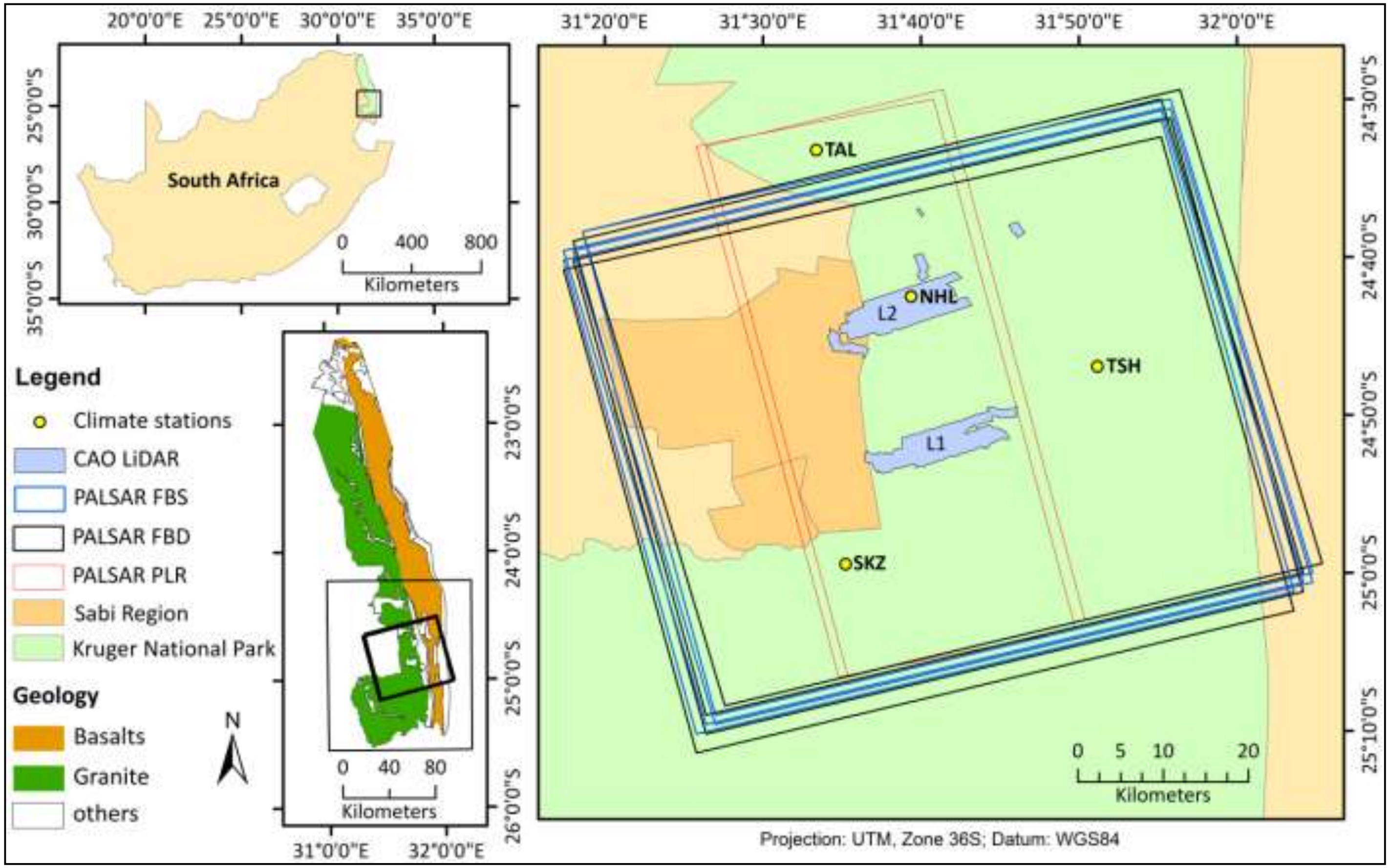

Fig. 2: Study area

(Weather stations acronyms: NHL: Nhlanguleni; SKZ: Skukuza; TAL: Talamati; TSH: Tshokwane)

Results/Discussion

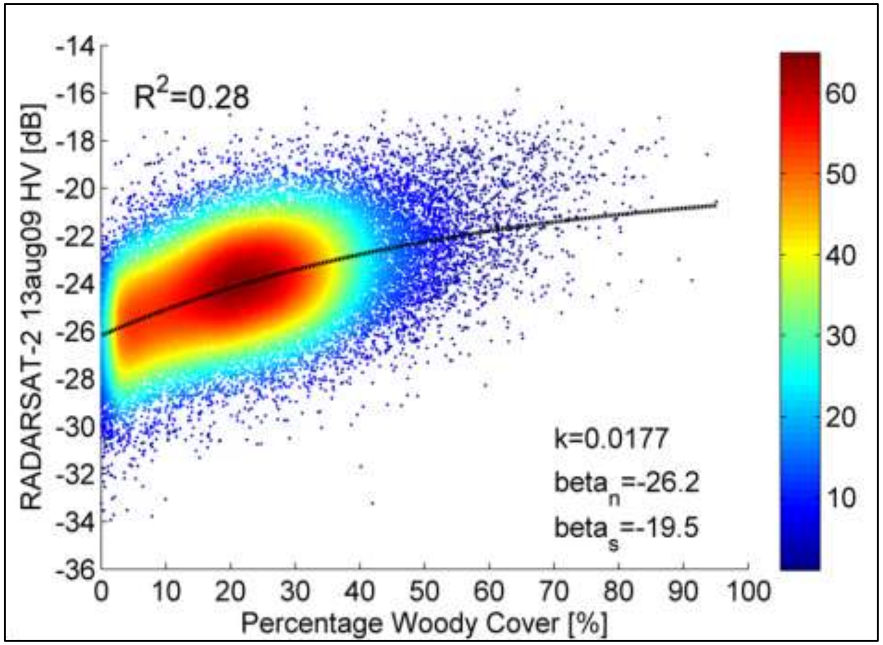

C-band

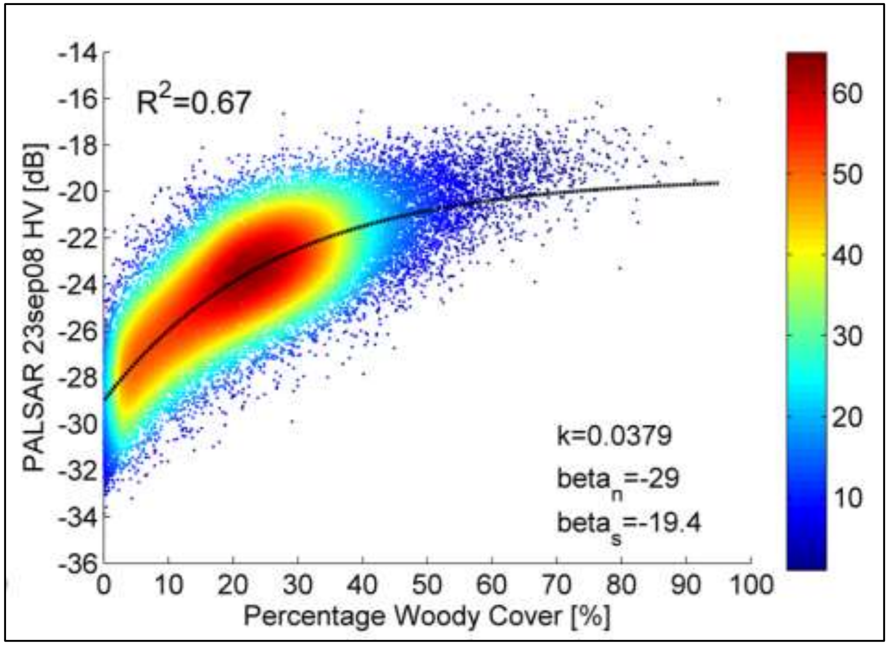

L-band

Results/Discussion

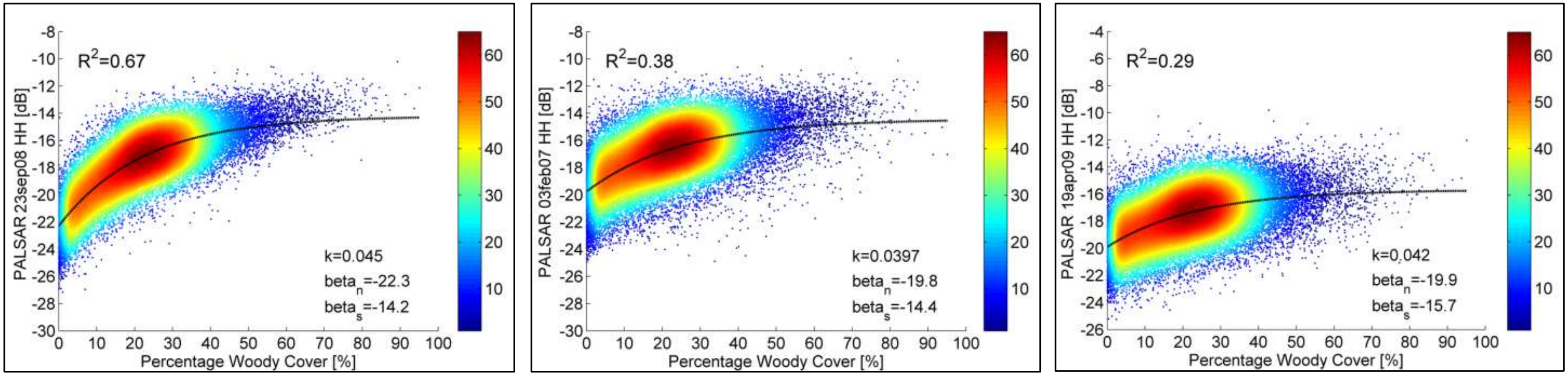

Dry season | Rainy season | End of rainy season

Results/Discussion

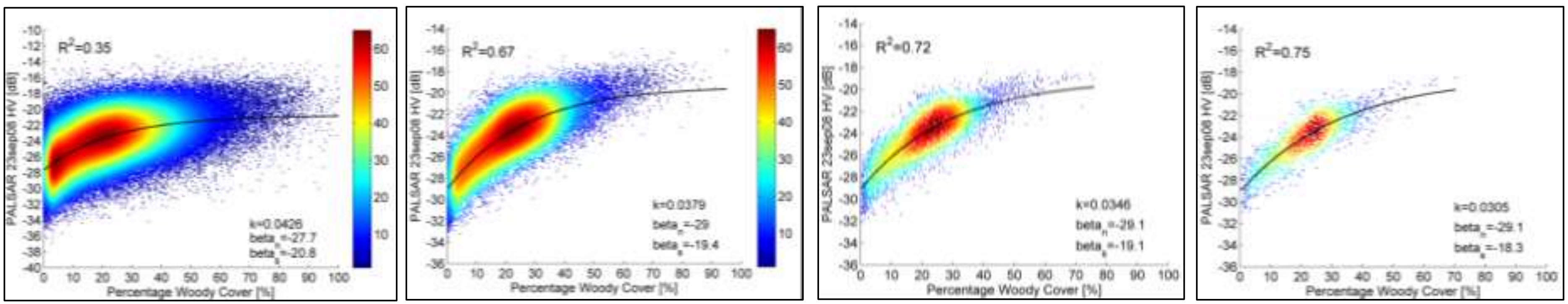

25 m 50 m 125 m 200 m

Pixel spacing

Results/Discussion

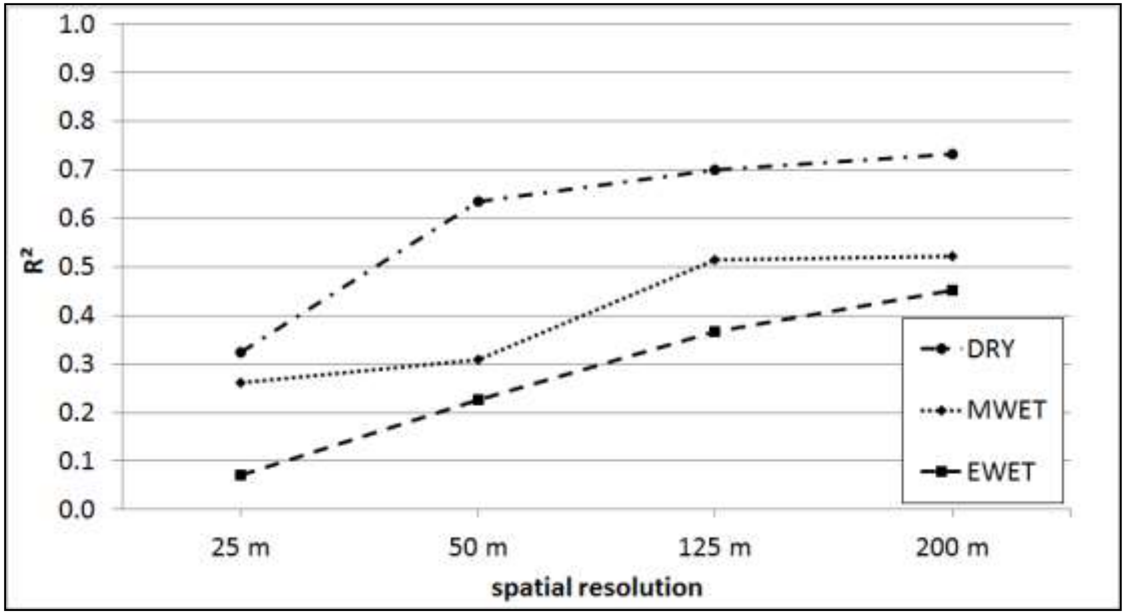

Fig. 4: Mean R^2 between PALSAR HH backscatter intensity and LiDAR-based woody cover for three seasons at four different aggregation levels (DRY dry season; EWET end of rainy season; MWET middle of rainy season)

Results/Discussion

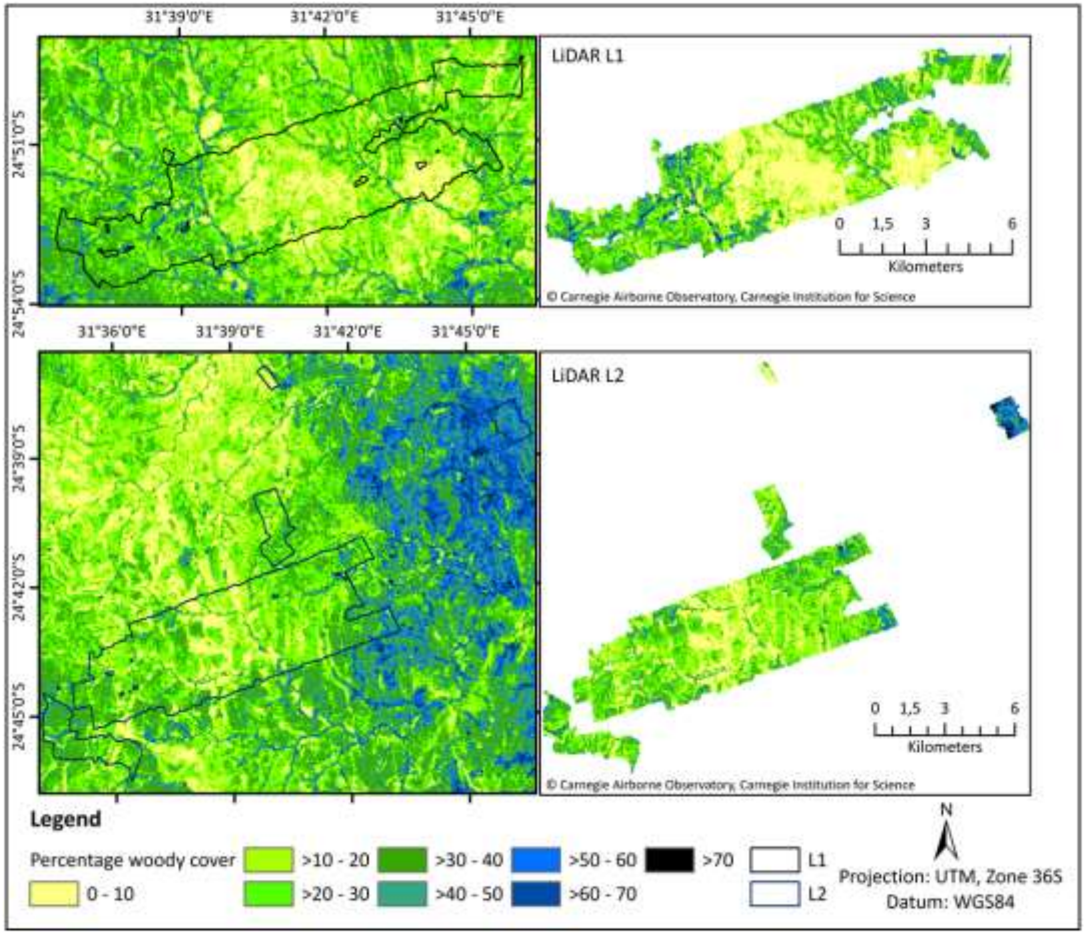

Fig. 5: Comparison between the PALSAR-based woody cover (left) and LiDAR-based woody cover (right) for the test sites L1 and L2

Results/Discussion

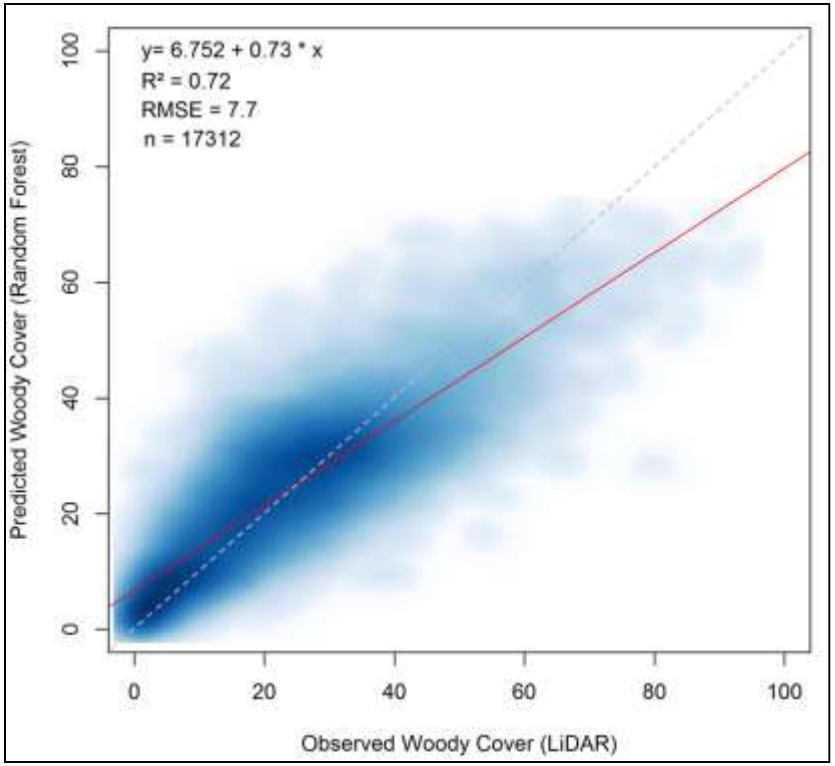

Fig. 6: SAR-based prediction of woody cover plotted again LiDAR-based observed woody cover. Red line is the regression line, and dotted line is the 1:1 line

SAR Techniques – Summarising Evaluation

1. **Backscatter** analysis (long wavelength, HV polarisation, the shorter the wavelength – the more images, summer data in boreal zone) – Sentinel-1, ALOS-2
2. **Interferometry: Coherence** analysis (shorter wavelengths require shorter temporal and spatial baselines, frozen conditions in the boreal zone), new results show great potential of single pass TanDEM-X coherence
3. **Interferometry: Phase** analysis (multi wavelength, polarisation, single-pass, acquisition conditions!) – no operational sensor constellation yet, but…
4. **Polarimetry** (long wavelength, high number of images) – still matter of research, some potential was demonstrated
5. **Polarimetric Interferometry** (long wavelength, spatial baseline, single-pass, acquisition conditions!) – no operational sensors yet, but…
6. **(Polarimetric) Tomography** (long wavelength, polarisation, spatial baselines, quasi single-pass, acquisition conditions!) – no operational sensors (and no planning for the future)